Impact of Wnt signalling on multipotent stem cell dynamics during Clytia hemisphaerica embryonic and larval development

Antonella Ruggiero

Université Pierre et Marie Curie

Ecole Doctorale Complexité du Vivant

Par Antonella RUGGIERO

Pour obtenir le grade de
Docteur de l'Université Pierre et Marie Curie

Impact of Wnt signalling on multipotent stem cell dynamics during *Clytia hemisphaerica* embryonic and larval development

Dirigée par Evelyn Houliston

Co-encadrant Carine Barreau

Soutenue publiquement le 24-11-2015 devant la commission d'examen constituée de:

Prof Agnes Audibert	Professor - UPMC Université Pierre et Marie Curie	**President**
Dr Peter Ladurner	Assistant Professor Institute of Zoology, University of Innsbruck	**Rapporteur**
Dr Fabian Rentzsch	Group Leader Sars Centre, Bergen	**Rapporteur**
Prof Paola Furla	Professor - UNS Université Nice Sophia Antipolis	**Examinateur**
Dr Evelyn Houliston	Directeur de Recherche - CNRS UMR 7009 Université Pierre et Marie Curie	**Directrice de thèse**

Ai miei genitori

“Chaque homme dans sa nuit s’en va vers sa lumière”

“Ciò che oggi fa notte dentro di noi, domani ci lascerà le stelle”

(V. Hugo)

Acknowledgement

First of all I would like to thank Evelyn Houliston for giving me the possibility to do my PhD in her Laboratory and to Carine Barreau for being present in everyday lab life.
Thank you for giving me the freedom to develop my style and my ideas and for taking care of me.

In particular I would like to say merci to Remi who offered me a helping hand.

I would like to say thanks to all the present and the past Lab members: Patrick, Pascal, Luca, Chiara, Sandra, Gonzalo, Tsuyo and Sophie. It has been a pleasure to work with you, thank you for the support (technical and moral!).
A special thanks to Pascal that was my big-brother (I would prefer to say *fratm*) and to Lucas and Chiara those were always there for me.
I am also very grateful to all the people in the unit that I have met over these four years, in particular to Janet for the hospitality and to Stefano who was the first to welcome me here.

Merci Sophie, Justine et Carole pour être toujours là dans cette longue marche dans le désert.

Vorrei ringraziare Stefania per essere stata allo stesso tempo: ricercatrice, capo, psicologa, mamma, amica... grazie per essere stata tutto questo!
Grazie di cuore alla mia famiglia e ai miei amici piu cari che mi hanno guardato da lontano!

General Summary

The aim of this work was to extend our understanding of the mechanisms regulating stem cell formation, specification and differentiation by studies in the non-bilaterian metazoan model *Clytia hemisphaerica*. *Clytia,* like other hydrozoan cnidarians, possess a particular population of multipotent stem cells called interstitial cells (i-cells), present during larval development and in the adult medusa, which are able to give rise both to somatic cell types and to gametes.

In bilaterian animals Wnt/β-catenin signalling regulates fundamental developmental processes such as germ layer segregation and primary body axis specification, but also regulates stem cell proliferation, lineage specification and differentiation.

I investigated the role of Wnt/β-catenin signalling in i-cell specification and differentiation. I established a set of markers for known i-cell derivatives: neural cells, nematocytes, gland cells and germ cells, which I used to monitor the presence of these cell types in Wnt3 morphant embryos. The results obtained suggest that Wnt/β-catenin signalling is involved in the last step of differentiation for certain neuronal cell types including nematocytes, but not for somatic cell fate choice from the multicellular i-cell pool. I found no evidence for germ cell fate specification from the multipotent i- cell pool prior to adult stages.

In the second part of my study I investigated the role of Wnt/β-catenin signalling in i-cell formation during embryogenesis. The results indicated that during normal development i-cell formation is Wnt/β-catenin independent and probably driven by inheritance of germ plasm containing localised mRNAs from the egg animal pole. In contrast in embryo re-patterning following embryo bisection, Wnt/β-catenin signalling appears to be necessary for *de novo* i-cell formation in the absence of germ plasm. Thus two distinct mechanisms can lead to i-cell formation during embryogenesis.

Overall the results obtained provided a better picture of how i-cells and their derivatives arise during embryogenesis and larval development.

TABLE OF THE CONTENTS

List of the Figures

INTRODUCTION

Our current understanding of stem cell biology comes mainly from studies in classical vertebrate and invertebrate model systems, however in light of the very strong evolutionary conservation of the signalling pathways involved (*e.g.* Wnt), non canonical model organisms can contribute extensively to extend our knowledge and unravel novel aspects of stem cell regulation.

Hydrozoan cnidarians were among the first non-bilaterian metazoan animals in which stem cells were described. A particular population of multipotent stem cells termed interstitial cells (i-cells) can differentiate into somatic cells such as nerve cells, gland cells and nematocytes, as well as into gametes.

My thesis work addressed the regulation of the i-cell population in the hydrozoan *Clytia hemisphaerica*. Various aspects of stem cell regulation were addressed, namely their formation during embryogenesis, proliferation, specification and differentiation of derivative fates. The main aspects treated in this manuscript will be specification (how the i-cells chose their fate), and differentiation (how once specified they reach their terminal state), as well as their embryological origin.

In the first part of this Introduction (1), I will describe general stem cell features and the mechanisms that regulate their formation and differentiation in various taxa and tissues.

The second part (2) is focussed on the cnidarian biology, in particular on i-cell biology.

I will describe in detail the known i-cell derivative cell types: their morphology and gene expression characteristics, and what is known about the molecular mechanisms controlling their specification and differentiation.

1) A general overview of stem cell features and regulation

1.1 Stem cell properties

A general definition of a stem cell, as commonly found in cell biology textbooks (*e.g.* Molecular Biology of the Cell, Alberts 2002), is as an undifferentiated cell capable of both self-renewal and multi-lineage differentiation, displaying an unlimited proliferative activity that lasts (*in vivo*) the lifetime of the animal. Based on this definition a stem cell should have the following characteristics:

- No particular morphological distinctive features.
- Be able to generate at least one daughter cell with the same potential as the mother cell.
- Unlimited mitotic proliferation.
- Potential to generate large numbers of differentiated functional progeny.

1.2 Stem cell potential

Based on their potential to differentiate into any particular type of cell, stem cells can be classified into 4 different categories: totipotent stem cells, pluripotent stem cells, multipotent stem cells and unipotent stem cells (Figure 1).

1) Totipotent stem cells: a totipotent cell can give rise to various differentiated cell types including those of extra-embryonic tissues. The zygote is considered by some to be totipotent stem cells, although it doesn't have the property of self-renewal, at least not directly.

2) Pluripotent stem cells: animal pluripotent stem cells are able to differentiate into all cell types of the three embryonic germ layers, *i.e.*, ectoderm, mesoderm, and endoderm. The best-know example is the embryonic stem cell (ES cell) (Martin 1981). In mammals, ES cells derive from the inner cell mass of the blastocyst. The inner cell mass comprises a group of cells arising very early during pre-implantation development, which give rise to the embryo proper. The outer cell layer of the blastocyst instead gives rise only to extra-embryonic tissues.

In all the animals that lack extra embryonic tissues, the terms totipotent and pluripotent are equivalent.

3) Multipotent cells: multipotent stem cells show a restricted pattern of differentiation into a limited number of cell types. A good example of a multipotent stem cell system is provided by the hematopoietic system, responsible for producing mature blood cells. Hematopoietic stem cells called hemocytoblasts give rise to "transit amplifying" progenitors of the myeloid and lymphoid lineages. Transit-amplifying cells are fated cells that proliferate and generate fully differentiated cells. The myeloid progenitor cells will then generate erythrocytes, megakaryocytes and myeloid cells, which in turn proliferate and differentiate into eosinophil, basophil, neutrophil and monocytes. The lymphoid cells produce T lymphocytes, B-lymphocytes and NK lymphocytes.

Multipotent stem cells are defined as adult stem cells if they are found in adult stage and can generate all the cell types of the tissue from which they originate, as is the case for the hematocytoblasts.

4) Unipotent stem cells: unipotent stem cells have a very restricted cell differentiation capacity, and can generate only one single type of cell. Melanocyte stem cells provide one example of unipotent stem cells, producing the pigmented cells (melanocytes) present in hair follicles and in epidermis. Melanocyte stem cell systems were characterised for the first time in mouse hair follicles (Nishimura et al. 2002). During each cycle of hair regeneration and regression, melanoblasts proliferate and differentiate into fully mature melanocytes, which enter into the developing hair.

As mentioned in the hematopoiesis example above, stem cells divide to generate intermediate cells, termed transit-amplifying cells. This type of temporal and developmental hierarchical organisation reduces the number of cell divisions that stem cells must undergo (Morrison & Spradling 2008). However this ordered progression, from stem cells to differentiated cells is not rigid. Indeed in particular conditions committed, differentiating or differentiated cells can revert to the self-renewing stem cells state. Thus tissue stem cells have the potential to revert (to dedifferentiate in the most extreme examples) to stem cells under certain circumstances. An example of this cellular plasticity is provided by studies of mouse spermatogonia (Nakagawa et al. 2010). Spermatogenic cells are organised within a compartment populated by germ cells and by somatic cells with support functions. The germ cell precursors, the spermatogonia give rise to the spermatocytes. Several subpopulations of spermatogonia, can be distinguished by morphology and by gene expression patterns reflecting different degrees of differentiation.

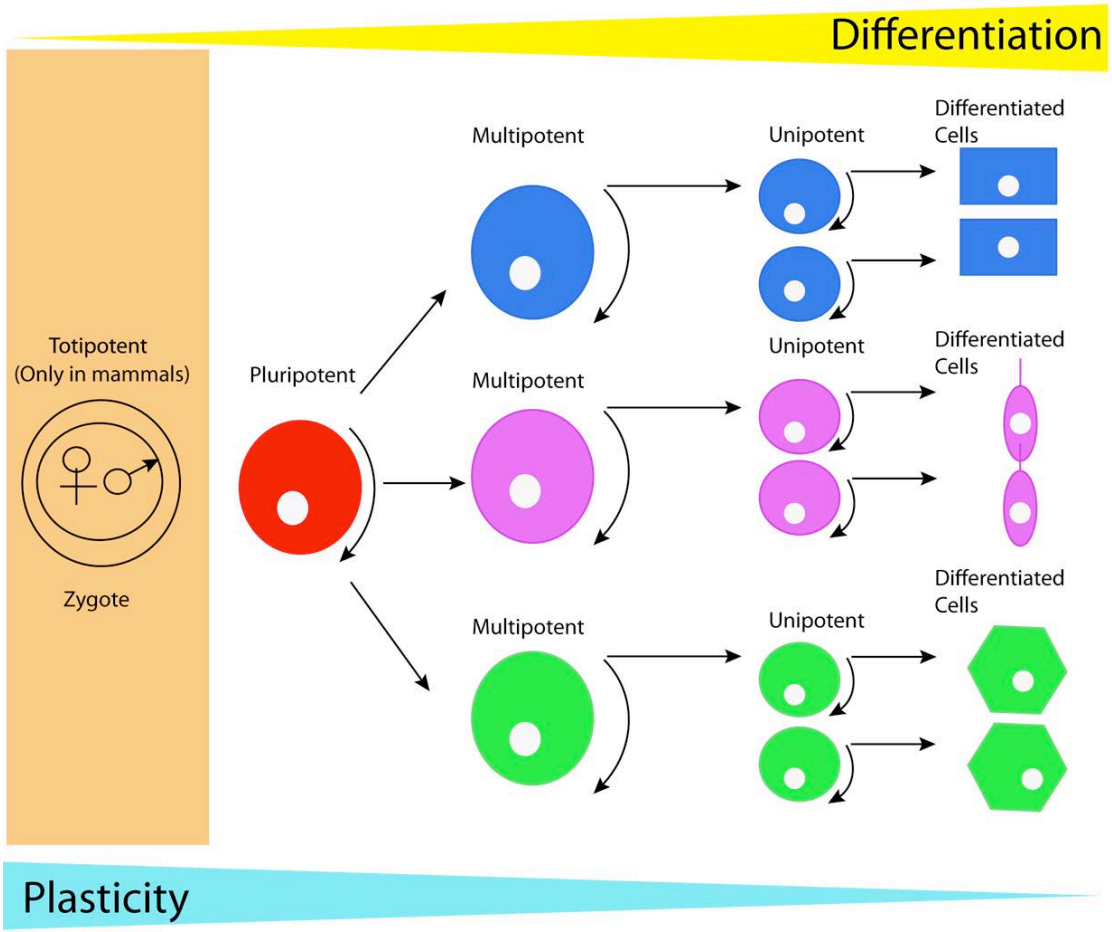

Figure 1: Stem cell potential.
The cartoon shows how stem cells gradually commit towards a differentiation pathway. The cells acquire a restricted fate, decreasing in potential. Pluripotent cells (in red) are able to give rise to multipotent stem cell here represented in three different colours (green, pink and blue). Multipotent stem cells have a reduced potential. Curved arrows illustrate the self-renewal ability of these stem cells. On the right, an illustration of the zygote that in mammals is a totipotent cell.

During regeneration after injury, spermatogonia at the most advanced differentiating stages contribute to the re-population of the spermatogenetic compartment by re-converting into stem cells.

1.3 Generating cell type progenitors

The progenitors of particular cell types are generated when stem cell progeny loses their stem cell properties (proliferation and self renewal) and moves on the pathway towards differentiation. In order to provide progenitors of particular differentiated cell types while

also renewing the stem cell population, the stem cells divide asymmetrically giving rise to two sister cells that have different fates, a feature that can be recognised by differences in size, morphology, gene expression pattern, or the number of subsequent cell divisions undergone by the two daughter cells (Horvitz & Herskowitz 1992). The asymmetric choice between self-renewal and differentiation can be regulated by extracellular cues coming from a "niche" acting preferentially on one of the daughter cell (a process termed environmental asymmetric cell division), or by intrinsic programs within the cell, which is known as divisional asymmetric cell division (Wilson & Trumpp 2006) or unequal segregation of localised cytoplasmic determinants (Figure 2).

In particular conditions such as during the formation of the stem cells pool, stem cell can divide symmetrically.

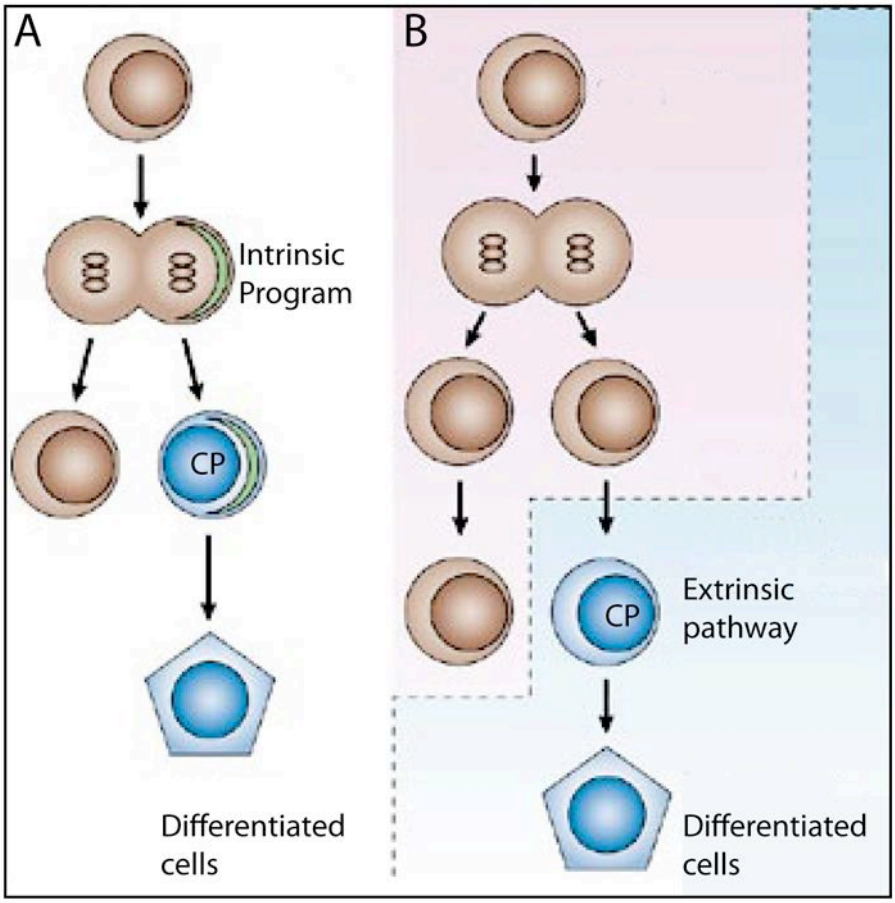

Figure 2: Asymmetric cell divisions.
A) Localised determinants direct the fate of the terminal differentiated cell, activating an intrinsic genetic program. B) Extrinsic cues determine the fate of one of the two daughter cells inducing the specification of cell precursor (CP) that will move into the differentiation pathway. Modified from Wilson & Trumpp (2006).

1.3.1. Generating progenitors via unequal determinant segregation

Two main events are necessary for setting up divisional asymmetric cell division: cell fate determinants have to be asymmetrically localised and the mitotic spindle has to be oriented with respect to the determinant axis (Betschinger & Knoblich 2004).

One example of asymmetric cell division of a stem cell involving unequal determinant distribution is seen in *Drosophila* neuroblasts (Knoblich 2001), which are central nervous system progenitor cells. Neuroblasts derive from the neuroectoderm tissue. Committed neuroblasts migrate into the sub neuroectodermal layer in a process termed delamination, and then generate by asymmetric cell division a small basal daughter cell called the ganglion mother (GMC) and a large apical daughter cell that retain a stem cell nature. The GMC is the neural progenitor as it will divide one more time and gives rise to two post mitotic neurons. In contrast the large apical cell retain a neuroblasts identity and continue to divide in a stem cell manner. The apical-basal polarity is set up by the PAR protein complex, which is localised apically. The PAR complex comprises a core of the three proteins: Par3, Par6 and aPKC (atypical Protein Kinase C), which have a role in asymmetric cell division across species and in different cell types (Guo & Kemphues 1995). The PAR complex regulates the localisation of the neural fate determinants in the GMC cells such as the membrane-associated Notch pathway suppressor Numb, the transcription factor Prospero, and specific adaptor proteins responsible for their basal localisation Miranda and Pon (Partner of Numb). Miranda is a coiled-coiled protein that binds Prospero and translocates it to the cell cortex, from where it is later released in the daughter cell to activate neural cell fate gene transcription.

1.3.2 Generating progenitors via environmental cues: the "Niche"

Stem cell "niches" are spatially distinct microenvironments that can include neighbouring cells, signalling molecules and other extracellular materials (Scadden 2006). These have been studied extensively in *Drosophila* and *Caenorhabditis elegans* gonads, which can be conveniently manipulated through genetic and molecular approaches. The *C. elegans* adult gonad shows an ordered progression in germ line formation from germ stem cells (GSCs) occupying the most distal extremity, to mature gametes positioned in the proximal part. A key population of undifferentiated somatic mitotic cells called "distal tip cells" (DTCs) covers the distal extremity of the gonad. DTCs are the major regulator of germ line

proliferation and are the main component of the gonad stem cell niche (Kimble & White 1981). The stem cell properties of the GSCs depend upon their contact with the DTCs. As GSCs move further away from the distal tip, they terminate their mitotic activity and enter into meiosis. DTCs cells control GSC differentiation through a Notch-like signal. DTCs express on the surface the delta-like ligand LAG-2, which activates the Notch-like receptor GLP-1, localised on the mitotic germ cells. In the cell contacting the DTCs, GLP-1 is activated and translocates to the nucleus, where it downregulates meiosis promoting genes like gld-1, gld-2 and nos3, required to maintain the stem cell state (Hansen 2004).

1.4 Maintaining the undifferentiated stem cell state

Maintenance of the undifferentiated stem cell state relies on a variety of regulatory mechanisms acting at different levels including transcriptional regulation, translational regulation and epigenetic modification of chromatin. During my thesis I used extensively as stem cell markers two genes involved in maintaining pluripotency through regulation of mRNA metabolism and translational control, *Piwi* and *Nanos*. Interestingly these two genes along with other mRNA binding proteins such as *Vasa* and *PL10* which have traditionally been considered as "germ line genes" because of their highly conserved expression in germ cell precursors (PGC), are now emerging as more widely functioning stem cell regulators with functions outside the germ line.
Before introducing *Piwi, Nanos* in more detail, I will mention briefly in this section the main actors in transcriptional regulation and epigenetic regulation of stem cell identity.

1.4.1 Transcriptional control

A set of transcriptional factors (TFs) have been well characterised in vertebrate embryonic stem cells, including Nanog, Oct4, Klf4 and Sox2, which act to repress somatic differentiation programs (Chambers et al. 2003; Niwa et al. 2000; Boyer et al. 2005). Discovered in 1998 Oct4 was characterised as an essential TF in maintaining the pluripotent state (Nichols et al. 1998). Oct4 belongs to the POU transcription factor family and can either activate or repress target gene expression by binding to the octameric sequence consensus motif AGTCAAAT. This consensus motif can be found in regulatory

sequences including those in introns. Although POU domains that bind this sequence are conserved across metazoans (Gold et al. 2014), Oct4 orthologs have not been identified outside vertebrates.

Nanog is required for the maintenance of a pluripotent state and to prevent the differentiation. It is a tripartite protein with a central homeodomain. Transcriptional regulation is mediated by the C-terminal domain, which is characterised by two subdomains, WR and CRD2 (Pan & Pei 2005). Recent phylogenetic analysis shows that Nanog like Oct4 is not present in *C. elegans* or in *Drosophila* or in non vertebrate-chordates like *Ciona* and *Amphiouxus* (Satou et al. 2008) but is present only in vertebrates (Ma et al. 2013). Sox2 belongs to the SR-HMG protein family. It is needed for the maintenance of a pluripotent state. Indeed loss of Sox2 causes the activation of differentiation pathways (Niwa 2007). Sox2 can cooperate with Oct3/4 in the control of target gene transcription. Kfl4 is a member of the KFL (Krüppel-like factor) transcription factor family. It is a zinc finger protein, which can activate or repress target genes involved in cell proliferation and or differentiation.

1.4.2 Epigenetic mechanisms

Stem cell regulation mechanisms involve epigenetic mechanisms and non-coding RNA-mediated gene silencing. Epigenetic in this context refers to changes in DNA structure without modifications of the DNA sequence. Epigenetic mechanisms include histone modifications and DNA methylation (chemical modifications to the cytosine residues of DNA). The tri-methylation of particular residues on the DNA sequence can identify the state of the chromatin. The methylation of the Lysine 4 on the Histone 3 (metK4H3), is correlated with transcriptional activity, while compact chromatin, not accessible for transcription, is marked by methylation of the Lysine 27 on Histone 3 (metK27H3). A protein complex involved in chromatin modification is the Polycomb group complex (PcG). PcG proteins function as a repressive complex, is required for the long-term silencing of chromatin and has an important role in the differentiation of stem cells as well as in early embryonic development (Simon & Kingston 2013).

Three proteins form the core complex: enhancer of zeste (Ezh2), embryonic ectoderm development (Eed) and suppressor of zeste 12 (Suz12). Eed binds Suz12, which is a histone

methyltransferase while EZh2 maintains the silent tri-methylated state of the Lysine 27 residue of the target DNA.

PcG proteins are highly conserved across animal species and have been studied also in two hydrozoans: *Podocoryne* (Lichtneckert et al. 2002) and *Hydra* (Khalturin et al. 2007; Genikhovich et al. 2006). The *Hydra* Eed ortholog HyEED is expressed in hydrozoan multipotent stem cells termed interstitial cells (i-cells) and in nematoblasts (stinging cells peculiar to cnidarians) (Khalturin et al. 2007; Genikhovich et al. 2006), which will be introduced in detail respectively in section 2.2.1 and 2.2.3 of this Introduction chapter. As HyEDD is expressed in the early-stage nematoblasts located in *Hydra* gastric region, but never detected in differentiated nematocytes located in the head and in the foot. Overexpression of a construct in which HyEED was fused to eGFP under a ubiquitous actin promoter, revealed degradation of the fusion protein, and thus probably of the endogenous protein, during nematocyte differentiation. Furthermore, following treatment with an inhibitor of the proteasome machinery (MG132), HyEED expressing cells were detected in mature nematocytes located at the extremity of the *Hydra* polyps. This study points to a role for EED in *Hydra* in preventing nematocyte differentiation from nematoblasts by polycomb type chromatin remodelling.

1.4.3 Regulatory RNAs

Small non-coding regulatory RNAs, along with epigenetic mechanisms, facilitate the continued expression of stem cell TFs. Stem cell TFs contribute to maintaining pluripotency by preventing stochastic and aberrant induction of differentiation. Thus regulatory RNAs, such as microRNAs (miRNA), endogenous small interfering RNAs (siRNA), long non-coding RNAs (LncRNA) and Piwi-interacting RNA (piRNA) play an important role in the control of pluripotency.

In the last few years the role of the LncRNAs has been widely investigated (Flynn & Chang 2014). LncRNAs are non-coding transcripts greater then 200 base pairs in length. A specific LncRNA has been identified that participates in the regulation of pluripotent ES cells (Guttman et al. 2011). Knockdown of these LncRNAs in mouse ES cells results in downregulation of the expression of pluripotency markers including Oct4, Nanog, Sox2 and Klf4.

siRNAs and miRNAs bind to Argonaute/Piwi family proteins of the Ago sub-type which are widely expressed in different tissue types (Wutz 2013). They are characterised by three highly conserved domains: the PAZ, MID and PIWI domains. The N-terminal PAZ domain and the MID domain together bind small RNAs (Song et al. 2005), while the C-terminal PIWI domain, whose structure is similar to that of RNase H enzymes, cleaves the RNA/DNA hybrids formed when the regulatory RNAs hybridise to complementary sequences in the genomic DNA (Okamura et al. 2004). Piwi proteins bind to a specific type of regulatory RNAs called piRNAs, which are mostly restricted to germ line and stem cells (Thomson & Lin 2009), as described in more detail in the following sections. piRNAs have sequence complementary to those of transposable elements : mobile DNA sequences that can insert themselves into new positions in the genome where they can cause genome instability and loss of long-term fitness. Piwi-piRNA interaction leads to the degradation of piRNA/transposable elements hybrids, thus preventing specific transposons from integrating into the genome (Brennecke et al. 2007). A major function of Piwi and of pi-RNAs is thus thought to be to protect the genome from transposable mobile elements.
More generally, RNA-binding proteins regulate every aspect of RNA metabolism, including pre-mRNA splicing, mRNA trafficking, stability, and translation. Among these, Nanos is an RNA binding protein with translational repressor function. In the next section I will give a more detailed introduction to the classical germ line genes, *Nanos* and *Piwi* that I used to track the multipotent stem cell population in *Clytia*.

1.5 A shared gene toolkit for stem cells and germ line

In the last few year molecular studies conducted in non-bilaterian organisms such as sponges and cnidarians, and in some invertebrates like planarians, have indicated the presence of a common molecular signature shared between some stem cell populations and the germ cells. These genes have been referred to as Germline Multipotency Program (GMP) genes (Juliano et al. 2010). The GMP gene set includes *Nanos*, *Piwi*, *Vasa* and *PL10*, all coding for RNA binding proteins. The GMP gene products have frequently been described as associated in granule-like structures in germ line cells variously termed *nuage*, chromatid bodies, germ plasm, and pole granules. These structures extensively described in primordial germ cells and developing oocytes, are composed of ribonucleoprotein

complexes located in the perinuclear region in PGCs which often translocate to subcortical regions of the oocyte during oogenesis (Kloc et al. 2004). Germ plasm presence in oocytes of different species is rather patchy across the animal phylogenetic tree leading to speculation that it may have arisen several times during evolution (Extavour & Akam 2003). Traditionally its role has been considered to be as a germ line determinant, which causes the cells of the embryo that inherit it to adopt a PGC fate. This determinant role for germ plasm has been shown by ablation or transplantation experiments in various insect species and in frogs (Kloc et al. 2004).

1.5.1 Piwi proteins in the germ line and stem cells

Piwi, Nanos and Vasa proteins and mRNAs, have repeatedly been found to be enriched in germ plasm in species where the germ plasm is present. More generally, across all species examined whether they have germ plasm in their oocytes or not, expression of the GMP genes is characteristic of the germ cell developmental lineage ('germ line'). In non-bilaterian animals, including sponges and cnidarians, as well as in some bilaterian species, expression of *Nanos*, *Piwi* and other "germ line" genes has been documented also in various populations of non-germ line multipotent stem cells. This has led to the idea that the presence of these proteins may be a molecular signature of pluripotent/multipotent stem cells rather than exclusively a germ cell marker. The findings relating to this conclusion are described in more detail in the following sections.

- *Piwi, a universal marker of germ line*

Historically *Piwi* (p-element induced wimpy testis) was identified in *Drosophila* from genetic screening for mutants defective in stem cell division. Characterisation of the Piwi phenotype revealed a role in germline stem cell (GSC) maintenance via self-renewal (Lin & Spradling 1997). In *Drosophila,* Piwi is expressed in the germ line and in a somatic population of cells located apically with respect to the GSCs (Cox et al. 1998). In *C. elegans* prg-1 and prg-2 (Piwi related genes) are required for the maintenance of mitotic germ cells. The zebrafish Piwi homolog *Ziwi* is also required for maintenance and development of germ cells (Houwing et al. 2007), while *Miwi* expression in mouse is restricted to the male germ line, and affects spermatogenetic progression (Deng et al. 2002). In the polychaete

Capitella teleta, two Piwi orthologs were found, *Ct-Piwi*1 and *Ct-Piwi2* (Giani et al. 2011). Expression pattern analysis detected these two transcripts in overlapping domains of proliferating somatic stem cell in the posterior growth zone and in the male and female PGCs, localised in the mature gonads.

- *Piwi a marker of stem cell in non-bilaterian metazoans*

After the discovery of Piwi, in 1998 Cox and colleagues were the first to hypothesise an extended role of the Piwi family protein. They proposed that Piwi represents the first of a group of genes that acts both in germ line and in somatic stem cells to regulate stem cell maintenance, proliferation and differentiation. This hypothesis has now been confirmed thanks to the increasing number of studies showing the presence of Piwi protein in somatic stem cells in a variety of animal species.

One example of multipotent stem cells expressing *Piwi* is sponge archeocytes, which display morphological and biological stem cells characteristics (Simpson 1984). Recent studies on the fresh water sponge (demonsponge) *Ehirava fluviatilis* demonstrate that archeocytes self-renewal, proliferate and possess the capacity to differentiate into several cell types including gametes (Funayama 2010). Archeocytes expressed two Piwi orthologs *EflPiwiA* and *EflPiwiB*. *EflPiwiA* is also expressed in another cell type specific to the sponge called choanocytes, flagellated cells whose main function is nutrient uptake. Upon spontaneous disorganisation and reorganisation of the cells in *Ehirava*, choanocytes can trans-differentiate into archeocytes and then re-differentiate into spermatocytes (Gaino et al. 1984).

In demosponges, it was recently proposed that a stem cell system based on two stem cells populations exist: the archeocytes and the choanocytes (Funayama 2013). The archeocytes give rise to all cell types (Funayama 2010) and the choanocytes manifest their stem cell potential in special conditions, during sexual reproduction or during regeneration. In the latter case choanocytes could accelerate the processes of sponge body recovery (Funayama 2013).

In the ctenophore *Pleurobrachia pileus,* two *Piwi* orthologs are found to be expressed in somatic stem cells and in germ cells (Alié et al. 2011). In particular Piwi proteins are

expressed in undifferentiated cells in tentacle roots, in the stem cells that give rise to neuronal types at the aboral pole, and in the ciliated polster cells in the combs.

Piwi gene expression is also characteristic of the i-cell population in *Hydra, Hydractinia* and *Clytia,* (Nishimiya-Fujisawa and Kobayashi 2012, Kanska and Frank 2013; Leclère et al. 2012; Denker et al. 2008).

A further example of Piwi expression in somatic stem cells is seen in planarian neoblasts. Neoblasts are totipotent stem cells that can generate all somatic cell types as well as the germ line (Baguna 1981). In the planarian *Schmidtea mediterranea* two *Piwi* orthologs have been identified: Smedwi1 and Smedwi2. Functional studies by RNAi treatments show that Smedwi2 is necessary for the production of neoblast progeny (Reddien et al. 2005).

Despite the reported expression of *Piwi* genes in a wide range of somatic stem cell types, their function in these cells remains unclear. They may be involved both in maintenance of the stem cell pool, as seen in the Smedwi2 case, and in protection of the genome from transposons, which may compromise regeneration capacity or the ongoing tissue renewal seen in hydrozoans, ctenophore tentacles and sponges.

1.5.2 Nanos regulates transcription and translation repression

Nanos is an RNA binding protein that contains a CCHC zinc finger domain with well-conserved functions involved both transcriptional regulation and translational repression. Nanos was first identified in *Drosophila* as an essential factor in early embryonic patterning (Wharton & Struhl 1991); however it has since become clear that this role is particular to *Drosophila*, while the conserved function of Nanos is associated with germ line.

- *Nanos is associated with germ line*

Nanos is expressed in primordial germ cells (PGCs) in widely divergent metazoans and its function is required for PGCs maintenance and migration in different organisms including zebrafish (Koprunner et al. 2001), *C. elegans* (Kraemer et al. 1999) and *Xenopus* (Lai et al. 2012). To execute its role as a translational repressor, Nanos acts together with a protein partner called Pumilio. mRNAs identified as Nanos/Pumilio targets have been characterised in several organisms and include the transcription factor Hunchback,

involved in the establishment of anterior-posterior polarity in *Drosophila* (Murata & Wharton 1995), and VegT an endoderm fate TF in *Xenopus* (Lai et al. 2012).
A role for Nanos in transcriptional repression in the germ line has also been shown in *Drosophila* where somatic gene transcription is prematurely activated in mutants lacking *Nanos* (Kobayashi et al. 1996).

- *Nanos somatic expression*

In *Drosophila*, Nanos also acts outside the germ line directing dendrite morphogenesis (Brechbiel & Gavis 2008) and some data also available suggest a possible function for Nanos in somatic stem cell maintenance. In the sponge *Sycon ciliatum, Nanos* is expressed in oocytes and in macromeres that give rise to the pynacoderm, the external layer of the adult sponge (Leininger et al. 2014). Thus sponge *Nanos* is expressed in both germ line and somatic cells. In several hydrozoan species examined, the Nanos1 genes are expressed in i-cells and germ cells. In contrast the paralog Nanos2 genes are additionally expressed at other sites, including the epithelial endodermal hypostome cells *in Hydra*. *Hydra Nanos2* expression increases during head regeneration, suggesting a role in head morphogenesis (Mochizuki et al. 2000). *Clytia* and *Hydractinia Nanos2* paralogs, beside i-cells and germ line, are expressed in differentiating nematoblasts (Leclère et al. 2012; Kanska & Frank 2013), indicating presumably a role for *Nanos2* in nematocyte formation. In the anthozoan cnidarian *Nematostella Nanos* orthologs have been characterised in two different studies. However the 2 reports show some discrepancies concerning the expression pattern of *Nanos1* and *Nanos2*. Torras and colleagues show a localised maternal distribution of *Nanos1* mRNA(Torras & González-Crespo 2005), while the results of Extavour and colleagues suggest that *Nanos1* is only expressed zygotically from the early gastrula stage, in a population of ectodermal scattered cells (Extavour et al. 2005). Torras and colleagues also claim that *Nanos2* is first detected at gastrula stage, then it localised in the posterior region of the planula larva and in developing tentacles, suggesting that *Nanos2* could regulate the formation of posterior structures (Torras & González-Crespo 2005). In contrast Extavour and colleagues provide a detailed *Nanos2* expression pattern showing for the first time the transcript at late blastula in a population of cells that in later stages will participate in the formation of the presumptive endoderm. In primary polyps *Nanos2* expression is restricted to distinguishable patches of cells localised along the length of the mesenteries. These cells

have the typical PGCs morphology (with large nucleus and *Nanos* cytoplasmic localisation). Moreover these cells are Vasa immunoreactive, suggesting that they might correspond to *Nematostella* PGCs. In *Nematostella* it remains to be resolved whether Nanos proteins have a somatic stem cell and/or germ line function.
In planarians expression of *Nanos*, unlike *Piwi*, is restricted to germ line precursors and its function is linked to gonad development and in gonad regeneration condition (Wang et al. 2007) while in ctenophores the *Nanos* expression pattern has not yet been described.

1.6 Wnt signalling: a candidate for stem cell regulation

Extrinsic factors, notably acting via intercellular signalling pathways, play a major role in regulating the balance between stem cell differentiation and maintenance (section 1.3.2). Many different signalling pathways including Wnt, *ERK*-MAPK, BMP-TFG*β*-Smad and Notch (Nusse et al. 2008; Zhang and Li 2005; Campos et al. 2004; Androutsellis-Theotokis et al. 2006) have been shown to regulate stem cell proliferation and/or differentiation in *vivo* and in *vitro*, in different species and in different contexts of development and tissue homeostasis. Ongoing studies in our group are focussed on the key participation of Wnt signalling in embryonic and larval development in *Clytia*, and so I addressed, during my thesis work the role of this pathway in i-cell development. In this part of the Introduction I will give an overview of the various Wnt signalling pathways.

- *Overview of Wnt signalling*

Wnt signalling regulates crucial aspects of cell fate determination, cell migration, cell polarity, organogenesis and primary body axis polarity during embryonic development. Wnt ligands and their Frizzled (Fz) receptors are evolutionary conserved during metazoan evolution. Indeed they are present throughout the animal kingdom (Croce & McClay 2008), including in organisms that diverged early from the bilaterians such as sponges and cnidarians, implying their presence in the metazoan common ancestor.
Wnt signalling can occur *via* β-catenin mediated regulation of gene transcription, described as the "canonical" or Wnt/β-catenin pathway (Figure 3A). Wnt signalling can also occur through β-catenin-independent pathways, including the Wnt/PCP (Figure 3B) and Wnt/Ca2+ (Figure 3C) pathways. The core proteins of the Wnt/PCP pathway regulate two different phenomena: coordination of individual cell polarity in the plane of the tissue

(Planar cell polarity), which can occur without Wnt ligands, and morphogenetic movements (Lapébie et al. 2011).

Wnt/Ca2+ pathway activation causes the release of intracellular Ca2+ with consequent activation of Cam Kinase II and Protein Kinase C which in turn drive the activation of nuclear factors like CREB and NFAT that promote the transcription of specific genes, including ones involved in organogenesis and establishment of the dorso-ventral axis (De 2011).

1.6.1 The Wnt/ β- catenin pathway

Wnt/β-catenin pathway core components include:

- Wnts Ligand.
- Receptors: Frizzled (Fz) family seven-pass-transmembrane proteins, and LRP5/6 co-receptors.
- The multi-domain protein Dishevelled (Dsh), which binds to the cytoplasmic domain of Fz.
- The transcriptional co-regulator β-catenin.
- A cytoplasmic destruction complex including the multi-domain protein adenomatous polyposis coli tumor suppressor (APC), the multifunction enzyme glycogen synthase kinase 3β (GSK3β), and the multidomain protein Axin.
- The transcription factor T-cell factor/lymphoid enhancing factor (TCF/Lef).

The Wnt/β-catenin pathway is activated by the binding of Wnt ligands to the Fz-LRP5/6 complex (Figure 3A). In the absence of Wnt ligands newly synthetized β-catenin accumulates in the cytosol and is phosphorylated by GSK3β. Phosphorylated β-catenin binds the APC-Axin destruction complex for degradation by the proteasome machinery**.** Upon Wnt/Fz interaction Dsh is phosphorylated and translocates to the plasma membrane (Rothbächer et al. 2000).

Phosphorylated Dsh recruits the APC-Axin destruction complex to the plasma membrane, thereby preventing destruction of β-catenin and resulting in its stabilisation and accumulation in the nucleus. Once in the nucleus, β-catenin interacts with the TCF/Lef transcription factor.

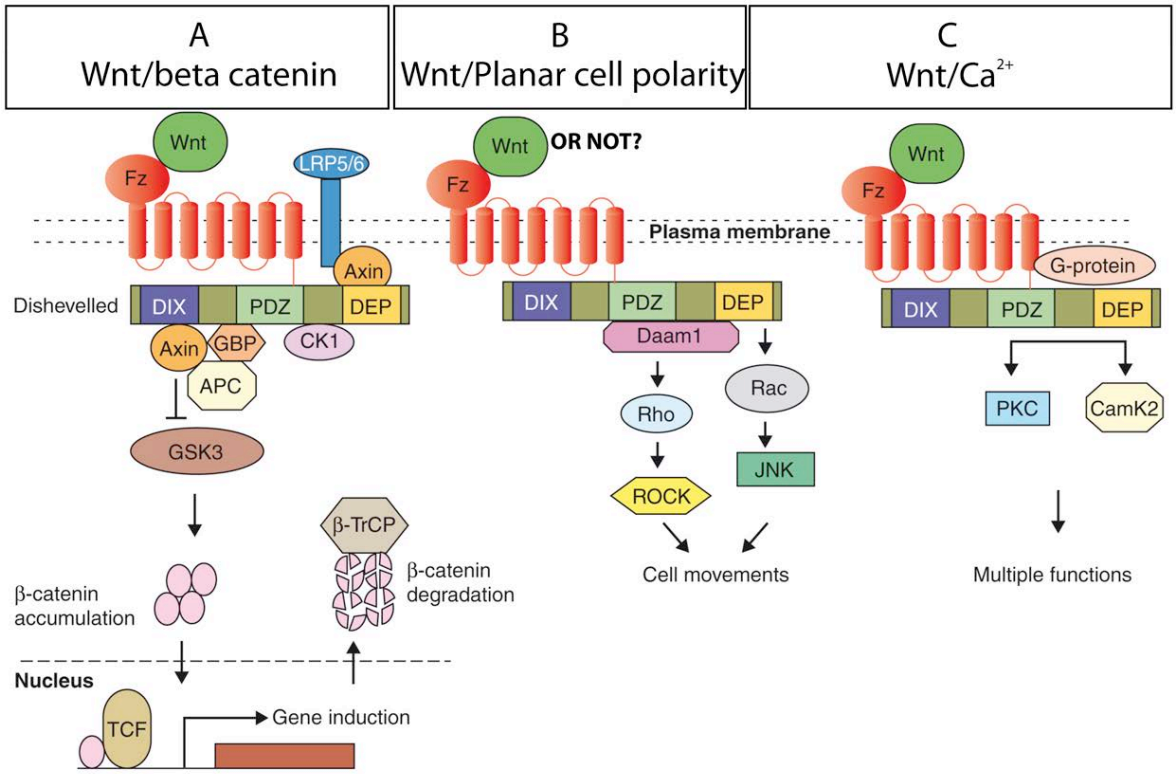

Figure 3: Wnt signalling pathways.
Diagram illustrating Wnt β-catenin dependent and independent signalling pathways.
A) The "canonical", β-catenin dependent pathway starts with the binding of the wnt ligands to the Frizzled (Fz) and LRP5/6 receptor complex. This complex induces the stabilisation of β-catenin *via* the bound protein Dishevelled (Dsh). Increased β-catenin stabilisation is accompanied by its translocation to the nucleus. In the nucleus, β-catenin bound to the transcriptional activator TCF/LEF induces the transcription of the genes normally suppressed by TCF/LEF in the absence of Wnt. In the absence of Wnt signalling, β-catenin associates with APC and AXIN in destruction complex.
B) Interactions between the Fz/PCP core components (Fz, Dsh, Strabismus and Prickle) to assure planar cell polarity do not require the Wnt ligand (see Figure 4). Wnt binding can, however, regulate downstream cell behaviours via the so-called Wnt-PCP pathway through Fz and Dsh, which activates the small GTPase RhoA and its effector ROK (Rho-associated kinase) in order to regulate the actin cytoskeleton. Another downstream effector of Dsh is JNK which can be activated by RhoA.
C) The Wnt-Ca^{2+} pathway is activated through wnt ligand binding to Fz receptors. Fz induces the activation of heterotrimeric G-proteins, which regulates calcium-calmodulin kinase 2 (CamK2) and protein kinase C (PKC). Modified from Habas & Dawid (2005).

In the Wnt-off state the TCF/Lef complex binds the transcription repressor Groucho, forming a repressive complex which blocks transcription of Wnt target genes. In the Wnt on state, Groucho is replaced by the β-catenin converting the TCF complex from a transcriptional repressor to a transcriptional activator.

The Wnt/β-catenin pathway can be negatively or positively stimulated by pharmacological treatments with molecules that target different components of the pathway, resulting in either its inhibition or activation. Commonly GSK3β has been targeted by treatments with LiCl or by paullone derivatives such as Alsterpaullone and BIO, resulting in artificial stabilisation of β-catenin and ectopic activation of the pathway.

1.6.2 The Wnt/ Planar cell polarity pathway

The use of the term "Wnt/PCP pathway" is rather confusing since Fz-mediated Planar Cell Polarity (PCP) does not necessarily involve Wnt. It was recently proposed to separate the effects mediated by the core components Fz, Dsh, Strabismus and Prickle into two pathways (Lapébie et al. 2011). One set of interactions termed Fz/PCP would coordinate planar cell polarity, while a second Wnt/Fz/Rho pathway involved in activating morphogenetic movements. These two pathways would act through different downstream modules.

- *Fz/PCP and tissue polarity*

In multicellular organisms, epithelial cells and other tissue sheets are not only polarized along the apicobasal axis, but also within the epithelial plane, a phenomenon known as planar cell polarity (PCP). In *Drosophila* PCP core components coordinate polarity between adjacent cells along the anterior-posterior axis of the embryo or the proximal-distal axis of the wings (Figure 4A). The PCP core components are Frizzled (Fz), Dishevelled (Dsh), the Lim domain protein Prickle (Pk), the four-pass-transmembrane protein Vang Gogh/Strabismus (Vang/Stbm), the ankyrin repeat protein Diego (Dgo) and the seven-pass-transmembrane atypical cadherin Flamingo/Starry night (Fmi/Stan) (Cho & Irvine 2004). One of the key features of this pathway is the asymmetric distribution of certain components between the two sides of the cell with respect to the direction of planar polarity. This asymmetrical distribution allows the propagation and coordination of the signalling from cell-to-cell (Figure 4B). The Stbm/Pk complex is localized on one side, while, Fz/Dsh/Dg complex is localised on the opposite side, such that Stbm and Fz interact extracellularly in neighbouring cells (Devenport 2014).

Fz/PCP was first described in the *Drosophila* adult wing to account for the polarity of

cuticular hairs and bristles that point towards the posterior pole (Gubb & Garcia-Bellido 1982) (Figure 4A). In vertebrates, PCP underlies the organisation and orientation of stereocilia in the sensory epithelium of the inner ear and the organisation of hair follicles (Figure 4A). PCP core components are extremely conserved throughout the animal kingdom. Their function in cilia orientation is conserved in hydrozoans, as is the case of *Clytia*. The *Clytia* Strabismus (Stbm) ortholog is required for the coordination of ectodermal cilia along the oral-aboral axis in the larva (Momose et al. 2012) (Figure 4A). Disrupting PCP in *Clytia* embryo by Stbm morpholino injection impairs cilia orientation.

- *Wnt/Fz/Rho: the Morphogenetic module*

In chordates the *Wnt/Fz/Rho* module has been shown to regulate different morphogenetic movements in the embryo, notably convergent extension in the so-called Keller explants.
The Keller explant is a piece of tissue including dorsal mesoderm and neural ectoderm from *Xenopus* early gastrula embryo. Two explants derived from two different embryos are cultured together. In wild type condition the neural ectoderm and the dorsal mesoderm undergo convergent extension (narrowing and elongating) forming a stereotyped morphology with two different domains (an elongated domain and a collar region interface). Keller explants are used to characterise the function of conserved heterologous proteins during gastrulation. Using this technique, it was shown that *Nematostella* Wnt5 and Wnt11 proteins impair convergent extension in *Xenopus* Keller explants (Rigo-Watermeier et al. 2012). Ectopic expression of *Nematostella* Wnt5 and Wnt11 induce opposite phenotypes. Wnt5 overexpression induces the formation of explants with a more elongating domain compared to the stereotyped morphology, whereas Wnt11 overexpression caused shorter explants, suggesting that these ligands affect cell convergent extension movements differently. It is not clear if Wnt5 and Wnt11 affect the establishment of the mesodermal cell polarity directly. Interestingly the overexpression of these two genes in *Xenopus* ventral blastomeres at the four-cell stage does not produce a secondary axis, unlike *Nematostella* Wnt1 overexpression. This suggests that Wnt5 and Wnt11 do not trigger the Wnt/β-catenin dependent pathway and that a β-catenin independent pathway was already present in the last common metazoan ancestor.

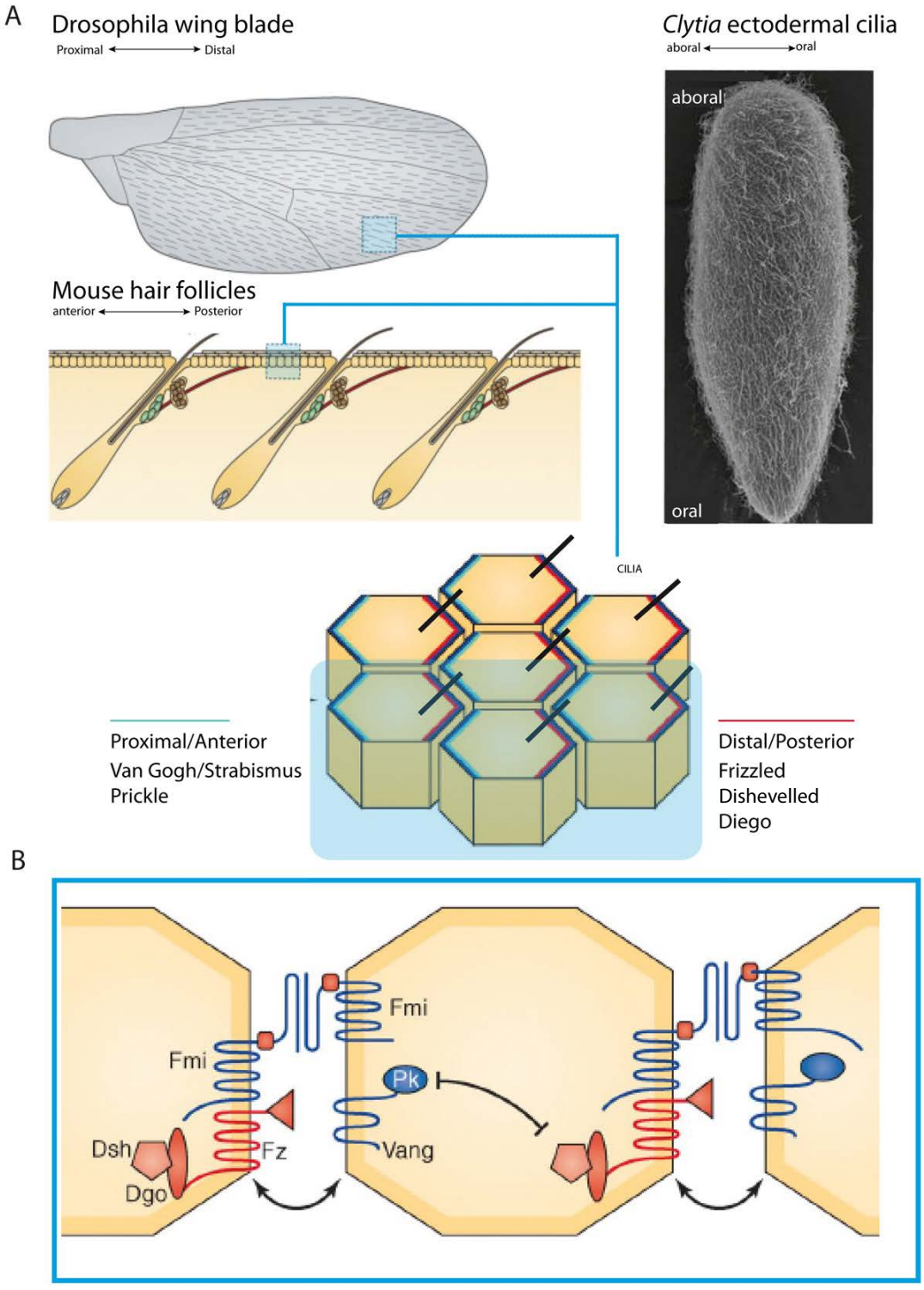

Figure 4: Planar cell polarity coordinates the orientation of cilia and hairs in metazoan tissues.
A) Examples of PCP coordination in the *Drosophila* wing blade, mammalian epidermis and *Clytia* planula ectodermal cilia. Cilia and hairs point in a single direction along the tissue axis, as indicated in the scheme. Ectodermal cilia in *Clytia* planula are oriented along the oral/aboral axis. Blue lines refer to a schematic illustrating that PCP components are localised at plasma membrane and are segregated along the epithelial plane. Red and green lines indicate the distribution of PCP core component at proximal/anterior to distal/posterior side. B) Asymmetrical distribution of PCP pathway components within neighbouring cells in the *Drosophila* wing blade. In blue Pk and Vang (Stbm) at anterior pole, in red Dg, Dsh and Fz localised at posterior side. Modified from Devenport (2014), Momose et al. (2012).

The Wnt/Fz/Rho module not only regulates morphognetic movements in vertebrates but also in cnidarians. In *Hydra* inhibition of JNK, one of the of the downstream elements of the Wnt/Fz/Rho module, by a chemical compound that specifically acts on JNK (not on p38 or ERK), impairs *Hydra* bud evagination (Philipp et al. 2009).In *Clytia*, it remains to be seen whether *Wnt/Fz/Rho* dependent movements, oriented by Fz/PCP, are responsible for elongation of the *Clytia* embryo during gastrulation, which is disrupted when Stbm is inhibited (Momose et al. 2012).

1.6.3 Developmental roles of Wnt/β- catenin pathway: Germ layers and body axis

Wnt/β-catenin signalling is widely deployed during early embryonic development to regulate germ layer formation and body axis (Clevers 2006; Amerongen & Nusse 2009), suggesting ancestral and highly conserved roles of this pathway. Wnt pathway *via* β-catenin stabilisation leads to endoderm/endomesoderm specification. This process has been demonstrated in a wide range of phyla including cnidarians, echinoderm, hemichordates and ascidians (Logan et al. 1999; Imai et al. 2000; Wikramanayake et al. 2003; Darras et al. 2011; Hudson et al. 2013). Studies in the solitary ascidians *Phallusia mammillata* and *Ciona intestinalis* revealed that the fate choice between endoderm and mesoderm is mediated through a β-catenin binary ON-OFF switch (Hudson et al. 2013). Hyperactivation or downregulation in isolated blastomere can convert the fate choice. For example it was shown that if an isolated blastomere retains an ON β-catenin state from 8 to 32 cell stage it will have an endoderm fate while in a OFF state the cell will give rise to the ectoderm (Hudson et al. 2013).

More widely discussed is the role of β-catenin nuclearisation as the key step in the establishment of the antero-posterior axis during bilaterian embryogenesis and the oral-aboral axis in non-bilaterian animals (Petersen & Reddien 2009; Marlow et al. 2013). During gastrulation β-catenin nuclearisation occurs and specifies oral-aboral identity, at the posterior pole in bilateria and the oral pole in cnidarians (Figure 5A). This correlation suggests that regionalised nuclear localisation of the β-catenin to establish embryo polarity was already a feature of embryogenesis in the common ancestor of metazoans.

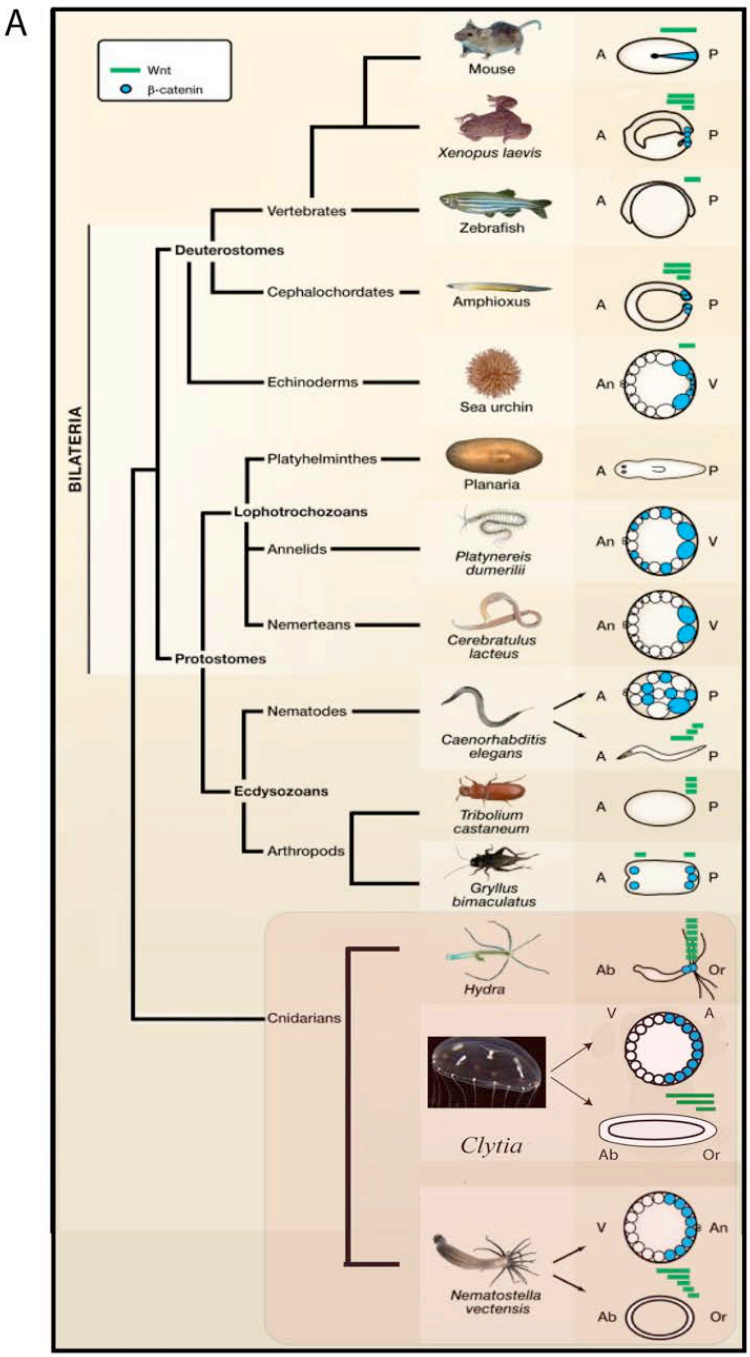

Figure 5: Embryonic axis and Wnt/β-catenin signalling.
A) Comparison of the axial localisation of Wnt transcripts and β-catenin nuclearisation in metazoans. Wnt expression domains are represented with green lines, while β-catenin localisation is illustrated with sky blue dots.
In cnidarians *Hydra, Clytia* and *Nematostella* (shaded in red), β-catenin nuclearisation occurs at the oral pole. (Modified from Petersen & Reddien 2009).

B) Model of axis determination in *Clytia*. Wnt/β-catenin pathway core components are distributed asymmetrically in the egg. On the animal side *Wnt3* mRNA (in red), *Fz1* mRNA (in green); on the vegetal side Fz3 mRNA (in blue). In *Clytia* embryos, β-catenin nuclearisation is restricted to the animal side and coincides with Wnt3 and Fz1 activity. Wnt3 and Fz1 *via* β-catenin drive the establishment of the oral identity. In contrast *Fz3* on the aboral side inhibits β-catenin localisation. From Momose et al. (2008).

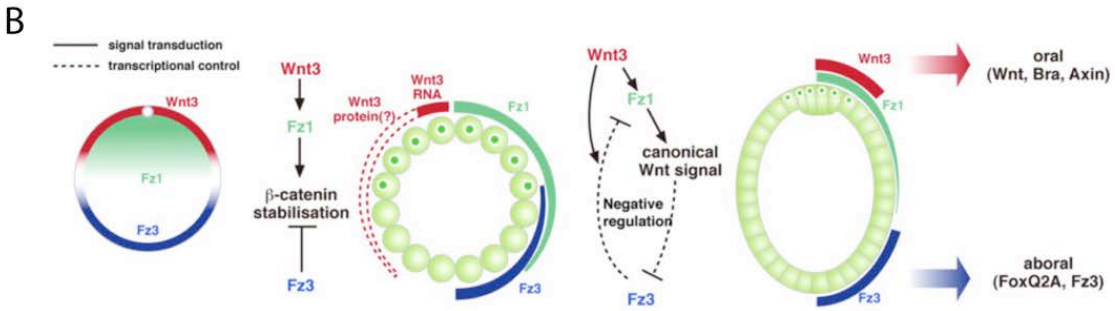

- *Wnt signalling in Cnidarians*

Genome and transcriptome analyses in cnidarian species have identified all the core components of Wnt and Fz/PCP signalling pathways, including Wnt ligands and Fz receptors (Kusserow et al. 2005; Guder et al. 2006; Lee et al. 2006). In cnidarians Wnt/β-catenin signalling has a key role in regulating axis formation, as well as other features of embryonic patterning, notably germ layer formation. This regulation of the cnidarian oral-aboral axis by Wnt signalling continues throughout the life cycle. In the anthozoan *Nematostella vectensis,* pharmacological activation of the Wnt/β-catenin pathway during development induces ectopic endoderm formation (Wikramanayake et al. 2003; Röttinger et al. 2012) while β-catenin knockdown, by morpholino injection into 1 cell stage embryos prevents endoderm formation and gastrulation (Leclère et. al under revision). Similarly in *Clytia,* downregulation of Wnt3 *(*to abolish β-catenin stabilisation) severely delays gastrulation, although endoderm formation recovers by the larva stage.

In *Hydra* and in *Hydractinia* polyps, hyperactivation of Wnt signalling, *via* pharmacological stabilisation of GSK3b, induces ectopic "oral identity" in the polyp body column (Hobmayer et al. 2000; Broun et al. 2005; Muller et al. 2007). Furthermore the transplantation of pieces of the "oralised" body column into a wild type polyps induce the formation of a second axis (Broun et al. 2005).

In *Clytia* developing embryos *Wnt3* ligand is expressed on the future oral side, derived from the egg animal pole along with the Frizzled receptor, *Fz1*, while a second Frizzled, *Fz3* is expressed at the opposite pole, (Figure 5B). Wnt β-catenin signalling through Fz1 specifies oral identity, while Fz3 acts as a Wnt/β-catenin pathway inhibitor and determines the aboral identity (Figure 5B). *Wnt3* is expressed earlier than any other Wnt ligand during *Clytia* embryogenesis, although 4 other ligands are later expressed in nested domains in the oral ectoderm (Momose et al. 2008). Moreover Wnt3 disruption *via* morpholino injections abolishes the expression of the other Wnt ligands consistent with its predominant role in axis formation. In *Clytia* that Wnt/β-catenin *(via* Wnt3) thus controls aboral-axis determination but is not essential for endodermal formation (Momose et al. 2008).

1.6.4 Wnt/β-catenin signalling and stem cell regulation

Wnt/β-catenin signalling not only specifies the anterior-posterior axis in many metazoan species (Petersen & Reddien 2009) but also has other developmental roles including the regulation of stem cell dynamics. Within different stem cell systems (*e.g.* hematopoietic, intestinal stem cell system), Wnt signalling has been found to act to maintain tissue cell homeostasis by the regulation of cell proliferation and differentiation, promoting lineage specification and maintaining a pluripotency state (Sokol 2011, Nusse et al. 2008).

One of the well-studied systems in which Wnt/β-catenin signalling controls cell homeostasis by regulating cell proliferation and differentiation is the mouse crypt-villus axis in the intestinal stem cell system. At the base of the villi are small invaginations termed crypts, which represent the functional unit of the intestinal epithelium. Stem cells of the crypt-villus system are located at the bottom of each crypt. These cells divide and produce transit-amplifying progenitors that will finally differentiate in the villus. In contrast Paneth cells, which are differentiated cells that control the intestinal microbial environment, are located below the stem cells. Wnt signalling can promote both the proliferation of the stem cell and the differentiation of the Paneth cells. In vivo studies using mouse transgenic lines showed that abolition of Wnt/β-catenin signalling has dramatic effects on the crypt compartments. Mice mutants lacking the transcription factor TCF4 show complete depletion of the crypt stem cells (Pinto et al. 2003), while the hyperactivation of Wnt/β-catenin promotes *de novo* formation of the Paneth cells (Andreu et al. 2008).

Wnt/β-catenin also controls neuronal lineage specification from neural crest cells. During the development of the vertebrate nervous system, neural crest cells generate peripheral nervous system neurons and several non-neural derivatives such as melanocytes (Dorsky et al. 2000). The activation of the β-catenin pathway in neural crest cells promotes neural fate specification, such that ablation of the β-catenin gene in mouse neural crest cells causes the loss of sensory cells and melanocytes (Hari et al. 2002). Conversely when β-catenin is constitutively activated the number of neural crest derivatives increases.

Going back to a stem cell system, Wnt/β-catenin signalling has been proposed to maintain self-renewal and pluripotency in mouse and human ES cells (Sato et al. 2004). The pharmacological hyperactivation of the Wnt/β-catenin pathway in ES cells promotes a state of pluripotency as suggested by morphological and molecular markers (*i.e.* increased levels of the pluripotent stem cell marker Oct3/4, as described in Introduction section 1.4).

The role of Wnt/β-catenin in stem cell regulation is not restricted to vertebrates. Studies on i-cells, in hydrozoans indicate that the Wnt/β-catenin pathway regulates the i-cells differentiation (Teo et al. 2006; Khalturin et al. 2007). In *Hydra* and in *Hydractinia* adult polyps, increasing Wnt/β-catenin signalling, *via* GSK3 inhibition induces ectopic differentiation of the nematocytes and nerve cells (only in *Hydractinia*). In *Hydra* the activation of Wnt/β-catenin, promotes the ectopic differentiation of the nematoblasts (see Introdution section 2.3.3). In *Hydra* activation of Wnt/β-catenin promotes the supernumerary differentiation of nematoblasts (see Introduction section 2.3.3). In *Hydractinia* nematogenesis is also stimulated, and it appears that pharmacological stabilisation of Wnt/β-catenin first causes a transient increase in proliferating cells as shown by BrdU labelling assays, followed by an increase in the number of differentiated nerve cells and nematocytes.

How are the functions of Wnt signalling in regulating body axis formation and maintenance, germ layer segregation, stem cell multipotency and fate commitment related and coordinated? This remains an important question to address.

2) Cnidarian models in developmental biology

Most studies in developmental biology involve a relatively small number of "model" organisms such as mouse, *C. elegans, Drosophila* and *Xenopus.* These are not sufficient to represent the wide diversity of life. It is becoming increasingly apparent that organisms outside these classical laboratory systems can make important contributions to understanding biological processes both evolutionary conserved and unique to particular animal groups.

In the last decade or so, the analysis of the increasing amount of genome and transcriptome data collected from non-conventional model species has revealed that most of the components of key signalling pathways involved in the regulation of fundamental developmental and cellular mechanisms are highly conserved across metazoans. For example genome analysis of the sponge *Amphimedon queenslandica* revealed the conservation of several gene families involved in fundamental mechanisms such as cell adhesion, body plan specification, and cell type differentiation (Srivastava et al. 2010).

More specifically in cnidarians, a large and diverse phylum positioned as sister group to the main animal clade of Bilateria (Figure 6), genome sequences analysis has revealed that their genomes share from many gene families with bilaterians (Putnam et al. 2007; Chapman et al. 2010; Hwang et al. 2007; Soza-Ried et al. 2010), even though cnidarians differ from bilaterian animals by the lack of key features such as mesoderm and a central nervous system. Cnidarians possess a "complete" Wnt gene repertoire (Lee et al. 2006; Kusserow et al. 2005) whose function in the establishment of the embryonic axis seems to be conserved as discussed above (see Introduction section 1.6.3).

Interest in using cnidarians as experimental models in developmental biology has grown, partly because of their morphological simplicity, high regenerative capabilities, and phylogenetic position but also because of their ontogenic plasticity. For example some cnidarians can rest in low metabolic states to survive a critical period, while in particular circumstances such as after an injury they can reactivate genetic cell proliferation and morphogenesis (Boero et al. 1992; Piraino et al. 2004). The addition of genomic data in recent years provides an opportunity to study these processes at molecular level in cnidarians.

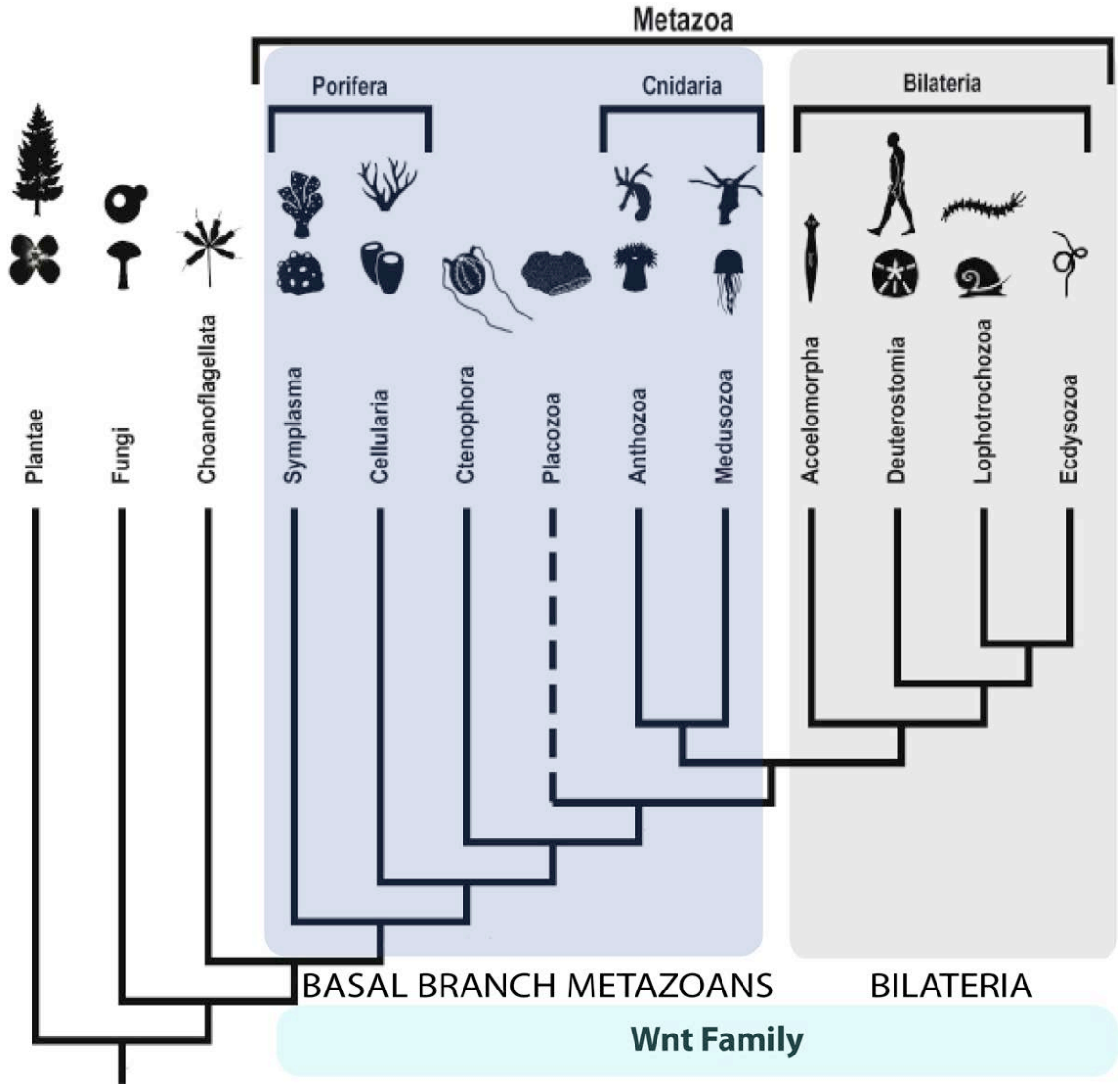

Figure 6: One hypothesis for the phylogenetic relationships between major metazoan clades.
Metazoan phylogenetic tree showing in light grey the Bilateria clade and in light blue the "basal branching" metazoans. Some of the topology is controversial but most recent studies agree that Cnidaria is the sister group to all bilaterinas. Cnidaria possess most of the key family genes involved in developmental mechanism, including a family of about 12 Wnt family genes.Modified from Ryan & Baxevanis (2007).

Cnidarians are subdivided in to two classes Anthozoa and Medusozoa (Figure 7A). The Medusozoa traditionally are split in four classes: Hydrozoa, Cubozoa, Scyphozoa, and Staurozoa. The Anthozoa (including sea anemones and corals), usually have larval and benthic polyp forms, the Medusozoa ancestrally have larvae, benthic polyps and free-swimming jellyfishes in their life cycles.

Cnidarians generally exhibit only one single body axis, the oral-aboral axis, with two germ layers (diploblastic): endoderm and ectoderm and are radially symmetric. However among

cnidarians some anthozoans possess a second body axis orthogonal to the oral aboral axis (directive axis) imparting bilateral symmetry (Figure 7B). In *Nematostella* the directive axis is defined by a plane that cuts symmetrically the mouth, the pharynx, the siphonoglyph and the retractor muscles.

Several cnidarian species have now been established as experimental models allowing gene function studies in developmental biology, notably *Nematostella* (Darling et al. 2005), *Hydra* (Galliot 2012) and *Hydractinia* (Plickerk et al. 2012) (Figure 7C) as well as less experimentally amenable species such as *Podocoryne* (Galliot and Schmid 2002) and *Acropora* (Ball et al. 2002). They have provided important insights into evolutionary questions such as the correspondence between the oral-aboral axis of Cnidaria and the anterior-posterior axis of Bilateria (Sinigaglia et al. 2013; Hobmayer et al. 2000), and the homology between the vertebrates striated muscle and the muscle of the medusa (Steinmetz et al. 2012). They have also been employed to address particular biology processes such as cell proliferation, differentiation (David 2012), and trans-differentiation (Schmid et al. 1982).

The hydrozoan *Clytia hemisphaerica* is a useful addition to these existing cnidarian models (Houliston et al. 2010), particularly to address developmental questions given the easy access to all embryonic stages, gonads and oocytes ,and regeneration questions, since the *Clytia* medusa displays whole body regeneration. Moreover *Clytia* embryos, larvae, polyps and jellyfishes are very robust, easy to handle and transparent. The time required to complete the full life cycle is relatively short (around three months) and *Clytia* is easily kept in laboratory conditions, where spawning can be experimentally controlled by light after a period of darkness (Houliston et al. 2010).

2.1 Clytia life cycle and development

Clytia is also known by other names including *Phialidium* and *Campanularia*. This confusion is due in part to the existence of multiple life stages, such that *Clytia* polyps and jellyfishes were not initially recognised as alternative forms of the same species.

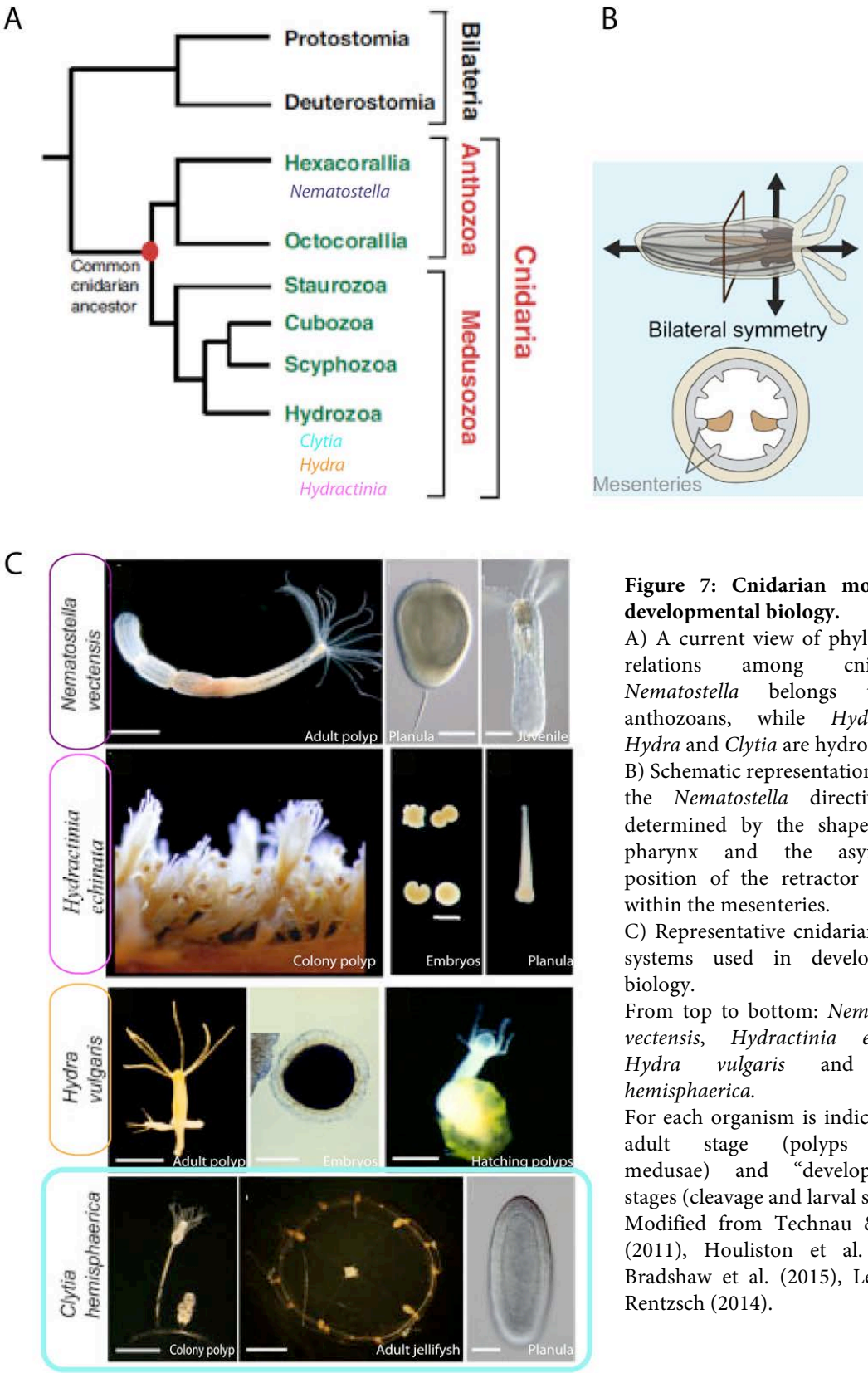

Figure 7: Cnidarian models in developmental biology.
A) A current view of phylogenetic relations among cnidarians. *Nematostella* belongs to the anthozoans, while *Hydractinia*, *Hydra* and *Clytia* are hydrozoans.
B) Schematic representation of the *Nematostella* directive axis determined by the shape of the pharynx and the asymmetric position of the retractor muscles within the mesenteries.
C) Representative cnidarian model systems used in developmental biology.
From top to bottom: *Nematostella vectensis*, *Hydractinia echinata*, *Hydra vulgaris* and *Clytia hemisphaerica*.
For each organism is indicated the adult stage (polyps and/or medusae) and "developmental" stages (cleavage and larval stages).
Modified from Technau & Steele (2011), Houliston et al. (2010), Bradshaw et al. (2015), Leclère & Rentzsch (2014).

Historically the polyp was named *Clytia (*Linnaeus 1767*)* and the medusa was named *Phialidium (*Leuckart 1856*). Clytia* has a tri-phasic life cycle: the free-swimming jellyfish, the larva and the polyp colony (Figure 8). Male and female adult *Clytia* have separate sexes (Figure 8b-c). Medusae spawn daily following a light-dark cycle, with a short light stimulus being sufficient to trigger oocyte maturation after 2 hours of darkness (Amiel et al. 2010). Following fertilisation, the egg (Figure 8d) develops into a planula larva (Figure 8e), which after 3 days is able to settle down onto a substrate and metamorphose to give rise to a colony of polyps.

In natural conditions, metamorphosis is induced by a bacterial film, so in sterile seawater planulae will not metamorphose. In laboratory conditions metamorphosis can be induced efficiently by GLWamide neuropeptides. GLWamides were first identified as metamorphosis inducing factors in the hydrozoan *Hydractinia* with the name metamorphosine A (Leitz et al.1994). *Clytia* undergoes very dramatic metamorphosis. The aboral pole of the planula attaches to the substrate and there is subsequently complete loss of larval structures before the polyp forms. The first structure to form is the primary polyp, which is the founder of the polyp colony (Figure 8f). It has been shown that cells from the oral pole of the larva contribute to the hypostome (mouth) of the primary feeding polyp (Freeman 1981b). Once it starts feeding, the primary polyp propagates vegetatively by extending stolons out across the seabed or other substrate. The mature colony is polymorphic with a connected system of feeding gastrozoid polyps (Figure 8h) and gonozoid polyps (Figure 8i) specialised for the budding of new baby medusae (Figure 8j). Gastrozoids produce new medusae clonally, and so laboratory medusae produced from a single colony are genetically identical. This is particularly advantageous for genetic studies, since polymorphism is highly reduced. In our laboratory most experiments have now been performed for over 10 years using 2 or 3 individual genotypes obtained from the same 'immortal' colonies. In collaboration with R. Copley (LBDV), M. Manuel's laboratory (UPMC Jussieu) and the Genoscope (Evry), the *Clytia* genome has been sequenced, assembled and is currently undergoing annotation (publication in preparation). An extensive *Clytia* transcriptome data set published last year (Lapébie et al. 2014) (see Result - II) is available on the Compagen web site, which is comparative genomic platform for early branching metazoans (www.compagen.org). A library containing about 8000 unique fully sequences cDNA sequences corresponding to about 90,000 ESTs is also available. Current

work in the laboratory is generating, using Illumina Seq technologies, further transcriptomic data to cover particular life stages or tissues (not published). These bioinformatics resources will be available in the near future to analyse gene expression profiles throughout the life cycle.

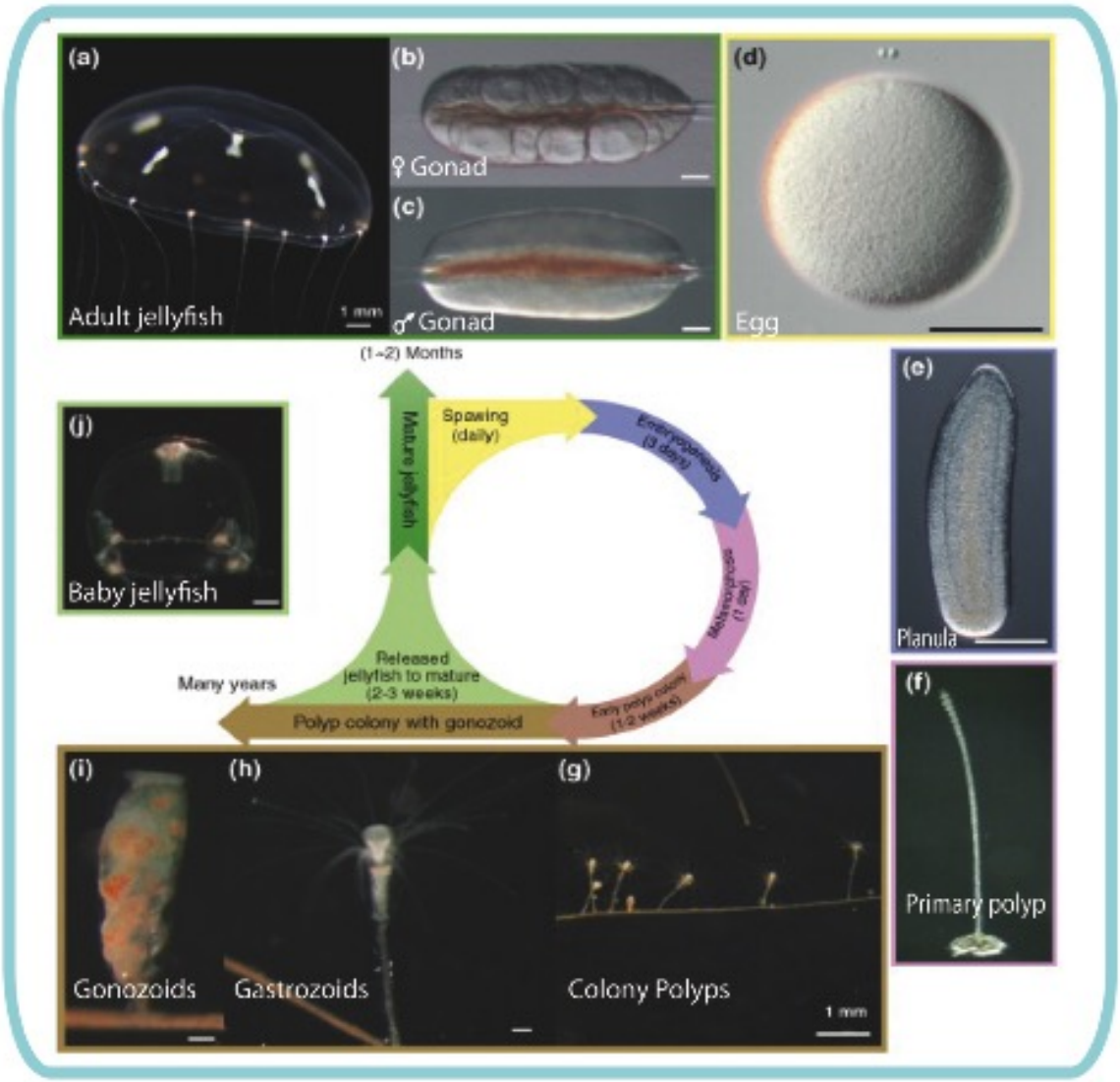

Figure 8: Clytia life cycle.
Clytia adult medusa (a) spawn daily after a short light stimulus. Female and male medusa release unfertilised eggs and sperm in the water (female and male gonads b-c). Following the external fecondation, the fertilised eggs cleave after 1 hour. Embryonic development generates the larval stage, about 48 hours post fertilisation at 18°C (d). The3-4 day old planula larva metamorphoses into a primary polyp (f) that is the founder of the polyp colony (g). The colony first develops the gastrozoids (h) that are the feeding zooids. Later, gonozoids, form that bud and release baby immature jellyfishes (j). Released baby jellyfishes are 1-3 mm in diameter and grow by feeding to become sexually mature after about 2-3 weeks in laboratory conditions, reaching a maximum size of 1-2 cm (a). Scale bar 1mm for adult jellyfishes and polyps, 100µm for the other stages.
Modified from Houliston et al. (2010).

2.1.1 *Clytia* embryogenesis and larval development

Clytia eggs are transparent and measure between 150 and 180 μm in diameter (Figure 8d). First cleavage is unipolar and occurs 50-60 minutes after fertilisation (Figure 9A). In hydrozoans the initiation site of the first cleavage coincides with the region of the egg that extruded the polar bodies (the animal pole), and later the site of cell ingression during gastrulation and the future oral pole of the larva (Freeman 1981a) (Figure 9A).

For experimental reproducibility we control the timing of developmental events in *Clytia* in the laboratory by maintaining a constant temperature (18-20^{0}C). During the first six hours of development at 18°C, a series of divisions, produces a single cell-layered blastula, covered by cilia for swimming, prior to the onset of gastrulation (Figure 9A). At 18°C Gastrulation starts, 10 hours post fertilization (hpf) by unipolar cell ingression at oral pole (Byrum 2001) (Figure 9A). Endodermal cells and *Piwi*/*Nanos1* positive-i-cells ingress to enter the cavity of the gastrula. Therefore a mixed population of cells that can be found inside the gastrula. Some of these cells will contribute to the endoderm (*i.e. FoxB* expressing cells), while others are founders of the i-cell lineage. After 24hpf, gastrulation is complete and planula larva elongates along the oral-aboral axis (Figure 9A), but endoderm is still not differentiated. Except at the mid-gastrula stage, embryos and planulae show a strong ability to re-pattern along the oral-aboral axis; when cut into presumptive oral and aboral halves they are able to reform well-patterned mini-larvae (Freeman 1981b). At 48hpf, ectoderm and endoderm are fully formed and are separated by a thin acellular mesoglea (Figure 9A-B). The ectodermal cells are ciliated and ectodermal cilia are oriented along the oral-aboral axis to drive the directional swimming towards the aboral pole, (Momose et al. 2012). At 48hpf planula stage the ectodermal layer shows the presence of several differentiated cell types: nematocytes, nerve cells and gland cells. In contrast, the endoderm hosts a population of endodermal gland cells and the multipotent i-cells stem cells (Figure 9B).

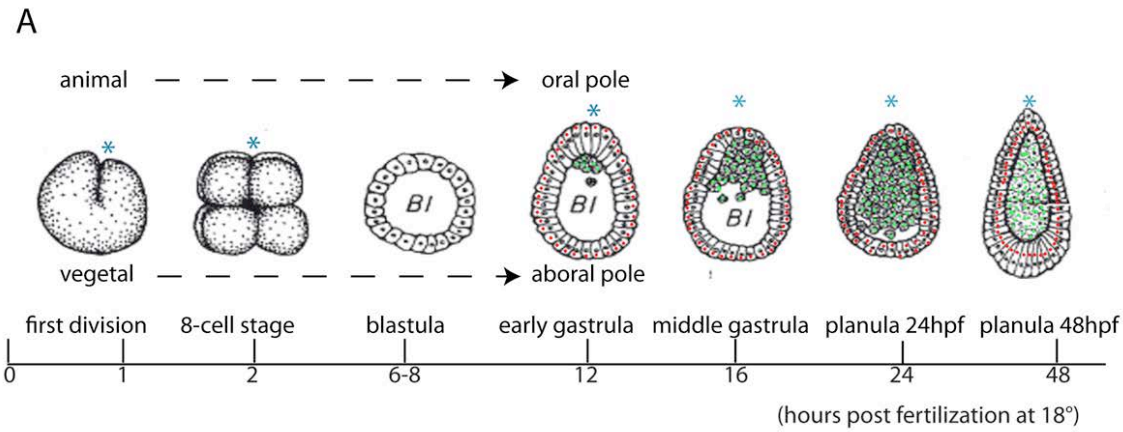

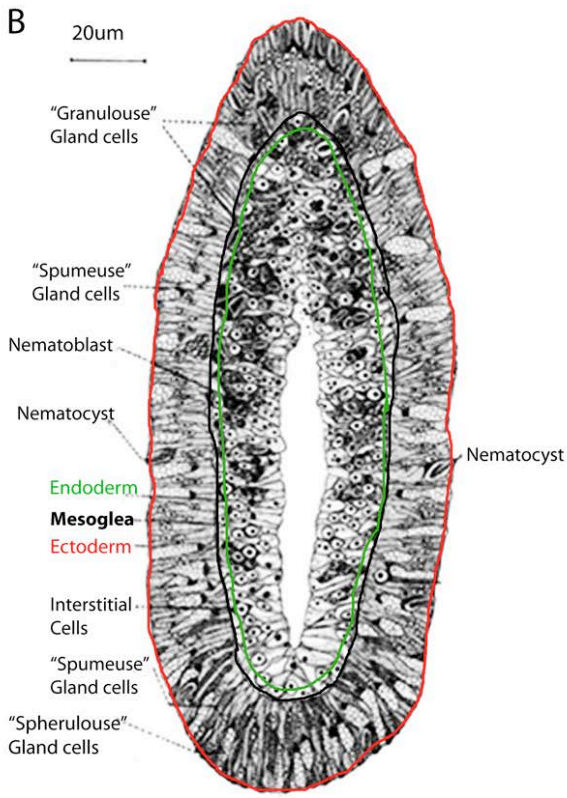

Figure 9: *Clytia* embryonic development.
A) Schematic illustration showing *Clytia* embryonic development. The site of the first cleavage, which is unipolar, corresponds to the oral pole of the planula (blue asterisks). After 6 hours, the embryo reaches the blastula stage. In some blastulae at this stage it possible to visualise the animal pole thanks to a deep cleft between the two lobes. At the early gastrula stage it is possible to recognise the first sign of polarity. Embryos acquire an ellipsoid shape and the cells are more elongated. At 24hpf gastrulation is complete, however presumptive endoderm is not yet differentiated (green cells). At 48hpf ectoderm (red cells) and endoderm (green cells) are well formed and the larva shows the typical torpedo shape. The line represent the developmental time in hours at 18°C.
Modified from Freeman (1981b).
B) Longitudinal section of a "late differentiated planula" (>48hpf). At this stage all the differentiated somatic cells are present as indicated by labels. Endoderm in green, ectoderm in red, mesoglea in black.
Modified from Bodo & Bouillon (1968).

2.1.2 *Clytia* medusa anatomy

The *Clytia* medusa is a small transparent jellyfish of about 1cm in diameter, with a laboratory life span of 2 to 3 months. The main anatomical feature of the jellyfish is the

bell-shaped umbrella (Figure 10A). The umbrella is convex above (exumbrella) and concave below (subumbrella) with the medusa manubrium and the mouth centrally positioned. The mouth has a single, cross-shaped opening connected to a large internal cavity that expands to form a simple stomach (Figure 10A). From the stomach four radial canals extend to the margin of the bell where tentacles are attached. The regions where the tentacles grow are defined as tentacle bulbs (Figure 10B). The tentacle bulbs are highly proliferative regions. *Clytia* gonads, the sexual organs of the medusa, are attached to the subumbrellar side of the umbrella on each of the four radial canals. Sensory organs are present in the form of simple statocysts (balance organs) located between tentacle insertion points. Two condensed nerve rings run around the periphery of the umbrella: one (outer ring) organised for integrating sensory inputs and the other (inner ring) for coordinating motor responses (Satterlie 2002) (Figure 10A). A diffuse nerve net runs through the subumbrella layer, which includes fast-contracting circular muscles for swimming, and the manubrium.

2.2 Hydrozoan cell types

Hydrozoans possess a relatively limited number of cell types compared to bilaterian animals. Medusae and larvae share to a large extent the same cellular components that will be described in the next section. The hydrozoan planula possesses two germ layers, the endoderm comprising endodermal gland cells, and endodermal epithelial cells, and the ectoderm include ectodermal epithelial cells, nerve cells, nematocytes and gland cells.
I-cells are distinct from any germ layers and migrate between the two depending on stage and structure, but in larval stages are located among the endodermal cells.

2.2.1 I-cells: a hydrozoan multipotent stem cell system

I-cells are migratory cells without any particular morphological distinctive feature such as neural processes or polarised granules. They are capable of generating daughter cells with the same potential as the mother cells, have unlimited proliferation potential and are able to produce differentiated functional progenies. Therefore i-cells can clearly be considered

to be a hydrozoan stem cell population. They have the particularity of being able to give rise to both somatic cell types and gametes (Figure 11A) (Bosch & David 1987; Bode 1996).

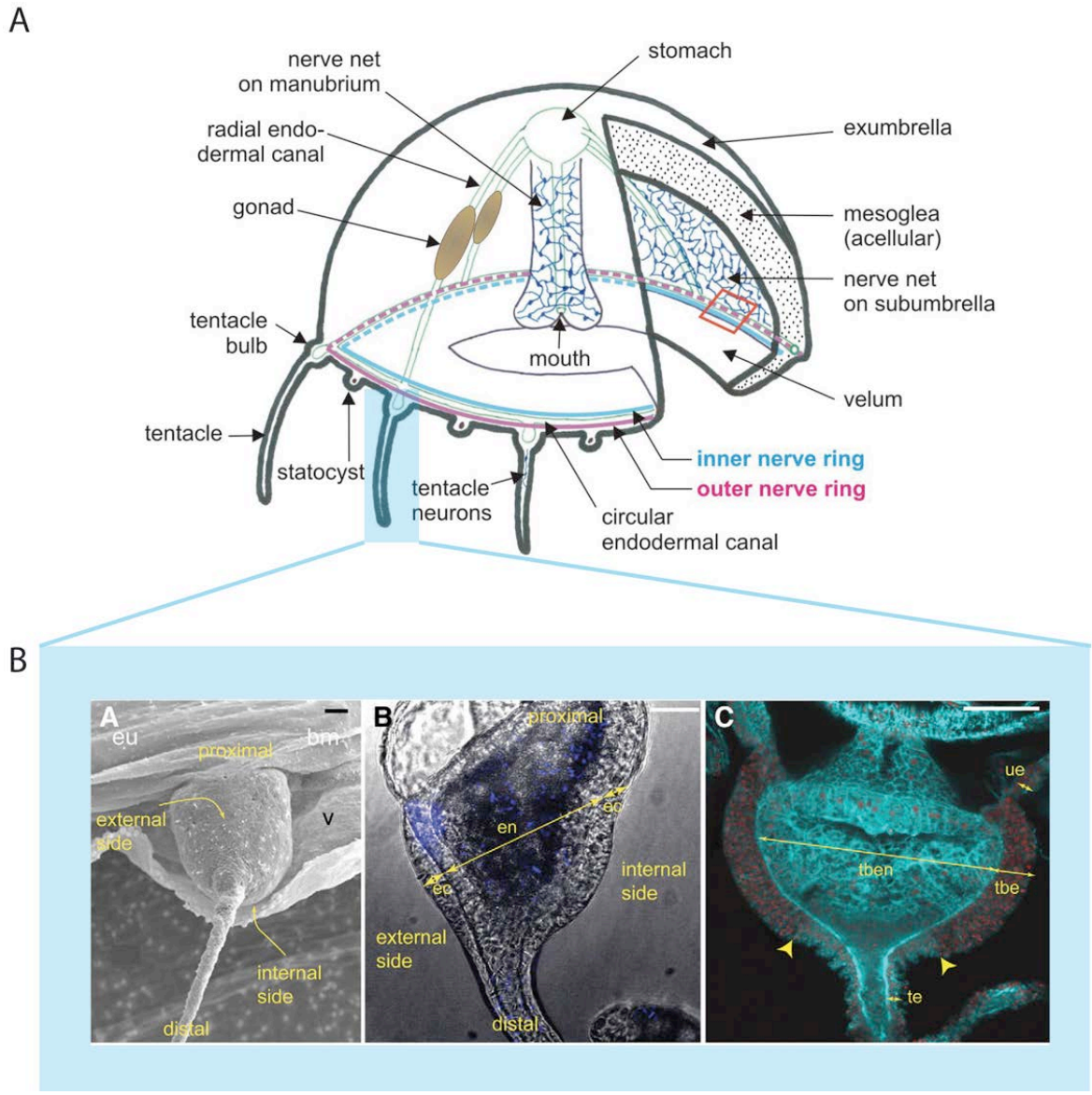

Figure 10: *Clytia* anatomy.
A) *Clytia* anatomical features The exumbrella and subumbrella are separated by a thick mesoglea. The nervous system includes a diffuse nerve net in the subumbrella region and in the manubrium, as well as inner and out nerve rings that run around the bell margin. From the stomach 4 radial canals extend to the bell margin. Each radial canal hosts one of the 4 gonads. B) Morphology of *Clytia* tentacles and tentacle bulbs (TBs). From left to right electronic microscopy picture of TB showing the site of the attachment to the bell margin; DIC image showing the internal cavity of the TB; Confocal optical section of an isolated TB stained with DAPI to visualise nuclei (red) and Phalloidin for cell contours (cyan). Scale bar 25µm. From Houliston et al (2010), Denker et al. (2008).

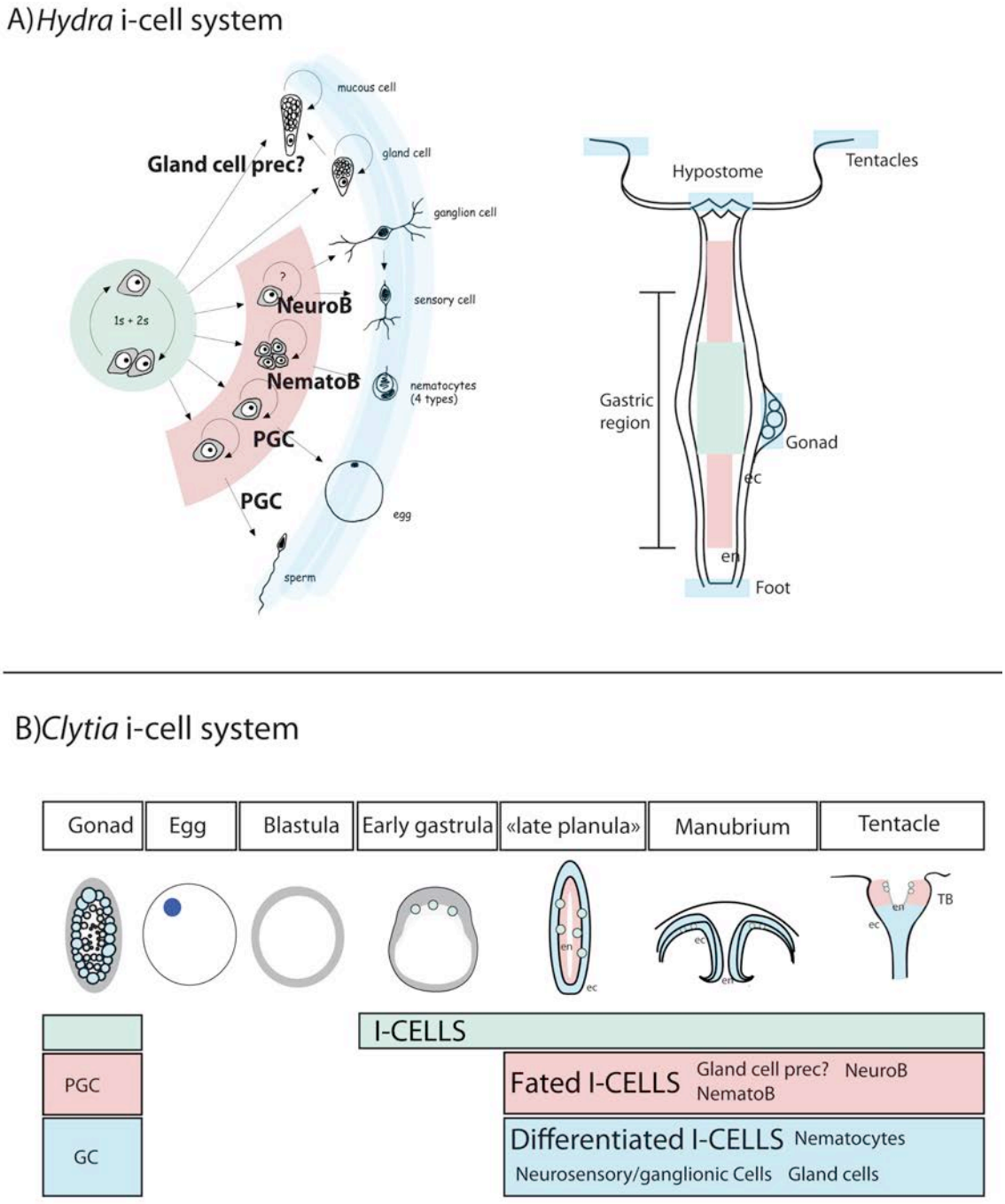

Figure 11: I-cell and i-cell derivatives in the *Hydra* polyps and in *Clytia* developmental stages and adult.
A) *Hydra* i-cell. Multipotent i-cell (green) give rise to all somatic progenitor (pink) and germ cell precursor (pink). All the progenitors differentiate producing mature cell types (sky blue). Prec: precursor, NeuroB: neuroblast, NematoB: nematoblast, PGC: germ cell precursor. In *Hydra* multipotent cell (green) are localised mostly in the gastric region in the interstitial spaces between the epithelial cells, differentiating cell are disperse throughout the *Hydra* body in the endodermal region (pink) while differentiated cells (sky blue) are mostly localised in the ectoderm layer at body extremities (tentacles, foot, hypostome). ec: ectoderm, en: endodermModified from Hobmayer et al. (2012).
B) *Clytia* i-cell. In *Clytia* i-cell are distinguishable, from a morphological point of view at early gastrula stage (green line). In adult stage the known site of i-cell localisation are the proximal part of the tentacle bulbs, the base of the manubrium and the gonads. Fated cell (pink line) have been characterised in the planula endoderm and in the medusa. Comparable to *Hydra* differentiated cells are located in the ectodermal layer, however mature gland cells are localised in both layer ectoderm and endoderm. ec: ectoderm; en: endoderm; TB: tentacle bulbs.

I-cells have been found exclusively in hydrozoans. Currently there is no evidence for the presence of this cell type, either in other medusozoan classes or in anthozoans . However the presence of multipotent stem cells in other cnidarians cannot be excluded. Several studies suggest that the amebocyte cells might be putative stem cells in anthozoans (Gold and Jacobs 2012).

August Weismann in 1883 was the first to detect the i-cells during his morphological studies on the *Hydractinia* adult polyps (Weismann A 1883). Weismann termed these cells *Stammzellen*, to illustrate their ability to generate committed progenitors (germ cells). Later i-cells were described in *Hydra* adult polyps, as small cell (5-6 μm diameter) with a round or spindle shape, large nucleus, a dense cytoplasm filled with ribosomes, few mitochondria, a small Golgi apparatus, and little endoplasmic reticulum (Lentz 1965). These morphological characteristics are common to all hydrozoans i-cells described so far.

A large part of the current extensive knowledge of i-cell biology and more generally of hydrozoan cell types derives from studies performed in *Hydra* and *Hydractinia*. Therefore I will first give a short introduction on i-cell distribution and molecular signatures in *Hydra* and in *Hydractinia*, followed by a more detailed description of what is known in *Clytia*.

I–cells localisation and molecular signature

- *Hydra and Hydractinia*

In *Hydra* adult polyps, i-cells are found in the gastric region between endodermal and ectodermal interstices (Figure11A). Within the i-cell population it is possible to distinguish two sub-populations: large and small i-cells. The large i-cells, found alone or in pairs, are referred to as true multipotent stem cells, while the small i-cells represent fate-committed i-cell populations, as shown for germ cells precursors (David & Plotnick 1980; Nishimiya-Fujisawa & Kobayashi 2012). Multipotent i-cells reside constantly in the body column, which can be considered to represent a stem cell niche. Even though several studies have addressed the structural details of the *Hydra* stem cell niche (Bosch et al. 2010, Bosch 2009b), at present little functional data is available to support the hypothesis that an "environmental" signal controls extrinsic or intrinsic cell program (see Introduction 1.3.1 and 1.3.2 sections of the Introduction). In contrast to the i-cell population, i-cell derivatives mainly reside at the body extremities (head and foot) (Figure 11A).

In *Hydractinia,* i-cells appear at early gastrula stage during development (Plickert et al. 1988; Frank et al. 2009). In the planula, they are located in the endoderm and some of them translocate through the mesoglea and migrate to the ectoderm. In the polyps, i-cells are mainly located in the stolonal compartment where they generate all the derivatives (Frank et al. 2009).

From a molecular point of view, i-cells, in both *Hydra* and *Hydractinia* express the germ cell/stem cell markers *Nanos* and *Piwi* (see section 1.5). In *Hydra* two Nanos gene paralog and the two *Piwi* paralog *Hywi* and *Hyli* are expressed both in multipotent i-cells and in committed i-cells, (Mochizuki et al. 2000, Nishimiya-Fujisawa & Kobayashi 2012). In *Hydractinia Nanos1* is female specific and is not detectable during development while *Nanos2* is maternally expressed in a germ plasm like structure, in the future oral pole (Kanska and Frank 2013; Plickert et al 2012).

In the less studied system *Podocoryne carnea, Piwi* transcripts have been detected throughout the life cycle in somatic and in germ line cells (Seipel et al. 2004).

Recently the expression pattern of *Nanos* and *Piwi* genes has been reported in Siphonophores, which are colonial hydrozoans. *Nanos* and *Piwi* positive cells were identified in the growth zone of the colony and in the female and male gonads (Siebert et al. 2014), showing again expression in germ cells and in somatic cells as for the other hydrozoans.

- *Clytia*

In the course of *Clytia* development, i-cells can be identified morphologically during gastrulation in ingressing cells in the oral region and then dispersed in the central core of the planula endoderm (Bodo et Bouillon 1968) (Figure 8B, 11B). Presumptive i-cell derived somatic cell types (ganglion cells, nematocytes, gland cells) are distributed in the late planula ectoderm and endoderm layers.

As in *Hydra* and *Hydractinia*, *Clytia* i-cells express *Nanos1, Piwi, Vasa, Nanos2 and PL10 genes* (Leclère et al. 2012). In this study I will focus on *Nanos1* and *Piwi*. In *Clytia* these genes are expressed throughout the life cycle (Figure 12A-B). Both genes are expressed maternally and the maternal mRNAs are localised within the egg in a "germ plasm-like" region surrounding the egg pronucleus. Transcripts of both genes are detected at cells located at the animal pole at the blastula stage and in ingressing cells at gastrula stage

(Figure 12A). Presumably during this period of development zygotic transcription of these genes starts and the spatial continuity suggests that new transcription could well begin in the same cells that inherit the maternal mRNA. In planula larvae *Piwi* and *Nanos1* are expressed in a population of cells with i-cell morphology (Figure 12A). In the adult medusa, *Piwi* and *Nanos1* expression is detected in male and female gonads, around the mouth and in the proximal part of the tentacle bulbs (Figure 12B). *Piwi* and *Nanos1* are not exclusively expressed in multipotent i-cells but also in some somatic fated cells and in germ cells (Figure 12B). *Piwi* and *Nanos1* expression in hydrozoans including *Clytia* is not restricted to multipotent, non-committed i-cells since it has also been reported in some early somatic derivative cells and in germ cells. These two genes may thus not be perfect markers to study i-cells ontogeny, but so far in *Clytia* I have been unable to uncover a marker specific to uncommitted i-cells (*i.e.* not expressed in germ cells or in somatic derivatives).

It is evident that there is a lack of information concerning i-cell ontogeny, since the majority of i-cell studies were carried out in the adult *Hydra* polyp. Even though a pioneer study in the hydrozoan *Pennaria tiarella* investigated the i-cell origin during embryonic development (Summers & Naynes 1969). In this studies i-cell presence were scored for the first time at planula stage in central endoderm, by morphological criteria. It is possible however that based on this this criteria delayed the timing of i-cell formation was incorrectly estimated. Interestingly in this study i-cells are thought to derive from endodermal cells rather than to arise as a germ layer-independent population. My study aims at compensating the lack of information with respect to i-cell origins during larval development. I investigated the appearance of i-cells during embryogenesis, and monitored i-cell derivatives appearance during *Clytia* larval development with the use of molecular markers.

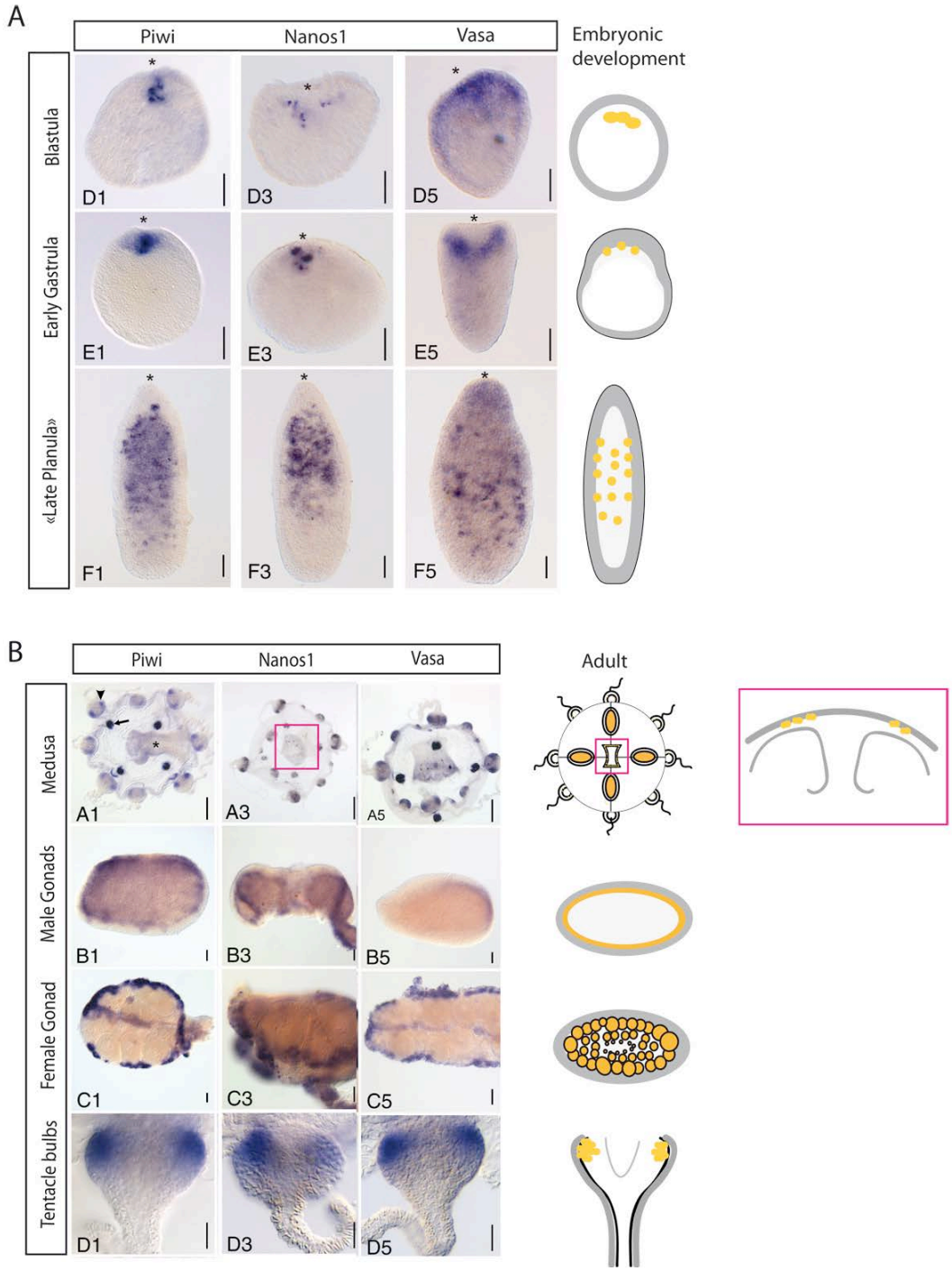

Figure12: Distribution of i-cells expressing *Piwi*, *Nanos1*,*Vasa* during larval development and in the medusa.

A) *Piwi*, *Nanos1* and *Vasa* expressing i-cells in embryos and larval stages. By *In situ* hybridisation *Piwi*, *Nanos1* and *Vasa* mRNAs are detected at the animal/oral pole during development. At the blastula stage the genes are expressed at the animal pole (on the two main lobes of blastulae showing a "peanut" morphology). At the early gastrula stage they are expressed at the oral pole, in cells that will ingress with the presumptive endoderm cells. In the planula the genes are expressed in a population of cells with morphological characteristics of i-cell interspersed in the endodermal region. Scale bar 50µm. On the left schematic representations of i-cell localisation (orange dots). Light grey: endoderm, dark grey: ectoderm.

B) *Piwi*, *Nanos1* and *Vasa* expression in the medusa. *Piwi, Nanos1*, *Vasa* mRNAs are detected in three main regions: the proximal area of the tentacle bulbs, at the base of the manubrium, and in the gonads. On the left schematic representation of i-cell distribution in the medusa (orange dots). In the pink square, schematic representation of the area boxed in A3, illustrating the medusa manubrium. Scale bar 100µm for the whole medusa, 25µm for the other images. From Leclère et al. (2012).

2.2.2 Nerve cells

The hydrozoan nervous system comprises morphologically distinct cell types, categorised as sensory cells and ganglion cells. Sensory cells convert specific chemical and physical stimuli such as light and touch into nerve impulses, while ganglion cells are often organised in intermediate stations termed plexuses that transmit impulses to other nerve elements. Some species, like the hydromedusa *Aglantha digitale*, possess specialised nerve cells with giant axons (Roberts & Mackie 1980). In *Aglantha* these nerve cells mediate the so-called escape swimming behaviour. Giant axon cells receive a sensory excitation from the bell margin, this signal is then conducted around the margin, provoking tentacles contraction (Roberts & Mackie 1980).

Even though the cnidarians (though hydrozoans) nervous system is considered to be one of the simplest metazoans nervous systems, it shows a wide diversity in its composition. In *Hydra* and in *Hydractinia* polyp nerve cells are localised in the ectodermal layer. In *Hydra* all the nerve cells are derived from the i-cells (Bosch & David 1987). The nerve cell precursors, called neuroblasts are localised in the gastric region and acquire their final fate only after reaching the ectodermal layer.

Morphological studies in *Clytia* planula described the presence of sensory and ganglionic cells in the planula ectoderm (Bodo & Bouillon 1968). Sensory cells are oriented perpendicular to the mesoglea placed at the base of the two epithelial layers, with the cell bodies located within the ectoderm (Martin 1988). Ganglion cells, (unipolar, bipolar or multipolar), are arranged in a nerve plexus oriented parallel to the mesoglea between the two epithelial sheets.

Unlike in *Hydra* polyps, nerve cells in *Clytia* larvae are not all i-cell derived. I-cell-depleted embryos are able to develop a subpopulation of neurosensory cells, but not ganglion cells, suggesting an ectodermal origin for some sensory cell types cells (Thomas & Martin 1987).

To describe the neuroanatomical features in planulae, jellyfishes and polyps of cnidarians, immunoreactivity toward some conserved neuropeptides is used as a common tool (Conzelmann & Jékely 2012). Neuropeptides are dominant transmitters molecules in cnidarians (Grimmelikhuijzen & Hauser 2012). The two types of antibodies used by the cnidarian community are those raised against RFamide and GLWamide neuropeptides. Ectodermal sensory cells expressing GLWamides have been described at the aboral pole in *Hydractinia echinata*, *Clava multicornis* and *Pennaria tiarella* planula (Piraino et al. 2011;

Gajewski et al. 1996; Plickert et al. 2003). RFamide positive ganglion cells are positioned at the base of the ectoderm and form a nerve net all along the mesoglea (Piraino et al. 2011; Plickert et al. 2003; Martin 1992). In *Hydra* polyps, RFamide neuropeptides are detected in the epithelial nerve net around the mouth (Figure 13G) while in the hydrozoans medusa *Eirene* RFamide neuropeptides are detected in the nerve ring and in the tentacle bulbs ectoderm (Figure 13F). However depending on the species, RFamides and GLWamides are not restricted to only one cell type as showed in *Clava multicornis* (Piraino et al. 2011).

Furthermore there may be several distinct precursors producing neuropeptides with slightly different sequences expressed in different cell populations and at different life cycle stages: for example there are 3 RFamide precursor genes in *Hydra* and two different GLWamide precursors in *Clytia, o*nly one of which is expressed in the larva.

It is clear that RFamide and GLWamide antibodies label different neural cell subpopulations (Piraino et al. 2011; Koizumi et al. 2014), and correspondingly that the two neuropeptides have different roles. Several reports indicate that GLWamides participate in the induction of metamorphosis (Plickert et al. 2003). In *Clytia* as in *Hydractinia* addition of some synthetic GLWamide peptides to the seawater can induce metamorphosis. In the light of wide utilisation of these two neuropeptides in cnidarians, I decided to use these two markers to monitor the appearance of differentiated neural cell types during *Clytia* larval development.

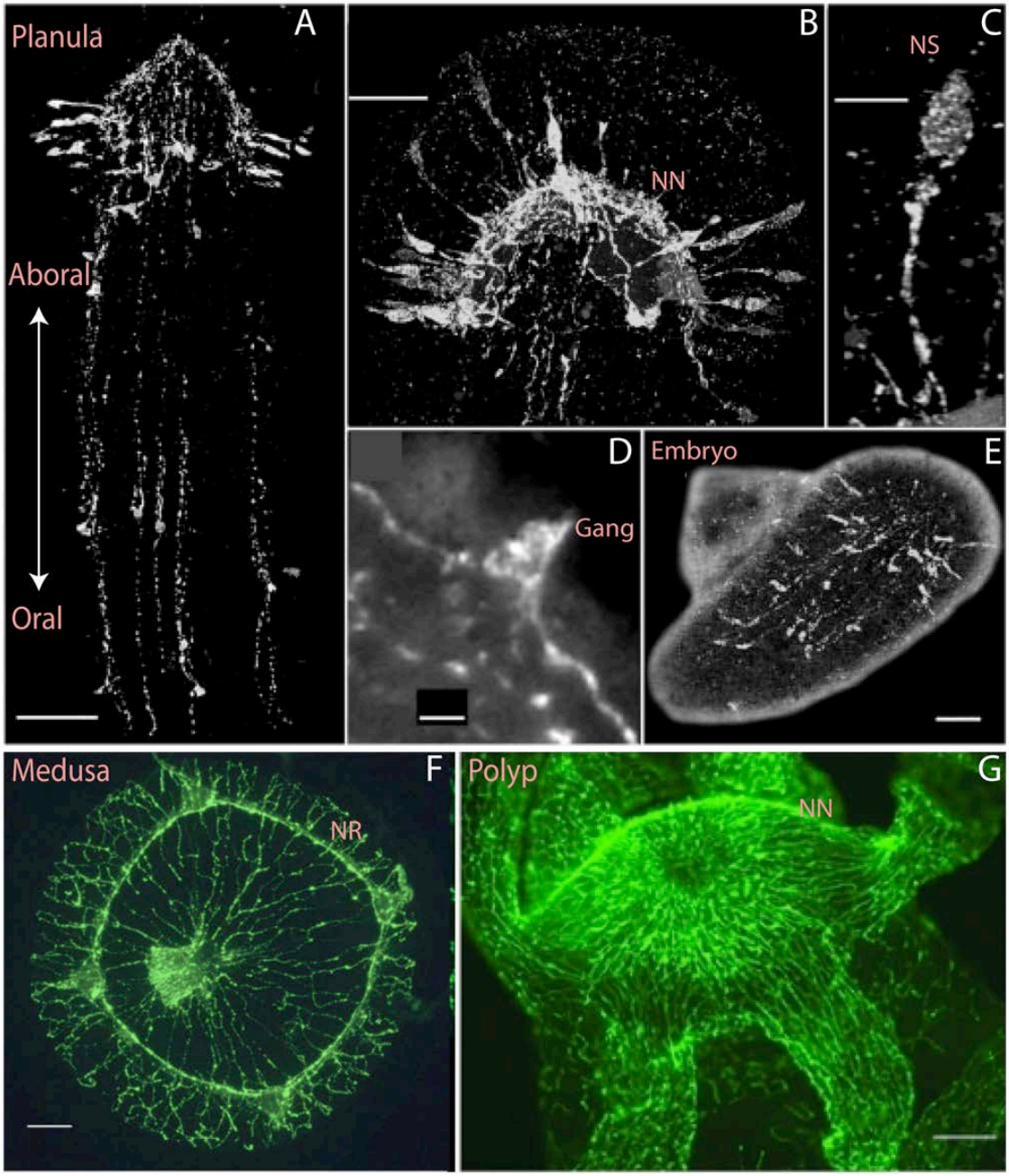

Figure 13: RFamide immunoreactivity in hydrozoan nervous systems.
Confocal images of different type of neurons immunodetected with a RFamide antibody in planulae, medusae, and polyps. (A-D) *Clava multicornis* planula (48hpf) showing an aboral neuronal plexus. In A punctuate staining characteristic of neuropeptide release is visible. B high magnification of the neural plexus, NN: nerve net. C high magnification showing a neurosensory cell (NS), D high magnification showing a ganglionic cell (Gang). E shows RFamide mature neurons at 36hpf. In the medusa *Eirene* (F), RFamide positive neurons are distributed in the nerve ring (NR) and in the manubrium. In *Hydra* polyps (G) an RFamide condensed nerve net (NN) is observed around the hypostome.
Scale bar: A 40µm, B 25µm, C 10µm, D 3µm, E 30µm, F 200µm, G 100µm. Modified from Piraino et al. (2011), Koizumi et al. (2014); Takahashi & Hatta (2011).

2.2.3 Nematocytes

In cnidarians, nematocytes are also known as stinging cells or cnidocytes. The terms "cnidocyte" and indeed "cnidarian" derive from the greek "cnida", meaning nettle. Nematocytes can be considered to be a neural cell type. They are specialised mechanosensitive neurosecretory cells, whose function is essentially in food capture and defence (Watanabe 2009, Galliot & Quiquand 2011).

Each nematocyte contains a special organelle called the nematocyst (the capsule) and a sensory apparatus termed the cnidocil. The nematocyst is a Golgi-derived capsule that contains a highly folded tubule that is expelled from the capsule where it is held under pressure upon stimulation to deliver a toxin into the prey or predator.

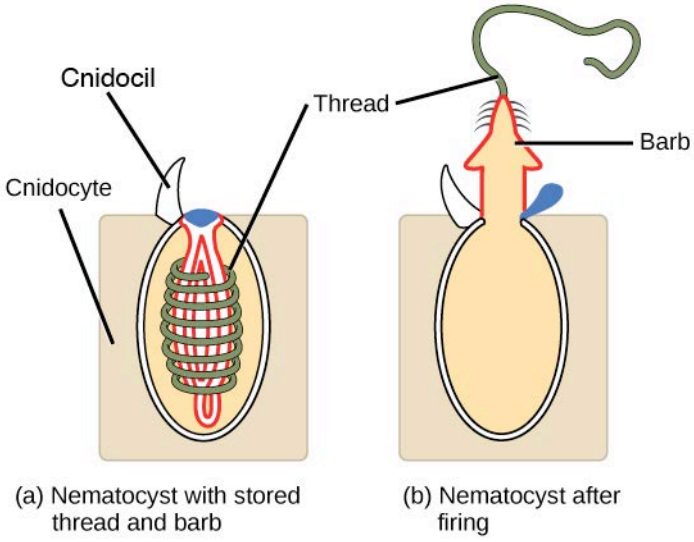

Figure 14: Nematocytes structures
The nematocyst is contained in the cnidocytes. The nematocyst consists of capsule to which is link a tube with a harpoon thread (a).
Upon cnidocil stimulation the folded tube is expulsed from the capsule and injected in the prey (b).
(From Boundless. "Phylum Cnidaria." *Boundless Biology*. Boundless, https://www.boundless.com/biology/textbooks/boundless-biology-textbook/invertebrates-28/phylum-cnidaria-167/phylum-cnidaria-644-12947/).

The nematocyst discharge mechanism is one of the fastest in nature and take less then 3 ms (Tardent 1984). The energy for the high intracapsular osmotic pressure is generated by a high concentration of the Poly-γ-glutamate (PGA) (Weber 1990). PGA is a polyanionic molecule that can bind to the cationic molecules (Szczepanek et al. 2002). Nematocyte capsules are birefringent, facilitating detection with polarized light and the intrinsic "chemical "nature of the nematocyte capsule allows a particular staining method to detect mature nematocytes (described in Material and Methods). During this study this technique was used to define when and where the first mature nematocyte appear in embryonic stages. In *Hydra* and *Hydractinia* polyps nematocytes are mostly located in the ectoderm at the extremities of the body, while their precursors termed nematoblasts are mostly

localised in the gastric body column. As it is the case for the nerve cells, nematoblasts acquire their final fate only in the ectoderm.

In *Clytia* planula, nematocytes are localised in the ectoderm when they are completely differentiated, while their intermediates, the nematoblasts are localised in the endodermal region. Thus nematoblasts migrate from the endoderm to the ectoderm to reach their final fate. In the adult jellyfish nematocytes are present thought the body but highly concentrated in the tentacles and in the mouth ectoderm (Denker et al. 2008).

2.2.4 Gland cells

From a morphological point of view gland cells are polarised cells, with granules concentrated in the cytoplasm toward the apical pole, and the nucleus located near the basal membrane. In cnidarians gland cells have secretory and digestive functions. In *Hydra* gland cells derive from the i-cells (Bode 1987, Siebert et al 2008) and are localised both in the endoderm and in the ectoderm. They are mostly scattered along the *Hydra* endoderm with a major density at the sub hypostomal region (Lentz, 1966, Chera et al. 2006).

In *Clytia* planulae, three different kinds of gland cells have been described: i) *glandulaire spumeuse* (hypostomal mucus cells) that arise at planula stage and persist in the aboral larval ectoderm; ii) *glandulaire spheruleus* (zymogen cells) that appear at the planula stage, located in the ectoderm but less numerous than the hypostomal mucus cells, and iii) *granuleuse* cells, present in the endoderm and in the ectoderm (Bodo & Bouillon 1968) (Figure 8B). In the adult jellyfish, gland cells are distributed in the gastrodermis in the manubrium and in the radial canal (Harrison and Westfall 1991). In particular the mouth opening is characterised by the presence of *spumeuse* and *spheruleus* gland cells (Bouillon 1966).

2.2.5 Gametes

Gametes and germ cell precursors are localised in the sexual organs in *Hydra* and in *Clytia* adult medusa gonads. *Clytia* gonads are attached to the subumbrellar side of the bell on each of the four radial canals. The oocytes are arranged on each side of the endodermal cavity (Figure 15). Proliferating germ cell precursors and oocytes undergoing the first stages of meiosis lie close to the medusa bell. Growing oocytes are positioned more distally.

Isolated *Clytia* gonads, can survive for 2-3 days. During this time they are still able to spawn in response to dark-light cycles, although they have lost physical contact with the rest of the medusa body. Thus isolated *Clytia* gonads can be used as a model to study mechanisms of oocyte maturation (Houliston et al. 2010).

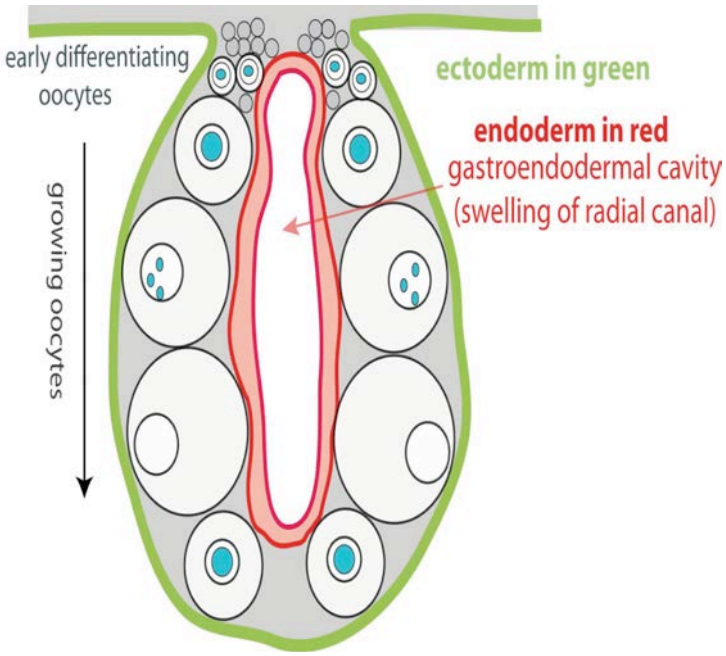

Figure 15: Structure of *Clytia* female gonad.
Schematic representation, of the female gonad. Oocytes are positioned between endoderm (red) and ectoderm (green) layers. Early oocytes are localised in the proximal region of the gonad (close to the bell margin), while the bigger late stage oocytes, are more common in the distal part of the gonad. From Amiel & Houliston (2009).

2.2.6 Epithelial cells

Among the few cell types that compose the hydrozoans body, epithelial cells represent the majority. Hydrozoan epithelial cells are the main component of the outer ectoderm and the inner endoderm. Both layers contain basal muscle processes that run parallel to the mesoglea. Muscle fibres are attached to the mesoglea and interconnect to form longitudinal and circular sheets that coordinate movement under neural control (Brusca and Brusca 2003). In *Hydra,* epithelial cells are considered as an additional stem cell lineage to the i-cells, because in the absence of i-cells (explained above) they are sufficient to drive morphogenesis and budding (Marcum and Campbell 1978). Further evidence of the role of the epithelial cells in morphogenesis was gained by *in vivo* tracking of epithelial cells (Wittlieb et al. 2006a). This technique allowed to determine the contribution of the GFP labelled endodermal epithelial cells in the bud formation. In *Hydractinia*, i-cells can give

rise to the epithelial cells, so the epithelial cells may not have to behave as stem cells (Plickert et al. 2012).

2.3 I-cell dynamics

The interstitial cell system provides a good model to investigate the specification and the differentiation of stem cells, since in planulae, polyps and medusae, the number of cells is limited and the final differentiated cells are common to all late stages. I-cells can give rise to nerve cells, nematocytes, gland cell and germ cells. Since the discovery of their multipotential capacity, i-cells have been the subject of numerous studies to unravel the basic mechanisms that regulate cell specification, proliferation and commitment.

2.3.1 Analysis of i-cell multipotency

In *Hydra*, analysis of i-cell potential was possible by using cytotoxic compounds that specifically eliminate i-cells, without killing the animal. Among these chemicals the most commonly used are Hydroxiurea (HU) and colchicine. HU blocks early S-phase cells by inactivating the nucleotide reductase enzyme, which is necessary for DNA synthesis, while colchicine is a microtubule inhibitor which causes M phase arrest. Following treatment by HU or colchicine, cell-cycle arrested and i-cells become susceptible to phagocytosis by epithelial cells (Campbell 1976), causing their loss. Treatments with colchicine and HU generate the so termed "epithelial polyps" or "i-cell free polyps". The cellular content of the epithelial polyps was analysed by *Hydra* maceration technique (David 1973). With this technique, *Hydra* tissues can be easily dissociated into individual cells, which retain their *in vivo* morphology and hence are recognizable as distinct cell types. Epithelial polyps lack nematocytes, all the nerve cell types and the gametes (Campbell 1976, Bode 1996).

Differently from polyps, in planula i-cells can be microsurgically deleted. Using this approach it was possible to investigate the origin of the i-cell derived nervous system in *Clytia* planula. During *Clytia* development, at middle gastrula stage, it is possible to separate an oral half containing oral ectoderm, presumptive endoderm and i-cells, and an aboral half composed only by the ectoderm. The planulae derived from the oral-half, form proper i-cells, and i-cell derivatives. In contrast the planula derived from the aboral-half lacked nematocytes and ganglion cells. Surprisingly the latter displayed the presence of

neurosensory cells. These observations suggest that in *Clytia* planula differently from *Hydra*, some sensory neurons derive from the ectodermal layer rather than from the i-cells (Martin and Thomas 1987), although the possibility of residual i-cells in the aboral part cannot be ruled out.

During the last 50 years, chemical and microsurgical techniques allowed, to unravel the i-cells potentialities. More recently the development of transgenic lines, in *Hydra* and in *Hydractinia* allowed *in vivo* i-cell tracking. With the help of this technique it was possible to validate the i-cell potentiality (Khalturin et al. 2007) and to investigate the migratory i-cell behaviour. When *Hydra* i-cells are transplanted in a wild type host polyp, they do not move, maintaining their position. Conversely, if the transplantation is done in epithelial polyps, i-cell began to move and to repopulate the i-cell free polyp (Boehm & Bosch 2012), suggesting that i-cell homeostasis is highly regulated.

2.3.2 Generating i-cell progeny: i-cell derivatives specification and differentiation

In *Hydra* polyps, and to some extent in *Clytia* planulae nematocytes and nerve cells originate from i-cells following distinct pathways of differentiation. The differentiation pathways of these two cell types are very different and are described below.

- *Nematocyte differentiation*

Nematocytes derive from precursor cells called nematoblasts, which are an i-cell derived cell population. The nematoblasts divide synchronously forming a cell cluster of 4 to 32 cells connected by intra-cytoplasmatic bridges (David & Gierer 1974). Once they stop proliferating the differentiation of the nematocytes capsule starts. During nematogenesis the Golgi complex enlarges and increases in size. In later stage of differentiation, the nucleus is displaced to one side of the cell and there is a strong increase in the amount and organisation of the ER. Vesicles fuse together to give rise to a tubule, which will generate the harpoon thread, and the cnidocil apparatus appears (Figure 14 A). In the last stage of differentiation, the tubule invaginates within the nematocyst, which reaches its maximum size, while the other organelles shrink and the ER system breaks down (Slautterback & Fawcett 1959). As a consequence of this final process of capsule maturation, the nematoblast cluster disperses and individual cells migrate into the ectodermal layer where the mature nematocytes become embedded into the epithelium. In *Hydra* nematoblasts

traverse long distances; nematogenesis occurs mainly in the central region of the polyp but differentiated nematocytes are particularly abundant in the head region, especially in the tentacles.

- *Neuronal differentiation*

Neurogenesis follows a more direct differentiation pathway than nematogenesis. In *Hydra* polyps the neural precursors, the neuroblasts, are located along the body column. Responding to local cues, differentiating neurons migrate toward the extremities of the body, (head and foot) to acquire their final fate. The analysis of the *Hydra* nervous system (including nematocytes and nerve cells) using molecular markers and functional assays has shown that, despite their distinct differentiation pathways, nematocytes and nerve cells derive from common precursors.

- *Genetic program modulating nematocytes and neural cell specification and differentiation*

Cnidarians possess transcription factors belonging to most of the groups known to be involved in neurogenesis from studies in bilaterian models. In bilaterians, the TF families that participate in neurogenesis include bHLH transcription factors, homeodomain proteins, Zinc finger proteins and Sox subgroup HMG box factors.

In cnidarians the bHLH repertoire is largely expanded (Gyoja et al. 2012). Bilaterian proneural bHLH factors belong to two main families: Atonal (ato) and Achete-scute (asc). In bilaterians, factors belonging to these two families are expressed in ectodermal cells where they are able to initiate neural development under the influence of Notch signalling (Bertrand et al. 2002).

In *Hydra,* the Achete-scute factor *CnAsh* is expressed in two distinct populations of cells, nerve cells developing in the apical/oral region and nematoblasts in polyp body column (Figure 16). In *Podocoryne*, two *Achaete-scute* genes have been characterised: *Ash1* and *Ash2* (Müller et al. 2003; Seipel et al. 2004a). *Ash1* expression is restricted to nematocytes, while *Ash2* is expressed in endodermal cells both, in the planula and in the medusa. In the planula these cells are positioned in the aboral endoderm, and in the medusa in the manubrium endoderm.

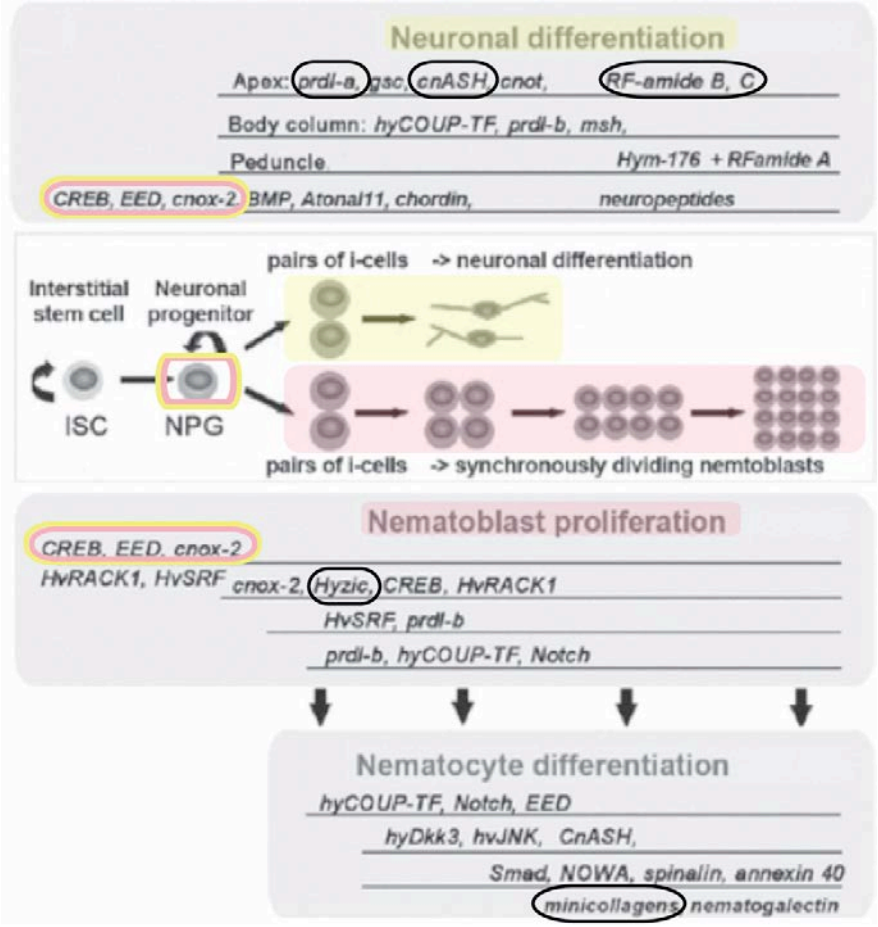

Figure 16: Genetic circuitry involved in nematocytes and neuronal cell specification. Diagram illustrating the genes that mediate nerve cells and nematocytes specification and differentiation in *Hydra*. Shaded in pink nematogenesis, shaded in yellow neurogenesis. Genes highlighted by double circles are expressed in the common neural progenitor (NPG). ISC :interstitial stem cell. Black encircled genes represent the family genes studied in this work. Modified from Galliot & Quiquand (2011).

The cellular identity of this cell population is not clear but they have been proposed to be neurosecretory cells on the basis of position and morphology. Phylogenetic analysis shows that *Ash2* belongs to the Asc-B family, and that it is an ortholog of the mouse gene *Ash3*. In mouse, *Ash3* is expressed in the gland cell lineage.

Among the class of homeodomain proteins present in cnidarians (Ryan et al. 2006), two genes belonging to the Paired-like class, *Prdl-a* and *Prdl-b* have been characterised in *Hydra* (Gauchat et al. 1998). *Prdl-a* is expressed in a subpopulation of apical neurons surrounding the hypostome ectoderm (Figure 16), however during head regeneration it is transiently expressed in the endoderm of the regenerative tip (Gauchat et al. 2004). *Hydra Prdl-b* is expressed in dividing nematoblasts net where nematocytes start to differentiate and migrate. Co-expression experiments using *Prdl-a* and *Prdl-b* probes reveal three different cell populations: a nerve cell population expressing *Prdl-a*, a dividing nematoblast population expressing *Prdl-b* and a third population expressing both genes, suggesting that nematocytes and nerve cell derive from the same neuronal precursor (Gauchat et al. 2004)(Figure 16).

Molecular studies such as these suggest that TF gene families involved in neurogenesis in vertebrates are involved in both neurogenesis and nematogenesis in hydrozoans, reinforcing the hypothesis that nematogenesis is a modified neural pathway (Watanabe et al. 2009). The *Hydra Zic* gene is another example of a neural gene involved in nematogenesis. Zic genes code for a family of C2H2 zing finger transcription factors. Vertebrate *Zic* genes are involved in germ layer differentiation, organogenesis, and have been shown to have a common role in neurogenesis by studies in cnidarians and ctenophores (Aruga et al. 2006; Layden et al. 2010). In *Hydra* polyps, *HyZic* is expressed in proliferative nematoblasts in the body column, (Lindgens 2004), prior to the expression of nematocyte structural genes such us *Nowa* (Figure 16). In *Nematostella* five *Zic* genes have been characterised. During development these genes are first expressed in the early gastrula at the aboral pole, while in the late planula and in the budding stage they are expressed in the presumptive and developing tentacles, in the ectoderm and in the endoderm.

Various studies in *Hydra* have indicated that neuroblasts and nematoblasts can derive from a common population of fate-committed i-cells. Another homeodomain TF, the *Gsx* orthologue *Cnox2*, appears to play a key regulatory function in these cells. *Cnox-2* is expressed in bipotent interstitial cells that give rise both to apical neurons and gastric nematoblasts. RNAi experiments indicate that *Cnox-2* functions upstream of *HyZic*, *Prdl-a*, and *CnAsh* in both nerve cell and nematocytes (Miljkovic-Licina et al. 2007), but upregulated the expression level of the TF COUP-TF. COUP-TF belongs to the steroid/thyroid hormone receptor superfamily of nuclear receptors, present across metazoans, whose members are involved in neurogenesis in vertebrates and in invertebrates (Gauchat et al. 2004; Galliot et al. 2009; Tang et al. 2010). In *Hydra COUP-TF* presents an expression pattern similar to *Prdl-b* and might promote the entry into nematocytes pathway (Miljkovic-Licina et al. 2007).

The *SOX* gene family is also commonly associated with neurogenesis. Sox proteins posses a highly conserved DNA binding domain termed HMG. These transcription factors maintain many cell homeostasis and self-renewal/differentiation pathways. *Sox* genes are often deployed as neurogenesis regulators in bilaterians, they can define neural identity, maintain neural stem cell populations and govern neural differentiation pathways (Pevny and Placzek 2005, Sandberg et al. 2005). At present among hydrozoans *Sox* genes have been characterised only in *Clytia* (Jager et al. 2006; Jager et al. 2011). In contrast *Sox* genes

have been widely studied in anthozoans (Magie et al. 2005; Shinzato et al. 2008; Richards & Rentzsch 2014). A recent study in *Nematostella* showed for the first time the existence of a neural restricted multipotent population expressing the ortholog of the conserved neurogenic gene *SoxB(2)*. This multipotent cell population divides asymmetrically, giving rise to sensory neurons, ganglion neurons and nematocytes (Richards & Rentzsch 2014) which represent the totality of neural cell types.

- *Clytia SOX complement*

In *Clytia* 10 *SOX* genes have been described (Jager et al. 2011). Based on their expression profiles they were grouped into three categories: endodermal genes (*SoxF*), genes expressed in stem cell/undifferentiated cells (*Sox3, Sox1, Sox12*) and nematocytes/neural genes (*Sox2, Sox13, Sox14, Sox15, Sox10*). For my study I was particularly interested in *Sox15*, which represented a good candidate for a role in neurogenesis/nematogenesis. *Sox15* in the adult jellyfish is expressed in the nematogenic tentacle bulbs ectoderm, while in the planula it is detected in an endodermal populations (putative nematoblasts), and in an ectodermal cell population identified as maturing nematocytes (Jager et al. 2011) (Figure 17).

- *Nematogenesis in Clytia tentacle bulbs*

Studies conducted in different cnidarian species identified minicollagen proteins as the major component of the nematocyst capsule (Kurz et al. 1991). Minicollagens are small collagen-like proteins, with long polyproline stretches flanked at the N and C-terminal by cysteine rich domains (CRD). These CRDs are responsible for stabilization of the capsule wall by disulphide bonds. *Minicollagen* mRNA is not detected in fully differentiated nematocytes either in *Hydra* or in *Nematostella*. Therefore minicollagen *in situ* hybridisation specifically identifies nematoblasts with an immature capsule in *Clytia* tentacle bulbs. In *Clytia* medusa the gene *Mcol3-4a* is expressed in the manubrium ectoderm and in the tentacle bulb ectoderm. *Clytia* medusa nematogenesis is particularly active in the tentacles bulbs (Denker et al. 2008), more precisely in the tentacle bulb ectoderm (TBE). An ordered progression of nematogenesis occurs along the proximal-distal axis of the tentacle, such that the TBE can be subdivided in four regions depending on their degree of differentiation and proliferation state (Figure 14 C). Interestingly, *Mcol3-4a* positive cells partially overlap with cell expressing the stem cell gene *Piwi*, suggesting that nematocyte-fated i-cells transiently retain *Piwi* expression. *Piwi* expressing

cells in the tentacle bulb are highly proliferative (Denker et al. 2008). *Clytia* tentacle bulbs, *Mcol3-4a* and *Sox15* expression domains overlap extensively (Figure 17C). I used these three genes to detect nematogenetic cells during *Clytia* embryonic development.

- *Gland cell formation*

I-cells also give rise to gland cells, however this i-cell differentiation pathway has been less studied. In *Hydra* the formation of gland cells was investigated by classical i-cell labelling approaches and recently by *in vivo* zymogen cell tracking (Schmidt & David 1986; Siebert et al. 2008). These *in vivo* tracking experiments show that mucous gland cell and zymogen cells are i-cell derived. *Hydra* gland cells express the serine protease inhibitor *Antistastin* (Holstein et al. 1992; Hwang et al. 2007).

Serine protease inhibitor (SPI) was characterised for the first time in salivary glands extract of the Mexican leech *Haementeria officinalis*. It has a potent anticoagulant action, (which inhibits blood coagulation factor Xa activity and disrupts the coagulation cascade) and an anti-metastatic effect (Tuszynskisb et al. 1987). In this study I used the *Clytia Antistasin* gene to describe the distribution of gland cells during embryonic development.

- *Germ cells origin*

In hydrozoans the germ line is not separated from somatic cell lineages. Indeed interstitial cells give rise to both lineages (Bosch & David 1987). The first to infer an i-cell origin for the germ cells was August Weissmann. He described, in *Hydractinia* histological preparation, the presence of a population of cells that he defined as "distinct population of cell, determined in advance, that undergo transformation in germ cells"(Weismann A 1883). However the first experimental evidence for an i-cell origin for germ cells dates back to 1957. Hauenschild performed transplantation experiments in the hydrozoan medusa *Eleutheria dichotoma*. He transferred i-cells from a sexual strain to an asexual medusa. Following the transplantation the medusa acquired the capacity to form gametes (Haueschild 1956). In *Clytia* the germ cell origin has been little investigated, but it appears that i-cells give rise to germ cells only within the gonads. In this study I sought to identify molecular markers expressed early during germ cell development from i-cells in order to assess whether i-cells committed to be germ cell precursors already arise during larval development.

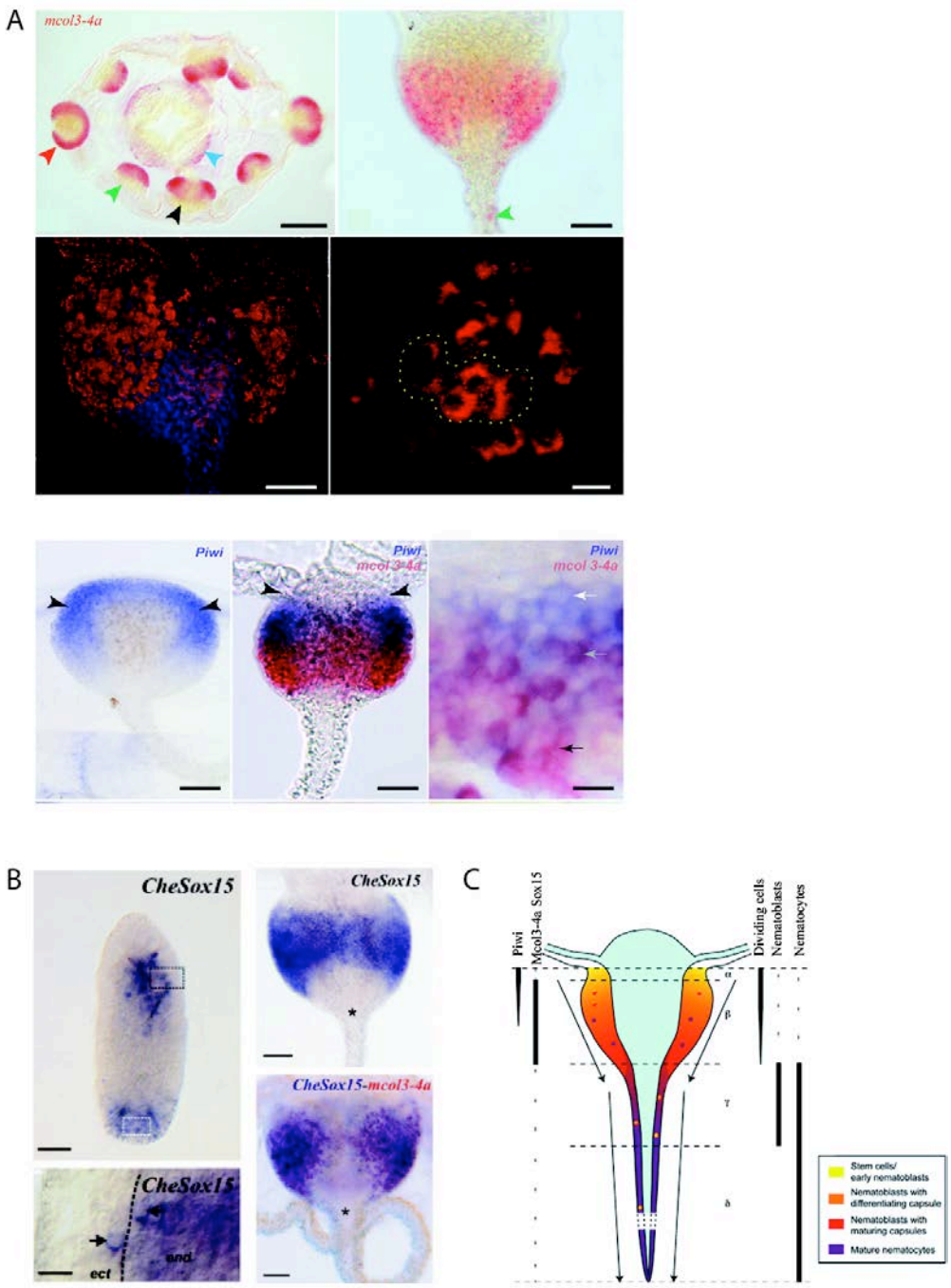

Figure 17: Molecular markers for *Clytia* Nematogenesis.
A) Expression pattern analysis of the nematogenic marker *Mcol3-4a* in the medusa. *Mcol3-4a* is expressed in the mouth and in the tentacle bulb ectoderm. Light blue and green arrowheads indicate *Mcol3-4a* expression at the base of manubrium and the base of the tentacle. On the right lower panel, high magnification of *Mcol3-4a*-expressing-cells in the tentacle bulb (external side). Yellow dotted lines highlight nematoblast nests as typical nematocytes conformation. *In situ* hybridisation showing overlapping expression domains of *Mcol3-4a* and *Piwi*. Scale bar First row: 250µm, second row: 25µm, 2.5µm, third row 25µm, 25µm, 10 µm
B) *Sox15* expression in adult medusa and planula. In late planula (>48hpf), *Sox15* mRNA is detected in a population of endodermal cells and in differentiating nematoblasts in the ectoderm, as shown by the high magnification in the lower right panel. In the medusa *Sox15* expression coincides with *Mcol3-4a* expression in tentacle bulbs. Scale bars 50µm, 10µm (planula), 20µm in tentacle bulbs.
C) Schematic representation of a tentacle bulb, including the distribution of the different cell types and molecular markers. From Jager et al. (2011), Denker et al. (2008).

Among conserved factors regulating gametogenesis, the Boule/Daz gene family is conserved across animal kingdom (Eirín-López & Ausió 2011; Kuales et al. 2011; Shah et al. 2010). Boule/DAZ genes play a variety of roles in germ cell development. For example, in the flatworm *Macrostomum lignano* three boule genes have been identified, of which *macbol1* and *macbol3* regulate respectively spermatogenesis and oogenesis (Kuales et al. 2011). In *C.elegans* DAZ-1 homolog was shown to be a crucial factor for female meiosis, while in *Drosophila* boule absence is associated with a defects in spermatogenesis (Karashima et al. 2000; Eberhart et al. 1996). Given the widespread involvement of Boule/DAZ genes in gametogenesis, I decide to identify and characterise for the first time *Boule* genes as potential early/specific expressed genes for germ cell in *Clytia.*

2.3.3 Wnt signalling regulates i-cell differentiation

As discussed above (section 1.6.4), in bilateria Wnt signalling regulates embryonic patterning and stem cell behaviour. The role of Wnt signalling in hydrozoan stem cell regulation was investigated in *Hydra* and *Hydractinia* polyps (Khalturin et al. 2007; Teo et al. 2006). The approach used in these two studies was similar. The authors hyperactive Wnt signalling by global treatment using inhibitors of the kinase GSK3b (a negative regulator of Wnt signalling). In *Hydra* Wnt signalling overexpression resulted in a change of the positional value along the oral-aboral axis, which affected the nematoblast population. Early nematoblasts expressing nbo35, located in the gastric region of the polyp were abolished following Wnt hyperactivation, while later nb031 expressing nematocytes, normally located in the tentacles became dispersed all along *Hydra* body. These results suggest that nematoblasts are forced to differentiate into nematocytes by the increase of the Wnt signalling, which promotes oral positional values. This hypothesis was confirmed by grafting experiments in which wild type i-cells were transferred in treated polyps. In these conditions i-cells behave as they have reached the final destination to become nematocytes. These observations suggest that Wnt signalling modulate i-cell differentiation in nematocytes by providing oral positional information.

Coherently with these results, hyperactivation of Wnt signalling in *Hydractinia* induces an increase in the number of nematocytes. In addition in these altered condition the numbers of RFamide positive neurons increased around the hypostome. Even though these results

clearly show an implication of Wnt in i-cell differentiation, it is still unclear whether Wnt signalling acts only via oral-aboral positional identity or also has a direct role in differentiation and/or earlier steps of neurogenesis or nematogenesis.

2.4 The embryological origin of i-cells

Clytia hemisphaerica i-cells express a set of conserved "germ cell/stem cell" markers including *Piwi* and *Nanos1*. In vertebrates, these genes are known to be part of the "germ plasm", a ribonucleopreotein complex inherited exclusively by the cells that will become germ cell precursors (See section 1.5). In *Clytia* these genes are expressed maternally and the mRNAs localise in a "germ plasm-like" region surrounding the egg pronucleus, as shown by electron microscopy (Figure 18). These mRNA are detected at the animal/oral pole during *Clytia* embryonic and larval development, (see Figure 12, Leclère et al. 2012). In *Hydractinia* eggs Vasa protein is concentrated in a similar position and is probably another germ plasm component (Rebscher et al. 2008). The presence of morphologically recognisable germ plasm structures, suggests that i-cell formation could be determined by inheritance of the germ plasm. Previous studies investigated the participation of the germ plasm into i-cell formation through the production of "germ plasm free" embryos. To separate animal (germ plasm present) and vegetal halves (germ plasm absent) embryos bisection experiment at 8-cell stage (single blastomeres isolation) and at blastula stage were performed (Figure 19). Fragments lacking germ plasm are able to re-generate *Piwi*-expressing i-cells (Figure 19), indicating the existence of cell-signalling mechanisms acting in *de novo* i-cell formation (Leclère et al. 2012).

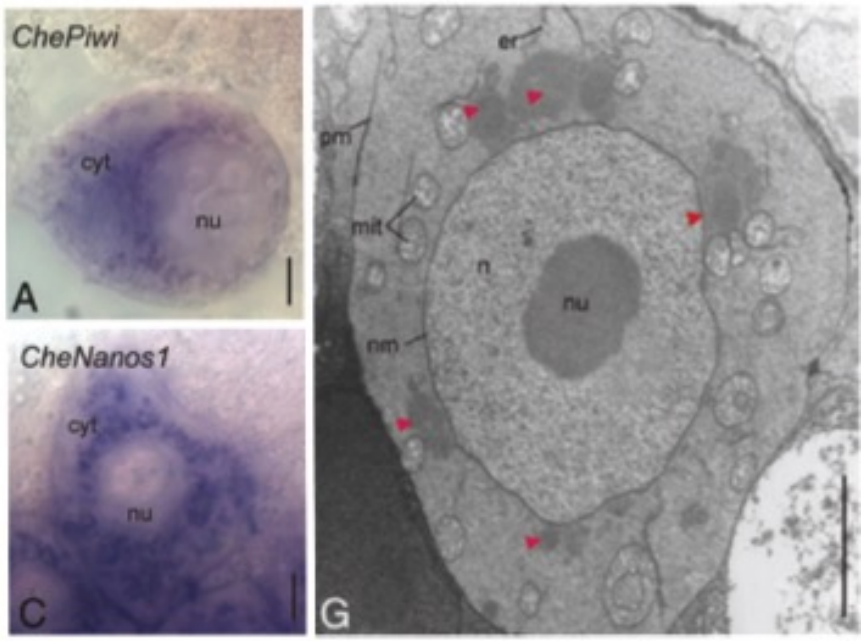

Figure 18: Morphological and molecular evidence for perinuclear germ plasm localisation in *Clytia* oocytes.
A, C: Characteristic perinuclear distribution of *Nanos1*and *Piwi* mRNAs in very early oocyte stages
G: TEM sections of growing oocytes. Perinuclear gem plasm is indicated by red arrowheads
er: endoplasmic reticulum, nm: nuclear membrane, pm: cell membrane, n: nucleus, nu: nucleolus, mit: mitochondria, cyt: cytoplasm, nu: nucleus, Scale bars 5µm. From Leclére et al. (2012).

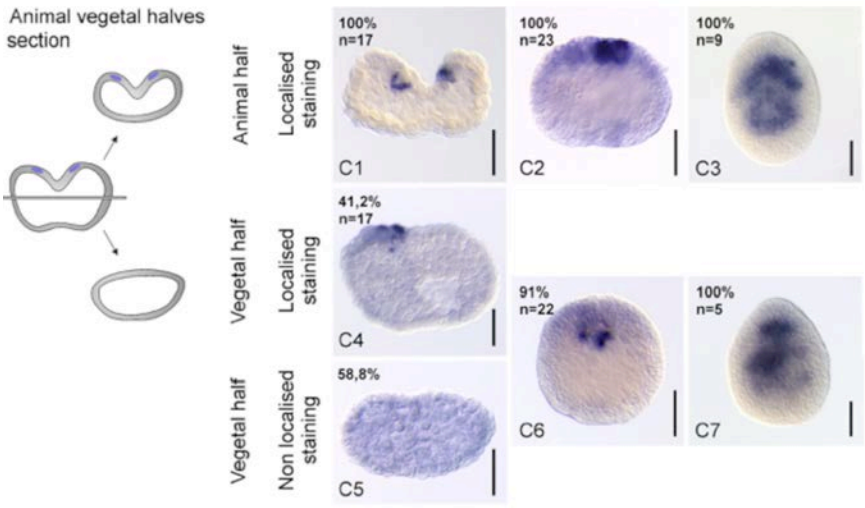

Figure 19: Piwi expressing i-cells can form from in both vegetal and animal regions. On the right, a schematic representation of the approach used to separate animal and vegetal halves at blastula stage. Note that at this stage the animal pole is distinguishable by the deeper cleft of the typical peanut shape. Bisection successfully eliminated germ plasm from about 60% of vegetal fragments, as assessed by immediate fixation prior to *Piwi in situ* hybridisation (C1, C4, C5). At the early gastrula stage (C2, C6) and at 24hpf (C3, C7) *Piwi*–expressing cells were detected in almost all samples, indicating that fragments lacking germ plasm are able to re-form i-cells. From Leclére et al. (2012).

Among the signalling pathways regulating stem cell formation the Wnt/β-catenin pathway is a prime candidate for regulating i-cells. Wnt/β-catenin signalling regulates proliferation and differentiation in *Hydractinia* and i-cell terminal differentiation in *Hydra* (Teo et al. 2006; Khalturin et al. 2007). In *Clytia* Wnt3 ligand expression at the " animal" or "oral" pole of the embryo during the larval development corresponds partially to the expression domain of *Nanos1* and *Piwi* as shown in figure 20.

Therefore in the present study I investigated the impact of Wnt/β-catenin signalling on:
- i-cell formation during undisturbed embryogenesis.
- *de novo* i-cell formation in isolated vegetal embryo fragments.
- fate specification and differentiation of i-cell derivatives.

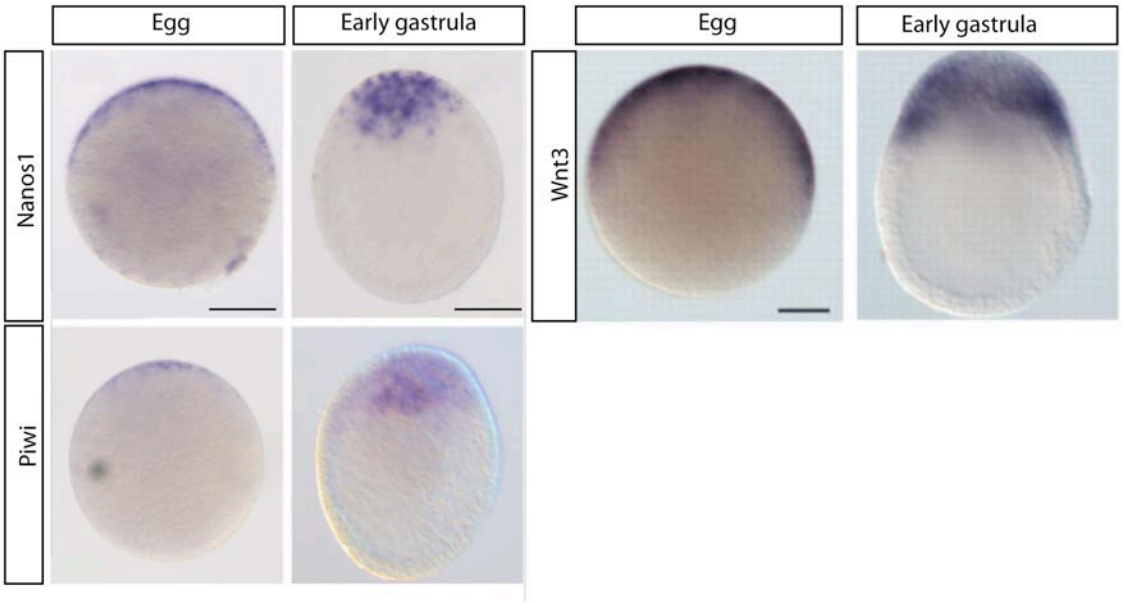

Figure 20: *Nanos1*, *Piwi* and *Wnt3* expression pattern in eggs and at early the gastrula stage. In *situ* hybridisation analysis shows that mRNAs for *Nanos1*, *Piwi* and *Wnt3* are all localised at the animal cortex in the unfertilised eggs (left panel for each line). At the early gastrula stage *Nanos1* and *Piwi* (right panel) are expressed in a population of ingressing cells at oral pole, while Wnt3 expression is detected mainly in the ectodermal cells. Scale bar 50μm.Left panel from Momose et al. (2008). Scale bar 40μm.

MATERIAL & METHODS

Animals

- *Culture system*

The complete *Clytia* life cycle is reproduced under laboratory conditions in a system of small aquaria each with a capacity of 5-6 litres, linked in series, and supplied by a circulating flow of artificial seawater. Some aquaria contain colonies of polyps, fixed on glass plates and other contains mature medusae, separated into males and females. Mature medusae are cultured in closed compartments in which the light is controlled by a day/night cycle, in order to synchronise spawning. Polyp colonies and jellyfishes are fed twice a day with *Artemia salina* larvae. More details of the *Clytia* culture system can be found at http://clytia.wikispaces.com/.

For all the experiments performed, *Clytia hemisphaerica* medusa cultured in Villefranche-sur-Mer from established laboratory colonies were used (Chevalier et al., 2006).

Clytia eggs were collected by placing the female medusae in glass beakers filled with artificial seawater (ASW- Red Sea Salt brand), and were allowed to settle by gravity. The sperm released by adult males was collected with a pipette and added to the collected eggs. In *Clytia* there is no obvious sign of successfully fertilisation. It is possible to estimate under the stereomicroscope if the amount of sperm surrounding the eggs is sufficient for fertilisation and successful development. At the four cells stage, embryos are transferred to clean glass beakers containing Millipore filtered Artificial seawater (MFSW). The embryos were cultured at 18 °C in MFSW.

- *Egg microinjection and embryo manipulation*

Morpholino oligonucleotides were suspended in water to a concentration of 4mM. As laboratory routine, a working solution of 1 mM morpholino oligos was prepared. The sequence of the morpholino oligonucleotide against Wnt3, injected at 200 µM have been already published (Momose et al. 2008). Microinjection in unfertilised egg was performed using an Eppendorf "Femtojet' microinjection system.

Embryos bisection experiments were performed at the 8-cell stage or blastula stage. Embryos were cut using fine tungsten needles on 2% agarose-coated Petri dishes. Embryo fragments were cultured in artificial filtered seawater. Although *Clytia* embryos exhibit variable morphologies during early development, for the cutting experiment at the blastula

stage we used only the "peanut" shape embryos in which the animal–vegetal axis can be deduced (Leclère et al 2012).

- **Phylogenetic analyses**

Alignments for the phylogenetic analyses were constructed using published sequences from previous work (Lapébie et al. 2014; Shah et al. 2010) and sequences retrieved by TblastN searches on public databases (Genbank) or at www.compagen.org (Hemmrich et al. 2012) for a set of representatives phyla . Sequences were aligned using CLUSTALW in the BioEdit package (A.Hall 1999) and the alignment corrected manually or using MUSCLE (Edgar 2004). Maximum-likelihood (ML) analyses were performed using the PhyML program. Trees were then visualised and annotated with FigTree v. 1.4.2 (http://tree.bio.ed.ac.uk/software/figtree/). Branch support was tested with bootstrapping (550replicates).

- **Single and double *in situ* hybridisation**

Single-probe in *situ* hybridisations was performed using the InsituPro robot (Intavis) as described previously (Lapébie et al. 2014). For double fluorescent in situ (FISH) using DIG-UTP and Fluorescein-UTP labelled probes, the protocol was modified as follows. Embryos were fixed overnight at 20°C in HEM buffer (0.1M Hepes pH 6.9, 50mM EGTA pH7.2, 10mM MgSO4), containing 3.7% formaldehyde, then washed five times in PBST (Phosphate Buffered Saline containing 0.1% Tween 20) for 10 minutes, dehydrated through a PBST/50% methanol step and stored in methanol at -20°C. After rehydration in PBST/50% methanol and three 5-minute washes in PBST, samples were transferred to the InsituPro robot plate. The robot program was as described previously with increased (12h) antibody incubation steps using peroxidase anti-DIG or anti-Fluorescein antibodies diluted 1:2000. Samples were then washed twice in fresh colour reaction buffer (0.0015 % H_20_2 in PBS) for 30 minutes. Signal was developed with fluorophore-conjugated tyramide (Perkin Elmer; 1:400 in colour reaction buffer) for 1hour. Residual enzyme activity was inhibited by10-minute incubation in 0.01N HCl followed by 2 PBST washes prior to addition and development of the second peroxidase-conjugated antibody. Following completion of the second colour reaction, samples were mounted in Citifluor mounting medium (Citifluor Ltd) and images acquired using a Leica SP5 microscope. To verify the

specificity of the images obtained for each probe combination, two controls were performed in parallel with single probe, imaging in both channels.

- **Cells counting procedure**

For co-expression studies the number of labelled cells was counted using the "cell Counter" ImageJ Plugin (cell_counter.jar). Cells were identified by HOECHST counterstaining and counted in each Z-plane, imaged using a Leica SP5 confocal microscope.

- **Nematocyst staining and Immunofluorescence**

Mature nematocytes were counted by staining the poly-γ-glutamate contents of their nematocyst capsules with DAPI, adapting a protocol from previous studies (Denker et al., 2008) and viewing them under the FITC channel of an epifluorescence microscope. Under these conditions only nematocyst capsules, and not nuclei, were visible.

Samples were fixed for 1 h in 3.7% formaldehyde/PBS at room temperature, washed 3 times in PBS for 10 minutes. They were incubated for 30 min in 50 µg/ml DAPI (from a 1mg/ml stock) in PBS. Samples were rinsed 3 times and mounted in Citifluor. Staining was observed by epifluorescence on a Zeiss Axiovert 200 microscope (excitation 450-490 nm, emission >515 nm).

Immunofluorescence was performed as previously described (Amiel and Houliston, 2009). RFamide positive neurons were visualised using a specific Clytia RFamide antibody (kindly gift of Dr. Gáspár Jékely, Max Plank Institute for developmental Biology, Tübingen, Germany), final dilution of 1:250, overnight at 4 °C, followed by a rhodamine coupled anti-rabbit IgG (Sigma, final dilution 1:100) for 3 h at room temperature, with Hoechst dye 33258 (Sigma, 0.3 µg/ml final) included to stain DNA. Specimens were mounted in Citifluor mounting medium (Citifluor Ltd) and imaged using a Leica SP5 confocal microscope.

RESULTS I:

Monitoring the spatial and temporal distribution of i-cell derivatives during *Clytia* larval development.

1.Background and Questions

In this chapter I will present the analyses that allowed me to achieve a first molecular cartography of i-cells and their derivatives during *Clytia* embryonic and larval development.

Whit the exception of an elegant histological description, which illustrates the different cell types of the *Clytia* planula larva (Bodo & Bouillon 1968; Figure 9B), and electron microscope descriptions of cell types in normal and i-cell–free larvae (Thomas and Martin 1987), little was previously known concerning the distribution of i-cells derivatives in the *Clytia* larva.

In order to track the appearance of different types of i-cell derivatives: nematocytes, nerve cells, gland cells and germ cells, I selected a set of potential molecular markers based on published work in *Clytia*, *Hydra* and *Podocoryne* (Hwang et al. 2007; Gauchat et al. 1998; Seipel et al. 2004; Jager et al. 2011; Leclère et al. 2012; Denker et al. 2008). In addition I took advantage of the transcriptomic data derived from sorted endodermal, ectodermal and *Nanos* expressing (i-cell lineage) cells in *Hydra* (Hemmrich et al. 2012 at http://compagen.zoologie.uni-kiel.de/blast.html) to verify that the genes with identifiable *Hydra* orthologs were expressed in *Hydra* multipotent i-cell lineage (Table 1 Annexes).

In this study I used *Piwi* and *Nanos1* interchangeably as i-cell markers. By co-localisation experiments (double *in situ* hybridisation) at different developmental stages I was able to show the two genes are largely expressed in the same cell population (Figure 21).

It should be noted that defining i-cells on the basis of *Piwi* and *Nanos1* expression means that both multipotent i-cells and some "fated i-cells" are included in the same population. Fated i-cells have already left the stem cell pool and chosen a particular differentiated cell type fate. I considered cells that co-express *Piwi*/*Nanos1* with early somatic markers to be fated i-cells; depending on the lineage these could be called for instance early nematoblasts or early neuroblasts.

To identify early progenitors and differentiated i-cells, I tried to identify markers for each step of differentiation. Because hydrozoan medusae and planulae share to a large extent the same cellular components, therefore I included in this study the adult jellyfish, in which structures are easier to recognise then in the planula. Comparison between the expression patterns in the planulae and in the medusae helped me to propose identities for the cells

expressing the genes. I also used other staining techniques to identify differentiated nematocytes and some neural sub-types.

This work was the first attempt to provide a molecular description of the appearance of the i-cell derivatives during *Clytia* larval development. It will provide a basic foundation for further molecular characterisation and for functional analyses on the regulation of i-cell dynamics (commitment and differentiation), and provided the background for the studies of Wnt signalling regulation of i-cells development presented in Results chapter II.

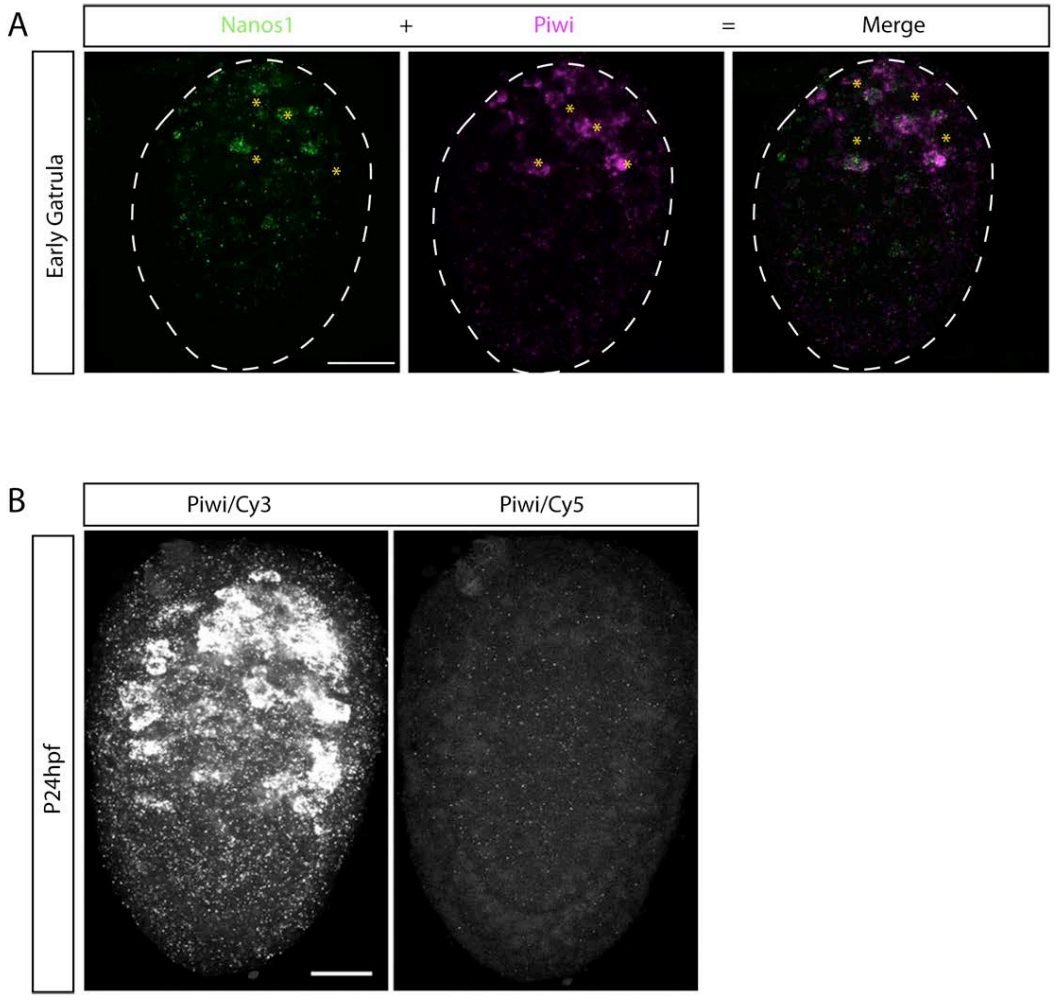

Figure 21: Co-localisation of *Piwi* and *Nanos1* transcripts. A) Representative confocal image showing co-localisation of *Nanos1* (green) and *Piwi* (pink) mRNA. Merged images show that *Piwi* and *Nanos1* co-localise at the early gastrula and at 72hpf (not shown). The identified cells, co-express both genes even though the superposition is not highlighted by a third different colour (*e.g* yellow). Scale bar 50µm. B) Negative control. Confocal image showing a single FISH, using *Piwi* probe (or *Nanos1*, not shown) at 24hpf. To verify the reliability and the specificity of the signal detected, the samples were incubated only with the *Piwi* probe and treated for a double FISH and imaged in both channels. Scale bar 50µm.

1.1 Nematogenesis progression during Clytia larval development.

In order to investigate the nematogenetic lineage during *Clytia* larval development I aimed to track the appearance of nematoblast progenitors (fated i-cells), nematoblasts and differentiated nematocytes. To do this I used a combination of approaches. I detected mature nematocytes using a DAPI staining technique (see Materials and Methods for details). At high concentrations, DAPI binds the anionic molecule poly-γ- glutamate that is one of the major components of the nematocyte capsule (Weber 1990) allowing the visualisation of the fully mature differentiated nematocytes under a FITC filter. These mature nematocyte cells also have a characteristic splinter-shaped morphology (Figure 22A) and are highly bi-refringent under polarised light.

From a molecular point of view, it has previously been shown that in the adult medusa and in the late planula (>48hpf) *Mcol3-4a* and *Sox15*, are expressed in nematoblasts and in nematocytes (Denker et al. 2008; Jager et al. 2011) (Figure 17 Introduction). Therefore I used these markers to follow the nematogenetic pathway during *Clytia* development.

1.1.1 Distribution of nematocytes during embryonic development

To determine exactly when and where mature nematocytes first appear during embryogenesis I scored the presence of nematocyte capsules by DAPI staining (Figure 22A) during development at 24, 36, 48, 72-hour post fertilisation (hpf). 24hpf corresponds to the end of gastrulation, with completion of the ingression of presumptive endoderm cells. By 48hpf the endodermal cells are organised into an endodermal epithelium and an internal cavity has formed through destruction and digestion of a central core of cells. At 72hpf larval development and cell type differentiation is complete and the planula is competent to metamorphose.

No nematocytes could be detected by DAPI staining in 24hpf planulae (Figure 22B), indicating that the nematocyte differentiation has not yet occurred. At 36hpf a few nematocytes (1-2 for each planula analysed) were detected in the ectodermal layer (Figure 22B). At 48hpf the average number of nematocytes in each planula increased to 25- 30. By 72hpf the number had further increased, to reach 30 to 50 nematocytes per planula (Figure 22B).

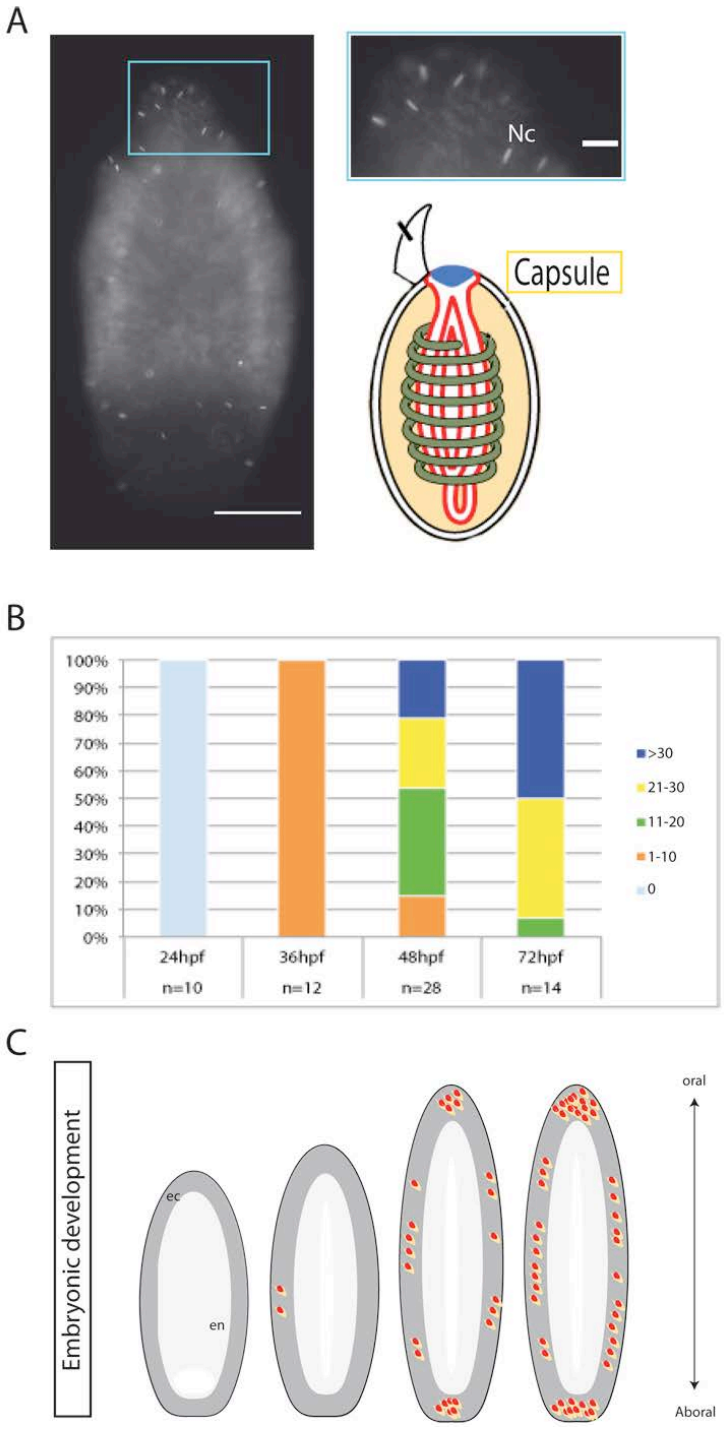

Figure 22: Appearance of nematocytes during larval development.
A) Nematocytes labelling. Nematocytes were labelled by incubation with high DAPI concentration; the image shows a 48hpf planula. Scale bar 50µm. In the right panel detailed view, of the area boxed in A. Nc: nematocytes capsule. Scale bar 10µm. Lower panel schematic illustration of the nematocytes and the nematocyst capsule. **B) Nematocytes counts.** Nematocytes were counted using epifluorescence microscopy and were grouped on the basis of nematocyte number. Light blue represents planulae with no detectable nematocytes, orange 1-10, green 11-20, yellow 21-30, dark blue more then 30 nematocytes detected. **C) Schematic representation of *Clytia* larval development,** indicating the nematocytes position during development. Nematocytes are represented using the same drawing in A. en: endoderm. ec: ectoderm. Oral pole at the top.

This observation shows that nematocytes first appear in the planula at around 36hpf and that their numbers then increase progressively, suggesting ongoing nematogenesis in the planula.

1.1.2 *Mcol3-4a*-expressing nematoblasts are largely restricted to the endodermal region

Minicollagens are the main component of the nematocytes capsule (Holstein et al. 1994), their transcripts can be detected prior the capsule formation, in the nematoblast cell population. Among several minicollagens genes characterised in cnidarians (David et al. 2008), to describe the distribution of nematoblasts in *Clytia* embryos and larvae I performed *in situ* hybridisation with the *Minicollagen 3-4a* gene (*Mcol3-4)* since it was previously shown to be expressed in the *Clytia* medusa nematoblast (Denker et al. 2008).
Expression of *Mcol3-4a* mRNA was detected for the first time at 24 hpf in cells concentrated in the oral 2/3 of the endodermal region (Figure 23A). As seen also in *Clytia* tentacle bulbs, *Mcol3-4a* expressing cells showed a typical nematoblast morphology and organisation (nests of 2,4 or 8 cells, known from *Hydra* studies to be interconnected by cytoplasmic bridges) (Figure 17 Introduction). In later stages, (48hpf and 72hpf) some cells expressing *Mcol3-4a* could be detected at the interface between endoderm and ectoderm layers suggesting that these cells are preparing to migrate into the ectoderm where they mature to form definitive nematocytes (see above). In fully differentiated nematocytes *Mcol3-4a* mRNA can no longer be detected.
In the adult medusa *Mcol3-4a* is expressed throughout the nematoblast population, including nematoblast progenitors in which *Piwi* is still expressed (Denker et al. 2008). To map the distribution of early stage nematoblasts at planula stages I performed co-expression studies using *Mcol3-4a* and *Piwi* probes. Using this approach I could distinguish three different cell populations (Figure 23B): *Piwi* expressing i-cells, (in red, including some multipotent i-cells and probably some early precursors of other cell lineages), early nematoblast progenitors (expressing both *Piwi* and *Mcol3-4a,* in yellow) and dividing nematoblasts organised in clusters (expressing only *Mcol3-4a,* in green). These three cell populations were all located in the central region of the planula endoderm but without any consistent relative distribution or position along the oral-aboral axis.
In the medusa, the expression of *Mcol3-4a* widely overlaps in nematoblasts with other genes including the *Clytia Sox* family transcription factors *Sox5, Sox13, Sox14, Sox12* and

Sox15 (Jager et al. 2011). I was particularly interested in *Clytia Sox15*, because of its very early Wnt3-dependent expression at the early gastrula stage (see Results II- PAPER 2) and its expression in both nematoblasts and differentiated nematocytes in the late planula (>48hpf) (Jager et al. 2011). Thus I combined analysis of the expression of *Sox15* and *Mcol3-4a* to map the appearance of nematoblasts and nematocytes during larval development.

1.1.3 *Sox15* is expressed during an extended period of nematogenesis

I performed *Sox15 in situ* hybridisation at the early gastrula, 24hpf and 48hpf planula stages. At the early gastrula stage, I detected *Sox15* expression in a subpopulation of ingressing cells at the oral pole, distributed in a similar manner to the i-cell markers, *Piwi* and *Nanos1* (Figure 24A, for *Piwi* and *Nanos1* see Figure 12, 44). Interestingly the expression of *Sox15* at this stage covers a broader domain then *Nanos1* and *Piwi*. At 24hpf *Sox15* mRNA was more weakly detected in the endoderm, with a few cells detected also in the ectoderm (Figure 24A). At this stage detection of the transcript was difficult, due to the weak intensity and diffuse distribution of the *in situ* hybridisation signal. This expression could reflect the onset of the expression of the gene in different cell populations dispersed in the planula ectoderm and endoderm. In contrast at 48hpf stage, *Sox15* expression was clearly detected in two different cell populations, one population scattered in the central endoderm and one in the ectoderm (Figure 24A-B). *Sox15* positive cells in the ectodermal layer had a characteristic morphology and are likely differentiating nematocytes (Jager et al. 2011).

Co-localisation studies using the *Mcol3-4a* probe in combination with the *Sox15* probe, showed that all *Mcol3-4a* positive cells also expressed *Sox15* (Figure 24B), and that *Sox15* is also expressed in differentiating nematocytes in the planula ectoderm, in which *Mcol3-4a* expression is no longer detected. These findings suggest that *Sox15* expression is maintained longer than the structural capsule gene *Mcol3-4a* and also that *Sox15* may be expressed in two different cell populations, rather than being restricted to the nematocytes.

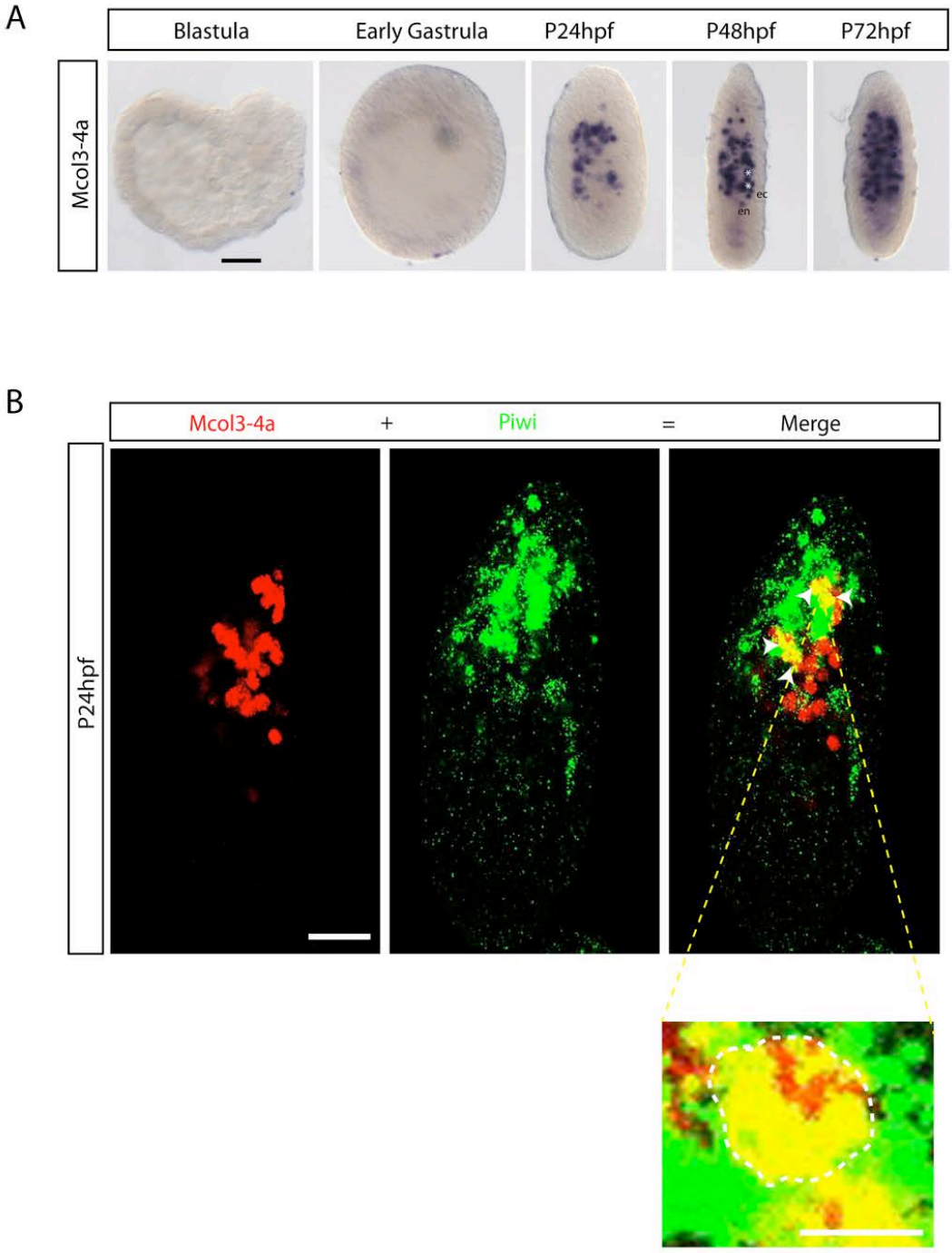

Figure 23: *Mcol3-4a* expression allows tracking of the nematoblast population during larval development.
A) *Mcol3-4a* mRNA is detected in cells in the planula endodermal region. In *situ* hybridisation with *Mcol3-4a* probe from blastula to planula 72hpf stages. From left to right: blastula, early gastrula, 24, 48, 72hpf planula stages. *Mcol3-4a* mRNA is not detected at blastula stage. Gene expression is detected at 24hpf in the endodermal region in a group of cells positioned mainly in the oral half. White asterisks indicate putative nematoblasts migrating into the ectoderm at 48hpf and at 72hpf.ec: ectoderm, en: endoderm. Scale bar 50µm.
B) *Mcol3-4a* expression coincides partially with *Piwi* expression. Confocal images showing the expression pattern of Mcol3-4a (red) and Piwi (green) at 24hpf planula. From right to the left: *Mcol3-4a*, *Piwi*, Merge (only one Z plane). Yellow colour indicates cells that show the co-expression of both genes. Oral pole at top. Scale bar 50µm. Lower image represent high magnification, showing a double-labelled cells (yellow). Scale bar 10µm.

In order to investigate whether *Sox15* is expressed in early nematoblasts, I performed co-localisation study using *Sox15* and *Piwi* at the early gastrula stage, the earliest stage in which *Sox15* is detected and before the onset of *Mcol3-4a* expression. It was possible to distinguish co-expression of *Sox15* and *Piwi* in a few cells, presumably corresponding to early stage nematoblasts expressing *Sox15* (Figure 24C). However it was unclear if there was a population of *Sox15*-expressing cells lacking *Piwi* expression. The *Hydra Sox15* ortholog is found to be weakly expressed in *Nanos* sorted i-cells, supporting the hypothesis of an i-cell origin for some of the *Sox15* positive cells (Table1 Annexes).

Based on these observations, it appears that *Sox15* represents a "pan nematogenetic", gene which has an early function in nematogenesis commitment and remains expressed right through the process of nematogenesis. Its function may not, however be restricted to nematogenesis, at least at early stages, accounting for the apparently wider distribution of *Sox15* expression across a broader oral domain in the early gastrula. In this context it cannot be excluded that *Sox15* is involved in both nematogenesis and neurogenesis. The timing and the localisation of *Sox15* expression are compatible with additional expression in a putative neuronal lineage, although we have yet to identify a neurogenesis gene expressed as early as the early gastrula stage (see following section). This scenario could thus be similar to the one described in *Nematostella*, in which *SoxB*(2) is expressed in common neuronal progenitors that give rise to nematocytes, neurosensory cells and ganglionic cells (Richards & Rentzsch 2014). Functional studies will be required to test the role of *Sox15* in *Clytia* nematogenesis and potentially in neurogenesis.

1.2 Neurogenesis during larval development

To follow neuroblasts and differentiated nerve cells I sought to use gene markers associated with neural fate choice and early neurogenesis (*eg* bHLH family genes) as well as late nerve cell markers.

In hydrozoans, transcription factors of the bHLH (Achaete-Scute, atonal-like), PRD (aristaless-like, prdl-a, prdl-b, gsc, rx, repo, PaxA / C, PaxB) and C2H2 Znf (Glis, Zic) families have been identified as regulators of neurogenesis (See introduction section 2.2.3 Reviewed in Galliot and Quiquand 2011).

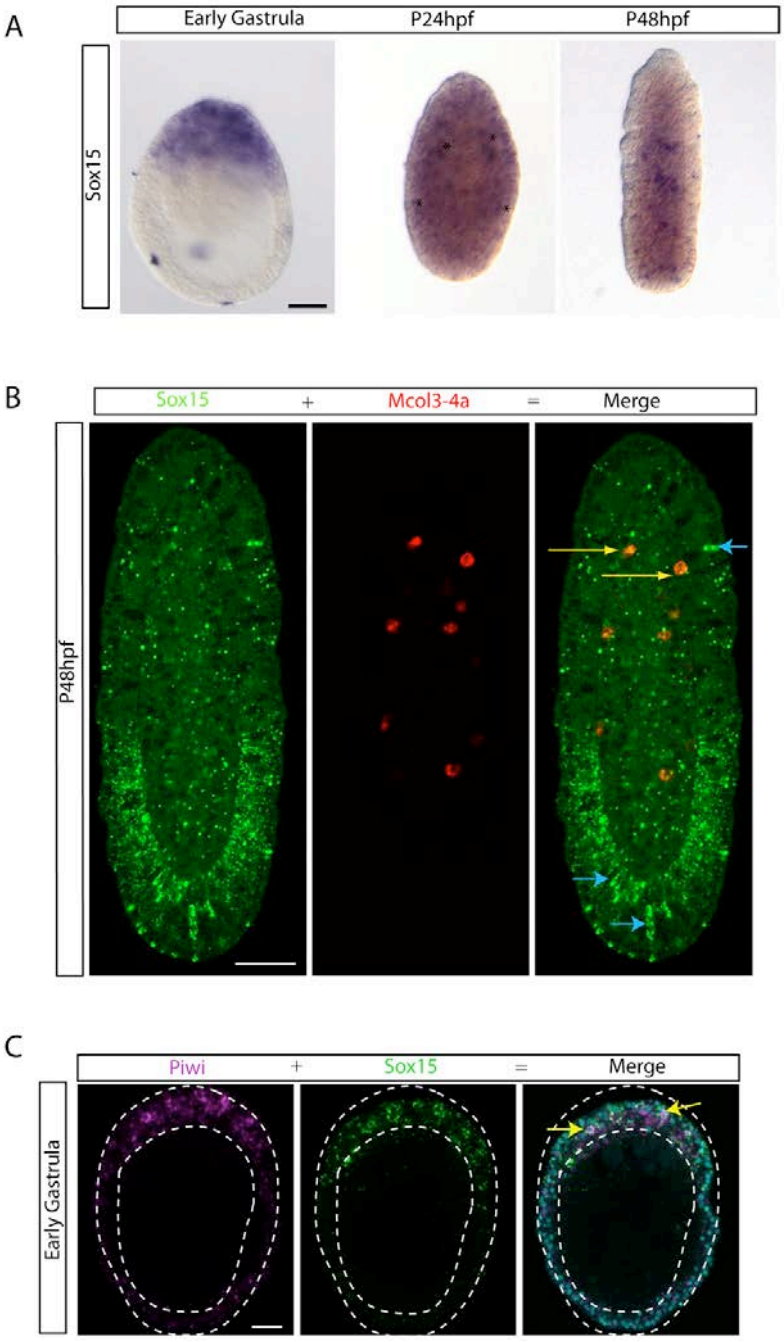

Figure 24: *Sox15* expression in nematoblasts and in differentiating nematocytes.
A) Expression pattern of Sox 15 during *Clytia* development. *In situ* hybridisation of *Sox15* from early gastrula to planula 48hpf. *Sox15* expression was detected at the oral pole in the early gastrula, in a wide population of cells. At 24hpf, it was weakly detected in few cells located both in the ectoderm and in the endoderm (black asterisks). At 48hpf *Sox15* mRNA was detected in two distinct cell populations, in the endoderm and ectoderm regions. Scale bar 50µm. **B) Some *Sox15* expressing cells in the endoderm are nematoblasts**. Confocal images showing the expression of *Sox15* (green) and *Mcol3-4a* (red), and the merged images (only one Z-plane) at 48hpf. *Mcol3-4a* expressing cells are restricted to the endoderm, while *Sox15* mRNA is found in the nematoblasts and in differentiating nematocytes (blue arrows). Yellow arrows indicate some cells expressing both genes, with a red core representing *Mcol3-4a* mRNA and green dots representing *Sox15* mRNA. **C) *Sox15* and *Piwi* double *in situ* at the gastrula stage**. Confocal image showing double FISH using *Piwi* (pink) and *Sox15* (green) probes. From left to right: *Piwi*, *Sox15*, Merged image. Yellow arrows indicate cells expressing both genes. Dashed lines represent the gastrula contour. Cyan: HOECHST stained nuclei. Oral pole at top of all the images. Scale bar 50µm.

I characterised some of these genes as putative candidates to follow *Clytia* neurogenesis. As potential markers of neural precursors I selected *Prdl-a*, *Asc-b* and *Zic-C*. As markers of differentiating and mature nerve cells, I used two neuropeptide precursors identified in the available *Clytia* transcriptome data. One was a precursor of the RFamide neuropeptide family, widely used as neurotransmitters in many animal species. The other coded for a GLWamide precursor known to be specifically involved in regulating larval settlement in hydrozoan planulae (Plickert et al. 2003).

I performed *in situ* hybridisation at successive developmental stages: early gastrula, 24hpf, 36hpf (intermediate stage between the end of gastrulation and full differentiation of the endodermal layer), 48hpf and 72hpf planula. None of the genes selected showed detectable expression at early gastrula stage (not shown) or at 24hpf, indicating that neural fate specification occurs only once the polarity of the developing larva is well established and gastrulation completed.

1.2.1 Clytia *Prdl-a* as putative neuronal marker

By reciprocal blast using the *Hydra Prdl-a* sequence I identified the *Clytia Prdl-a* ortholog from the available *Clytia* transcriptome (validated through phylogenetic analysis; Figure 25). *Prdl-a* codes for a homeodomain proteins belonging to the wider Paired family. In *Hydra* polyps, Prdl-a acts as regulator of neurogenesis during head regeneration. It is expressed in a subpopulation of neurons localised around the *Hydra* hypostome and also transiently in the endoderm during regeneration (Gauchat et al. 1998). During embryonic development *Clytia Prdl-a* expression was detected beginning at 36hpf in cells scattered through the aboral half of the planula endodermal region (Figure 26A), suggesting that these cells are ready to migrate into the ectoderm prior to differentiation. Others *Prdl-a* positive cells were positioned more centrally and showed an i-cell- like morphology (round shape with a large nucleus, Figure 26B) consistent with expression in nematoblasts. At later stages (48hpf and 72hpf) the expression of *Prdl-a* was only weakly detectable, suggesting that wave of production of a wave of *Prdl-a* expressing neurons is followed by reduced expression in later stages of development (Figure 26A).

To validate *Prdl-a* as a neural marker I analysed its expression pattern in the adult jellyfish (Figure 26C). *Prdl-a* expression was detected in the tentacle bulb on the proximal side of

the differentiation zone (Figure 26C), defined as the β region by Denker et colleagues, (see introduction section 2.2.3 Figure 17) and in a subset of ectodermal nerve cells in the manubrium ectoderm (Figure 26C). To confirm the neural identity of these *Prdl-a* expressing cells, it would be useful to examine their morphology in more detail, or by comparing their distribution with that of neurons expressing different neuro-transmitters.
The *Hydra Prdl-a* gene is similarly expressed in neurons surrounding the mouth (Gauchat et al. 1998). No *Prdl-a* expression was detected in the gonads, in the nerve ring or in the circular canal (Figure 26C). These observations indicate that *Prdl-a* is expressed in a sub-population of nerve cells of the medusa, but also in some putative neuroblasts. This hypothesis is supported by the analysis of expression of the *Hydra Prdl-a* ortholog in sorted i-cells (Table1 Annexes). To address this hypothesis I performed double *in situ* hybridisation using *Prdl-a* probes in combination with *Piwi* probes at larval stages. I was unable to demonstrate any co-expression, however this result is not conclusive because of the relatively weak expression of *Prdl-a.*
To resolve this question it would be useful to perform co-localisation experiments at the medusa stage, to see if *Piwi* and *Prdl-a* have overlapping expression domains, as is the case for *Piwi* and *Mcol3-4a* (see Figure 17 introduction).

1.2.3 Clytia *Asc-b* is a expressed in the endoderm in both planulae and medusae

Among the many described proneural gene families I decided to investigate a member of the Achete scute family, *Clytia* Asc-b. Asc proteins form a subfamily of the wider bHLH transcription factor family, involved in promoting neural progenitor commitment (Bertrand et al. 2002). *Clytia Asc-b* was isolated as a full-length clone by BLAST searches using the *Hydra CnASH* sequence from available *Clytia* transcriptome data. In *Hydra CnASH* is expressed both in differentiating sensory neurons (Hayakawa et al. 2004) and in differentiating nematoblast (Lindgens 2004). A detailed phylogenetic analysis, including bHLH proteins from *Nematostella, Hydra*, *Acropora*, *Drosophila*, and *Human* (sequences extracted from (Gyoja et al. 2012), determine the relationships between 29 *Clytia* bHLH proteins (Figure 27). These included *Clytia* orthologs of numerous proneural genes including human *Neurogenin* a key regulator of neuronal fate (Kageyama et al. 2005). The

Clytia gene that I had selected, for further analysis, *Asc-b*, was found to be the ortholog of *Podocoryne Ash2* gene (Seipel et al. 2004) and not of *CnASH (Asc-a)*.

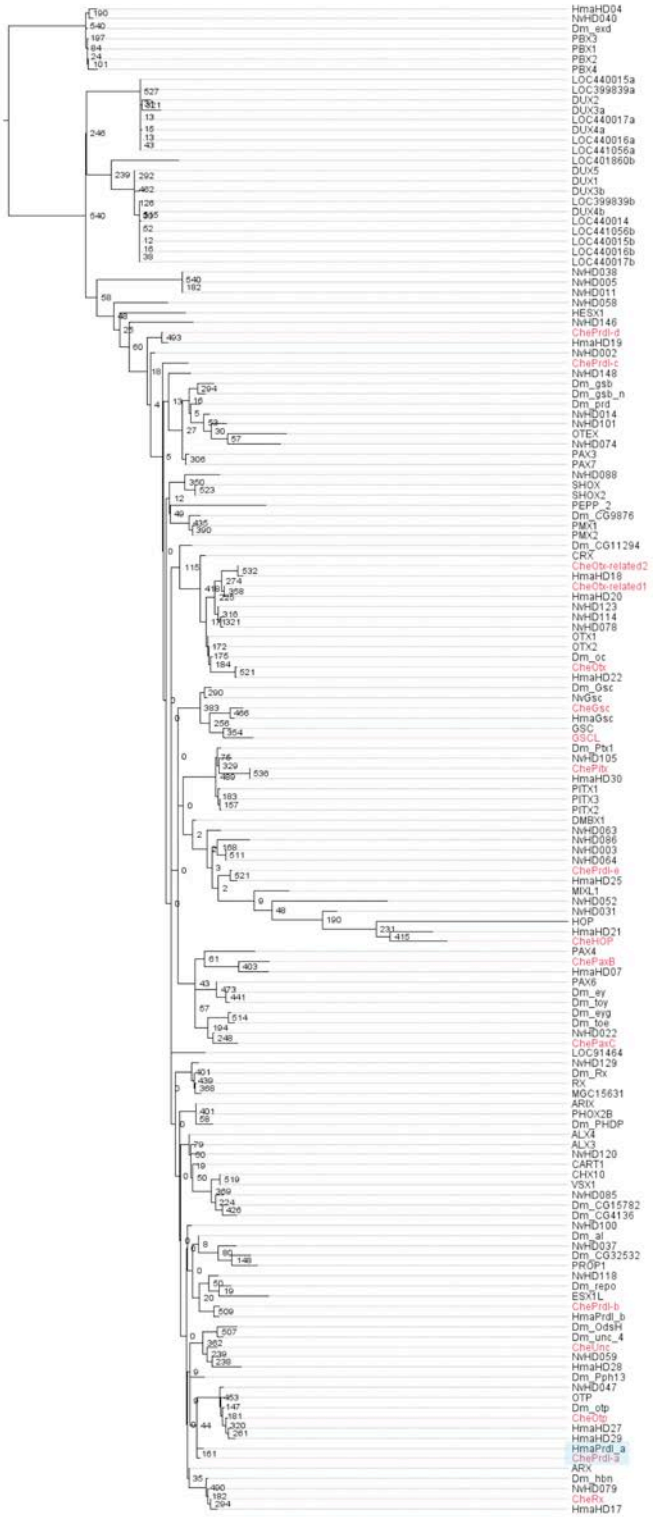

Figure 25: Gene orthology of metazoan paired-class homeobox transcription factors.
Phylogenetic analysis of Prdl-a transcription factors.
The amino-acid alignment of paired subfamily sequences was extracted from (Lapébie et al. 2014; Ryan et al. 2006). *Clytia* and Hydra *Prdl-a* orthologs pairs can be clearly identified (shaded in blue). *Clytia* genes are indicated in red.
The following sequences from *Clytia hemisphaerica* have been added
(Sequence name: Accession number).
Prdl-b:KT318135,
Prdl-d:KT318136,
HOP: KT318137,
Pitx: KT318138,
Rx: KT318139,
Otx-related-2:KT318140,
Ot: KT318141,
Otx: KT318142,
Otx-related-1: KT318143,
Prdl-e: KT318144,
Prdl-c:KT318145,
Unc:KT318146,
PaxB:KT318147,
PaxC :T318148

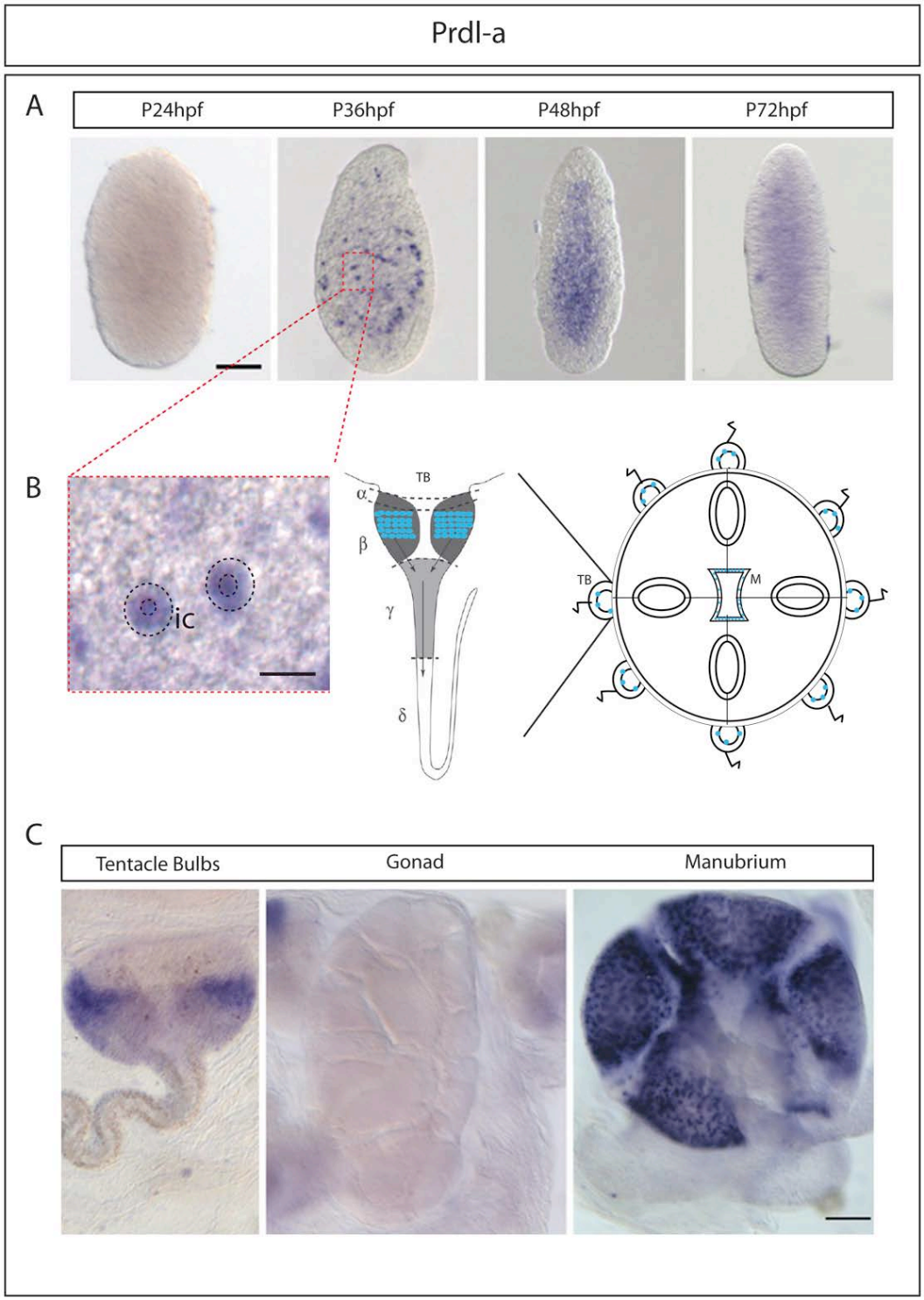

Figure 26: *Prdl-a* expression during larval development and in the adult medusa.
A) ***In situ* hybridisation of *Prdl-a* during larval development at 24,36, 48 and 72 hpf.** *Prdl-a* mRNAwas first detected at 36hpf, concentrated in the aboral endoderm. A later stages the expression is more widespread but weaker. Scale bar 50µm. Oral pole at the top of all the images.
B) High magnification showing cell morphology of *Prdl-a* expressing cells at 36hpf. Scale bar 10µm. ic: i-cells. **C) Medusa stage.** *Prdl-a* expression was detected in a subpopulation of ectodermal cells in the upper part of the tentacle bulbs, and in subpopulation of ectodermal cells in the manubrium. Scale bar 100µm. Tentacle bulbs are oriented with their proximal pole on the top, manubrium oriented with mouth on the bottom, in all images. The Medusa cartoon shows the site of *Prdl-a* expression (light blue) in the adult, in particular in tentacle and tentacle bulbs (TB) (corresponding to the differentiation region β, modified from Denker et al. 2008) and in the manubrium (M).

In *Podocoryne Ash2* expression is restricted to the endoderm, both in medusa and in planula. It is unclear which type of cells expresses the gene, but they were tentatively proposed to be secretory cells in *Clytia* developing larvae *Asc-b* expression was observed in few endodermal cells at 36hpf, restricted to the aboral half of the embryo. At 48hpf the expression was weaker and at 72hpf the expression was barely detectable (Figure 28A). Expression of this gene at medusa stage was detected in the endodermal cells of the tentacle bulbs, in the circular canal endoderm and in the manubrium endoderm. No expression was detected in gonad endoderm (Figure 28B) or in the radial canals. I could not identify with certainty the cell types in which *Asc-b* is expressed. *Asc-b*, as seems the case of *Ash2* in *Podocoryne* (see Introduction 2.3.2) may not be expressed in neurons. Detailed morphological analysis, combined perhaps with histological characterisation (*e.g.* PAS staining) would be useful to determine the cell type that expresses *Asc-b*. Whatever the identity of these cells, they are probably derived from i-cells since the *Hydra Asc-b* ortholog is expressed in i-cell sorted population (Hemmrich et al. 2012) (see Table1 Annexes).

1.2.4 *Zic-C* is expressed in a sub-type of neural cells specific to medusa tentacles.

Zic family genes encode C2H2-type zinc finger transcription factors. In vertebrates, *Zic* genes are present in multiple copies (5 copies in mice and in *Xenopus*) and are involved in a plethora of biological events at different times during development. For example, during gastrulation *Zic* genes are involved in germ layer specification while during organogenesis they are required for neural tube formation. Moreover, *Zic* genes show a redundant role in central nervous system development (Houtmeyers et al. 2013). Several studies in cnidarians and ctenophores suggest an ancestral role for *Zic* genes in neuronal development (Layden et al. 2010; Lindgens 2004). In *Nematostella* five *Zic* genes have been identified. These genes show overlapping expression domains in presumptive tentacle ectoderm in the planula and in tentacle ectoderm in the polyps, which are considered highly neurogenic structures. In *Hydra Hyzic* is expressed in early nematoblast precursors, thus it implicated in the nematogenesis process (Lindgens 2004).

At start of this study I could only identify one *Zic* gene in the available *Clytia* transcriptome dataset. Phylogenetic analysis revealed that this gene is the ortholog of *Nematostella Zic-C* (Figure 29), and so the gene was named *Zic-C* and that it groups in a clade with other

cnidarian genes. A second *Clytia Zic* gene (named *CheZic*), found later is the ortholog of the *Hydra Hyzic*.

I investigated the expression pattern of *Clytia Zic-C* gene during embryonic development and in the adult medusa. In planulae *Zic-C* mRNA was weakly detected at the aboral pole, at 48 and 72hpf (Figure 30A). In contrast, in the medusa, *Zic-C* expression was strongly detected in the tentacle and in the tentacle bulb ectoderm. *Zic-C* expressing cells are most likely neurosensory cells as indicated by their neuronal process (Figure 30-B). *Zic-C* neuronal cells appear to be specifically associated with the tentacles, since no expression was detected in the manubrium ectoderm or in gonad ectoderm or in nerve ring.

Consistently with previous data in non-bilaterian species, these observations indicate that *Zic-C* is expressed late during development and in a tentacle specific neuronal subtype.

In support of this hypothesis the *Hydra Zic-C* ortholog is not enriched in sorted i-cell population (Table1 Annexes).

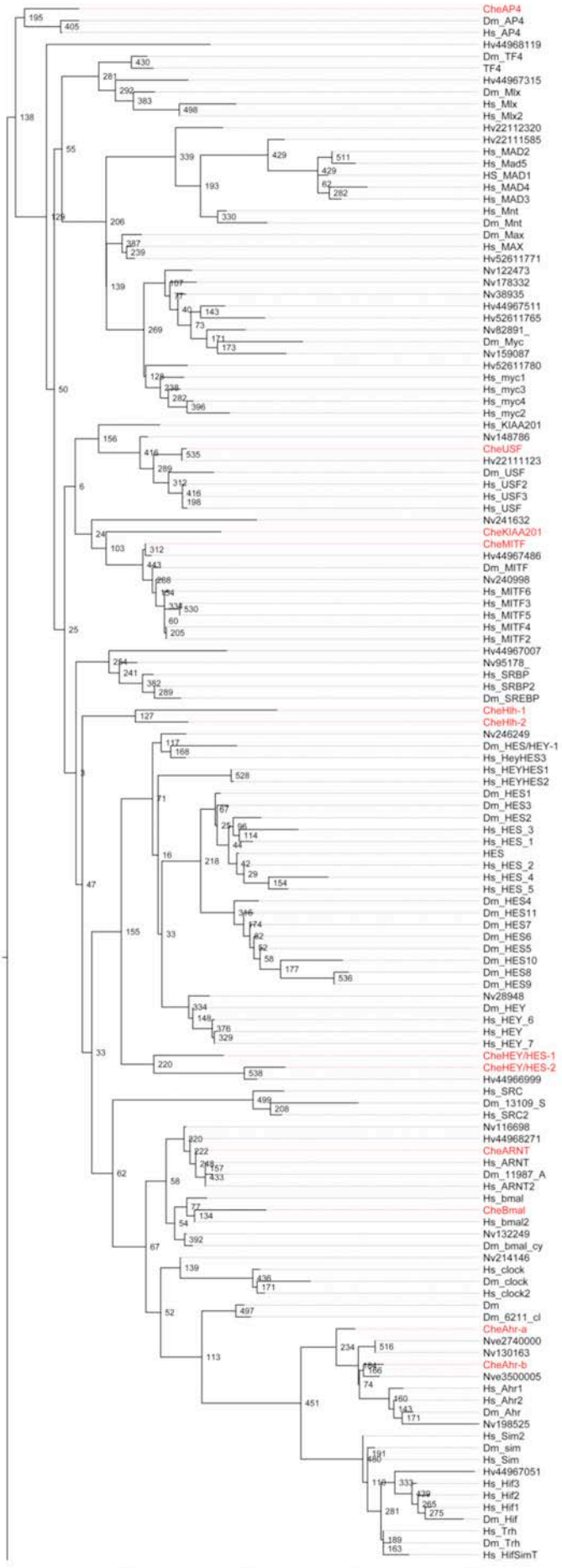

Figure 27: Gene orthology of metazoan bHLH family.
Phylogenetic analysis of bHLH transcription factor domain-containing sequences. The sequence were extracted from (Lapébie et al. 2014). The analysis confirms the placement of the *Clytia* proteins within the Achaete-scute family. Asc-b is the ortholog of *Podocoryn*e Ash2, *Hydra vulgaris HvAsh-like* and *Human Ascb3 (*Grey box*)*. Note that the *Clytia* gene *HlhIE1* belongs to the same clade but it was named previously according to its expression characteristics. *Clytia* genes are indicated in red. The following sequences from *Clytia hemisphaerica* have been added (Sequence name: Accession number)
PTFb: KT318149,
Neurogenin: KT318150,
Paraxis: KT318151,
AP4: KT318152,
Asca-1: KT318153,
Hlh-4: KT318154,
HEY/HES-2: KT318155,
HAND: KT318156,
Hlh-6: KT318157,
Twist: KT318158,
Net: KT318159,
Hlh-5:KT318160,
Hlh-1: KT318161,
Hlh-2: KT318162,
HEY/HES-1:KT318163,
USF:KT318164,
KIAAA2018: KT318165,
Bmal: KT318166,
Hlh-3: KT318167,
Ahr-b: KT318168,
ARNT: KT318169,
MITF: KT318170,
Asca-2: KT318171,
MIST-b: KT318172,
Ahr-a: KT318173,
MIST-a: KT318174.

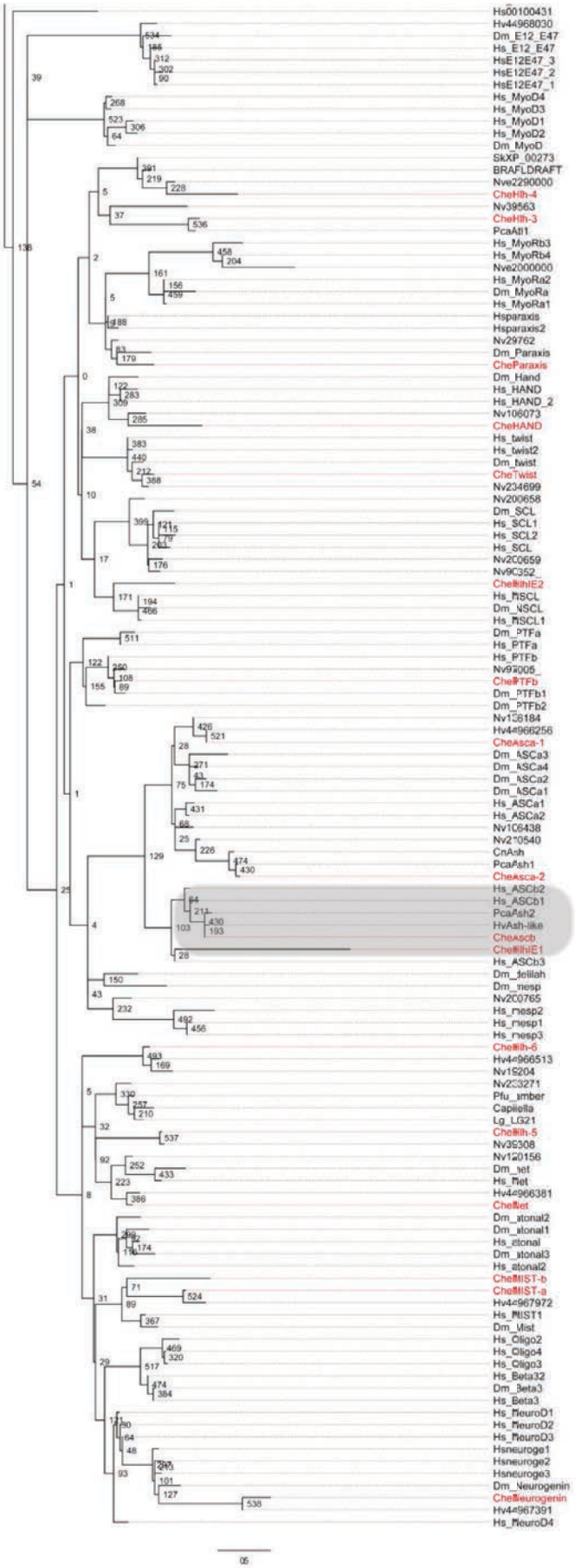
Hs00100431
Hv44968030
Dm_E12_E47
Hs_E12_E47
HsE12E47_3
HsE12E47_2
HsE12E47_1
Hs_MyoD4
Hs_MyoD3
Hs_MyoD1
Hs_MyoD2
Dm_MyoD
SkXP_00273
BRAFLDRAFT
Nve2290000
CheHlh-4
Nv39563
CheHlh-3
PcaAtl1
Hs_MyoRb3
Hs_MyoRb4
Nve2000000
Hs_MyoRa2
Dm_MyoRa
Hs_MyoRa1
Hsparaxis
Hsparaxis2
Nv29762
Dm_Paraxis
CheParaxis
Dm_Hand
Hs_HAND
Hs_HAND_2
Nv106073
CheHAND
Hs_twist
Hs_twist2
Dm_twist
CheTwist
Nv234699
Nv200658
Dm_SCL
Hs_SCL1
Hs_SCL2
Hs_SCL
Nv2C0659
Nv9C352_
CheHlhE2
Hs_NSCL
Dm_NSCL
Hs_NSCL1
Dm_PTFa
Hs_PTFa
Hs_PTFb
Nv99005_
ChePTFb
Dm_PTFb1
Dm_PTFb2
Nv136184
Hv4e966256
CheAsca-1
Dm_ASCa3
Dm_ASCa4
Dm_ASCa2
Dm_ASCa1
Hs_ASCa1
Hs_ASCa2
Nv106438
Nv2C0540
CnAsh
PcaAsh1
CheAsca-2
Hs_ASCb2
Hs_ASCb1
PcaAsh2
HvAsh-like
CheAscb
CheHlhE1
Hs_ASCb3
Dm_Jelilah
Dm_nesp
Nv200765
Hs_nesp2
Hs_nesp1
Hs_nesp3
CheHlh-6
Hv4e966513
Nv19204
Nv233271
Pfu_amber
Capitella
Lg_LG21
CheHlh-5
Nv36308
Nv120156
Dm_Net
Hs_Net
Hv4e966381
CheNet
Dm_atonal2
Dm_atonal1
Hs_atonal
Dm_atonal3
Hs_atonal2
CheMIST-b
CheMIST-a
Hv4e967972
Hs_MIST1
Dm_Mist
Hs_Olig02
Hs_Olig04
Hs_Olig03
Hs_Beta32
Dm_Beta3
Hs_Beta3
Hs_NeuroD1
Hs_NeuroD2
Hs_NeuroD3
Hsneuroge1
Hsneuroge2
Hsneuroge3
Dm_Neurogenin
CheNeurogenin
Hv4e967391
Hs_NeuroD4
05

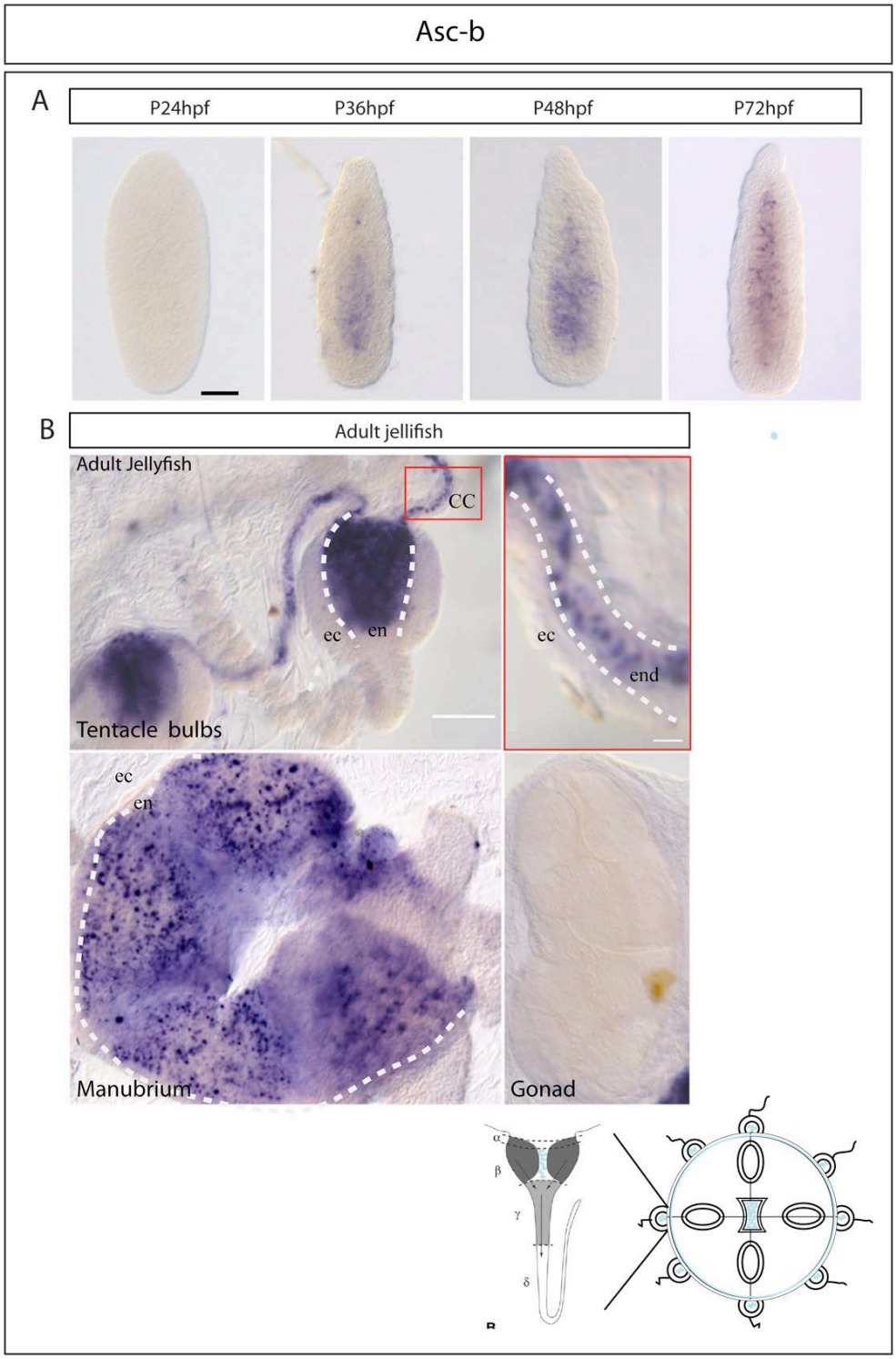

Figure 28: *Asc-b* expression during larval development and in the adult medusa.
A) *In situ* hybridisation of *Asc-b* at 24,36, 48, 72 hpf. *Asc-b* was first detected at 36hpf, weakly in the aboral region of the endoderm. Scale bar 50µm.
B) Medusa stage. *Asc-b* mRNA was detected in a subpopulation of cells in the endodermal region of tentacle bulbs. Scale bar 10µm. Boundary between ectoderm and endoderm indicated by white dotted lines. On the left, a higher magnification view of the area boxed in red showing *Asc-b* expression in the endoderm of the circular canal (cc). Scale bar 10µm.
Asc-b expression in the manubrium endoderm. No expression was detected in mature female gonads. Ec: endoderm, ec: ectoderm, cc: canal circular. The Medusa cartoon shows the site of *Asc-b* gene expression (Cyan) in the adult, in particular in tentacles and tentacle bulbs (modified from Denker et al 2008).

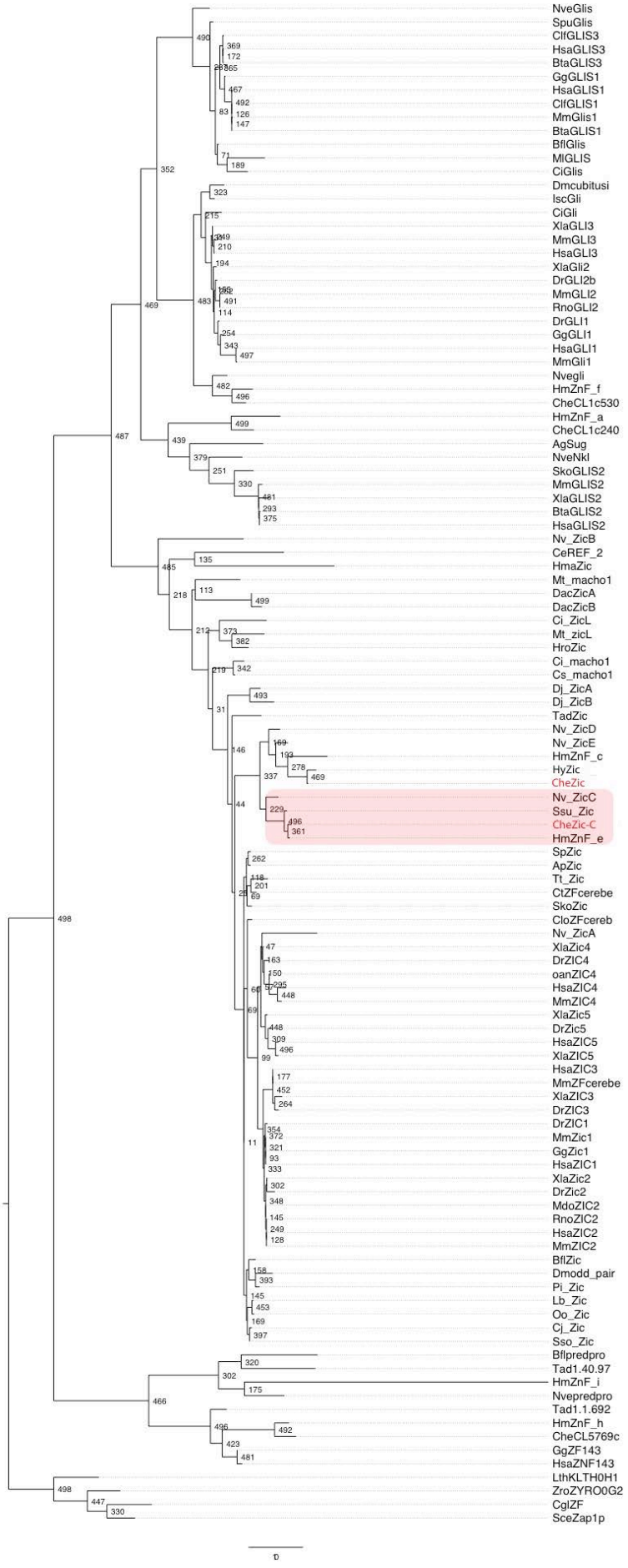

Figure 29: Gene orthology of metazoan Gli/Zic superfamily.

Phylogenetic analysis of Zic/Gli family zinc finger motifs. The sequence were extracted from (Layden et al. 2010). Genes identified in this study are in red.

Clytia Zic-C groups with the uncharacterised gene *Hydra* gene *HmZnfe* with *Nematostella Zic-C,* and with *Scalionema suvaense Zic gene* (shaded in red). The additional *Clytia* sequence that was found is orthologous of the *Hydra* gene *HyZic*, involved in early nematogenesis (Lindgens 2004).

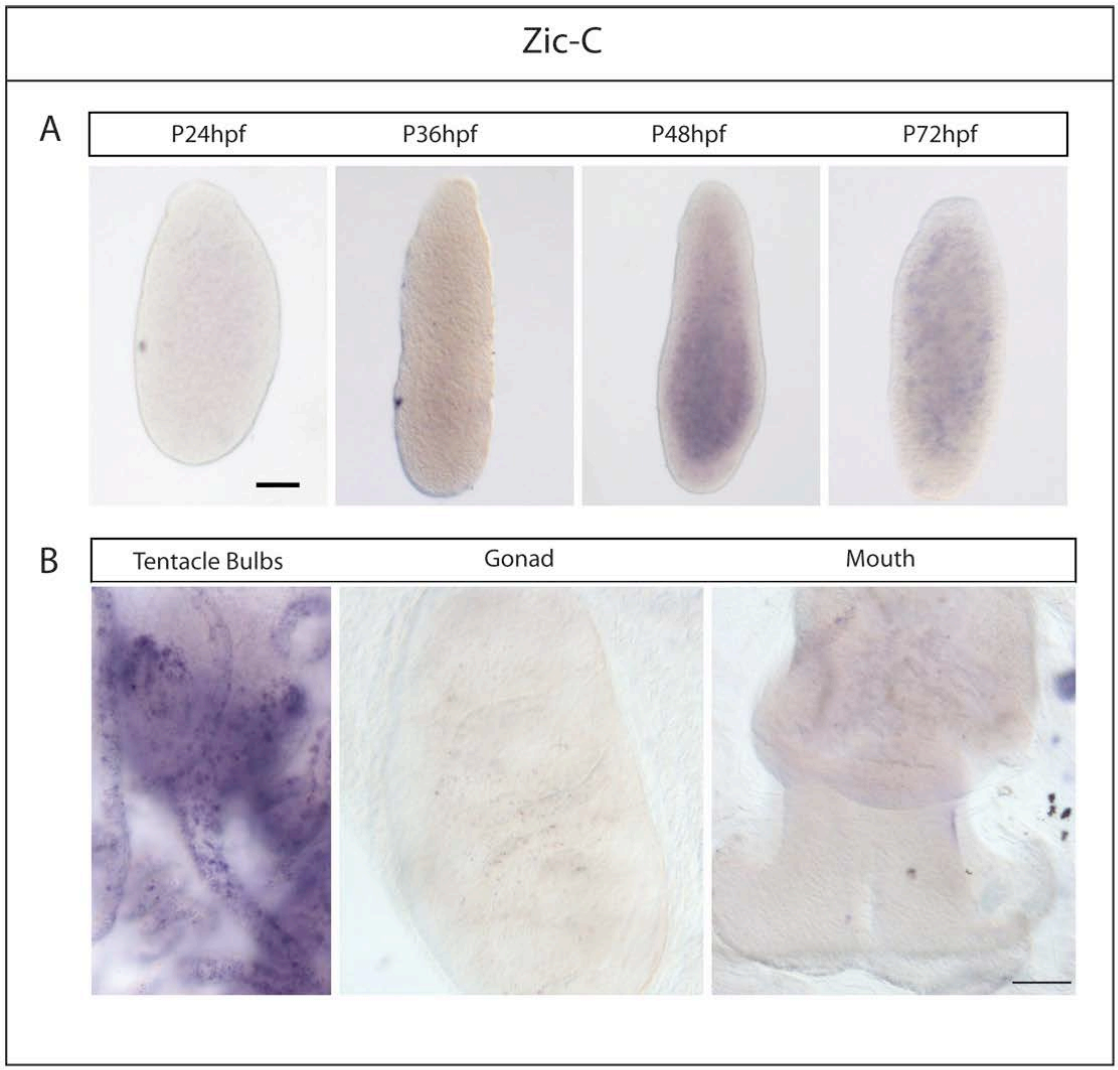

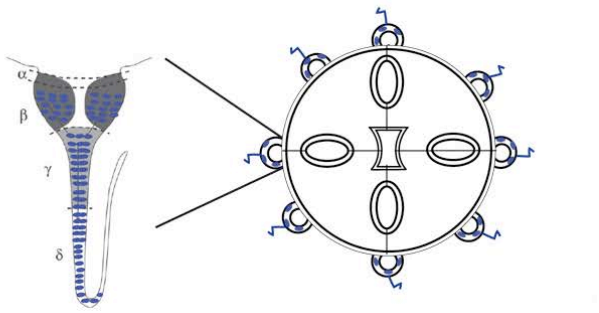

Figure 30: *Zic-C* expression during larval development and in the medusa.
A) *In situ* hybridisation of *Zic-C* during larval development at 24, 36,48, 72hpf. *Zic-C* mRNA was first detected at low levels at 48hpf stage in the aboral endoderm. Scale bar 50µm. **B) Medusa stage**. Zic-C was detected strongly in cells in the tentacle and tentacles bulbs ectoderm; *Zic-C* was not detected either in the manubrium ectoderm or in the gonad ectoderm, or in the radial/circular canal or in the nerve ring. Scale bar 100µm. Medusa cartoon showing the site of *Zic-C* gene expression (dark blue) in the adult, in particular in tentacle and tentacle bulbs (corresponding to the β, γ, δ differentiating/ differentiated tentacle areas, modified from Denker et al. (2008).

1.2.5 Neuropeptide expression defines mature neural subpopulations

Neuropeptides are major neurotransmitter molecules in cnidarians (Grimmelikhuijzen et al. 1996) and have been used extensively to visualise the cnidarians nervous system (see Introduction 2.2.2). To monitor nerve cells differentiation I used GLWamide and RFamide neuropeptide precursors as markers. The mRNA of one of the RFamide precursor transcript (PP5) was detected in few ectodermal cells at 36hpf planula stage (Figure 31A). At 48hpf PP5 expression was detected in cells positioned in the lateral ectoderm along the oral-aboral axis (Figure 31A), but mainly excluded from the polar region, as reported for the other hydrozoan planulae (Plickert et al. 2003).

Immunostaining with a *Clytia* specific RFamide antibody (kindly gift of Dr. Gáspár Jékely Max Plank Institute for developmental Biology, Tübingen, Germany) showed an extensive nerve net between lateral ectoderm and endoderm of the planula (Figure 31B). Cells-bodies were positioned at the base of the ectoderm. These RFamide neuropeptide expressing cells have been described as ganglionic cells (Martin 1988).

In the medusa *PP5* mRNA was detected throughout the manubrium ectoderm, in the medusa tentacle, in the tentacle bulb ectoderm and in the nerve ring (Figure 31C).

In *situ* hybridisation revealed that expression of the GLWamide precursor *PP2* is restricted to larval stages (Figure32A). At 36hpf, only a few cells express the *PP2* transcript, while the number of cells increases at 48 and 72hpf. The mRNA was detected in a band of cells localised around the aboral pole from which neural projections connect the outer and the inner cell layer, typical of sensory cells (Figure 32A).

These observations indicate that differentiated nerve cells first start to appear at 36hpf, and that *Clytia* RFamide and GLWamide neuropeptides are expressed in two different populations of neurons, likely corresponding to ganglionic and sensory neuron respectively. The absence of the PP2 GLWamide precursor in medusae (Figure 32B) is consistent with its specific role only in metamorphosis. A second GLWamide precursor named PP11 is expressed in the medusa (G. Quiroga and P. Lapébie, unpublished results).

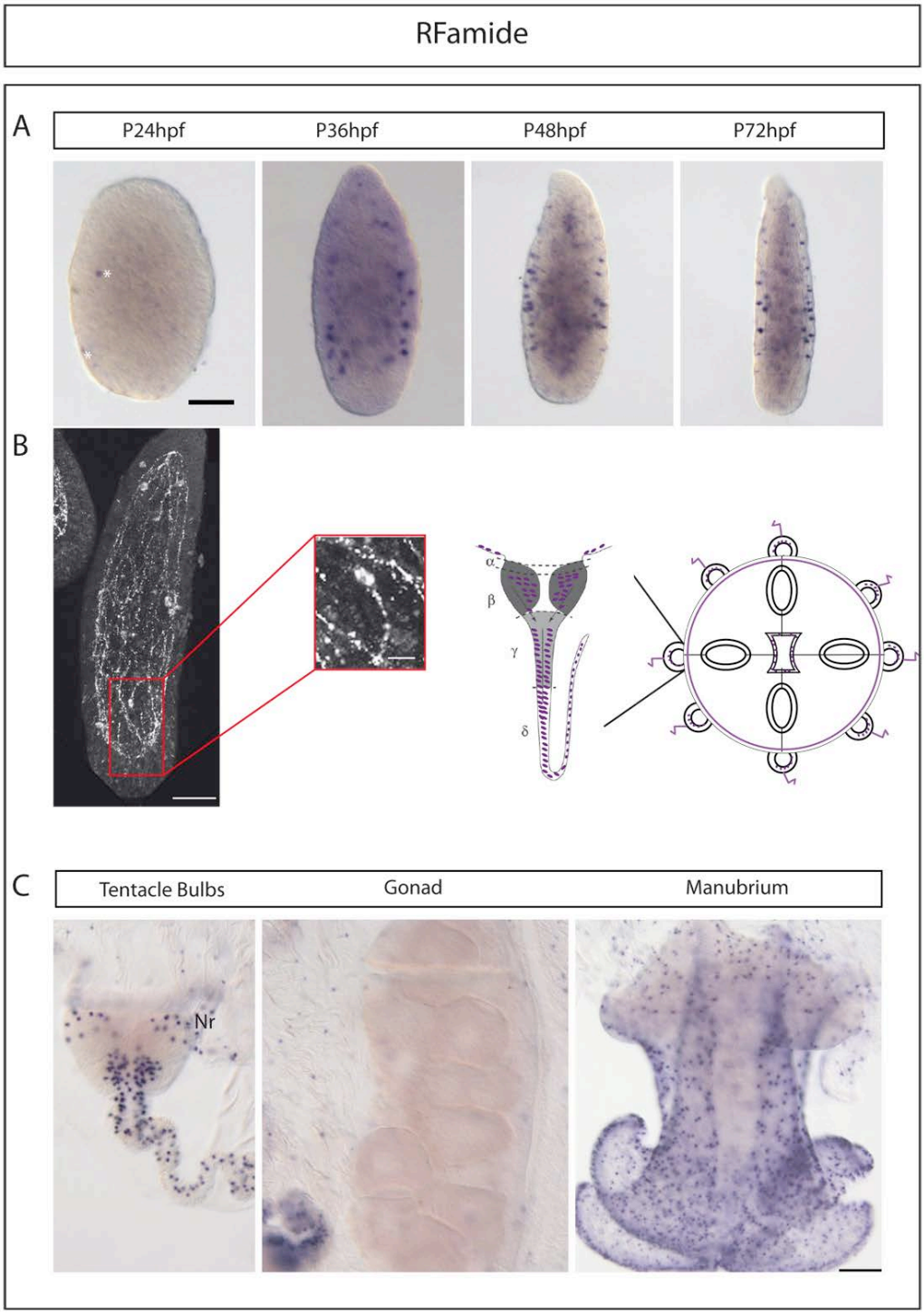

Figure 31: *RFamide* expression during larval development and in the adult medusa.
A) ***In situ* hybridisation of the *RFamide* precursor gene PP5 during larval development at 24, 36,48, 72 hpf.** *PP5* mRNA is detected in ectodermal cells, and starting from 36hpf, in the lateral ectoderm. Scale bar **50**µm**.** B) ***Clytia* specific RFamide** antibody staining at 48hpf. On the left a higher magnification view of the area boxed in red, showing the morphology of neuronal RFamide expressing cells**.** Scale bar 10µm.
C) **Medusa stage**. *RFamide* expressing neurons are strongly detected in tentacles, in tentacle bulb ectoderm and in the nerve ring (Nr), as well as in scattered cells in the bell epithelia. Scale bar 100µm. Nr: nerve ring. The Medusa cartoon shows the site of *PP5* expression (purple) in the adult, in particular in tentacle and tentacle bulbs (corresponding to the β, γ, δ differentiating/ differentiated tentacle areas, modified from Denker et al 2008).

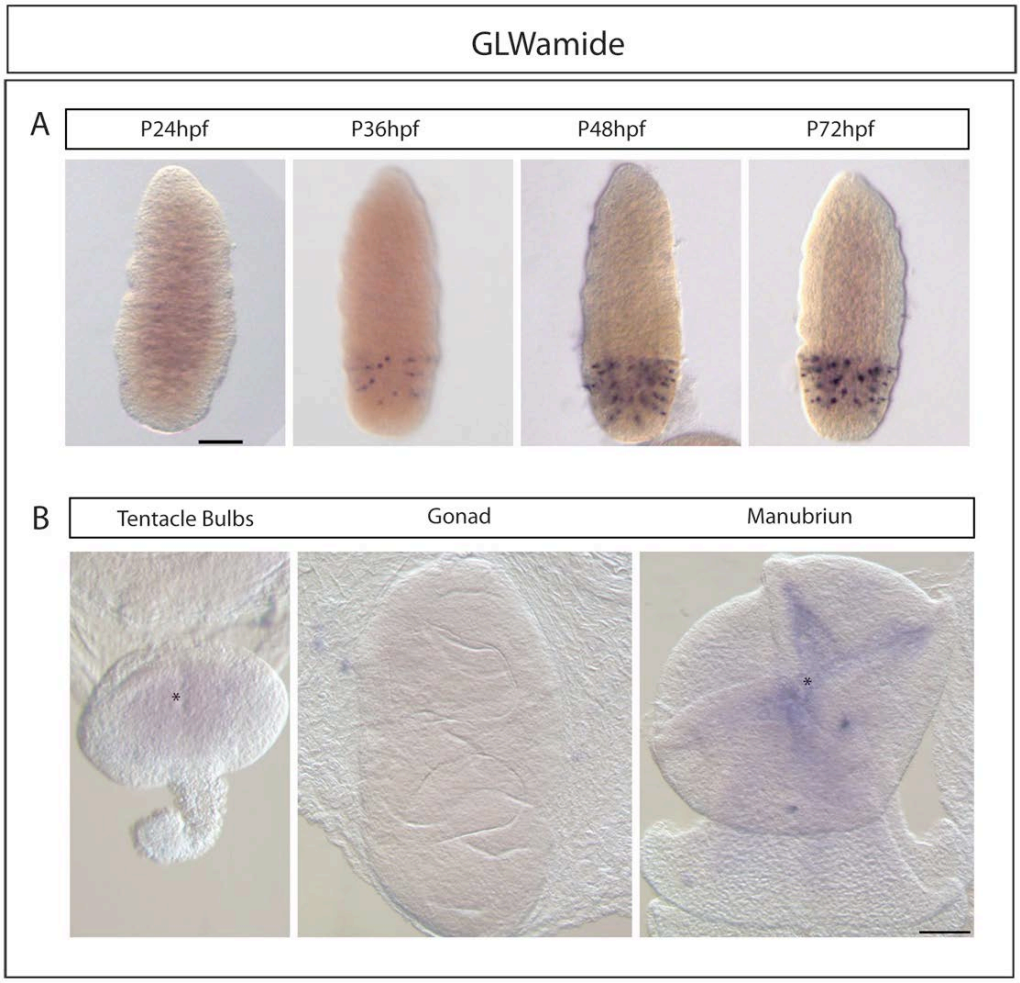

Figure 32: *GLWamide* expression during larval development and in the adult medusa.
A) ***In situ* hybridisation of the GLWamide precursor PP2 during larval development at 24, 36,48, 72 hpf**. PP2 mRNA in the planula is detected in ectodermal cells starting for 36hpf, positioned at the aboral pole. Scale bar 50µm**. B) Medusa stage**. *PP2* mRNA could not be detected in the medusa. Black asterisks indicate non specific signal. Scale bar 50µm.

1.3 Gland cell formation in Clytia planulae and in the medusae

I followed gland cell formation during *Clytia* larval development and in the medusa by *in situ* hybridisation using the *Antistasin* gene

Antistasin is a serine protease inhibitor detected in *Hydra* gland cells with a digestive function (zymogen cells). Sequence analysis revealed that *Clytia* Antistasin contains seven antistasin domains, confirming that it belongs to the antistasin multigenic family. It was not possible to perform a phylogenetic analysis since the number of domains and the type of domain is highly variable among species. *Antistasin* expression analysis revealed that at 24hpf, the transcript is expressed in the oral endodermal region. At later stages, *Antistasin* expressing cells increased in number and were found through the endoderm (Figure 33A),

with some cells also detected weakly in the ectoderm at 72hpf (Figure 33A), where other types of gland cell have also been described (Bodo and Bouillon 1968).

To confirm the identity of the *Antistasin* expressing cells I performed expression analysis in the medusae. At this stage *Antistasin* was detected strongly and exclusively in gland cells of the manubrium (Figure 33B). These cells show a club shape, typical of zymogen cells (Figure 33C) and are located in the manubrium endoderm and more specifically in the stomach region.

These observations suggest that *Antistasin* positive cells are gland cells and that in the planula they could correspond to the "*granuleuse*" gland cells described by Bodo and Bouillon (1968) since they are the only type of gland cells described in both layers at this stage. In addition an i-cell origin for *Antistasin* positive gland cells is supported by the level of *Hydra* Antistasin ortholog in separated i-cells and in the endodermal cells (Table 1, Annexes).

1.4 Germ cell genes in Clytia

It is not known when the germ cells fate is specified during the *Clytia* life cycle, *i.e.* whether this fate choice is already made for some cells from i-cell in the planula, in the circulating i-cells in the stolon system of the polyp colony or not until i-cells reach the gonad in the medusa stage. To try to identify germ cell precursors during larval stages in *Clytia*, I tested multiple members of several conserved gene families associated with germ cell formation in bilaterian species, specifically the Boule/DAZ family and Tudor domain proteins. Boule/DAZ family members are RNA binding proteins and include Boule, DAZ and DAZL. Ten Boule-related sequences were identified from the *Clytia* transcriptome collection and three full-length cDNA clones were retrieved from a cDNA library for which ESTs were available (Chevalier et al 2006). Seven sequences from the *Hydra vulgaris* genome and four sequences from the *Nematostella vectensis* genome were also identified as belonging to the *Boule/DAZ* family. Phylogenetic analysis suggested that a duplication event occurred specifically in the cnidarian lineage (Figure 34A). I selected three boule genes for *in situ* hybridisation: *Boule1-a*, one of the two orthologs of the Bilaterian Boule/Daz gene, as well as genes from a cnidarian specific group, *Boule-like-1a,* and *Boule-like-1-b.* The Boule 1-a amino acid sequence includes the conserved motifs RNP1 and RNP2, as well as conserved amino acids present at diagnostic positions considered as the

molecular signature of Boule proteins (Figure 34B). The *Boule1*-a transcript was detected exclusively in the germ cells in both male and female *Clytia* jellyfish gonads (Figure 35A), but not at other i-cell sites such as tentacle bulbs. The profile of expression of *Boule-1a* in both male and female gonads was very similar to that reported for *Nanos1* and *Piwi*, suggesting the *Boule1-a* is expressed in i-cells but only in the gonads. Conversely during embryonic development no *Boule-1a* expression was detected. In contrast, *Boule-like1-a* and *Boule-like-1b* transcripts were detected both during larval development and in the medusa. *Boule-like-1a* transcripts were detected for the first time at 24hpf in scattered cells located between the endodermal and the ectodermal layers (Figure 35A), as described for *Nanos1* and *Piwi* (Leclère et al. 2012). In the adult medusa its expression appeared restricted to tentacle bulbs, in a population of cell located between ectoderm and endoderm. *Boule-like1-b* mRNA was detected in both ectoderm and endoderm at 24 and 48hpf, while it was barely detectable at 72hpf (Figure 35A). In the adult *Boule-like1b* expression was restricted to female gonads and it was ubiquitously expressed in oocytes and eggs (Figure 35-B). These results suggest that *Boule1-a* is exclusively expressed in germ cells and can therefore be used as a specific germ cells marker and that germ cell fate is not specified until the medusa stage. Tudor domain proteins are characterised by the presence of the tudor domain (Ponting 1997), but can also contain other domains in a variety of combinations. This is reflected in the diversity of biological processes in which tudor domain proteins are involved. The role of *Tudor* itself in germ cell formation has been demonstrated in different taxa. *Drosophila tudor* mutants fail in to form pole cells (Thomson & Lasko 2005), while *Tdrd1/Mtr1* gene deletion in mouse leads to complete male sterility (Chuma et al. 2006).

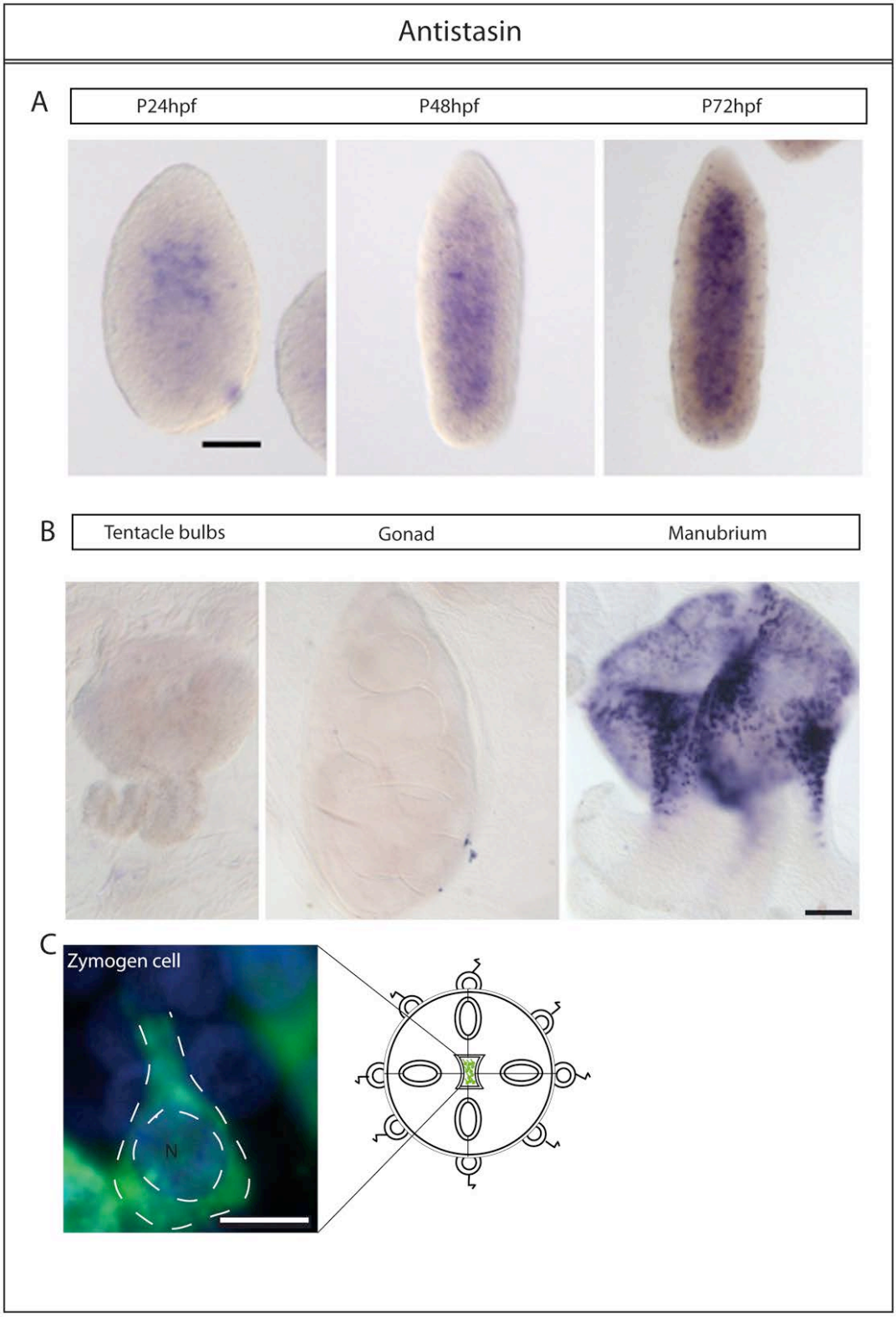

Figure 33: *Antistasin* expression during larval development and in the adult medusa.
***In situ* hybridisation of *Antistasin* during larval development at 24,48,72 hpf.** *Antistasin* is first detected at24hpf stage in the oral endodermal region. At later stages the gene expression territory extends throughout planula endoderm. At 72hpf some Antistasin-expressing gland cells are found in the ectoderm. Scale bar 50µm. **B) Medusa stage**. In medusae, *Antistasin* expression is restricted to gland cells located in manubrium endoderm. Scale bar 100µm**. C) High magnification showing *Antistasin* cell morphology following fluorescence *in situ* hybridisation**: *Antistasin* (green), Hoechst stained nuclei (blue). Scale bar 10µm**.** The Medusa cartoon shows the site of *Antistasin* gene expression (green).

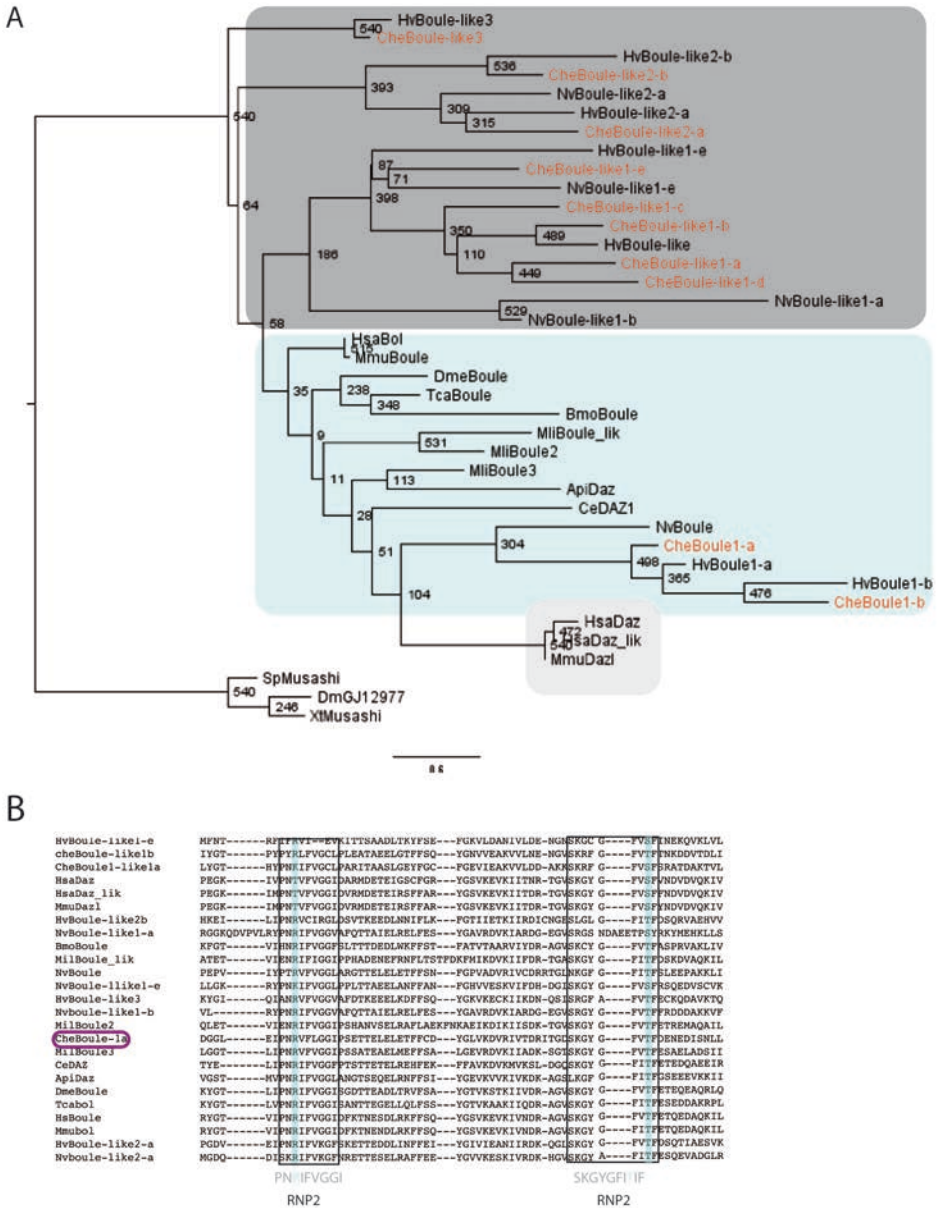

Figure 34: Gene orthology of metazoan Boule/DAZ family member.

A) Phylogenetic analysis using the RRM domain. Numbers below the branches are maximum likelihood bootstrap values. Note the lineage specific duplication event in cnidarians. *Clytia* genes are indicated in red. Members of the Musashi orthology group from Drosophila, Xenopus and sea urchin were chosen as outgroup. Species abbreviations: Api (*Apis millifera),* Bmo (*Bombix mori*) Che(*Clytia hemisphaerica*), Cte (*Capitella teleta*), Ce(*Caenorhabditis elegans*), Hv (*Hydra vulgaris*), Hs (*Homo sapiens*) Mli (*Macrostoma lignanum*), Mmu (*Mus musculus*), Xt (*Xenopus tropicalis*), Nv (*Nemtostella vectensis*), Tca (*Trichoplax adherens*), Sp(*Strongylocentrotus purpuratus).* Sequence name: Accession number
HvBoule-like3: XP_012556641.1, NvBoule-like1-a: XP_001620626.1, HvBoule-like1-e: XP_004211430.1, NvBoule: XP_001632599.1, HvBoule-like2b: XP_004207589.1, NveBoule-like1-e: XP_001635220.1, NveBoule-like1-b: XP_001637248.1, HvBoule-like2-a: XP_002163170.2, NvBoule-like2-a: XP_001623902.1, DmGJ12977: XP_002046609.1, XtMusashi :XP_012816891.1, SpMusashi: XP_001199490.2, CheBoulelike1-c: KT318175, CheBoulelike3: KT318176, CheBoulelike1-d: KT318177, CheBoule1-b: KT318178, CheBoulelike1-e: KT318179, CheBoulelike2-a: KT318180,

B) RRM sequence alignment. Alignment of RRM sequences; the highly conserved motifs RNP-1 and RNP-2 are indicated in grey. The two amino acids present in all Boule ortholog are highlighted in blue.

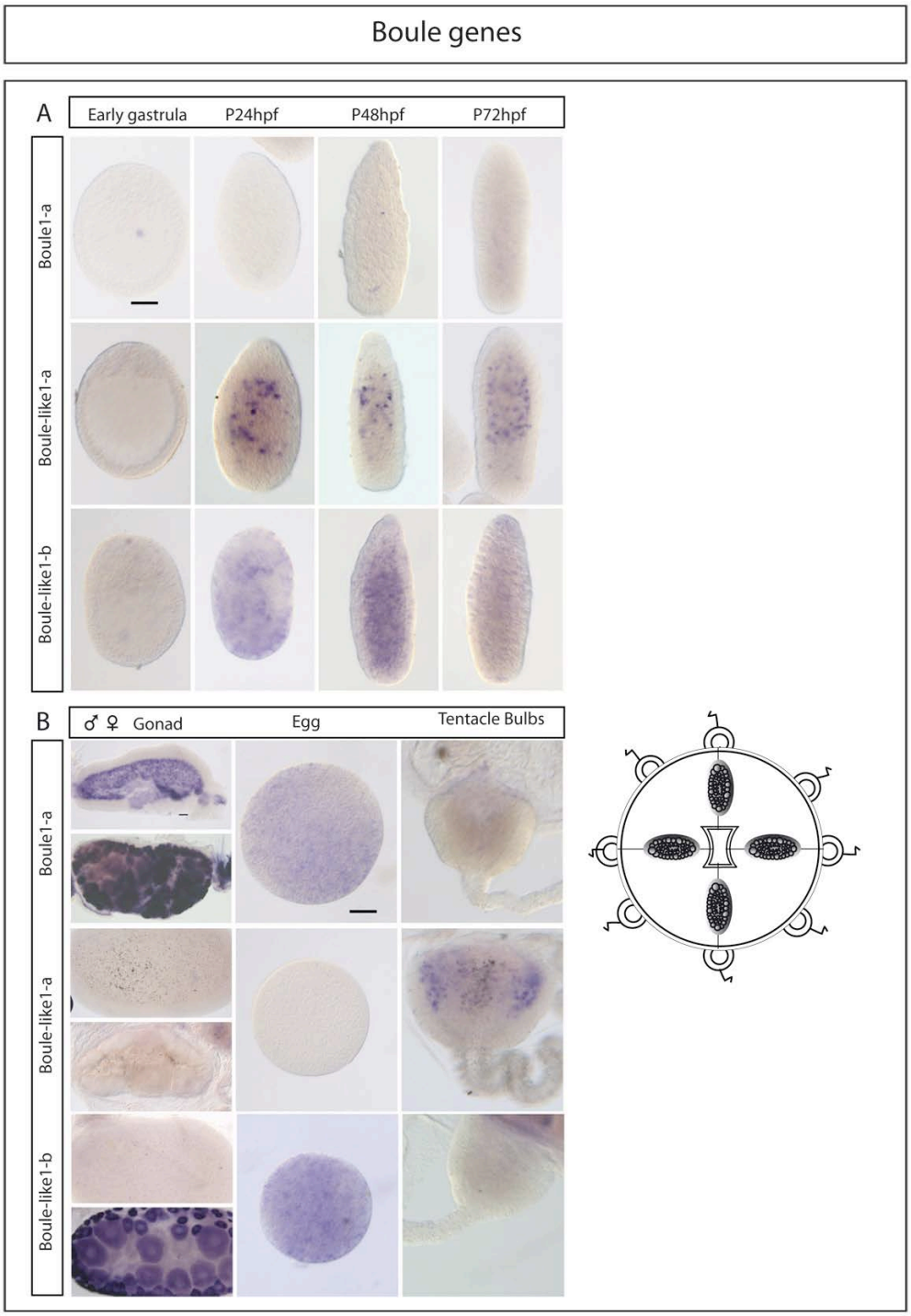

Figure 35: Boule/Daz family gene expression during larval development and in the adult medusa.
A) *In situ* hybridisation of *Boule1-a, Boule-like1-a, Boule-like1-b* during larval development at early gastrula 24,48,72hpf. *Boule-like1-a* and *Boule-like1-b* were first detected at 24hpf. During development, Boule like1-a expressing cells were found in the oral endodermal region, in a similar distribution to the one reported for *Nanos1* and *Piwi*. *Boule like1-b* was detected in both ectodermal and endodermal layers at 24, 48 and weaker at 72hpf. Scale bar 50µm. *Boule1*-a was not detected in the larva. Scale bar 50µm.
B) Medusa stage. *Boule1-a* expression in the adult was detected only in male and female gonads. *Boule1-a* mRNA was distributed uniformly in the unfertilised egg. *Boule-like1-a* mRNA was detected exclusively in the tentacle bulbs, in two lateral patches of cell localised at boundary between endoderm and ectoderm. *Boule-like1-b* gene expression was only detected in the female gonad and the mRNA was ubiquitously expressed in the unfertilised egg. Scale bar 50µm. Medusa cartoon showing the site *Boule1-a* gene expression.

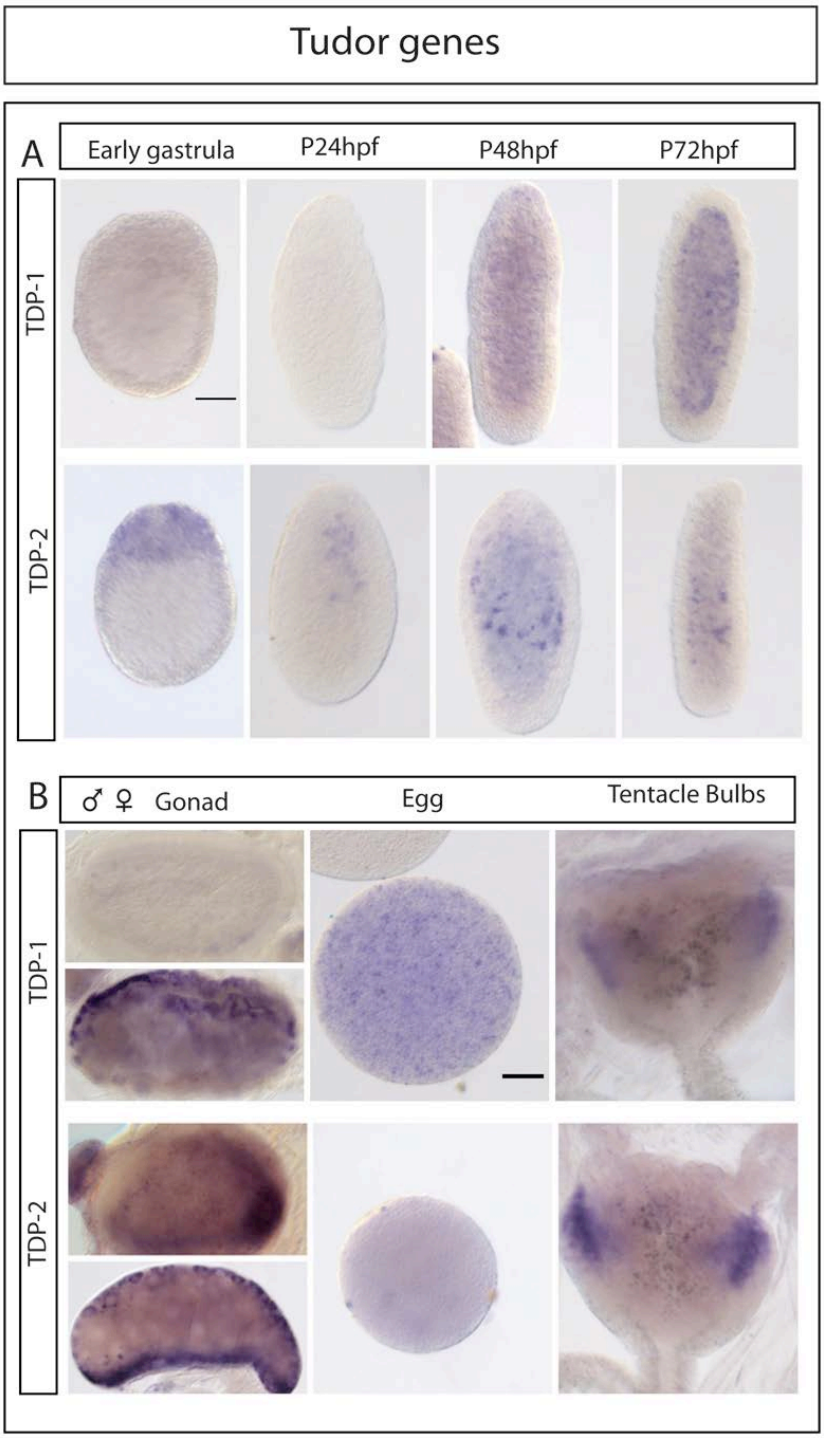

Figure 36: Tudor-domain gene expression during larval development and in the adult medusa. A) ***In situ*** **hybridization of** ***TDP-1 and TDP-2*** **during larval development at early gastrula 24,48,72hpf.** TDP-1 mRNA was detected for the first time at planula 48hpf, and was broadly distributed in the endoderm also at later stages. TDP-2 transcripts were detected for the first time in the early gastrula at future oral pole (gastrulation site). During development it is expressed in a population of cells located within the endoderm region which could correspond to an i-cell subpopulation. Scale bar 50μm. **B) Medusa stage.** TDP-1 expression detected in the medusa was female specific, with ubiquitous mRNA distribution detected in the developing oocytes. The transcript was detected also in the tentacle bulbs at the boundary between endoderm and ectoderm. TDP-2 mRNA was detected in both male and female gonads and in tentacle bulbs, at the interface between endoderm and ectoderm. Scale bar 50μm.

In the *Clytia* transcriptome I identified two tudor domain containing proteins, baptised TDP-1 and TDP-2. Expression pattern analysis showed that TDP-1 can be first detected at 48hpf, in the endodermal region and in a few cells in the ectoderm towards the oral pole, while at later stages *TDP-1* expression appears restricted to the endodermal region (Figure 36-A). In the medusa *TDP-1* mRNA was barely detectable in male gonads, while in female gonad it was detected in oocytes of all stages of oogenesis, and in tentacle bulbs at the boundary between endoderm and ectoderm (Figure 36B). In contrast *TDP-2* was detected already at early gastrula stage, widely across the gastrulation site at the future oral pole. At larval stage (24,48,72hpf) *TDP-2* transcripts were detected in a few cells located in the central endodermal region which might correspond to an i-cell subpopulation (Figure 36A).This hypothesis is supported also by high level of *Hydra* TFDP-2 ortholog in separated i-cells population (Table1 Annexes). In the medusa TDP-2 was detected in both male and female gonads, (predominantly in small oocytes) and in the tentacle bulbs, at the boundary between endoderm and ectoderm (Figure 36B). Interestingly TDP-2 sequence analysis reveals the presence of two dimethylarginine/lysine binding sites. Recently it has been showed that PIWI proteins contain dimethyl arginine residues. Certain Tudor domain proteins can through the dimethyl/arginine binding sites, associate specifically with PIWI proteins (Siomi et al. 2010). This could suggest a specific function of this *Clytia* tudor protein in i-cell regulation through Piwi (*e.g.* genome protection). Neither of the Tudor domain proteins chosen here for analysis have the profile characteristics expected for germ cell fate specification genes, both being expressed in the tentacle bulbs, but they may have a wider roles in i-cell biology. I identified the gene *Thyn1* as an additional putative germ-cell specific marker. Originally I selected this gene on the basis of reported i-cell lineage specific expression in a micro-array based screen in *Hydra* (Hwang et al. 2007). Thyn1 stays for thymocyte nuclear protein 1. This gene was originally identified is a screen in avian lymphocyte cultures, as a cellular protein that mediates apoptotic events. *Thyn1* gene is present in a single copy for each species (see phylogenetic analysis Figure 37A) and the proteins appear to be highly conserved among bacteria, plants, and throughout the animal kingdom (Miyaji et al. 2002). These proteins are characterised by the presence of the so-called EVE domain, whose function is still unknown (Figure 37B). The EVE domain belongs to the PUA domain superfamily involved in RNA binding. The role of this protein has been little studied in vertebrates. Functional analysis in thymocyte cell cultures show

that it prevents apoptosis, and that increased protein levels correlate with a decrease of apoptosis (Toyota et al. 2012). I found that *Clytia Thyn1* expression was restricted to the male and female gonads, and that the mRNA is distributed uniformly in the eggs (Figure 38). The expression of *Thyn* was very strong in the male gonad. It is known that the apoptosis mechanism used to regulate the number of proliferating germ cells and it has been shown in *Hydra* spermatogenesis is regulated through apoptotic event (Kuznetsov et al. 2001).

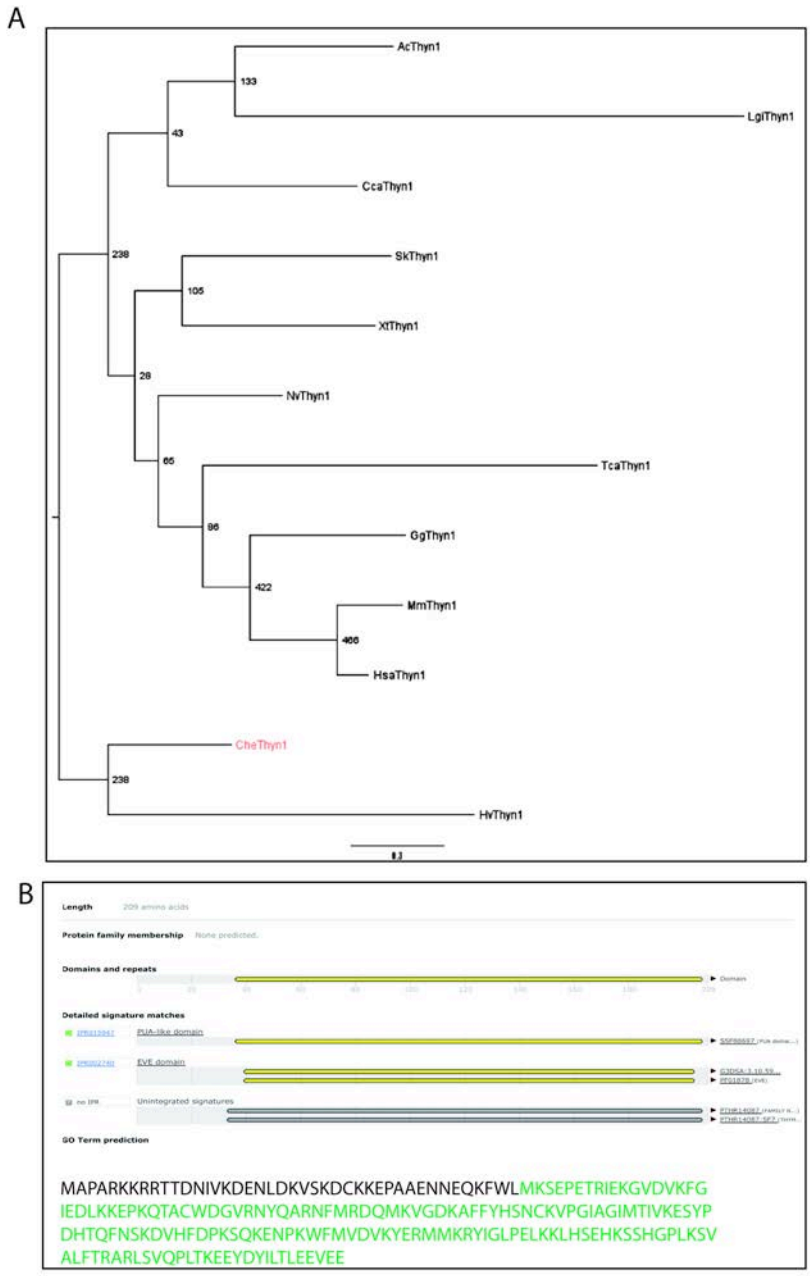

Figure 37:Phylogenetic analysis of metazoan EVE domains proteins Thyn1 proteins are highly conserved from bacteria to mammals. Sequences from *Aplysina californica, Capitella teleta,Saccoglossus kowalevskii, Lottia gigantean,Xenopus tropicalis, Nematostella vectensis, Trichoplax adherens, Gallus gallus, Mus musculus, Clytia hemisphaerica, Hydra vulgaris, Homo sapiens,* were identified as belonging to Eve family by reciprocal blast. Species abbreviations:Ac (Aplysina californica), Cte (Capitella teleta), Sk (Saccoglossus kowalevskii), Lgi (Lottia gigantea), Xt (Xenopus tropicalis), Nv (Nematostella vectensis), Tca (Trichoplax adherens), Gg (Gallus gallus), Mm (Mus musculus), che (Clytia hemisphaerica), Hv (Hydra vulgaris), Hsa (Homo sapiens).The following sequences containing Eve domain were used for phylogenetic analysis. Sequence name;: Accession numberLgiThyn1: XP_009059928.1, TcaThyn1: XP_009059928.1,HvThyn1: XP_012558048.1, AcThyn1: XP_005096716.1, XtThyn1 :NP_001120782.1, CteThyn1: ELU16431.1GgThyn1 :NP_989618.1, MmThyn1: XP_006510751.1, HsaThyn1: NP_054893.1, SkThyn1: XP_006821718.1, NvThyn1: XP_001635839.1 **B) EVE domain analysis.** Amino acid sequence analysis shows the presence of the EVE domain in the Thyn1 protein sequence (in green).

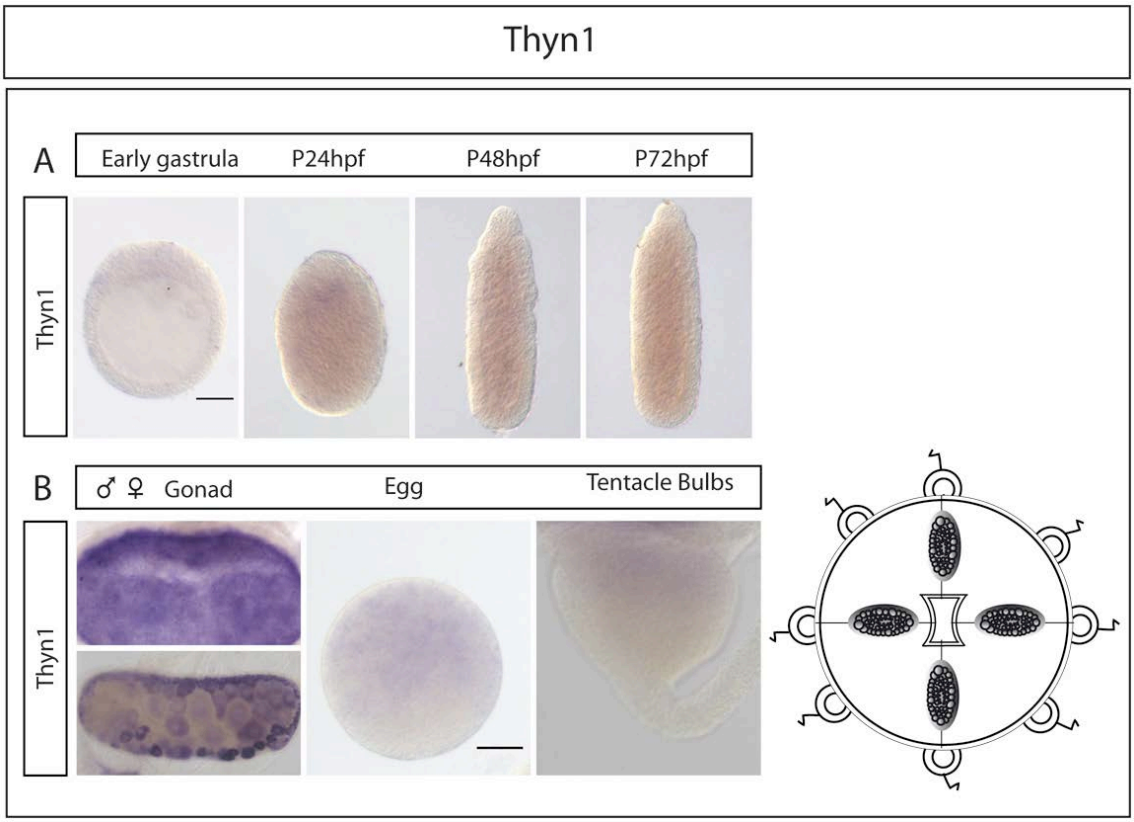

Figure 38: *Thyn1* expression during larval development and in the adult medusa.
A) ***In situ* hybridisation of Thyn1 during larval development at 24, 36,48, 72 hpf**. Thyn1 mRNA could not be detected during larval development. Scale bar 50 µm**. B) Medusa stage**. *Thyn1* mRNA is detected only in female and in male gonads. Scale bar 50 µm**.** The Medusa cartoon shows the site of *Thyn* gene expression (grey).

Potentially Thyn1 could thus be involved in regulating germ cell degeneration in *Clytia* gonads. The restriction of its expression to the gonad, as in the case of *Boule-1a*, is consistent with a scenario in which germ cell fate specification occurs only in sexually mature medusae.

Overall these data suggest that *Boule-1a* and *Thyn1* are germ cell markers, and indicate that germ cell specification occurs only after larval metamorphosis. It will be interesting to test the functional role of these putative germ cell specific genes during germ cell development. The level of these two transcripts could be downregulated using RNAi (currently being tested in the group, S. Chevalier unpublished) on the whole medusa (at different stages of sexual maturation, or on the isolated gonads techniques), or by gene editing using the efficient CRISPR-Cas9 approach (T. Momose, unpublished).

RESULTS II:

Wnt/β-catenin signalling in embryonic patterning, i-cell formation and i-cell differentiation during *Clytia* embryionic and larval development

2. Background and Questions

Depending on the cellular context, Wnt ligands activating the Wnt/Fz/β-catenin pathway regulate embryonic axis polarity, maintain stem cell populations, control cell proliferation and govern cell fate decisions throughout the animal kingdom.

As described in the Introduction, in hydrozoans, including *Clytia*, Wnt/β-catenin dependent signalling (Figure 3A) drives oral/aboral axis formation. During *Clytia* embryonic development the Wnt/β-catenin pathway specifically establishes the oral pole through the activation of the Wnt3 ligand and the Fz1 receptor produced from maternal mRNAs localised in the egg animal half (Momose et al. 2008)(see Introduction 2.1.3). In *Hydra* and *Hydractinia* polyps Wnt/β-catenin signalling controls body axis polarity, but it is also involved in the regulation of i-cell differentiation (Introduction, sec 1.6.4). In *Hydra* the hyperactivation of the Wnt/β-catenin signalling *via* GSK3 inhibition, induces ectopic nematocyte differentiation; in *Hydractinia* it also causes an increase in the number of nematocytes and of RFamide neural subpopulations. These observations suggest that in both these hydrozoan polyps Wnt signalling controls i-cell differentiation.

The experiments described in this chapter address the functions of the Wnt/β-catenin signalling in *Clytia* i-cell regulation in relation to axis establishment in the embryo and larva. The chapter includes two manuscripts, one in preparation for publication in *Developmental Biology* (Ruggiero et al *in prep*) (**PAPER 1**) and one published in 2014 (Lapebie, Ruggiero at al., PLoS Genetics 2014) **(PAPER 2)**.

PAPER 1 addresses the function of the Wnt/β-catenin pathway in the formation and differentiation of i-cell during embryonic development by a loss of function approach.

For **PAPER 2,** I participated in the identification of additional and novel genes expressed differentially along the developing oral-aboral axis and implicated in embryonic development. The genes were identified by comparing the transcriptomes of unmanipulated early gastrulae and of early gastrula in which the Wnt/β-catenin pathway was inactivated.

2.1 PAPER 1: Summary of the results

2.1.1 Investigating Wnt/β-catenin signalling in i-cell formation and differentiation during *Clytia* embryonic development.

In order to investigate the influence of the Wnt/β-catenin signalling activity on i-cell dynamics during *Clytia* embryonic development I monitored the presence of i-cell and i-cell derivatives: nerve cells, gland cells and nematocytes in embryos in which Wnt signalling was abolished by Wnt3 morpholino injection (Wnt3 morphants).
To verify if i-cell differentiation was affected in Wnt3 morphants at different developmental stages (early gastrula, 24 and 48hpf), I used the set of i-cell derivatives markers described in the previous ResultI chapter.
To assess the involvement of the Wnt/β-catenin pathway in i-cell maintenance and i-cell proliferation I used both *Nanos1* and *Piwi* i-cell markers. The main finding were as follows:

- *I-cell formation is Wnt3 independent*

Wnt3 morphants have a slightly delayed gastrulation, have a spherical shape and lack polarity as indicated by the loss of orientation in their swimming behaviour and by loss of expression of oral markers such as the *Clytia Brachyury* ortholog *Bra1* (Momose et al. 2008). Wnt3 morphant embryos fail to elongate even at 24 and 48hpf, making it easy to verify in each experiment that Wnt/β-catenin signalling has been largely inhibited. Despite the very different morphology I could not distinguish any difference between wild type embryos and Wnt3 morphants with respect to i) the timing of onset of *Nanos1* and *Piwi* expression, ii) the number of cells expressing *Nanos1* and *Piwi* (Figure 39). Corresponding analysis of expression levels of these genes in Wnt3-MO embryos showed no significant difference (Figure 43).
These observations suggest that i-cell formation is not dependent on the Wnt/β-catenin pathway and therefore that formation and maintenance of the i-cell population is regulated independently from axial polarity.

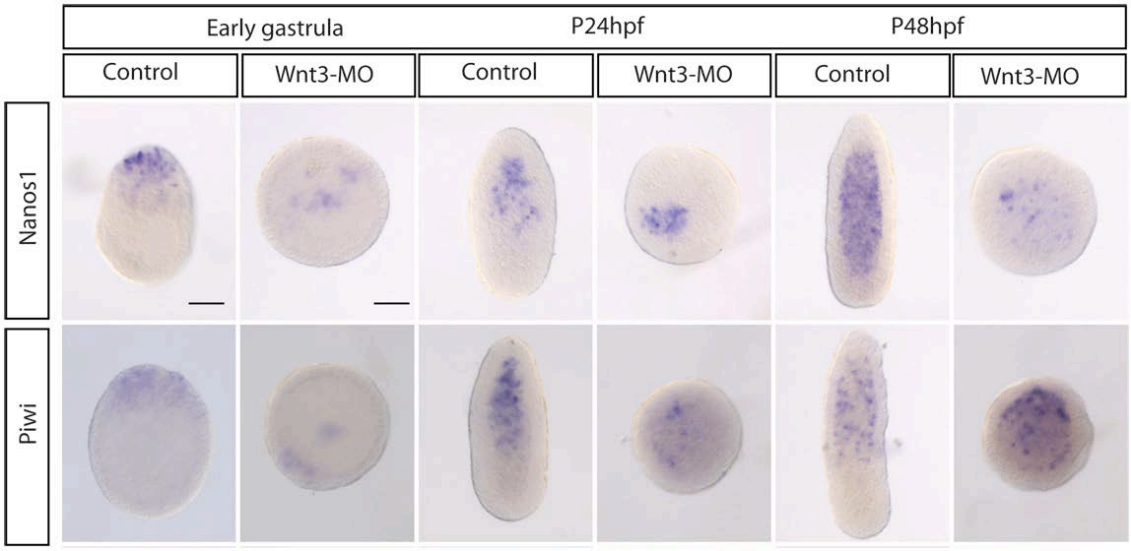

Figure 39: *Nanos1* and *Piwi* expression is not inhibited in Wnt3 morphants.
In situ hybridisation of *Nanos1* and *Piwi* in untreated (left panels) and Wnt3 morphants (right panels) at early gastrula and planula 24,48hpf. At the early gastrula stage *Piwi* mRNA expression in Wnt3 morphants embryos is slightly weaker than in untreated embryos. In later stages the expression of *Piwi* and *Nanos1*in Wnt3 morphants is comparable to the untreated embryos. All control embryos are oriented with the oral pole at the top. Scale bar 50μm.

- *Wnt/β-catenin signalling is required for the final differentiation of the neural cell types*

To check if Wnt3 had a role in neurogenesis, I assessed the presence of neural cell types: neuroblasts, nematoblasts, differentiated nerve cells and nematocytes. To characterise the presence of these four cell populations I used a combination of *in situ* hybridisation and microscopy approaches. To detect nematocytes capsules I used DAPI staining, and *in situ* hybridisation to score nerve cells and nematoblast using *Prdl-a* and *Mcol3-4a* markers. To detect differentiated nerve cells I performed *in situ* hybridisation with the *PP5* (RFamide precursor), and *PP2* (GLWamide precursor) probes. Expression of *Prdl-a* and *Mcol3-4a* was not affected or slightly delayed (*Mcol3-4a*) in Wnt3 morphants, however RFamide but not GLWamide expression was completely abolished at 48hpf Wnt3-MO planulae (Figure 40). 48hpf Wnt3-MO planulae also lacked nematocytes as shown using DAPI staining, and by 72hpf only a few nematocytes (between 5-7) could be detected in Wnt3 morphants in comparison with controls that had between 70-80 nematocytes per planula.

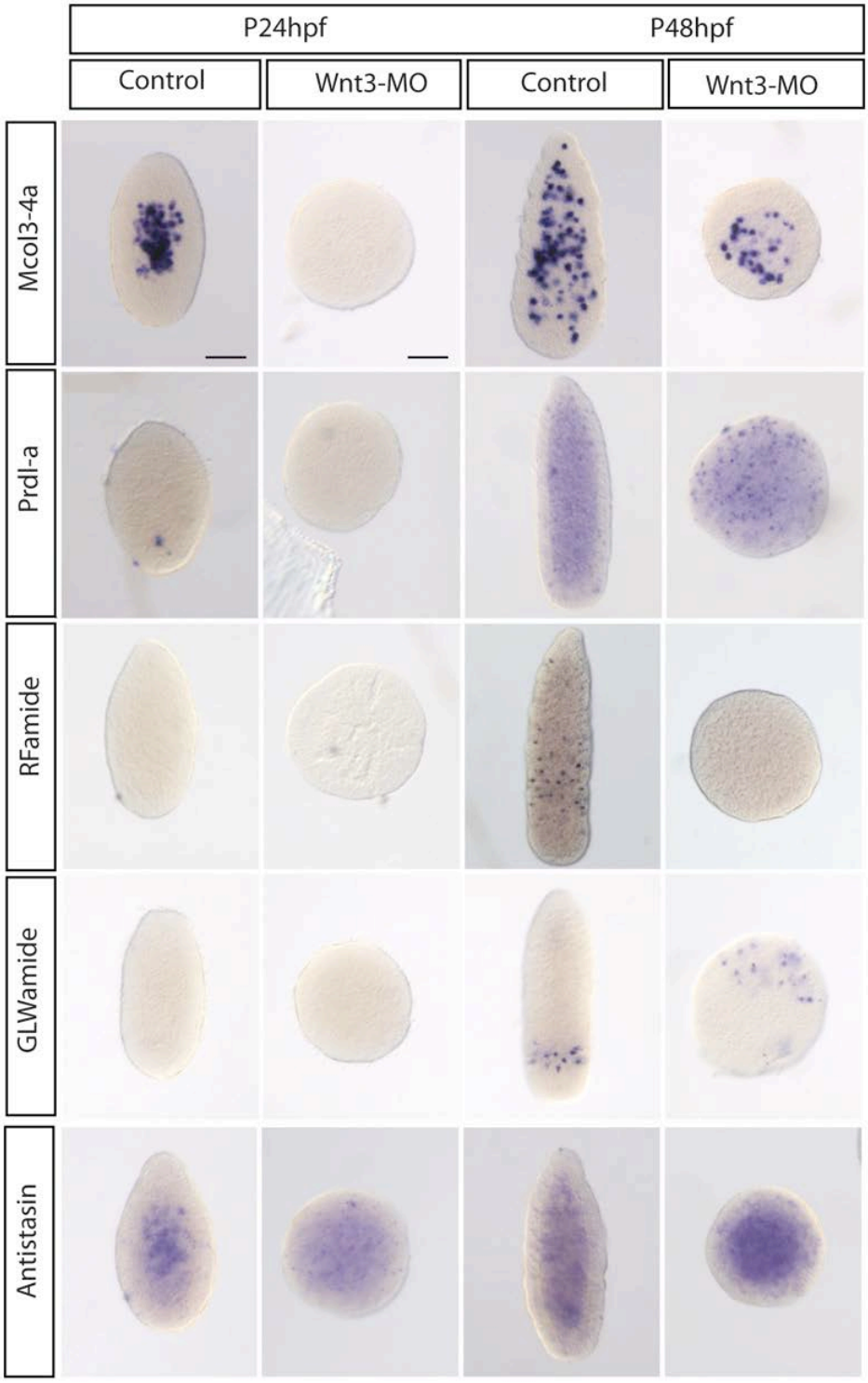

Figure 40: Wnt3 is required for the differentiation of the RFamide neurons.
In situ hybridisation of *Mcol3-4a, Prdl-a, PP5* (RFamide precursor), *PP2* (GLWamide precursor*), Antistasin* in untreated (left panels) and Wnt3 morphants (right panels) at 24hpf and 48hpf. *Prdl-a*, *RFamide* and *GLWamid*e mRNAa were not detected at 24hpf in the control or in Wnt3 morphants. At 24hpf *Mcol3-4a* expression is absent in Wnt3 morphants, however at 48hpf *Mcol3-4a* transcript became detectable. At 48hpf, the expression of *Prdl-a* and *PP2* was detected in Wnt3 morphants, while *PP5* expression was completely absent. Antistasin was detected in control and in Wnt3 morphants at 24,48hpf planula. Scale bar 50μm.

These observations suggest that loss of Wnt3 function directly or indirectly prevents the last step of differentiation of some neural cell types, including nematocytes and RFamide expressing ganglion cells. These two cell types reach their final fate in the ectoderm, and show a specific distribution along the Oral-Aboral (O-A) axis: both cells types are present along the lateral ectoderm and nematocytes are also concentrated at the oral pole. Both cell types are largely excluded from the aboral pole region. My results are compatible with the results obtained in *Hydra* and in *Hydractinia* in which the hyperactivation of Wnt/β-catenin signalling stimulates the differentiation of both nematocytes and RFamide neural cell type (Khalturin et al. 2007; Teo et al. 2006). More specifically, "oralised" *Hydra* polyps treated with alsterpaullone, (ALP, which inhibits the negative Wnt regulator GSK3b kinase) show ectopic expression of a specific tentacle nematoblast marker *nbo31* in the gastric region. Indeed the gastric nematoblasts acquire the fate of the tentacle nematobasts (that normally expressed the *nbo31* gene) and stop expressing the *nbo35* gene that is a marker of this population. This is consistent with the role of Wnt/β-catenin signalling in defining positional information along the O-A axis. Consistently, grafting experiment in which untreated i-cells were transplanted to ALP treated polyps showed that i-cells behaved as if they had reached their final destination in the tentacles in terms of neural marker expression (Khalturin et al. 2007). *Hydractinia* polyps treated with ALP showed an increase in the number of nematocytes (by morphological analysis) and RFamide cells, suggesting that also in *Hydractinia* polyps Wnt signalling influences the final differentiation of neural cell types. In *Clytia* the absence of Wnt3 in the oral ectoderm, with consequent down regulation of the Wnt/β-catenin signalling prevented the formation of the nematocytes and the RFamide nerve cells. This is again consistent with a role for Wnt/β-catenin signalling in promoting differentiation of oral type nerve cells. Interestingly the GLWamide neuronal subpopulation was not affected by the absence of Wnt/β-catenin signalling. This population is also positioned in the ectoderm, but at the aboral pole of the planula. This is consistent with a model in which neuroblasts can differentiate into GLWamide cells at a lower level of Wnt/β-catenin signalling, Wnt ligands in *Clytia* planulae are probably distributed in a gradient from oral to aboral pole because of a nested/overlapping expression of several ligands in the planula (Momose et al. 2008). In accordance with this model genes expressed in the neural and nematocyte precursors (*e.g. Mcol3-4a*, *Prdl-a*) are not inhibited by Wnt3 downregulation (Figure 41).

- *Wnt3 does not affect gland cells formation*

I monitored the expression of the gland cell marker *Antistasin* in Wnt3 morphants, to see whether gland cell formation is Wnt/β-catenin dependent. The *Antistasin* transcript could be detected in Wnt3 morphants in 24hpf and 48hpf planulae. As in the controls, *Antistasin* expression was strongly detected in the endoderm and also in the ectoderm (Figure 40-41). These data indicate that Wnt3 is not involved in gland cell development or differentiation.

Taken together these data indicate that:

- ✓ i-cell formation during embryonic development is Wnt/β-catenin pathway (*via* Wnt3) independent
- ✓ Wnt/β-catenin signalling regulates, directly or indirectly, the final step of differentiation for the oral/lateral neural cell types including nematocytes and RFamide neurons.
- ✓ Somatic commitment for i-cells is not regulated by Wnt/β-catenin signalling
- ✓ Gland cell formation is not Wnt/β-catenin signalling dependent

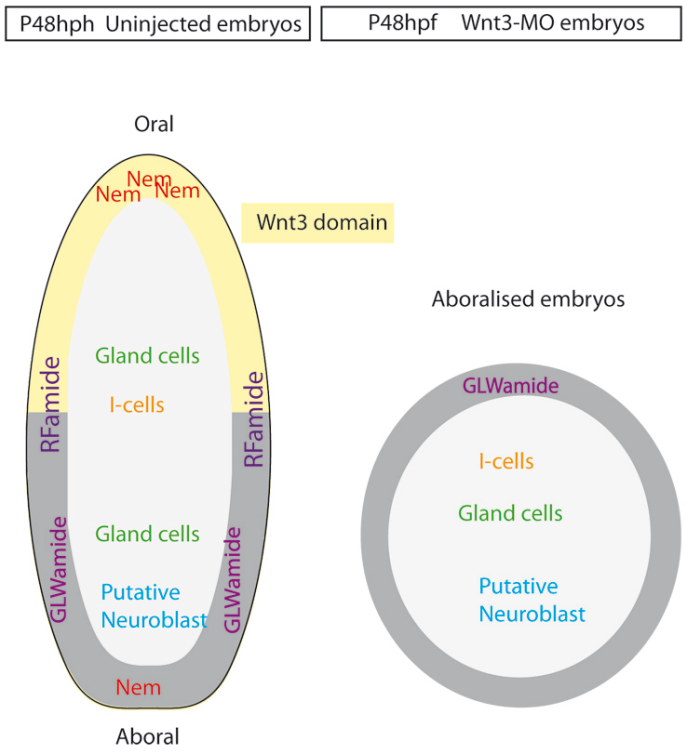

Figure 41:A Wnt gradient is require for neural fate acquisition. Schematic illustration of untreated planula 48hpf and Wnt3 MO at the same stage of development. The distribution of the different somatic cell types is represented according to the expression profile of the gene markers and to morphological features: Nem = nematocytes, i-cells (*Piwi* and *Nanos1*), Gland cell (*Antistasin*), putative neuroblast precursors (*Prdl-a*). RFamide and LWamide indicate two different neuronal cell subpopulations. Wnt3 morphants lack oral identity, but gastrulate forming ectoderm (grey) and endoderm (light grey). Wnt3 expression domain indicated in yellow, correspond to the ectodermal oral pole absent in Wnt3 morphants. Wnt3 morphants lack nematocytes and RFamide neuronal cell type.

- *Wnt/β-catenin signalling contributes to i-cell formation in embryos lacking germ plasm*

Previous work (Leclère et al. 2012) left open the question of whether i-cells formation during *Clytia* development occurs by inheritance of maternal germ plasm (containing *Piwi* and *Nanos1* mRNAs) (see Introduction 2.4) from the egg animal pole. I-cells can also form "*de novo*" in isolated vegetal embryos fragments, implying that signalling mechanisms also contribute to their formation. These fragments can restore an oral -aboral axis, despite the loss of much of the maternal Wnt3 and Fz1, concentrated in animal half of the embryos. The results presented in the previous section show that Wnt/β-catenin signalling is not required for i-cell formation during normal embryonic development, but I wanted to test its role also in i-cell formation during embryo re-patterning. The presence of i-cells was monitored by *in situ* hybridisation with probes for *Piwi* or *Nanos1*. These mRNAs are detectable in the i-cells and in the germ plasm-bearing blastomeres at early stages. To generate i-cell depleted embryos, animal/oral halves containing germ plasm, and vegetal/aboral halves lacking germ plasm were separated by bisection. To investigate the role of Wnt/β-catenin pathway on i-cell formation in the context of axis re-patterning, Wnt3-MO was injected into unfertilised eggs, and embryo bisection performed at the blastula stage. At this stage the morphology of most embryos allows the A-V axis to be distinguished. Alternatively, blastomeres were separated individually at 8-cell stage. The presence of *Piwi* or *Nanos1* expressing cells was assessed in the planulae after one or two days of development. There was a clear difference in the ability of embryo vegetal halves or vegetal 1/8 blastomeres to support i-cell formation in the presence or absence of Wnt signalling. While almost all vegetal fragments from uninjected embryos formed i-cells, a significant numbers failed to reform i-cells following Wnt3-MO injection.
From these results the following conclusion can be made:

- ✓ Germ plasm contributes to i-cell formation
- ✓ Two distinct mechanisms can ensure the formation of i-cells during embryogenesis
- ✓ Wnt3 drives (directly or indirectly) the formation of i-cells in germ plasm-depleted embryos.

In this scenario Wnt/β-catenin signalling is potentially the inductive signal responsible for i-cell formation in the absence of germ plasm. It is likely that Wnt signalling acts indirectly,

allowing the re-establishment of an oral pole territory, which is a pre-requisite for i- cell restoration. Other signalling pathways such as peptide-based signalling, TGFb or Notch signalling could be more directly involved in the homeostasis of the i-cell population downstream of Wnt signalling.

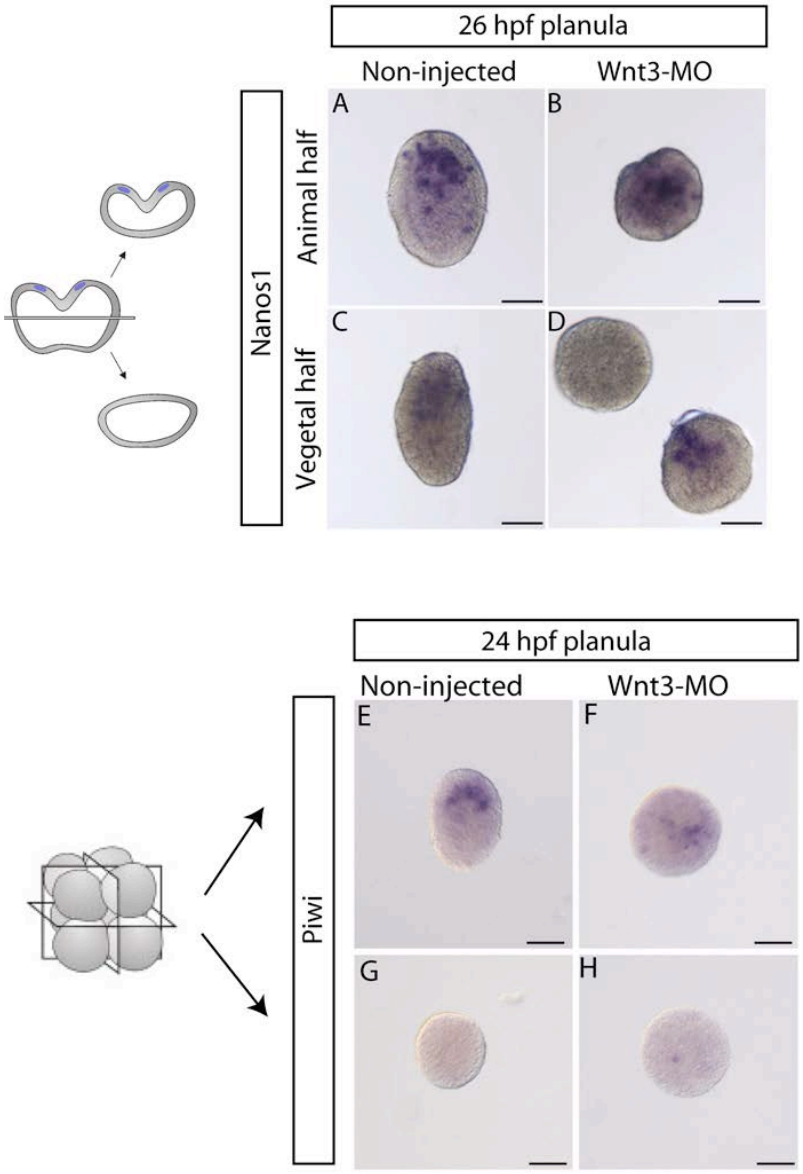

Figure 42: Wnt3 signalling is required for *de novo* i-cell formation.
In situ hybridisation using *Nanos1* (A-D) *and Piwi* (E-H) probes on non-injected and Wnt 3 morphants following animal/vegetal separation. A-D embryo bisection experiment performed at blastula stage. All the mini planulae (non injected and Wnt3 morphants) animal-derived (A-B) present *Nanos*1expression, while only the 50% of the Wnt3 injected vegetal -halves present *Nanos1* expression. In 24hpf larvae derived from separated 8-cell stage blastomeres (E-H), *in situ* hybridisation using *Piwi* probe revealed that 30% of the non-injected embryos are spherical and lack *Piwi*-expressing cells (G), as compared to 56% in the case of Wnt3-MO injection (H). Scale bars: 50μm for A-H.

PAPER 1:

Wnt signalling in multipotent stem cell formation and differentiation in *Clytia hemisphaerica* larval development

Antonella Ruggiero, Pascal Lapébie , Carine Barreau and Evelyn Houliston

Manuscript in preparation for submission to Developmental Biology

Wnt signaling in multipotent stem cell formation and differentiation during larval development in the hydrozoan *Clytia*

Antonella Ruggiero, Pascal Lapébie , Carine Barreau and Evelyn Houliston

Sorbonne Universités, UPMC Univ. Paris 06, CNRS, Laboratoire de Biologie du Développement de Villefranche-sur-mer (LBDV), 06230 Villefranche-sur-mer, France.

Corresponding author**:** Evelyn Houliston (+33) 493763983, houliston@obs-vlfr.fr

Keywords: stem cell, hydrozoan, Wnt, neurogenesis, germ plasm

Abstract

In hydrozoan cnidarians, germ cells but also several somatic cell types derive from multipotent stem cells called interstitial cells (i-cells). How i-cell development is regulated during embryogenesis remains unclear. In *Clytia hemisphaerica,* the i-cell lineage appears to inherit "germ plasm" containing Piwi, Nanos1 and Vasa mRNAs from the egg animal pole, suggesting a determinant–based mechanism, but it can also develop when germ plasm is absent. We tested the role of Wnt/b-catenin signaling in i-cell formation using morpholinos targeting the maternal ligand Wnt3, essential for oral-aboral polarity development (Wnt3-MO). I-cell formation and maintenance were not inhibited in Wnt3-MO embryos, or in larvae derived from animal (germ plasm-containing) halves of either uninjected or Wnt3-MO blastulae. In contrast the i-cell forming ability of vegetal blastula halves was severely compromised by Wnt3-MO. The number of "mini-embryos" generated from isolated 8-cell stage blastomeres to develop i-cells was similarly reduced by Wnt3-MO. Subsequent events including maintenance of the i cell pool and somatic fate determination steps were found to be insensitive to Wnt3-MO; the expression of gland cell (*Antistasin*) and neurogenesis (*Prdl-a*) markers occurred on schedule in developing Wnt3-MO larvae, while the first steps of nematogenesis occurred with a delay. In contrast, final differentiation of neurons and nematocytes was inhibited by Wnt3-MO, and also by late treatments with the b-catenin/TCF inhibitor PKF118-310. No expression of the novel germ cell precursor markers *Boule1-a* and *Thyn1* could be detected in larvae, consistent with restriction of germ cell fate specification to adult stages.

We conclude that during *Clytia* embryogenesis Wnt signaling is required for i-cell formation in the absence of germ plasm (directly or through axis establishment) and for nematocyte and neuronal differentiation, but not for somatic cell fate specification from i-cells. Our findings also support a role for germ plasm in i-cell fate determination during normal embryogenesis.

Highlights

- Germ plasm inheritance determines i-cell fate during normal embryogenesis
- I-cell formation in the absence of germ plasm is possible via Wnt signaling
- Somatic fate specification from i-cells in the larva is Wnt independent.
- Final differentiation of nematocytes and some neurons requires Wnt signaling
- No evidence for germ cell lineage specification during larval development.

Introduction

Hydrozoan cnidarians are animals which have certain biological features more frequently associated with plants. They typically propagate vegetatively as well as by sexual reproduction, and also show exceptional regeneration properties including restoration of missing parts of the three possible life cycle forms: planula larva, polyp and medusa. Central to these two related features is a remarkable population of multipotent stem cells called interstitial cells (i-cells), present through the entire life cycle (Watanabe et al., 2009) (Bosch et al., 2010) (Plickert et al., 2012; Watanabe et al., 2009). The i-cells are small cells with rounded morphology and relatively large nuclei that occupy spaces at the bases of the two layers of self-maintaining epitheliomuscular cells. The epitheliomuscular cells are the basic cell type of the two cnidarian germ layers (ectoderm and endoderm) and can also generate certain specialized epithelial cell types as well as some sensory neurons (Bosch et al., 2010; Martin and Thomas, 1981a; 1981b). I-cells have been extensively characterised in *Hydra* polyps, where they have been shown to generate multiple somatic cell types including secretory gland cells, nerve cells and nematocytes (the stinging cells characteristic of cnidarians, which can be considered to be specialised mechanoreceptor cells), as well as germ cells (Bosch and David, 1991; David, 2012; Galliot and Quiquand, 2011; Khalturin et al., 2007; Watanabe et al., 2009). In the colonial polyps of *Hydractinia,* i-cells have an even wider potential, being able in experimental tests to generate all adult cell types including epitheliomuscular cells (Müller et al., 2004; Plickert et al., 2012). Once committed to different somatic cell fates, neuronal and nematocyte precursors migrate into the ectodermal layer to take up their positions along the body axis, termed oral-aboral (OA) in cnidarians, and complete differentiation. These processes have been described not only to hydrozoan polyps, but also at the "planula" larva stage (Martin, 1990; Martin and Archer, 1986). In hydrozoan planula larvae i-cells are largely confined to the inner layer of endoderm cells (Bodo and Bouillon, n.d.; Leclère et al., 2012; Plickert et al., 2012), despite early histological suggestions of an ectodermal origin in some species (see discussion in (Genikhovich et al., 2006).

With the notable difference that they generate somatic cell types as well as germ cells, hydrozoan i-cells in many ways resemble a classical animal "germ line", a developmental cell lineage devoted to producing gametes which in many animals is segregated from the "soma" early during embryogenesis. Thus i-cells are the source of

germ cells, and express orthologues of many genes associated with totipotency and commonly considered to be germ line markers, such as Nanos, Piwi, PL10 and Vasa (Genikhovich et al., 2006; Leclère et al., 2012; Rebscher et al., 2008). Furthermore, during embryonic development *Clytia* i-cells arise near the site of endoderm formation derived from the egg animal pole, mirroring the endoderm-primordial germ cell association seen in many chordate species in which both derive from the egg vegetal hemisphere. Correspondingly the animal region of hydrozoan eggs and vegetal region of bilaterian eggs harbor two types of developmental determinant: maternally localized mRNAs that contribute to endoderm fate, and "germ plasm". Germ plasm is a morphologically distinguishable egg cytoplasmic material containing localized germ line mRNAs and/or proteins inherited by primordial germ cells, which in species of anuran amphibians, nematodes and insects has been demonstrated experimentally to determine germ line fate (Extavour, 2003; Ikenishi, 1998). Germ plasm like material has been detected in hydrozoan eggs as animal pole aggregates of Vasa protein in *Hydractinia* (Rebscher et al., 2008) and of Vasa, Nanos1, Nanos2, Piwi, PL10 mRNAs in *Clytia* (Leclère et al., 2012). Although i-cells are first detected in the corresponding future oral pole region (cell ingression site) at the early gastrula stage in *Clytia*, there is no experimental evidence that this germ plasm contributes to determining their fate. Indeed, germ plasm inheritance is certainly not the exclusive route to i-cell formation, since both animal and vegetal blastomeres from 8 cell stage embryos can develop into "mini-larvae" containing i-cells (Leclère et al., 2012). This observation suggests that the intercellular signaling mechanisms responsible for the strong re-patterning ability of vegetal embryo fragments (Freeman, 1981) can promote i-cell formation ectopically in the absence of germ plasm.

We have addressed the intercellular interactions regulating different aspects of i-cell regulation during larval development in *Clytia*: their initial formation, the commitment to different derivative fates through the specification of progenitor cell populations, and the differentiation of final specialized cell types. We focussed on Wnt signaling, known for its role in regulating stem cell dynamics in mammalian stem cells (Reya and Clevers, 2005). Two previous studies in hydrozoan polyps found that over-stimulation of the Wnt/b-catenin pathway by pharmacological inhibition of the negative regulator GSK3b caused excess formation of nematocytes and of some nerve cell types at the expense of progenitors (Hensel et al., 2014; Khalturin et al., 2007; Teo et al., 2006). Interpretation of the exact role

of Wnt signaling in stem cell regulation from these studies is complicated by its simultaneous function in defining positional values along the OA axis, because Wnt activation confers oral identity in cnidarians(Brouns, 2012; Duffy et al., 2012; Hobmayer et al., 2000; Kusserow et al., 2005; Wikramanayake et al., 2003) probably reflecting an ancient role in animal body axis specification(Petersen and Reddien, 2009). The critical role of Wnt signaling in axial patterning is well illustrated during *Clytia* embryogenesis. In the future oral half of the early embryo, the ligand Wnt3 and receptor Fz1, both synthesized from animally localized maternal mRNAs, activate the Wnt/b-catenin ('canonical') pathway to cause stabilization and nuclear localization of the transcriptional co-regulator b-catenin, while the negatively acting receptor Fz3 blocks this pathway in the future aboral territory (Momose et al., 2008; Momose and Houliston, 2007). Wnt-dependent gene transciption in the oral territory shows two main expression patterns, one involved in axial patterning through maintained expression at the oral tip throughout larval development, and the other distinguishing various ingressing cell populations including presumptive endoderm cells but also the i-cell progenitors (Lapébie et al., 2014).

Using molecular markers for i-cell derivatives we mapped their appearance and differentiation patterns in relation to the developing OA axis of embryos and larvae. We then assessed the influence of Wnt/b-catenin signaling on different aspects of i-cell development, achieving inhibition of this pathway by injection into the egg of Morpholino oligonucleotides targeting Wnt3 (Wnt3-MO), previously demonstrated to prevent b-catenin cytoplasmic accumulation and nuclear localisation (Momose et al., 2008). We also used in some experiments the pharmacological inhibitor PKF118-310, which interferes with the interaction between b-catenin and the conserved transcription factor Tcf/LEF, required to regulate gene expression via this pathway (Lepourcelet et al., 2004).

Materials and Methods

Manipulation of Eggs and Embryos

Eggs obtained by light-induced spawning of laboratory-raised medusae were microinjected with Wnt3-MO prior to fertilization as described previously (Momose and Houliston, 2007). At the four or eight cell stage, any unfertilized or abnormally dividing embryos were removed. Planulae were fixed for *in situ* hybridization after 24, 48 or 72 hours of culture (hpf for hours post ferilization) at 18°C in Filtered Artificial Sea Water (FASW; Red Sea Salt brand). Blastula bisection and blastomere separation were performed using fine Tungsten wire loops in agar-lined petri dishes as described previously (Leclère et al., 2012). PKF118-310 was used at 0.9 μM in FASW, diluted from a 15 mM stock immediately before use.

Gene cloning and in situ hybridization

In *situ* hybridization probes were synthesized from cDNA clones retreived from our EST collection when available. For the remaining sequences, cDNAs were cloned by PCR using the pGEM-T Easy system (Promega). All sequences were verified before probe synthesis. DIG-labeled and Fluorescein-labeled antisense RNA probes for in *situ* hybridization were synthesized using Promega T3/T7/Sp6RNA polymerases, purified using ProbeQuant G-50 MicroColumns (GE Healthcare) and taken up and stored at -20°C in 100 ml of 50% formamide.

In *situ* hybridization was performed using the InsituPro robot (Intavis) as described previously (Lapébie et al., 2014).

Immunofluorescence and nematocyte staining

Immunofluorescence was performed as previously described (Amiel and Houliston, 2009). RFamide positive neurons were visualized using a commercial FMRF-amide antibody (Immunostar, final dilution of 1:800) overnight at 4 °C, followed by a rhodamine coupled anti-rabbit IgG (Sigma, final dilution 1:100) for 3 h at room temperature, with Hoechst dye 33258 (Sigma, 0.3 μg/ml final) included to stain DNA. Specimens were mounted in Citifluor mounting medium (Citifluor Ltd) and imaged using a Leica SP5 confocal microscope. The nematocyte staining protocol was adapted from previous studies (Denker

et al., 2008; Wolenski et al., 2013). Samples were fixed for 1 h in 3.7% formaldehyde/PBS at room temperature, then washed 3 times in PBS for 10 minutes. They were incubated for 30 min in 50 µg/ml DAPI (from a 1mg/ml stock) in PBS. Samples were rinsed 3 times and mounted in Citifluor. Staining was observed by epifluorescence on a Zeiss Axiovert 200 microscope (excitation 450-490 nm, emission >515 nm).

Sequence analysis

In order to assign orthology to newly-identified *Clytia* genes, we performed phylogenetic analysis for the multigenic families, retrieving homologous protein by reciprocal blast from our transcriptome collection and from publicly available genomic database (NCBI). We checked the domain composition characteristic to the protein family using EXPASY PROSITE domain prediction tools on-line, and added sequences to previously published alignments when available. Species were selected to represent the different taxa (Deuterostomes, Lophotrochozoa, Ecdysozoa) and the cnidarians *Hydra vulgaris* (Hydrozoa) and *Nematostella vectensis* (Anthozoa). Sequences were aligned using MUSCLE (Edgar, 2004)at http://www.ebi.ac.uk/Tools/msa/muscle/. Maximum Likelihood analysis using the MPI version of PhyML 2.4 was run on the Observatoire de la Cote d'Azur calculation cluster using the LG amino-acid substitution model {Le:2008fp}. Gamma shape parameters and the proportion of invariable sites were estimated, and 4 substitution rate categories were used. Phylogenetic trees are available in File S2. For Antistasin and Tudor-containing proteins, whose domain sequence alignment was unsatisfactory, BLAST and domain analysis identified putative orthologues in the closely related species *Hydra vulgaris.*

Accession numbers for the newly identified sequences are given in Table S3. This table also lists *Hydra magnipapillata* and *Hydra vulgaris* orthologues of these genes, and the number of matching reads from the transcript dataset (HAEP) available at http://compagen.zoologie.uni-kiel.de/blast.html (Hemmrich et al., 2012) for separated cell populations (endoderm, ectoderm and nanos-positive cells), normalized with respect to total read number.

Results

I-cells can form by Wnt3 dependent and independent mechanisms

To test the role of wnt signaling in i-cell formation we blocked Wnt/b-catenin signaling during embryogenesis by injection prior to fertilization of Wnt3-MO (Momose et al., 2008) and monitored i-cell formation by in situ hybridization using Piwi and Nanos1 probes. The i-cells detected by these two probes detect both the multipotent stem cell population and some cells already embarked on the developmental pathway to form derivative cell types such as nematocytes, as shown by double fluorescent in situ with the nematoblast-expressed gene Minicollagen 3/4a (Denker et al., 2008) (data not shown). In Wnt3-MO embryos fixed at the early gastrula stage, 24 hpf (early planula) and 48 hpf (mid planula), i-cells were clearly detected in the vast majority of embryos in parallel with their appearance in non-injected controls, despite the spherical morphology indicating loss of the oral territory (Fig. 1A-L). These observations indicate that during normal development neither Wnt signaling nor oral fate determination is required for i-cell formation or maintenance of the population, and are compatible with a direct mechanism of i-cell fate determination by inherited germ plasm. We addressed this possibility using the two different embryo manipulation approaches employed previously (Leclère et al., 2012), blastula bisection or separation of blastomeres at the 8-cell stage.

Non-injected and Wnt3-MO pre-injected blastula–stage embryos (about 5-6 hpf) were bisected into putative animal and vegetal halves, using the distinctive lobed morphology observed in some embryos to orient the OA axis. Immediate fixation of a sample from each group followed by *in situ* hybridization with Nanos1 probe confirmed that germ plasm was detectable in nearly 100% of "animal" fragments (11/11 and 20/21 in the two experimental conditions), but in less than 50% of "vegetal" fragments (5/8 and 6/12). This residual germ plasm in the "vegetal" fragments is almost certainly the result of inaccurate bisection, which left behind a very low numbers of Nanos1 expressing cells in the embryo vegetal half (Table 1, data not shown). The remaining half blastulae were cultured until 26 hpf before fixation and Nanos1 *in situ* hybridization (Table 1, Figure 1M-P). From uninjected embryos, all the "animal" group non-injected planulae and most (11/12) of those in the vegetal group developed clearly detectable i-cells (Figure 1M, O). Nearly all "animal" blastula halves from Wnt3-MO also developed clear i-cells by 26 hpf

(Figure 1N), however those in the "vegetal" group showed no detectable i–cells in 9/18 cases (Figure 1P). These data indicate that i-cell formation in the vegetal region is Wnt3 dependent. Development of i-cells in 50% of half-planulae in the "vegetal group" could be accounted for by contamination with animal material including germ plasm at about this frequency (see above).

Similar results were obtained following separation of individual blastomeres from non-injected and Wnt3-MO embryos at the 8-cell stage. For each embryo, 4 blastomeres (derived from the egg animal hemisphere) will contain germ plasm and the other 4 will be germ plasm free in most cases (Leclère et al., 2012). This blastomere-separation approach has the advantage of more reliable separation of germ plasm from non-germ plasm regions, but the disadvantage that it is not possible to distinguish animal from vegetal blastomeres due to a lack of polarity landmarks at the 8-cell stage. In the experimental conditions used for this experiment, 1 or 2 of the 8 mini-embryos derived from each 8-cell stage embryo failed to develop an OA axis, as assessed by elongation and directional swimming, even at 48 hpf (data not shown). This suggests that some vegetal-blastomere derived mini-embryos lacked sufficient "organizer" activity to re-establish an oral peak of Wnt/b-catenin signaling necessary for axis recovery. We observed a correlation between axis formation and i-cell development; Piwi-expressing cells could clealy be detected in 36/51 (70%) of mini-embryos derived from uninjected 8-cell stage embryos, which had all attained an elongated morphology 24 hpf , while the remaining mini-embryos showed spherical morphology and no i-cells could be clearly distinguished (Table 2, experiment 1) . For mini-embryos derived from Wnt3-MO embryos, which were all spherical, the number that developed Piwi-positive i-cells was further reduced to 56% (31/55 in Table 2, expt1; Figure 1Q-T). The most likely explanation for this result is that the mini-embryos generated from germ plasm-containing animal blastomeres can develop i-cells despite the lack of OA polarity, while those generated from vegetal blastomeres cannot.

Taken together these results indicate that two distinct mechanisms can generate i-cells during *Clytia* larval development. During normal development Wnt is not required, likely because of fate determination by inherited germ plasm. In fragments lacking germ plasm, however Wnt signaling is required for a distinct i-cell specification process, either directly or indirectly through its role in re-establishing the OA axis.

Sequential specification of i-cell derivatives during larval development

To address the involvement of Wnt signaling in cell fate choice from i-cell pool, we developed a panel of gene markers for likely i-cell derivative cell types, focusing on the known i-cell derivatives in *Hydra*: gland cells**,** nerve cells and nematocytes (Figure 2; see Supplementary file S1 for expression patterns of these genes in adult medusae) and germ cells (Figure 3).

As a gland cell marker we adopted the *Clytia* orthologue of the *Hydra* gene *Antistasin,* a serine protease inhibitor suggested to protect endodermal cells from their own secreted digestive enzymes (Holstein et al., 1992), whose expression in the *Clytia* medusa was strongly detected in the digestive part of the manubrium (Supplementary file S1). In *Hydra* all endodermal gland cells (mucous gland cells and zymogen cells) are i-cell derived (Siebert et al., 2008), however some mucous cells in the *Clytia* larva may not be (Martin and Thomas, 1981a). During larval development we could detect weak *Antistasin* expression as early as 24 hpf, ie in the very early planula just completing gastrulation (Figure 2A-C). Expression was largely confined to the central presumptive endoderm region consistent with expression in cells that participate in the formation of the central endodermal cavity by autolysis.

To follow nematocyte formation we used as a marker the *Minicollagen 3/4a* gene, which codes for a structural component of the nematocyst capsule (Denker et al., 2008). Minicollagen 3/4a mRNA could be detected from 24 hpf through larval development in the nematoblasts and differentiating nematocytes in the central part of the endodermal region, but not during later stages of differentiation and migration into the ectoderm (Figure 2D-F). Finally, to characterise neurogenesis we identified the *Clytia* orthologue of the *Hydra* paired-class homeobox gene *Prdl-a* (phylogenetic analysis in Supplementary file S2), expressed in subset of i-cell derived neural cells occupying the head region of *Hydra* and *Podocoryne* polyps (Gauchat et al., 1998; Reya and Clevers, 2005). In *Clytia* medusae, *Prdl-a* was similarly expressed in a population of cells with neural-like morphology in the manubrium ectoderm and in the proximal part of the the tentacle bulb ectoderm (Supplementary file S1). During larval development we could first detect *Prdl-a* expression in the endodermal region at 36 hpf (not shown), its expression at 48 hpf and 72 hpf being slightly less concentrated towards the oral pole (Figure 2G-I). We found that a basic Helix Loop Helix (bHLH) gene related to the *Drosophila* neurogenic gene *Achaete Scute, Asc-b,*

showed a very similar expression profile to *Prdl-a* through larval development (Fig. 2J-L). *Clytia Asc-b* is the orthologue of *Podocoryne Ash2* (phylogenetic analysis in Supplementary file S2), expressed in putative secretory cells in the endoderm (Hensel et al., 2014; Khalturin et al., 2007; Seipel et al., 2004; Teo et al., 2006). Expression of *Clytia Asc-b* in medusa was confined to cells in endodermal structures (circular but not radial canals and manubrium), whose precise identity remains to be established (Figure S1). Trancriptomic data from separated cell populations from *Hydra* polyps (Hemmrich et al., 2012) supported an i-cell origin for *Prdl-a*, *Asc-b* and *Antistasin*–expressing cells, since *Hydra* ortholog transcripts for all these genes were all detected in Nanos-positive cells, and more strongly in endodermal cells for *Asc-b* and *Antistasin* (Table 3). The timing of *Clytia Prdl-a* and *Asc-b* expression compared to *Minicollagen 3/4a* expression indicates that neurogenesis occurs later than nematocyte differentiation during *Clytia* larval development, although this should be confirmed by identifying genes expressed earlier during neurogenesis. We cannot rule out the possibility of a common neural-nematogenesis precursor as described in *Nematostella* (Richards and Rentzsch, 2014) and in *Hydra* (Galliot et al., 2009).

Finally to map the formation of differentiated neurons we identified the *Clytia* cDNA sequences coding for precursors of RFamide neuropeptides, widely expressed in cnidarian i-cell derived ganglionic cells (Hayakawa et al., 2004; Martin, 1990; Momose et al., 2008; Momose and Houliston, 2007), and one of two GLWamide precursor genes identified in the *Clytia* transcriptome, *PP2*. GLWamides are expressed in sensory neurons concentrated at the aboral pole of hydrozoan larvae and are involved in triggering metamorphosis (Piraino et al., 2011; Takahashi and Hatta, 2011). All the neurons expressing GLWamide precursor genes in *Hydra* are absent in i-cell free polyps (Lapébie et al., 2014; Mitgutsch, 1999), implying an i-cell origin, although we cannot rule out the possibility that the sensory neurons of ectodermal origin described in hydrozoan larvae (Martin and Thomas, 1981a; Momose et al., 2008; Thomas et al., 1987) may include ones expressing GLWamide. In *Clytia* larvae both RFamide and GLWaII precursor mRNAs were first detected in ectodermal cells at 36 hpf (not shown), and showed the expected lateral and aboral ectoderm distributions respectively along the body axis (Figure 2M-R).

No evidence for germ cell precursor formation during larval development

In hydrozoans, differentiating germ cells detected by morphological criteria have only been described in adult stages (medusae or polyps, depending on the species life cycle), either in the gonads or in some cases migrating towards them (Künzel et al., 2010; Momose and Houliston, 2007). To address whether committed germ line precursors might already be generated during larval stages, we sought to identify early-expressed molecular markers of the germ line in *Clytia* by testing in adult medusae the expression of six candidate genes identified in our *C. hemisphaerica* transcriptome (Lapébie et al., 2014; Leclère et al., 2012) coding for various putative RNA binding proteins, 3 Boule/DAZ related proteins, 2 Tudor domain proteins and the EVE domain nuclear protein Thyn1. Boule/DAZ family members have a characteristic combination of RRM domains and Daz repeats and are widely associated with germ cell development across the animal kingdom {Fu:2015cv} but have not been previously characterised in cnidarians. *Clytia Boule1-a* is an orthologue to all bilaterian Boule genes (including the Daz or DAZL subfamily specific to vertebrates), while *Boule like1-b* and *Boule like 1-a* result from independent expansion of the Boule/DAZ family in the cnidarian linage (Phylogenetic analysis in Supplementary File S2). Tudor domain proteins also have widespread roles in RNA metabolism including the piRNA processing and DNA damage responses, but also in pole cell formation in *Drosophila* (by the original *Tudor* gene) and mammalian spermatogenesis(Pek et al., 2012; Thomson and Lasko, 2005). The two *Clytia* Tudor Domain Proteins TDP-1 and TDP-2 that we tested contain four or six Tudor domains respectively, as well as one RING domain and one BBOX protein domain for TDP-1, while TDP-2 contains two binding sites for dimethylated arginin providing a putative binding site for Piwi proteins. The *Clytia Thyn1* gene was selected for characterization due to the i-cell restricted expression of the *Hydra* ortholog Hmp_06895 (Hemmrich et al., 2012; Hwang et al., 2007). Thyn1 (For Thymocyte nuclear protein 1) proteins show wide sequence conservation of the "EVE" putative RNA binding motif among animals and plants and even bacteria (Phylogeny in Supplementary File S2), but little is known about their function, except for the regulation of apoptosis and cell cycle progression in thymocytes by mammalian and avian Thyn1 proteins (Miyaji et al., 2002; Momose et al., 2008; Toyota et al., 2012).

In situ hybridization patterns in adult medusae (Figure 3) identified two of the six candidate markers tested, *Clytia Boule1-a* (Fig. 3A) and *Thyn*1 (Fig. 3F) as early germ line

makers. Expression of these two genes was detected exclusively in developing male and female germ cells and in the region of the adult gonad close to the bell where i-cells and the early stages of germ cell development are most concentrated (Amiel and Houliston, 2009; Denker et al., 2008). Germ-line restricted expression of *Clytia Boule1*-a is consistent with a highly conserved germ line role across animal species, whereas the *Clytia Thyn1* expression was unexpected given its wider i-cell expression in *Hydra* (Hwang et al., 2007). Expression of , *TDP-1* and *TDP-2* was also detected in male and/or female germ cells but also in other sites, notably in the i-cell rich region at the base of the tentacle bulbs (Figure 3C, D, E), suggesting wider or multiple developmental roles. *Boule like1-a* was not expressed in the gonad, while *Boule like1-b* was expressed in developing female but not male germ cells (Figure 3B).

No expression of either of the putative germ line specific genes that we identified, *Boule1-a* or *Thyn1,* was detected in planula larvae, even at 72 hpf when the larvae are fully developed and competent to metamorphose. These analyses thus support a model in which commitment of i-cells to a germ cell fate is delayed until adult stages in the *Clytia* life cycle.

Wnt signaling is not required for i-cell somatic fate choices

We tested the requirement for wnt signaling in somatic cell type generation from i-cells using the molecular markers characterised above (Figure 4) as well as other staining techniques to detect differentiated neurons and nematocytes (Figure 5). In Wnt3-MO larvae, *Antistasin* (Fig. 4A-B), *Prdl-a* (Fig. 4E-F) and *Asc-b* (Fig. 4G-H) expression was detectable at 48 hpf as it was in uninjected controls, despite the spherical phenotype, showing that neither Wnt3 function nor oral territory development are required for gland cell or nerve cell development. *Minicollagen 3-4a* expression (Fig.4C-D) also was clearly detected at 48 hpf but not at 24 hpf, indicating that nematoblast formation occurs with a delay. Despite the Wnt3 independence of neural and nematocyte precursors formation, we found that the numbers of differentiated nematocytes and of some neural cells types was severely reduced in Wnt3-MO embryos. Intact 48 hpf and 72 hpf planulae showed on average 23 and 69 nematocytes respectively as visualised with DAPI staining (Fig. 5A, C; n=22 and n=21 embryos respectively). In contrast, no nematocytes were detected in Wnt3-MO planulae at 48 hpf and 72 hpf (Fig.5B, D; average=0 and 0,7 for n=26 and 33 respectively). RFamide expressing neurons were not detectable in Wnt3-MO planulae at 48 hpf by either *in situ* hybridization (Figure 4J) or immunofluorescence (Fig. 5E-F). On the

other hand GLWamide expressing sensory neurons were clearly detectable in the Wnt3-MO larvae at 48 hpf (Figure 4K-L). These observations suggest that differention of some i-cell derivatives may depend on Wnt3 signaling, either directly or through its role in patterning the OA axis.

b-catenin nuclear localisation is abolished in Wnt3-MO embryos, at least until the early gastrula stage, and the expression of two Wnt ligands expressed orally during later stages is also prevented(Momose et al., 2008), but we cannot exclude the possibility that other Wnt ligands function during later periods of larval development. To address this possibility we treated larvae from 24 hpf to 48 hpf with the TCF/ß-catenin interaction inhibitor PKF118-310 (Figure 6). In PKF118-310 treated larvae, *Piwi* (Fig. 6B) and *Minicollagen 3-4a* (Fig. 6D) expression was detectable by *in situ* hybridization at 48 hpf as it was in non treated controls (Fig.6A, C) and in Wnt3-MO larvae (Fig.1F and Fig. 4D), showing that Wnt signaling is dispensable for maintenance of i-cells and nematoblast formation. On the other hand RFamide precursor (PP5) and GLWamide precursor (PP2) expression was abolished, suggesting that Wnt signaling acts at later stages of larval development. Assessment of the numbers of final nematocytes by DAPI staining and RFamide expressing cells by immunostaining confirmed this conclusion (data not shown). These PKF118-310 experiments are consistent with the Wnt3-MO findings, but have to be treated with caution since we cannot rule out non-specific effects of the drug.

Discussion

The hydrozoan planula larva offers an excellent opportunity to undertand how alternative somatic cell types can be generated from a common stem cell pool and also to address the embryological origin of i-cells. In this study we followed successive steps of i-cell development during embryogenesis and larva formation in *Clytia*, and defined successive distinct roles for Wnt signaling. We found that Wnt signaling is not essential either to establish or to maintain the i-cell pool during normal development, nor for them to engage in somatic fate pathways via the formation of nematoblasts, neuroblasts or gland cells. Wnt/ß-catenin inhibition did, however, prevent terminal differentiation of nematocytes and some ganglionic cell types. We also uncovered another significant feature of i-cell regulation which requires, directly or indirectly, Wnt signaling: their formation by a 'recovery' pathway activated in the absence of maternal germ plasm from the egg animal pole.

The two principal areas addressed by our study are discussed in more detail below: defining the Wnt dependent steps of somatic cell development from i-cells, and uncovering alternative mechanisms to specify formation of the initial i-cell pool. Another point of interest in this study was our identification of two genes expressed early during germ line development, *Boule1-a* and *Thyn1*. No expression of either of these could be detected in the planula, supporting a model in which germ cell fate specification in *Clytia* is delayed until adult stages, for instance being induced by signals from the somatic gonad tissues.

Wnt signaling is not required to specify i-cell somatic fates but for their differentiation.

Our conclusion that the appearance during *Clytia* larva development of precursor cells of various somatic i-cell derivatives does not require Wnt signaling, but that final differention of nematocytes and some neural cell types does so, is compatible with most of the observations from previous studies in *Hydractinia* and *Hydra.* We found a strong reduction in the number of differentiated nematocytes in *Clytia* Wnt3-MO and PKF118-310 treated embryos, while in polyps of both the other species, treatment with paullones to stimulate b-catenin accumulation by blocking GSK-3b resulted in a large excess of developing and mature nematocytes(Khalturin et al., 2007; Teo et al., 2006). In *Hydra* polyps the increase in late stages of nematocyte differentiation induced by alsterpaullone was found to occur at the expense of cells expressing the "nematoblast nest" marker nb035.

We can thus propose that in both these species of hydrozoan polyp as well as the *Clytia* planula larva, Wnt signaling drives the terminal steps of nematocyte differentiation. Wnt expression in the planula ectoderm is organised as overlapping/nested domain of several ligands (Momose et al., 2008), which could produce an oral-aboral descending gradient of Wnt/b-catenin activity. The oral pole peak coincides with a concentration of nematocytes at this site (Bodo and Bouillon, n.d.; Plickert et al., 2012) (Figure 5). Likewise in *Hydra* it has been proposed that Wnt activity promotes nematocyte differentiation relating to hyper-development of mouth and tentacle structures at the oral tip of the polyp where this pathway is locally favored (Bosch and David, 1991; Hobmayer et al., 2000; Khalturin et al., 2007; Lengfeld et al., 2009).

While all three studies of Wnt function during i-cell development support a stimulatory role for Wnt signaling in nematogenesis, interpretations vary concerning which steps are being regulated. The *Hydra* study (Khalturin et al., 2007) and our *Clytia* data indicate that neither maintenance of the multipotent i-cell pool nor initial entry into the nematogenesis pathway are regulated by Wnt signaling. In apparent contradiction, transient stimulation of cell proliferation and b-catenin nuclear localization in cells of the endodermal region was observed in alsterpaullone-treated *Hydractinia* larvae and polyps (Teo et al., 2006), but it is possible that the cell population affected by Wnt pathway stimulation in that study was not restricted to the i-cell lineage. The delay we observed in *Minicollagen 3-4a* expression in Wnt3-MO *Clytia* embryos also appears at first sight to contradict the hypothesis that early nematogenesis steps are Wnt-independent, but may reflect the general delay in zygotic gene expression in i-cells and other cells that ingress during gastrulation when the translation of Wnt3, Fz1 or the PCP core component gene Strabismus are disrupted (Lapébie et al., 2014).

As for nematogenesis, Wnt signaling was found to affect final differentiation but not early regulatory steps during i-cell derived neurogenesis. In *Clytia*, *Prdl-a* expression occurred on schedule in Wnt3-MO embryos, but we observed cell-type specific effects on neuronal differentiation. The sensitivity of these cell types correlates with their distribution along the OA axis. Thus RFamide ganglion cells formation along the sides of the *Clytia* planula, may be stimulated by "higher" values of a Wnt gradient in the ectoderm along the OA axis, as may the RFamide neurons preferentially associated with tentacles and other oral structures in *Hydractinia* polyps (Teo et al., 2006). Conversely development of aboral

localized neurons such as GLWamide expressing sensory neurons in the *Clytia* planula does not seem to be sensitive to Wnt3 down-regulation, although it was disrupted by the TCF pharmacological inhibitor, indicating that GLWamide neuron differntiaton could require a lo Wnt/β-catenin w level of Wnt/β-catenin signaling. In *Hydra,* paullone treatments had no obvious effects on neuronal populations expressing the peptide Hym355, which is expressed extensively along the body column (Khalturin et al., 2007), and thus not obviously under the influence of the oral Wnt source (Hobmayer et al., 2000; Lengfeld et al., 2009). Oral specific effects of Wnt signaling on neural differentiation could well be mediated by peptides secreted by the epithelial cells that could affect interstitial cell differentiation by inhibiting commitment or migration of nerve precursor cells (Bosch, 2003; Watanabe et al., 2009). In *Hydra*, Hym-355 (a PRGamide) produced by neurons stimulates neural differentiation while –PW family peptides secreted by epithelial cells inhibit it (Takahashi and Fujisawa, 2009). Wnt3/β-catenin

Finally, endodermal digestive cell differentiation, as assayed by *Antistasin* expression, was not affected in *Clytia* Wnt-3 MO embryos. Since Wnt expression in the planula is restricted to the ectoderm, the endodermal region may be largely out of the influence of Wnt signaling both for early and late stages of i-cell development.

To conclude, studies of Wnt signaling in hydrozoan polyps and larvae can be reconciled according to a model in which Wnt signaling stimulates the final differentiation of nematocytes (normally concentrated at the planula oral pole and in polyp oral tentacles), and also neuronal differentiation in ectodermal ganglion cells. In future experiments it would be interesting to address the signaling pathways responsible for the i-cell regulation processes occuring in the endodermal region of the planula; drug experiments in *Hydra* suggest that the Notch pathway is involved in nematoblast specification (Käsbauer et al., 2007; Khalturin et al., 2007) while secreted peptides may be involved in the feedback regulation that maintains the i-cell pool (Steele, 2002). Cnidarian-specific secreted peptides and 7tm receptors expressed preferentially in the cells that ingress during gastrulation (including i-cells) (Lapébie et al., 2014) provide candidates for these signals.

Two mechanisms for i-cell fate determination during Clytia embryogenesis

Previously we showed that germ plasm including Vasa, PL10, Nanos1 and Nanos2 mRNAs is positioned around the female pronucleus at the egg animal pole. In this position it is inherited by the i-cell precusors, although inheritence by this lineage has not been

demonstrated. This would require tracking of the germ plasm in live animals, perhaps in the future by gene editing to tag UTRs of the mRNA allowing their detection with fluorescent binding proteins, for instance using the MS2 system (Bertrand et al., 1998). In this study we provide the first experimental evidence that germ plasm has i-cell fate determining activity in *Clytia*. We found that i-cells could develop in whole embryos and in (germ plasm containing) animal embryo fragments whether or not Wnt signaling was inhibited, and thus irrespective of OA axis development. In contrast, i-cells did not form from (germ plasm free) vegetal regions if Wnt signaling was inhibited. The most simple explanation for this result is that the Wnt independent i-cell formation is driven by germ plasm inherited from the egg animal pole.

Although we can thus be reasonably confident that germ plasm participates in determining i-cell fate during normal embryogenesis, clearly an alternative mechanism is available to account for i-cell formation from vegetal fragments. Germ line specification in many animals is delayed until late stages of embryogenesis, despite deriving in undisturbed embryos from an identifiable cell lineage (Juliano et al., 2010). The sea urchin embryo provides an example in which plasticity of the germ line lineage has been demonstrated experimentally; germ line cells normally derive from the small micromere lineage (which actually generates the entire adult primordia ahead of larval metamorphosis) but when the small micromeres are removed, regulatory mechanisms allow fertile adults to develop. The *Clytia* example is, however, the first case to our knowledge of germ line restoration following precursor ablation in an animal where "germ plasm" in undisturbed conditions contributes to determining the fate of the germ cell lineage. The germ plasm in this case contains aggregates of mRNAs from several germ lines genes (Vasa, PL10, Piwi, Nanos1, Nanos2) and also probably the Vasa protein as observed in *Hydractinia* (Rebscher et al., 2008), but it is important to note that these mRNAs are also present throughout the embryo in a less organised state, which may facilitate formation of i-cells following animal pole removal (Leclère et al., 2012; Momose et al., 2008). A variety of post transcriptional mechanisms may contribute to mRNA and protein accumulation during this process, as described for sea urchin Vasa and Nanos (Gustafson et al., 2011; Oulhen et al., 2013; Yajima et al., 2014).

In *Clytia,* i-cell regeneration was found to be Wnt3 dependent, both from vegetal blastula halves and from isolated 8-cell stage blastomeres. This could mean that Wnt/b-

catenin signaling directly stimulates i-cell formation, and/or that it does so indirectly by allowing restoration of the OA axis via formation of an oral organizer region, as characterised in *Hydra* polyps (Broun, 2005; Hobmayer et al., 2000). New transcription of the germ plasm genes would not be required, at least initially, since their maternal mRNAs are present in a diffuse form in the vegetal region as well as in animal pole aggregates (Leclère et al., 2012).

Our findings in Wnt3-MO embryos were reinforced by the observation that some vegetal blastomeres from uninjected 8-cell stage embryos failed to recover OA axes and also to "regenerate" i-cells. This failure of some vegetal blastomeres to recover axial polarity was somewhat surprising given the high recovery rates reported previously from similar experiments in *C. gregaria* (Freeman, 1981) and *C. hemisphaerica* (Leclère et al., 2012). It partially resembled the results obtained in *Podocoryne carnea* (Momose and Schmid, 2006) or *Nematostella vectensis* (Fritzenwanker et al., 2007; Lee et al., 2007), in which axis restoration capacity is animally localized. Axis re-patterning ability in *C. hemisphaerica* may be sensitive to variation in experimental/culture conditions. This ability depends initially on the balance between the pathway activators Wnt3 and Fz1 provided from animal localized maternal mRNAs, and the inhibitory Fz3 from vegetally localized mRNAs (Momose et al., 2008; Momose and Houliston, 2007). Subsequently secreted factors produced orally and aborally are proposed to act to maintain polar identities (Lapébie et al., 2014). The failure of vegetal fragment to form an oral pole could thus reflect a failure of residual Wnt3/Fz1 signaling to overcome Fz3-mediated inhibition of oral identity during these processes. Whatever the reasons, this failure provided us with a useful confirmation of the correlation between axis re-patterning and i-cell regeneration capacities in the *Clytia* larva.

Acknowledgements :

We thank Sandra Chevalier for invaluable technical assistance and Doug Houston (Iowa) for his participation in cutting experiments. We also thank Doug and all our group members, especially Lucas Leclère and Chiara Sinigaglia for stimulating discussions.

References

Amiel, A., Houliston, E., 2009. Three distinct RNA localization mechanisms contribute to oocyte polarity establishment in the cnidarian Clytia hemisphaerica. Dev. Biol. 327, 191–203.

Bertrand, E., Chartrand, P., Schaefer, M., Shenoy, S.M., Singer, R.H., Long, R.M., 1998. Localization of ASH1 mRNA particles in living yeast. Molecular Cell 2, 437–445.

Bodo, F., Bouillon, J., n.d. Etude histologique du développement embryonnaire de quelques Hydroméduses de Roscoff. Cahiers de Biologie Marine IX, 69–79.

Bosch, T.C., David, C.N., 1991. Decision making in interstitial stem cells of Hydra. In Vivo 5, 515–520.

Bosch, T.C.G., 2003. Ancient signals: peptides and the interpretation of positional information in ancestral metazoans. Comp. Biochem. Physiol. B, Biochem. Mol. Biol. 136, 185–196.

Bosch, T.C.G., Anton-Erxleben, F., Hemmrich, G., Khalturin, K., 2010. The Hydra polyp: nothing but an active stem cell community. Dev. Growth Differ. 52, 15–25.

Broun, M., 2005. Formation of the head organizer in Hydra involves the canonical Wnt pathway. Development 132, 2907–2916.

Brouns, S.J.J., 2012. A Swiss Army Knife of Immunity. Science 337, 808–809.

David, C.N., 2012. Interstitial stem cells in Hydra: multipotency and decision-making. Int. J. Dev. Biol. 56, 489–497.

Denker, E., Manuel, M., Leclère, L., Le Guyader, H., Rabet, N., 2008. Ordered progression of nematogenesis from stem cells through differentiation stages in the tentacle bulb of Clytia hemisphaerica (Hydrozoa, Cnidaria). Dev. Biol. 315, 99–113.

Duffy, D.J., Millane, R.C., Frank, U., 2012. A heat shock protein and Wnt signaling crosstalk during axial patterning and stem cell proliferation. Dev. Biol. 362, 271–281.

Edgar, R.C., 2004. MUSCLE: multiple sequence alignment with high accuracy and high throughput. Nucleic Acids Research 32, 1792–1797.

Extavour, C.G., 2003. Mechanisms of germ cell specification across the metazoans: epigenesis and preformation. Development 130, 5869–5884.

Freeman, G., 1981. The role of polarity in the development of the hydozoan planula larva. Rouxs Arch Dev Biol 190, 168–184.

Fritzenwanker, J.H., Genikhovich, G., Kraus, Y., Technau, U., 2007. Early development and axis specification in the sea anemone Nematostella vectensis. Dev. Biol. 310, 264–279.

Galliot, B., Quiquand, M., 2011. A two-step process in the emergence of neurogenesis. Eur. J. Neurosci. 34, 847–862.

Galliot, B., Quiquand, M., Ghila, L., de Rosa, R., Miljkovic-Licina, M., Chera, S., 2009. Developmental Biology. Dev. Biol. 332, 2–24.

Gauchat, D., Kreger, S., Holstein, T., Galliot, B., 1998. prdl-a, a gene marker for Hydra apical differentiation related to triploblastic paired-like head-specific genes. Development 125, 1637–1645.

Genikhovich, G., Kürn, U., Hemmrich, G., Bosch, T.C.G., 2006. Discovery of genes expressed in Hydra embryogenesis. Dev. Biol. 289, 466–481.

Gustafson, E.A., Yajima, M., Juliano, C.E., Wessel, G.M., 2011. Developmental Biology. Dev. Biol. 349, 440–450.

Hayakawa, E., Fujisawa, C., Fujisawa, T., 2004. Involvement of Hydra achaete-scute gene CnASH in the differentiation pathway of sensory neurons in the tentacles. Dev. Genes Evol. 214, 486–492.

Hemmrich, G., Khalturin, K., Boehm, A.-M., Puchert, M., Anton-Erxleben, F., Wittlieb, J., Klostermeier, U.C., Rosenstiel, P., Oberg, H.-H., Domazet-Lošo, T., Sugimoto, T., Niwa, H., Bosch, T.C.G., 2012. Molecular signatures of the three stem cell lineages in Hydra and the emergence of stem cell function at the base of multicellularity. Molecular Biology and Evolution 29, 3267–3280.

Hensel, K., Lotan, T., Sanders, S.M., Cartwright, P., Frank, U., 2014. Lineage-specific evolution of cnidarian Wnt ligands. Evol. Dev. 16, 259–269.

Hobmayer, B., Rentzsch, F., Kuhn, K., Happel, C.M., Laue, von, C.C., Snyder, P., Rothbächer, U., Holstein, T.W., 2000. WNT signalling molecules act in axis formation in the diploblastic metazoan Hydra. Nature 407, 186–189.

Holstein, T.W., Mala, C., Kurz, E., Bauer, K., Greber, M., David, C.N., 1992. The primitive metazoan Hydra expresses antistasin, a serine protease inhibitor of vertebrate blood coagulation: cDNA cloning, cellular localisation and developmental regulation. FEBS Letters 309, 288–292.

Hwang, J.S., Ohyanagi, H., Hayakawa, S., Osato, N., Nishimiya-Fujisawa, C., Ikeo, K., David, C.N., Fujisawa, T., Gojobori, T., 2007. The evolutionary emergence of cell type-specific genes inferred from the gene expression analysis of Hydra. Proceedings of the National Academy of Sciences 104, 14735–14740.

Ikenishi, K., 1998. Germ plasm in Caenorhabditis elegans, Drosophila and Xenopus. Dev. Growth Differ. 40, 1–10.

Juliano, C.E., Swartz, S.Z., Wessel, G.M., 2010. A conserved germline multipotency program. Development 137, 4113–4126.

Käsbauer, T., Towb, P., Alexandrova, O., David, C.N., Dall'Armi, E., Staudigl, A., Stiening, B., Böttger, A., 2007. The Notch signaling pathway in the cnidarian Hydra. Dev. Biol. 303, 376–390.

Khalturin, K., Anton-Erxleben, F., Milde, S., Plötz, C., Wittlieb, J., Hemmrich, G., Bosch, T.C.G., 2007. Transgenic stem cells in Hydra reveal an early evolutionary origin for key elements controlling self-renewal and differentiation. Dev. Biol. 309, 32–44.

Kusserow, A., Pang, K., Sturm, C., Hrouda, M., Lentfer, J., Schmidt, H.A., Technau, U., Haeseler, von, A., Hobmayer, B., Martindale, M.Q., Holstein, T.W., 2005. Unexpected complexity of the Wnt gene family in a sea anemone. Nature 433, 156–160.

Künzel, T., Heiermann, R., Frank, U., Muller, W., Tilmann, W., Bause, M., Nonn, A., Helling, M., Schwarz, R.S., Plickert, G., 2010. Migration and differentiation potential of stem cells in the cnidarian Hydractinia analysed in eGFP-transgenic animals and chimeras. Dev. Biol. 348, 120–129.

Lapébie, P., ruggiero, A., Barreau, C., Chevalier, S., Chang, P., Dru, P., Houliston, E., Momose, T., 2014. Differential Responses to Wnt and PCP Disruption Predict Expression and Developmental Function of Conserved and Novel Genes in a Cnidarian. PLoS Genet 1–23.

Leclère, L., Jager, M., Barreau, C., Chang, P., Le Guyader, H., Manuel, M., Houliston, E., 2012. Maternally localized germ plasm mRNAs and germ cell/stem cell formation in the cnidarian Clytia. Dev. Biol. 364, 236–248.

Lee, P.N., Kumburegama, S., Marlow, H.Q., Martindale, M.Q., Wikramanayake, A.H., 2007. Asymmetric developmental potential along the animal–vegetal axis in the anthozoan cnidarian, Nematostella vectensis, is mediated by Dishevelled. Dev. Biol. 310, 169–186.

Lengfeld, T., Watanabe, H., Simakov, O., Lindgens, D., Gee, L., Law, L., Schmidt, H.A., Ozbek, S., Bode, H., Holstein, T.W., 2009. Multiple Wnts are involved in Hydra organizer formation and regeneration. Dev. Biol. 330, 186–199.

Lepourcelet, M., Chen, Y.-N.P., France, D.S., Wang, H., Crews, P., Petersen, F., Bruseo, C., Wood, A.W., Shivdasani, R.A., 2004. Small-molecule antagonists of the oncogenic Tcf/beta-catenin protein complex. Cancer Cell 5, 91–102.

Martin, V.J., 1990. Development of nerve cells in hydrozoan planulae: III. Some interstitial cells traverse the ganglionic pathway in the endoderm.

Martin, V.J., Archer, W.E., 1986. Migration of interstitial cells and their derivatives in a hydrozoan planula. Dev. Biol. 116, 486–496.

Martin, V.J., Thomas, M.B., 1981a. Elimination of the interstitial cells in the planula larva of the marine hydrozoanPennaria tiarella. J. Exp. Zool. 217, 303–323.

Martin, V.J., Thomas, M.B., 1981b. The origin of the nervous system in Pennaria tiarella, as revealed by treatment with colchicine.

Mitgutsch, C.E.A., 1999. Expression and Developmental Regulation of the Hydra-RFamide and Hydra-LWamide Preprohormone Genes in 1–15.

Miyaji, H., Yoshimoto, T., Asakura, H., Komachi, A., Kamiya, S., Takasaki, M., Mizuguchi, J., 2002. Molecular cloning and characterization of the mouse thymocyte protein gene. Gene 297, 189–196.

Momose, T., Derelle, R., Houliston, E., 2008. A maternally localised Wnt ligand required for axial patterning in the cnidarian Clytia hemisphaerica. Development 135, 2105–2113.

Momose, T., Houliston, E., 2007. Two oppositely localised frizzled RNAs as axis determinants in a cnidarian embryo. PLoS Biol. 5, e70.

Momose, T., Schmid, V., 2006. Animal pole determinants define oral-aboral axis polarity and endodermal cell-fate in hydrozoan jellyfish Podocoryne carnea. Dev. Biol. 292, 371–380.

Müller, W.A., Teo, R., Frank, U., 2004. Totipotent migratory stem cells in a hydroid. Dev. Biol. 275, 215–224.

Oulhen, N., Yoshida, T., Yajima, M., Song, J.L., Sakuma, T., Sakamoto, N., Yamamoto, T., Wessel, G.M., 2013. The 3'UTR of nanos2 directs enrichment in the germ cell lineage of the sea urchin. Dev. Biol. 377, 275–283.

Pek, J.W., Anand, A., Kai, T., 2012. Tudor domain proteins in development. Development 139, 2255–2266.

Petersen, C.P., Reddien, P.W., 2009. Wnt Signaling and the Polarity of the Primary Body Axis. Cell 139, 1056–1068.

Piraino, S., Zega, G., Di Benedetto, C., Leone, A., Dell'Anna, A., Pennati, R., Carnevali, D.C., Schmid, V., Reichert, H., 2011. Complex neural architecture in the diploblastic larva of Clava multicornis (Hydrozoa, Cnidaria). J. Comp. Neurol. 519, 1931–1951.

Plickert, G., Frank, U., Müller, W.A., 2012. Hydractinia, a pioneering model for stem cell biology and reprogramming somatic cells to pluripotency. Int. J. Dev. Biol. 56, 519–534.

Rebscher, N., Volk, C., Teo, R., Plickert, G., 2008. The germ plasm component vasa allows tracing of the interstitial stem cells in the cnidarian Hydractinia echinata. Dev. Dyn. 237, 1736–1745.

Reya, T., Clevers, H., 2005. Wnt signalling in stem cells and cancer. Nature 434, 843–850.

Richards, G.S., Rentzsch, F., 2014. Transgenic analysis of a SoxB gene reveals neural progenitor cells in the cnidarian Nematostella vectensis. Development 141, 4681–4689.

Seipel, K., Yanze, N., Schmid, V., 2004. Developmental and evolutionary aspects of the basic helix–loop–helix transcription factors Atonal-like 1 and Achaete-scute homolog 2 in the jellyfish. Dev. Biol. 269, 331–345.

Siebert, S., Anton-Erxleben, F., Bosch, T.C.G., 2008. Cell type complexity in the basal metazoan Hydra is maintained by both stem cell based mechanisms and

transdifferentiation. Dev. Biol. 313, 13–24.

Steele, R.E., 2002. Developmental signaling in Hydra: what does it take to build a “simple” animal? Dev. Biol. 248, 199–219.

Takahashi, T., Fujisawa, T., 2009. Important roles for epithelial cell peptides in Hydra development. Bioessays 31, 610–619.

Takahashi, T., Hatta, M., 2011. The Importance of GLWamide Neuropeptides in Cnidarian Development and Physiology. J Amino Acids 2011, 424501.

Teo, R., Möhrlen, F., Plickert, G., Müller, W.A., Frank, U., 2006. An evolutionary conserved role of Wnt signaling in stem cell fate decision. Dev. Biol. 289, 91–99.

Thomas, M.B., Freeman, G., Martin, V.J., 1987. The Embryonic Origin of Neurosensory Cells and the Role of Nerve Cells in Metamorphosis in Phialidium gregarium(Cnidaria, Hydrozoa). International Journal of Invertebrate Reproduction and Development 11, 265–285.

Thomson, T., Lasko, P., 2005. Tudor and its domains: germ cell formation from a Tudor perspective. Cell Res 15, 281–291.

Toyota, H., Jiang, X.-Z., Asakura, H., Mizuguchi, J., 2012. Thy28 partially prevents apoptosis induction following engagement of membrane immunoglobulin in WEHI-231 B lymphoma cells. Cell. Mol. Biol. Lett. 17, 36–48.

Watanabe, H., Hoang, V.T., Mättner, R., Holstein, T.W., 2009. Immortality and the base of multicellular life: Lessons from cnidarian stem cells. Seminars in Cell & Developmental Biology 20, 1114–1125.

Wikramanayake, A.H., Hong, M., Lee, P.N., Pang, K., Byrum, C.A., Bince, J.M., Xu, R., Martindale, M.Q., 2003. An ancient role for nuclear beta-catenin in the evolution of axial polarity and germ layer segregation. Nature 426, 446–450.

Wolenski, F.S., Layden, M.J., Martindale, M.Q., Gilmore, T.D., Finnerty, J.R., 2013. Characterizing the spatiotemporal expression of RNAs and proteins in the starlet sea anemone, Nematostella vectensis. Nat Protoc 8, 900–915.

Yajima, M., Gustafson, E.A., Song, J.L., Wessel, G.M., 2014. Piwi regulates Vasa accumulation during embryogenesis in the sea urchin. Dev. Dyn. 243, 451–458.

Figure legends

Figure 1. Wnt3 requirements for i-cell development in embryos and embryo fragments.
Images showing in situ hybridization using *Nanos1* (A-F) *and Piwi* (G-L) probes on non-injected and Wnt 3-MO embryos fixed at the early gastrula stage (A, B, G, H) and in planula larvae fixed at 24 hpf (C, D, I, J) and 48 hpf (E, F, K, L). Cells expressing both probes were detected at all three developmental stages, in intact embryos as well as in embryos lacking Wnt3. In 26 hpf embryos derived from animal (M-N) or vegetal (O-P) halves of blastula stage embryos, clear *Nanos1* expressing cells were detectable in all the non-injected or Wnt3-MO injected mini-planulae except for 50% of the "vegetal" group Wnt3-MO injected (P), in which Nanos1 signal is absent. In 24 hpf larvae derived from separated 8-cell stage blastomeres (Q-T), *in situ* hybridization using *Piwi* probe revealed that 30% of the non-injected embryos are spherical and lack Piwi-expressing cells (S), as compared to 56% in the case of Wnt3-MO injection (T). Scale bars: 50 μm for M-T.

Figure 2. Expression of putative i-cell somatic derivative markers during larval development.
Images showing in situ hybridization on planula larvae fixed at 24 hpf and 48 hpf using *Antistasin* (A-C) probes for gland cells, *Minicollagen 3-4a* (D-F) for nematocytes, *Prdl-a* (G-I) for differentiating neurons, *Asc-b* (J-L) for an uncharacterised endoderm-associated cell population, the RFamide precursor gene PP5 (M-O) for ganglionic neurons and the *GLWamide precursor PP2* (P-R), for aboral sensory neurons. Scale bars: 50 μm.

Figure 3. In situ hybridization analysis of potential germ line markers.
In situ hybridization images of *Clytia* medusae and planula larvae to characterize expression of a set of potential germ cell expressed genes, *Boule-1a* (A1-A7) , *Boule like1-b* (B1-B7), *Boule like1-a* (C1-C7), *TDP-1* (D1-D7), *TDP-2* (E1-E7) and *Thyn1* (F1-F7). TDP-1 expression in adult medusa was detected only in female gonads. The strong signal in small oocytes (red arrows in A1') is typical of oocyte expressed genes. The only genes exclusively expressed in the germ line, *Boule-1a* and *Thyn1*, were not detectably expressed in larval stages. AI', BI,'CI',DI',EI',FI' high magnification of the areas boxed in AI,BI,CI,DI,EI,FI,.

Red dashed lines in CIII show the boundary between endoderm and ectoderm. en: endoderm, ec:ectoderm. Scale bars: A-AI,B.B-BI,C-CI,D-DI,E-EI,F-FI 150 µm, AII-FII: 50 µm, AIII-FIII 100 µm, AIV-AVII 50 µm, AV-FVII 50 µm.

Figure 4. I-cell derivative expression in Wnt3-MO embryos.

In situ hybridization images of planula larvae fixed at 24 hpf and 48 hpf developed in parallel from non-injected (left panels) and Wnt3-MO injected (right panels) eggs. Probes used: *Antistasin* for gland cells *(*A-B), *Minicollagen 3-4a* for nematocytes (C-D), *Prdl-a* for differentiating neurons (E-F), *Asc-b* for undefined endoderm-associated cells (G-H), *PP5* for RFamide ganglionic neurons (I-J) and *PP2* for GLWamide aboral sensory neurons (K-L). Scale bars: 50 µm.

Figure 5. Wnt3 is required for nematocyte and ganglion cell differentiation.

A-D) Poly-gamma-glutamate staining of nematocytes capsules using DAPI at high concentration. Needle shape capsules are clearly visible in 48 hpf planulae (A). Their numbers increase at 72 hpf (C). In Wnt3-MO embryos, no nematocytes were detected (B, D).

E-F) RFamide antibody staining of 48 hpf non-injected (E) or Wnt3-MO injected (F) planula larvae. Ganglion cells stained in non-injected condition are totally absent from Wnt3-MO larvae. Neuronal cell bodies are indicated by red arrows. Scale bars: X for A-D; 50 µm for E-F

Figure 6. The Pharmacological TCF inhibitor PKF118-310 disrupts neural differentiation

Images showing *in situ* hybridization on planula larvae fixed at 48 hpf in untreated embryos and following 0.9 µM PKF118-310 treatment from 24 to 48 hpf using *Piwi* (A-B) probe for i-cells, *Minicollagen 3-4a* (C-D) for differentiating nematocytes, *PP5* (E-F) for RFamide ganglionic neurons and *PP2* (G-H) for GLWamide aboral sensory neurons. Scale bars: 50 µm.

Tables

TABLE 1: I-cell development following Blastula bisection.

6 hpf blastula 30min after blastula bisection	Non-injected			Wnt3-MO injected		
	Uncut	Animal half	Vegetal half	Uncut	Animal half	Vegetal half
Embryos with Nanos1 positive cells (%)	100	100	38	100	91	50
Embryos without Nanos1 positive cells (%)	0	0	62	0	9	50
Total	26	11	8	24	22	12
26 hpf planula 20h after blastula bisection	Non-injected			Wnt3-MO injected		
	Uncut	Animal half	Vegetal half	Uncut	Animal half	Vegetal half
Embryos with Nanos1 positive cells (%)	100	100	92	100	95	50
Embryos without Nanos1 positive cells (%)	0	0	8	0	5	50
Total	27	14	12	30	21	18

TABLE 2: I-cell development following blastomere isolation at the 8-cell stage.

	Experiment 1 - Piwi				Experiment 2 - Piwi				Experiment 3 - Piwi				Experiment 4 – Nanos1			
24 or 25 hpf planula pre-cutted at 8-cell stage	Non-injected		Wnt3-MO injected		Non-injected		Wnt3-MO injected		Non-injected		Wnt3-MO injected		Non-injected		Wnt3-MO injected	
	Uncut	Cut	Uncut	Cut	Uncut	Cut	Uncut	Cut	Uncut	Cut	Uncut	Cut	Uncut	Cut	Uncut	Cut
Embryos with Piwi or Nanos1 positive cells (%)	100	70	60	44	100	50	92	40	87	31	93	25	93	46	93	25
Embryos without Piwi or Nanos1 positive cells (%)	0	30	40	56	0	50	8	60	13	69	7	75	7	54	7	75
Total	30	51	15	55	13	12	52	42	15	61	15	60	15	24	15	36

TABLE 3: Gene names, accession numbers, and expression data in sorted cell types for Hydra orthologues.

Clytia gene name	accession number	Ortholog in Hydra magnipapillata	Ortholog in Nematostella vectensis	Ortholog in H. vulgaris transcriptomic dataset HAEP-T-CDS	ECTO	ENDO	NANOS	Podocoryne Orthologs
Asc-b	CEG06181.1	AAR0587.1	001622360.1	HAEP_T-CDS_v02_14032	0	7	4	AAQ75376.1
Prdl-a		CAA75668.1		HAEP_T-CDS_v02_8796	3	0	22	
Boule-1a		None						
Boule like1-b		XP_002157877.1		HAEP_T-CDS_v02_9288	0	0	0	
Boule like1-a		AFM91092.1		HAEP_T-CDS_v02_9098	0	0	0	
TDP-1		XP_012563744.1		HAEP_T-CDS_v02_6974	12	13	107	
TDP-2		XP_012556899.1		HAEP_T-CDS_v02_5242	33	24	69	
Thyn1		XP002162584.1		HAEP_T-CDS_v02_4726	134	180	1685	
Antistasin		CAA47864.1		HAEP_T-CDS_v02_5764	5	109	16	
				HAEP_T-CDS_v02_5763	4	76	17	
Piwi	EU199802	XM_002155877		HAEP_T-CDS_v02_104 l	134	45	192	
RFamide		XP_002164214.3		HAEP_T-CDS_v02_1089	5	0	0	
				HAEP_T-CDS_v02_12198	2	0	0	
GLW		XP_002164748		HAEP_T-CDS_v02_43727	15	8	7	
				HAEP_T-CDS_v02_8405	2	9	3	
Minicollagen 3/4a	ABW02882.1	DAA34982.1 (minicollagen8)		HAEP_T-CDS_v02_48708	10	0	26	
		DAA34987.1 (minicollagen 13)		HAEP_T-CDS_v02_859	4	2	1	

FIGURE 1

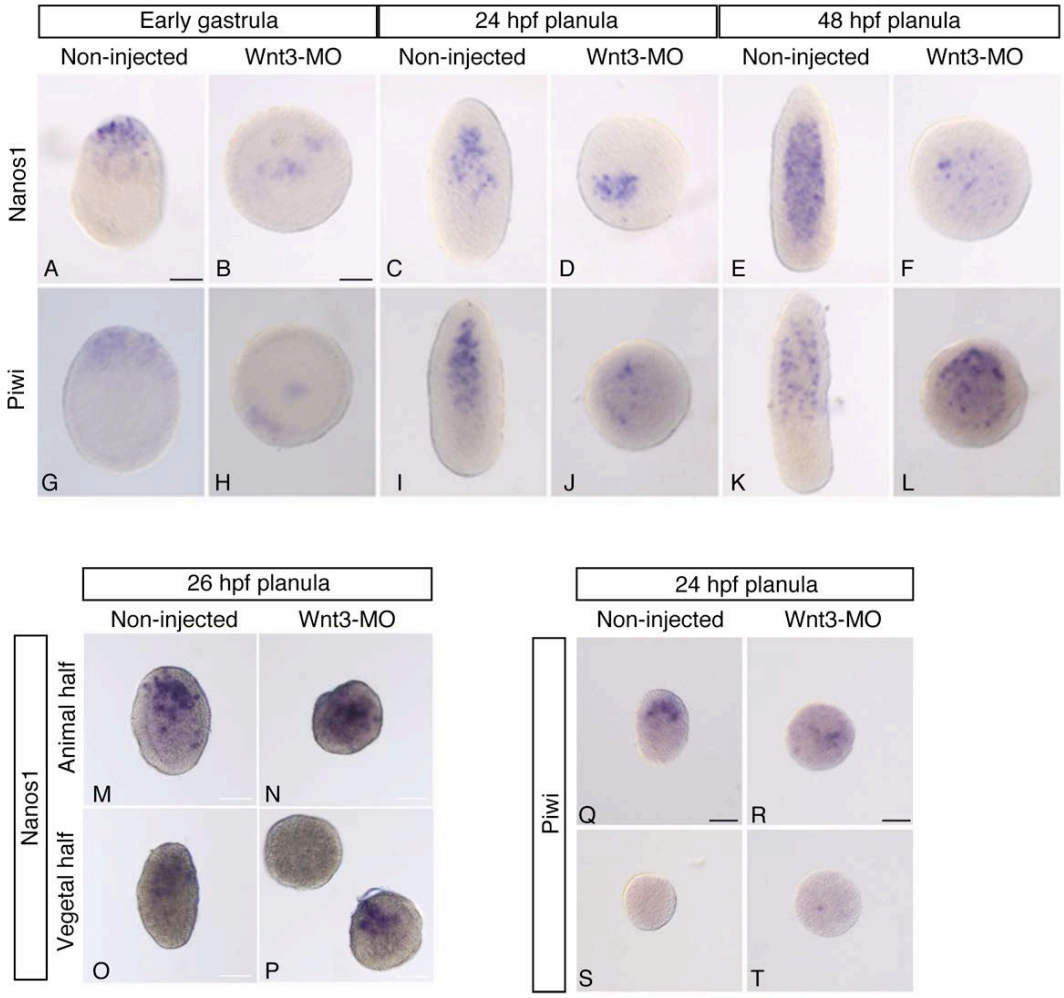
Early gastrula
24 hpf planula
48 hpf planula
Non-injected
Wnt3-MO
Non-injected
Wnt3-MO
Non-injected
Wnt3-MO
Nanos1
Piwi
A
B
C
D
E
F
G
H
I
J
K
L
26 hpf planula
Non-injected
Wnt3-MO
Nanos1
Animal half
Vegetal half
M
N
O
P
24 hpf planula
Non-injected
Wnt3-MO
Piwi
Q
R
S
T

FIGURE 2

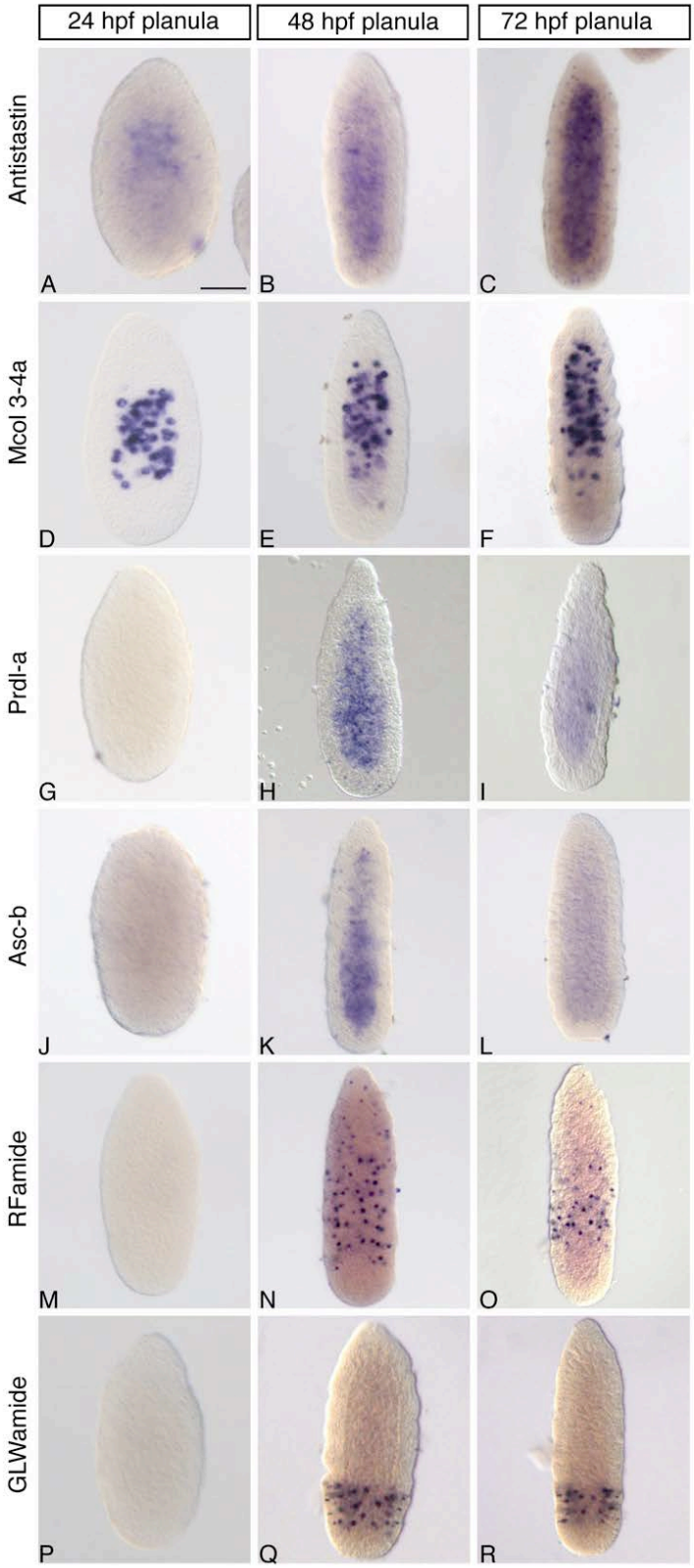
24 hpf planula
48 hpf planula
72 hpf planula
Antistastin
Mcol 3-4a
Prdl-a
Asc-b
RFamide
GLWamide
A
B
C
D
E
F
G
H
I
J
K
L
M
N
O
P
Q
R

FIGURE 3

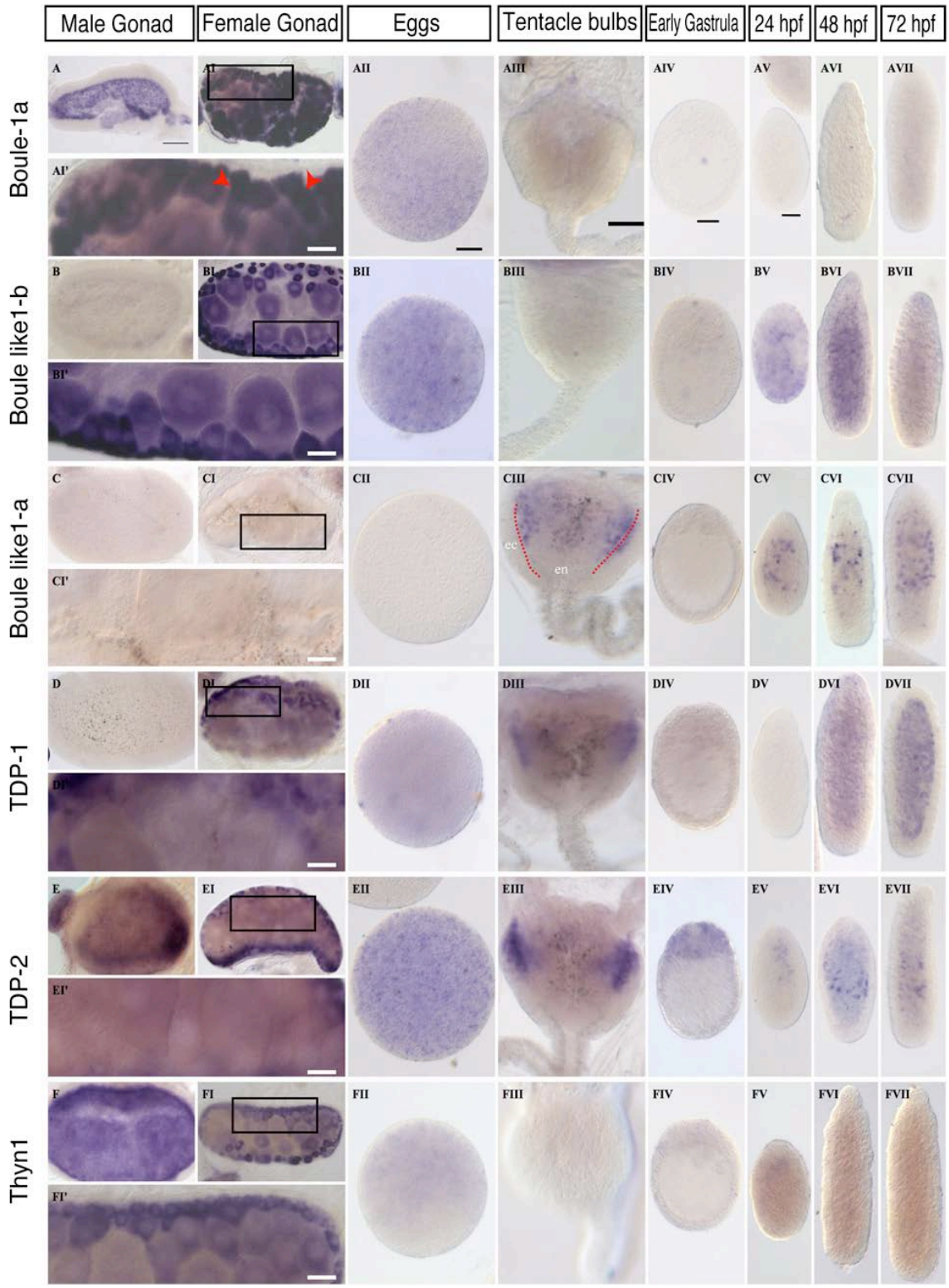
Male Gonad
Female Gonad
Eggs
Tentacle bulbs
Early Gastrula
24 hpf
48 hpf
72 hpf
Boule-1a
Boule like1-b
Boule like1-a
TDP-1
TDP-2
Thyn1
A
AI
AI'
AII
AIII
AIV
AV
AVI
AVII
B
BI
BI'
BII
BIII
BIV
BV
BVI
BVII
C
CI
CI'
CII
CIII
CIV
CV
CVI
CVII
ec
en
D
DI
DI'
DII
DIII
DIV
DV
DVI
DVII
E
EI
EI'
EII
EIII
EIV
EV
EVI
EVII
F
FI
FI'
FII
FIII
FIV
FV
FVI
FVII

FIGURE 4

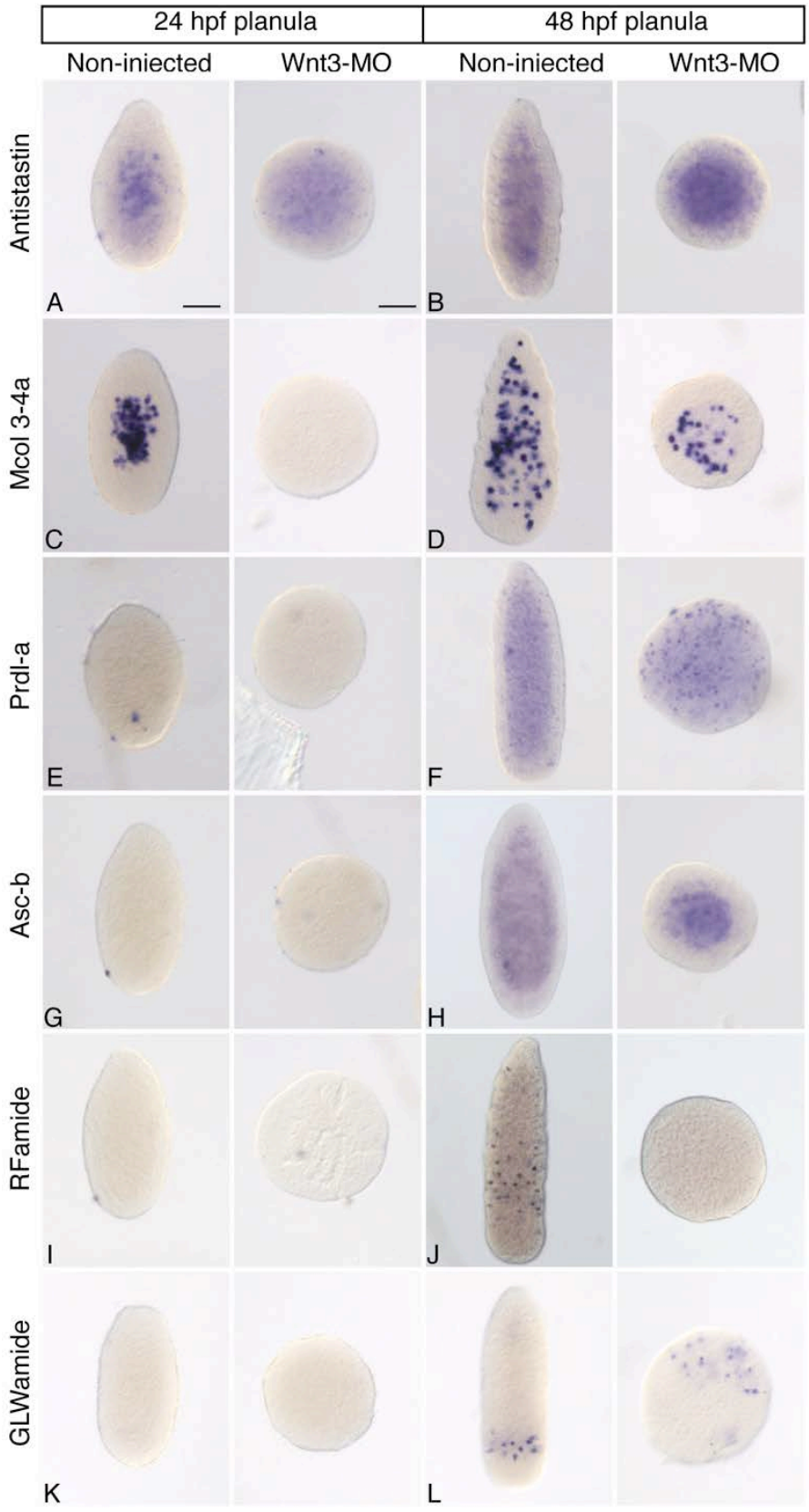
24 hpf planula
48 hpf planula
Non-iniected
Wnt3-MO
Non-iniected
Wnt3-MO
Antistastin
Mcol 3-4a
Prdl-a
Asc-b
RFamide
GLWamide
A
B
C
D
E
F
G
H
I
J
K
L

FIGURE 5

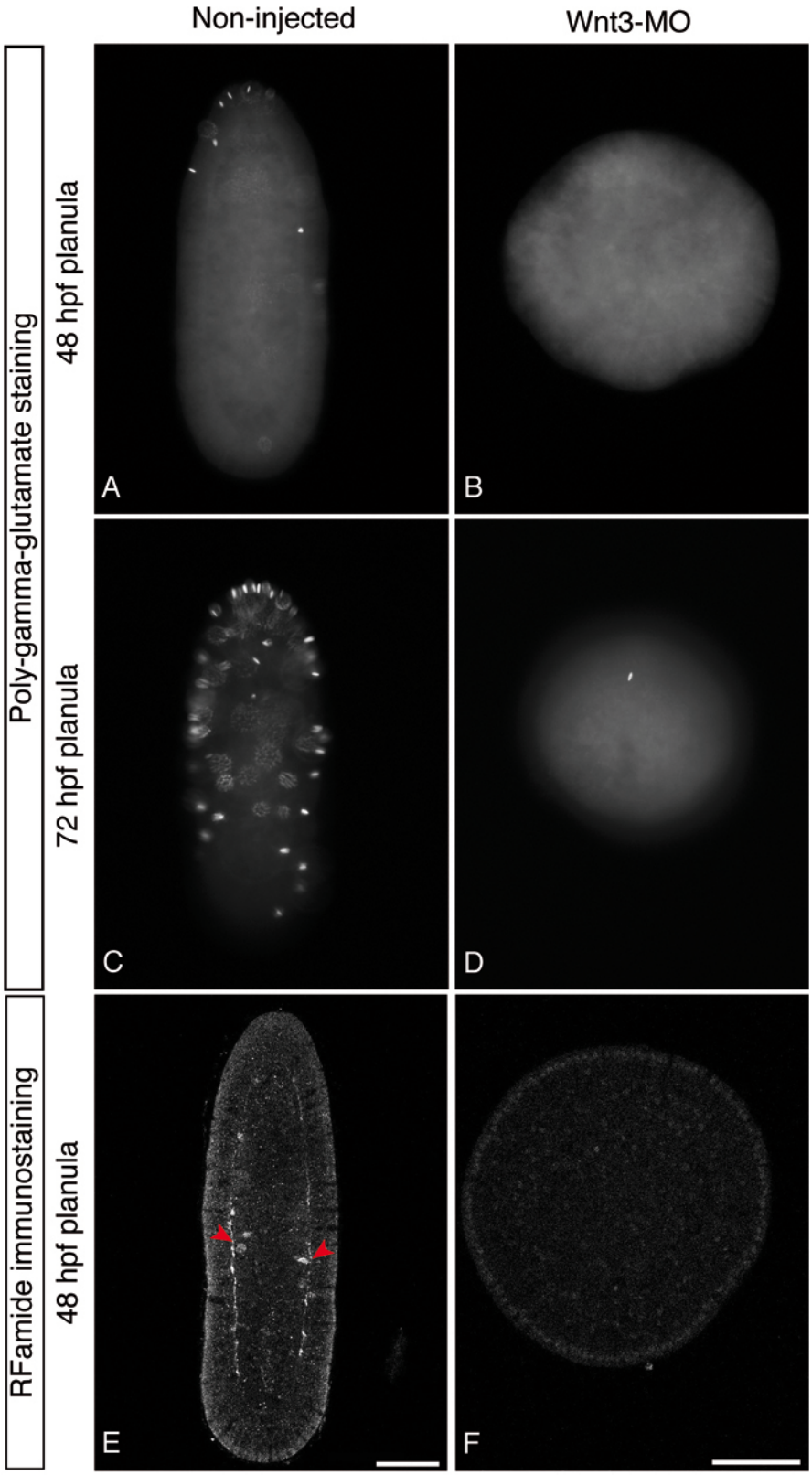
Non-injected
Wnt3-MO
Poly-gamma-glutamate staining
RFamide immunostaining
48 hpf planula
72 hpf planula
48 hpf planula
A
B
C
D
E
F

FIGURE 6

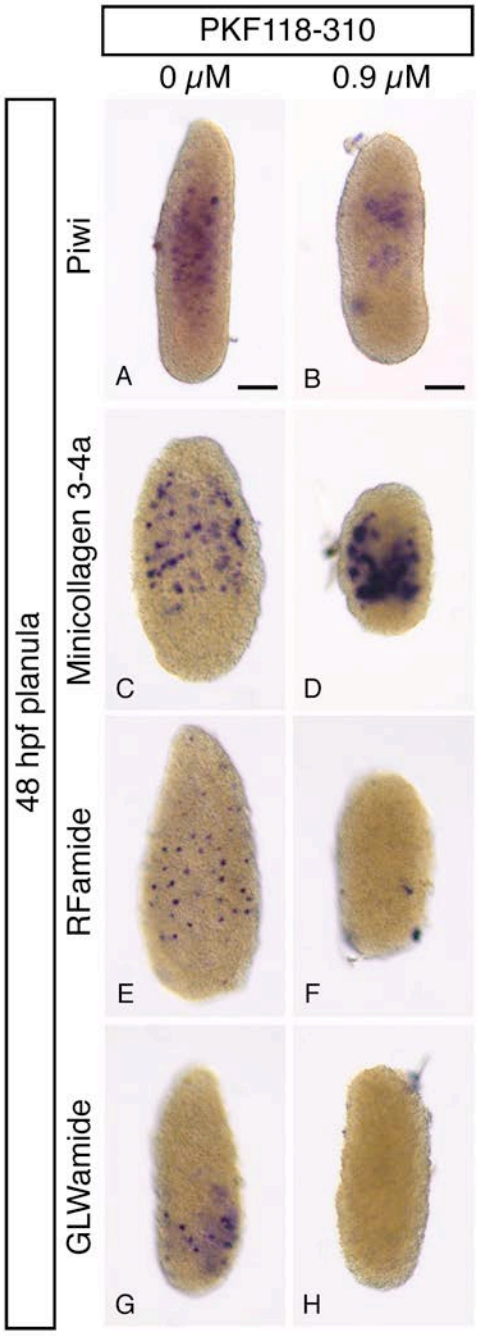
PKF118-310
0 μM
0.9 μM
48 hpf planula
Piwi
Minicollagen 3-4a
RFamide
GLWamide
A
B
C
D
E
F
G
H

SUPPLEMENTARY Files

Supplementary Figure S1

S1) Putative somatic i-cell derivative gene expression in adult medusa

Images showing in situ hybridization on adult medusa using Antistasin (A-C) probes for gland cells, Prdl-a (D-F) for differentiating neurons, Asc-b (G-I) for an uncharacterised endoderm-associated cell population, the RFamide precursor gene PP5 (J-L) for ganglionic neurons and the GLWamide precursor PP2 (M-O), for aboral sensory neurons. Scale bars: 50 µm.

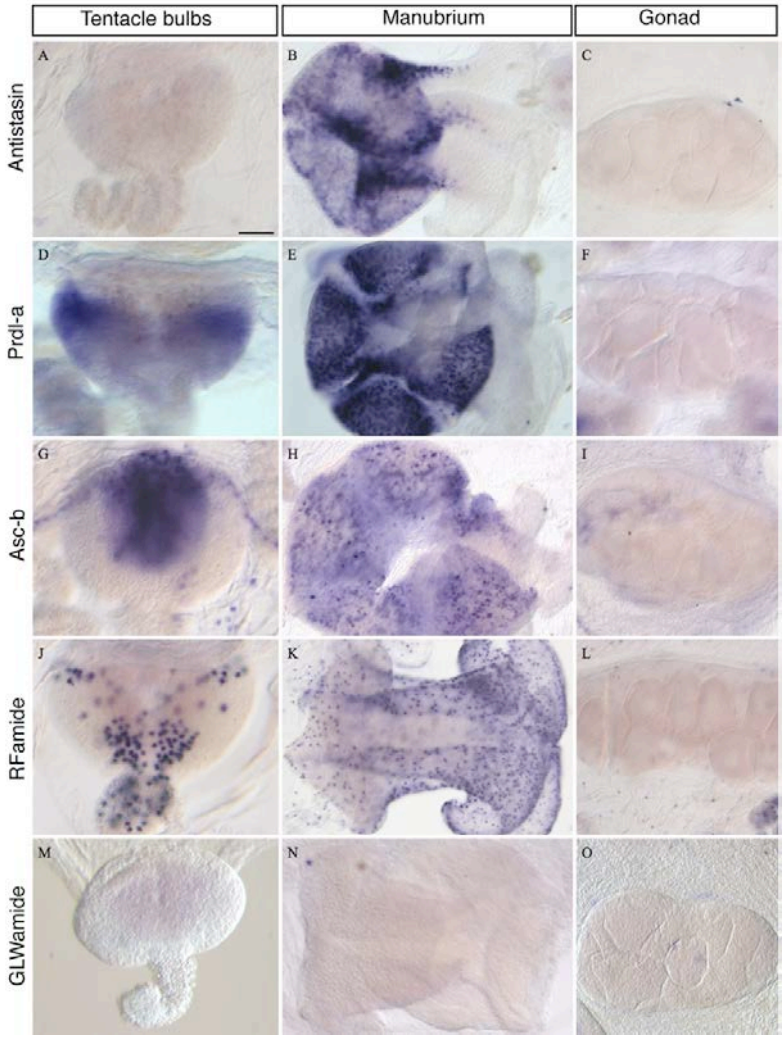

S2) Phylogenetic analyses of the genes newly characterised in this study

Hlh family (Asc-b gene)

Phylogentic analysis of cnidarian bHLH transcription factors. Maximum likelihood tree with bootstrap values next to each node. *Clytia* genes are indicated in red. Scale bar represents 0.6 substitions per site.
The following *Clytia hemisphaerica* sequences were added to the alignment provided in (Lapébie et al. 2014). Accession numbers in parentheses.
PTFb (KT318149); Neurogenin (KT318150); Paraxis: (KT318151); AP4: (KT318152); Asca-1: (KT318153); Hlh-4 (KT318154); HEY/HES-2 (KT318155); HAND (KT318156); Hlh-6 (KT318157); Twist (KT318158); Net (KT318159); Hlh-5 (KT318160); Hlh-1 (KT318161); Hlh-2: KT318162); HEY/HES-1: (KT318163); USF (KT318164,KIAAA2018: KT318165, Bmal: (KT318166); Hlh-3: (KT318167); Ahr-b: (KT318168); ARNT (KT318169); MITF (KT318170); Asca-2: (KT318171); MIST-b: (KT318172); Ahr-a: (KT318173); MIST-a: (KT318174); Asc-b (XXX).

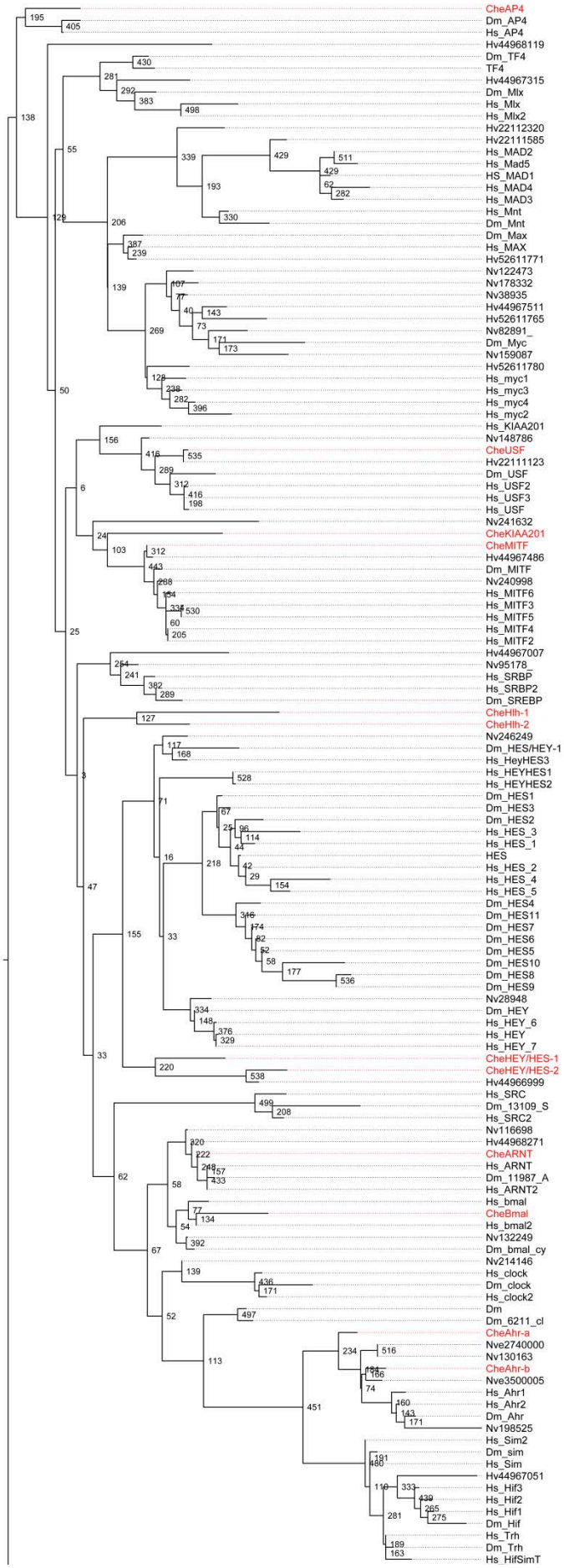
CheAP4
Dm_AP4
Hs_AP4
Hv44968119
Dm_TF4
TF4
Hv44967315
Dm_Mlx
Hs_Mlx
Hs_Mlx2
Hv22112320
Hv22111585
Hs_MAD2
Hs_Mad5
HS_MAD1
Hs_MAD4
Hs_MAD3
Hs_Mnt
Dm_Mnt
Dm_Max
Hs_MAX
Hv52611771
Nv122473
Nv178332
Nv38935
Hv44967511
Hv52611765
Nv82891_
Dm_Myc
Nv159087
Hv52611780
Hs_myc1
Hs_myc3
Hs_myc4
Hs_myc2
Hs_KIAA201
Nv148786
CheUSF
Hv22111123
Dm_USF
Hs_USF2
Hs_USF3
Hs_USF
Nv241632
CheKIAA201
CheMITF
Hv44967486
Dm_MITF
Nv240998
Hs_MITF6
Hs_MITF3
Hs_MITF5
Hs_MITF4
Hs_MITF2
Hv44967007
Nv95178_
Hs_SRBP
Hs_SRBP2
Dm_SREBP
CheHlh-1
CheHlh-2
Nv246249
Dm_HES/HEY-1
Hs_HeyHES3
Hs_HEYHES1
Hs_HEYHES2
Dm_HES1
Dm_HES3
Dm_HES2
Hs_HES_3
Hs_HES_1
HES
Hs_HES_2
Hs_HES_4
Hs_HES_5
Dm_HES4
Dm_HES11
Dm_HES7
Dm_HES6
Dm_HES5
Dm_HES10
Dm_HES8
Dm_HES9
Nv28948
Dm_HEY
Hs_HEY_6
Hs_HEY
Hs_HEY_7
CheHEY/HES-1
CheHEY/HES-2
Hv44966999
Hs_SRC
Dm_13109_S
Hs_SRC2
Nv116698
Hv44968271
CheARNT
Hs_ARNT
Dm_11987_A
Hs_ARNT2
Hs_bmal
CheBmal
Hs_bmal2
Nv132249
Dm_bmal_cy
Nv214146
Hs_clock
Dm_clock
Hs_clock2
Dm
Dm_6211_cl
CheAhr-a
Nve2740000
Nv130163
CheAhr-b
Nve3500005
Hs_Ahr1
Hs_Ahr2
Dm_Ahr
Nv198525
Hs_Sim2
Dm_sim
Hs_Sim
Hv44967051
Hs_Hif3
Hs_Hif2
Hs_Hif1
Dm_Hif
Hs_Trh
Dm_Trh
Hs_HifSimT

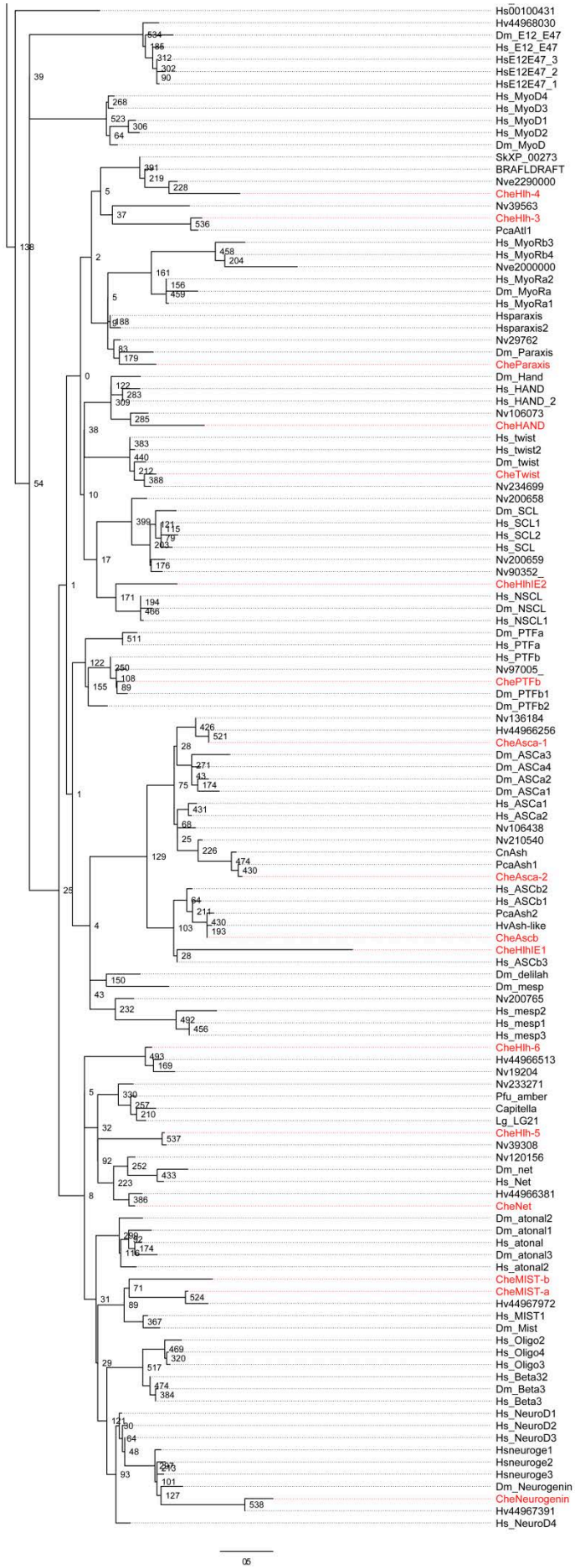
Hs00100431
Hv44968030
Dm_E12_E47
Hs_E12_E47
HsE12E47_3
HsE12E47_2
HsE12E47_1
Hs_MyoD4
Hs_MyoD3
Hs_MyoD1
Hs_MyoD2
Dm_MyoD
SkXP_00273
BRAFLDRAFT
Nve2290000
CheHlh-4
Nv39563
CheHlh-3
PcaAtl1
Hs_MyoRb3
Hs_MyoRb4
Nve2000000
Hs_MyoRa2
Dm_MyoRa
Hs_MyoRa1
Hsparaxis
Hsparaxis2
Nv29762
Dm_Paraxis
CheParaxis
Dm_Hand
Hs_HAND
Hs_HAND_2
Nv106073
CheHAND
Hs_twist
Hs_twist2
Dm_twist
CheTwist
Nv234699
Nv200658
Dm_SCL
Hs_SCL1
Hs_SCL2
Hs_SCL
Nv200659
Nv90352_
CheHlhE2
Hs_NSCL
Dm_NSCL
Hs_NSCL1
Dm_PTFa
Hs_PTFa
Hs_PTFb
Nv97005_
ChePTFb
Dm_PTFb1
Dm_PTFb2
Nv136184
Hv44966256
CheAsca-1
Dm_ASCa3
Dm_ASCa4
Dm_ASCa2
Dm_ASCa1
Hs_ASCa1
Hs_ASCa2
Nv106438
Nv210540
CnAsh
PcaAsh1
CheAsca-2
Hs_ASCb2
Hs_ASCb1
PcaAsh2
HvAsh-like
CheAscb
CheHlhE1
Hs_ASCb3
Dm_delilah
Dm_mesp
Nv200765
Hs_mesp2
Hs_mesp1
Hs_mesp3
CheHlh-6
Hv44966513
Nv19204
Nv233271
Pfu_amber
Capitella
Lg_LG21
CheHlh-5
Nv39308
Nv120156
Dm_net
Hs_Net
Hv44966381
CheNet
Dm_atonal2
Dm_atonal1
Hs_atonal
Dm_atonal3
Hs_atonal2
CheMIST-b
CheMIST-a
Hv44967972
Hs_MIST1
Dm_Mist
Hs_Oligo2
Hs_Oligo4
Hs_Oligo3
Hs_Beta32
Dm_Beta3
Hs_Beta3
Hs_NeuroD1
Hs_NeuroD2
Hs_NeuroD3
Hsneuroge1
Hsneuroge2
Hsneuroge3
Dm_Neurogenin
CheNeurogenin
Hv44967391
Hs_NeuroD4
05

PRDL subfamily

Phylogenetic analysis of metazoan paired-class homeobox transcription factors. The predicted amino acid sequences of Paired subfamily proteins was extracted from(Ryan et al. 2006; Lapébie et al. 2014). Maximum likelyhood tree with bootstrap values next to each node. *Clytia* genes are indicated in red. *Clytia hemisphaerica* Prdl-a and Prdl-b were named according to their orthology with *Hydra* Prdl-a and Prdl-b. Scale bar represents 0.6 substitions per site.
The following *Clytia hemisphaerica* sequences were added to the alignment provided in (Lapébie et al. 2014). Accession numbers in parentheses.
Prdl-a (???); Prdl-b (KT318135); Prdl-d (KT318136); HOP (KT318137); Pitx (KT318138, Rx (KT318139); Otx-related-2 (KT318140); Ot (KT318141); Otx (KT318142); Otx-related-1 (KT318143); Prdl-e (KT318144); Prdl-c: (KT318145); Unc (KT318146); PaxB (KT318147); PaxC (T318148).

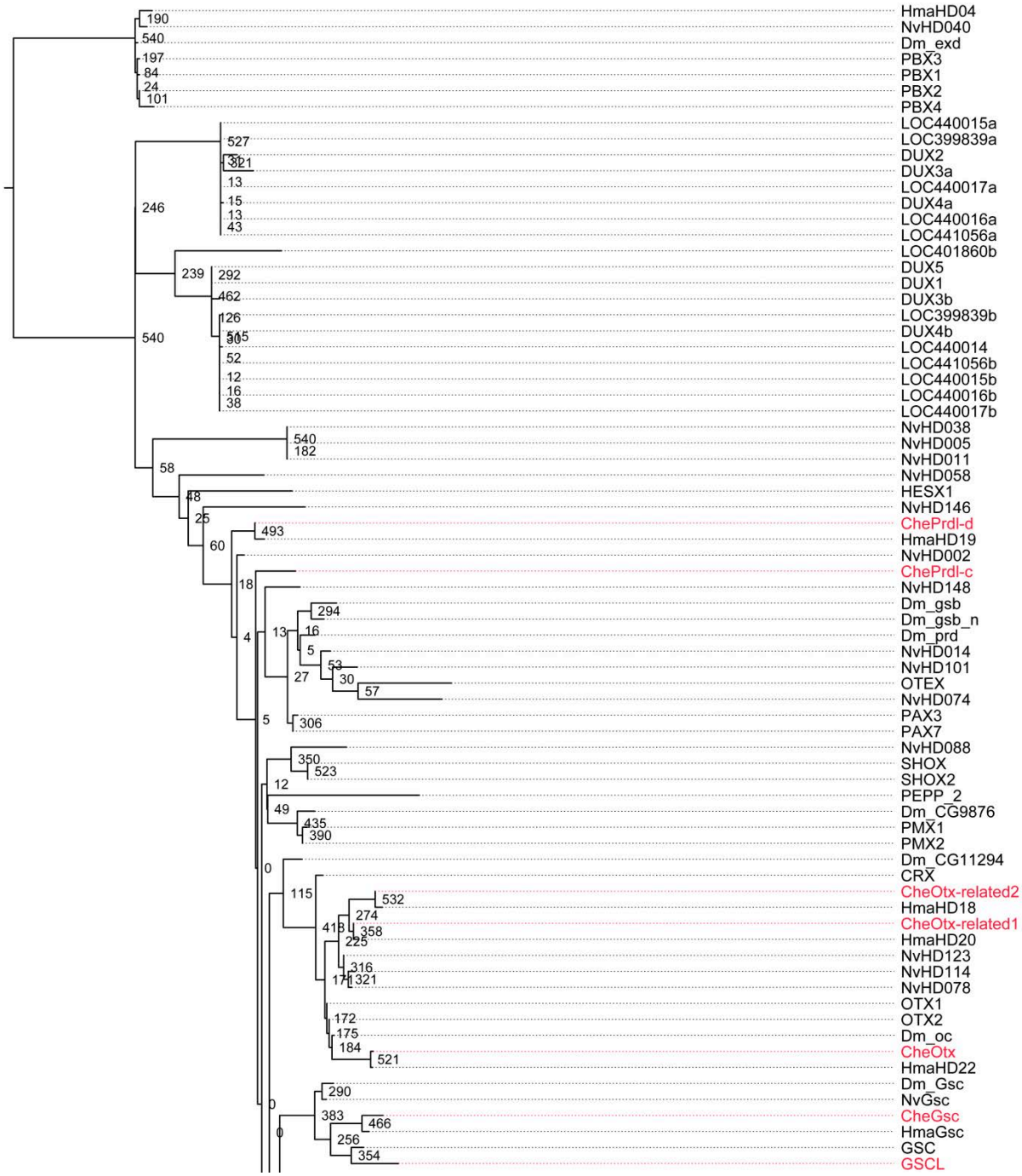
HmaHD04
NvHD040
Dm_exd
PBX3
PBX1
PBX2
PBX4
LOC440015a
LOC399839a
DUX2
DUX3a
LOC440017a
DUX4a
LOC440016a
LOC441056a
LOC401860b
DUX5
DUX1
DUX3b
LOC399839b
DUX4b
LOC440014
LOC441056b
LOC440015b
LOC440016b
LOC440017b
NvHD038
NvHD005
NvHD011
NvHD058
HESX1
NvHD146
ChePrdl-d
HmaHD19
NvHD002
ChePrdl-c
NvHD148
Dm_gsb
Dm_gsb_n
Dm_prd
NvHD014
NvHD101
OTEX
NvHD074
PAX3
PAX7
NvHD088
SHOX
SHOX2
PEPP_2
Dm_CG9876
PMX1
PMX2
Dm_CG11294
CRX
CheOtx-related2
HmaHD18
CheOtx-related1
HmaHD20
NvHD123
NvHD114
NvHD078
OTX1
OTX2
Dm_oc
CheOtx
HmaHD22
Dm_Gsc
NvGsc
CheGsc
HmaGsc
GSC
GSCL

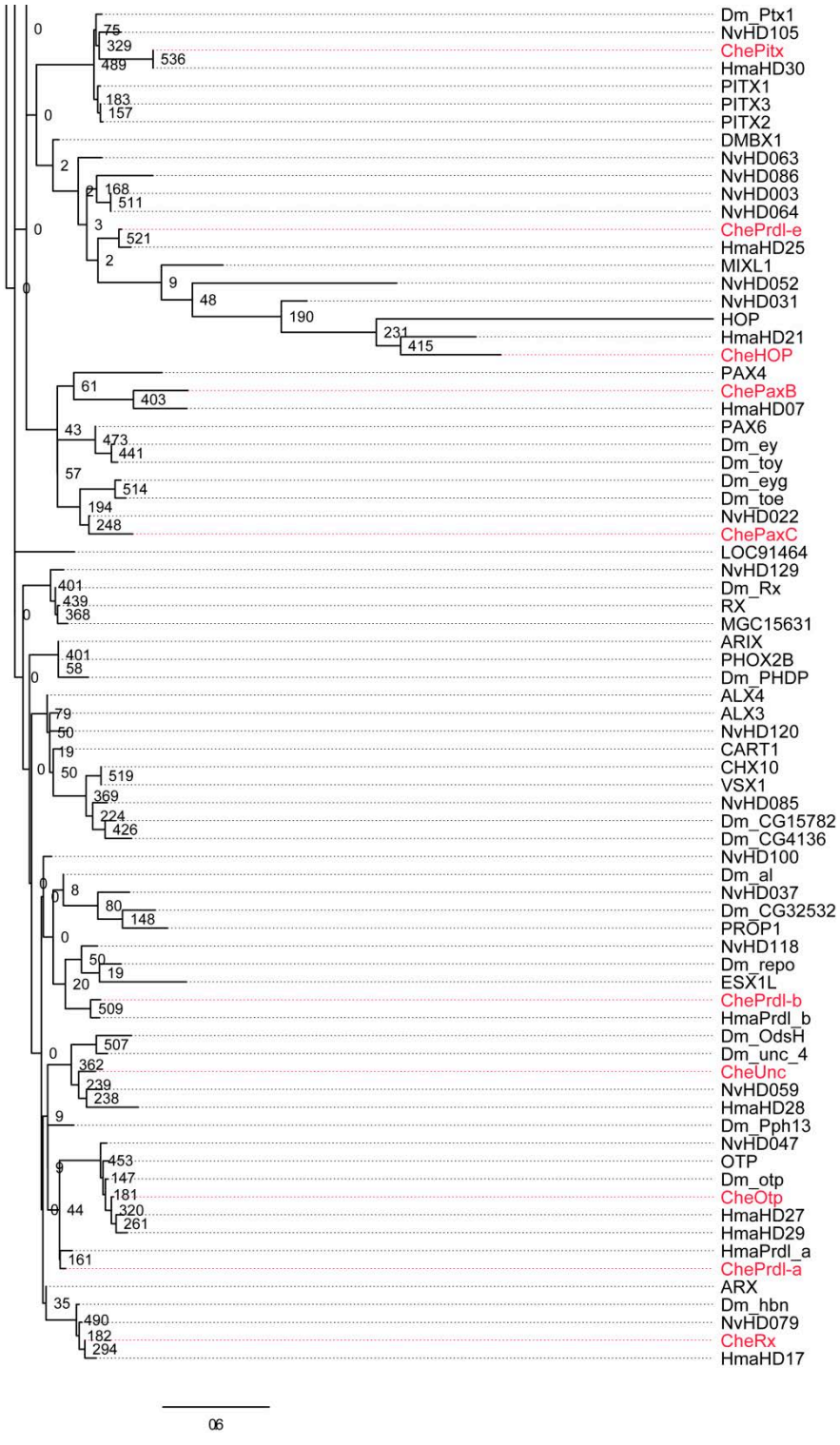
Dm_Ptx1
NvHD105
ChePitx
HmaHD30
PITX1
PITX3
PITX2
DMBX1
NvHD063
NvHD086
NvHD003
NvHD064
ChePrdl-e
HmaHD25
MIXL1
NvHD052
NvHD031
HOP
HmaHD21
CheHOP
PAX4
ChePaxB
HmaHD07
PAX6
Dm_ey
Dm_toy
Dm_eyg
Dm_toe
NvHD022
ChePaxC
LOC91464
NvHD129
Dm_Rx
RX
MGC15631
ARIX
PHOX2B
Dm_PHDP
ALX4
ALX3
NvHD120
CART1
CHX10
VSX1
NvHD085
Dm_CG15782
Dm_CG4136
NvHD100
Dm_al
NvHD037
Dm_CG32532
PROP1
NvHD118
Dm_repo
ESX1L
ChePrdl-b
HmaPrdl_b
Dm_OdsH
Dm_unc_4
CheUnc
NvHD059
HmaHD28
Dm_Pph13
NvHD047
OTP
Dm_otp
CheOtp
HmaHD27
HmaHD29
HmaPrdl_a
ChePrdl-a
ARX
Dm_hbn
NvHD079
CheRx
HmaHD17
06

Boule/DAZ family

Phylogenetic analysis of metazoan DAZ/Boule family RRM proteins. Sequences from *Hydra vulgaris* and *Nematostella vectensis* genomes and *Clytia hemisphaerica* transcriptomes were identified as belonging to Boule/Daz family by reciprocal blast and added to the sequence list below. Species abbreviations: Api (*Apis millifera),* Bmo (*Bombix mori*) Che(*Clytia hemisphaerica*), Cte (*Capitella teleta*), Ce(*Caenorhabditis elegans*), Hv (*Hydra vulgaris*), Hs (*Homo sapiens*) Mli (*Macrostoma lignanum*), Mmu (*Mus musculus*), Xt (*Xenopus tropicalis*), Nv (*Nemtostella vectensis*), Tca (*Trichoplax adherens*), Sp(*Strongylocentrotus purpuratus)*
Members of the Musashi orthology group from *Drosophila, Xenopus* and sea urchin were been chosen as an outgroup. Divergent parts of the alignment have been removed, and the RRM domain and Daz repeats retained. The sequences published in (Tsai et al. 2014) have been used , and the following sequences from *Clytia, Nematostella* and *Hydra* have been added, with Accession numbers in parentheses.
HvBoule-like3 (XP_012556641.1); NvBoule-like1-a (XP_001620626.1); HvBoule-like1-e (XP_004211430.1); NvBoule (XP_001632599.1); HvBoule-like2b (XP_004207589.1); NveBoule-like1-e (XP_001635220.1); NveBoule-like1-b (XP_001637248.1); HvBoule-like2-a (XP_002163170.2); NvBoule-like2-a (XP_001623902.1); DmGJ12977 (XP_002046609.1); XtMusashi (XP_012816891.1); SpMusashi (XP_001199490.2);, CheBoulelike1-c (KT318175); CheBoulelike3 (KT318176); CheBoulelike1-d (KT318177); CheBoule1-b (KT318178); CheBoulelike1-e (KT318179); CheBoulelike2-a (KT318180) CheBoule1-a (XXXX); CheBoule1-like-1a (xxxx); CheBoule1-like1-b (xxx).

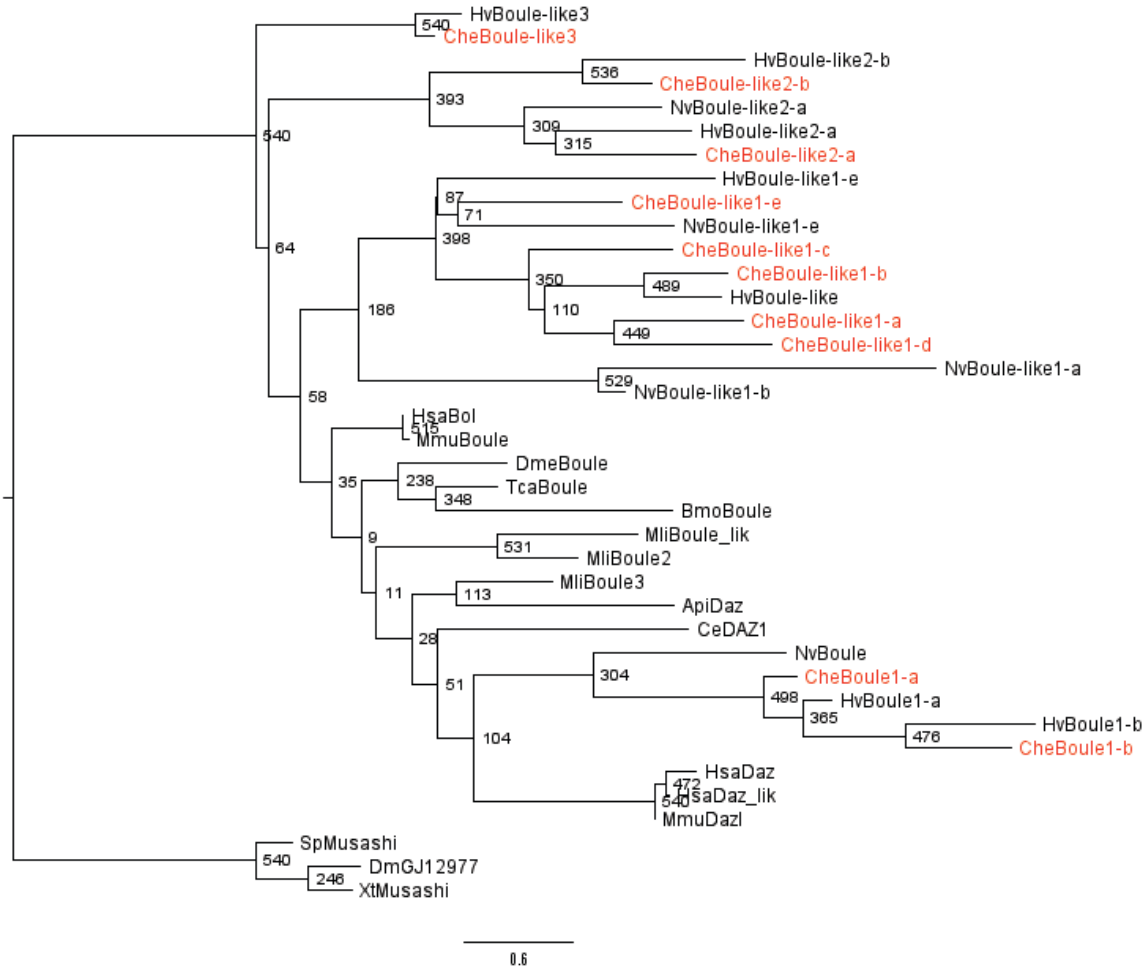
HvBoule-like3
CheBoule-like3
HvBoule-like2-b
CheBoule-like2-b
NvBoule-like2-a
HvBoule-like2-a
CheBoule-like2-a
HvBoule-like1-e
CheBoule-like1-e
NvBoule-like1-e
CheBoule-like1-c
CheBoule-like1-b
HvBoule-like
CheBoule-like1-a
CheBoule-like1-d
NvBoule-like1-a
NvBoule-like1-b
HsaBol
MmuBoule
DmeBoule
TcaBoule
BmoBoule
MliBoule_lik
MliBoule2
MliBoule3
ApiDaz
CeDAZ1
NvBoule
CheBoule1-a
HvBoule1-a
HvBoule1-b
CheBoule1-b
HsaDaz
HsaDaz_lik
MmuDazl
SpMusashi
DmGJ12977
XtMusashi
0.6

Thyn1

Phylogenetic analysis of metazoan Eve domain proteins. Thyn1 proteins are highly conserved, identifiable in both bacteria and mammals. Amino acid sequences from *Aplysina californica (Ac , Capitella teleta* (Cte)*; Saccoglossus kowalevskii* (Sk)*; Lottia gigantean* (Lgi)*; Xenopus tropicalis* (Xt)*; Trichoplax adherens (Tca); Gallus gallus* (Gg); *Mus musculus* (Mm)*; Clytia hemisphaerica* (Che)*; Hydra vulgaris* (Hv)*; Homo sapiens* (Hsa)*; Nematostella vectensis* (Nv), were identified by reciprocal blast. The following sequences containing Eve domain were used for phylogenetic analysis. Accession numbers in parentheses
LgiThyn1 (XP_009059928.1); TcaThyn1 (XP_009059928.1); HvThyn1 (XP_012558048.1); AcThyn1 (XP_005096716.1); XtThyn1 (NP_001120782.1); CteThyn1 (ELU16431.1); GgThyn1 (NP_989618.1); MmThyn1 (XP_006510751.1); HsaThyn1 (NP_054893.1); SkThyn1 (XP_006821718.1); NvThyn1(XP_001635839.1); CheThyn1 (XXX)

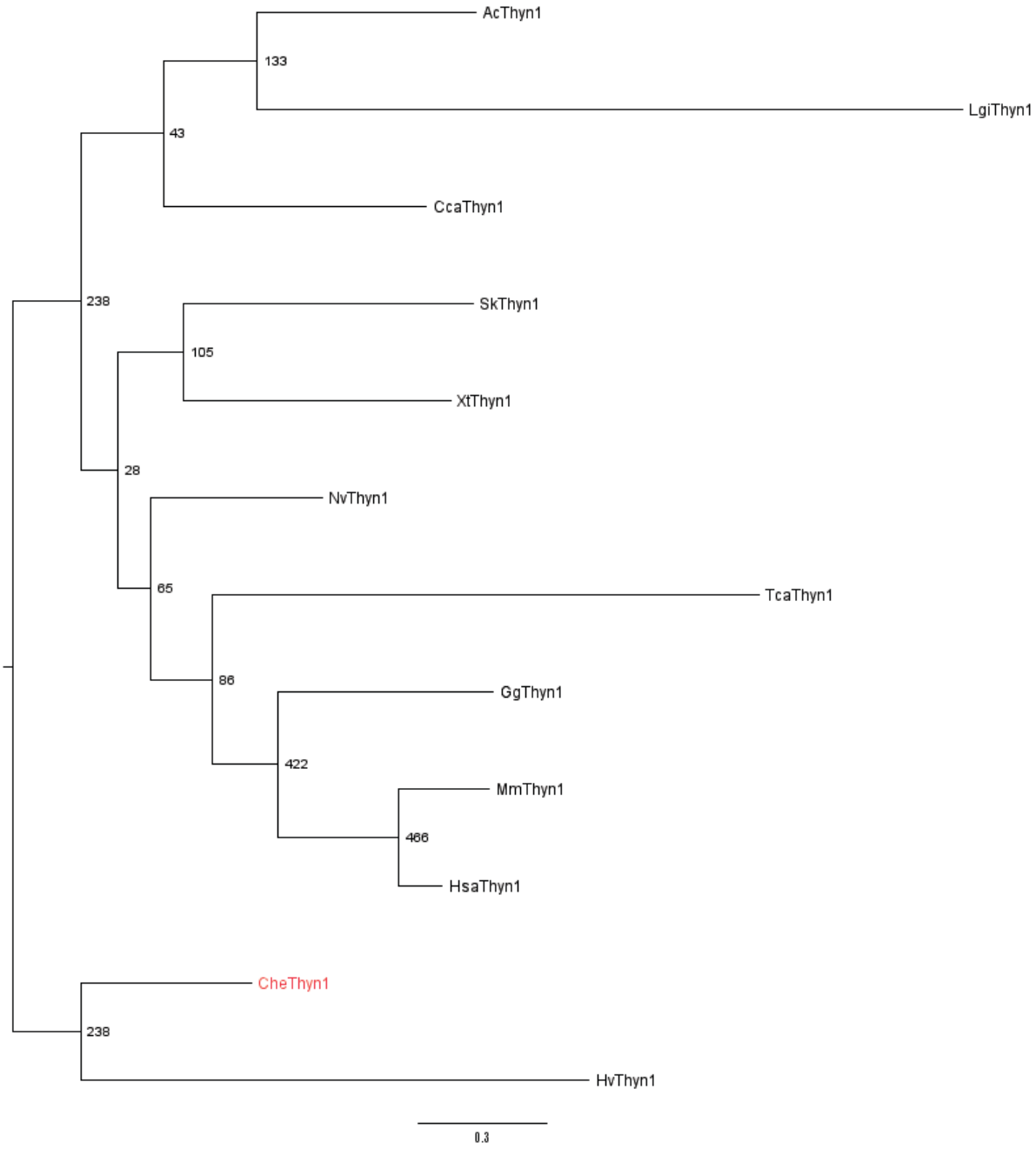
AcThyn1
133
LgiThyn1
43
CcaThyn1
238
SkThyn1
105
XtThyn1
28
NvThyn1
65
TcaThyn1
86
GgThyn1
422
MmThyn1
466
HsaThyn1
CheThyn1
238
HvThyn1
0.3

References

Lapébie, P., Ruggiero, A., Barreau, C., Chevalier, S., Chang, P., Dru, P., Houliston, E., Momose, T., 2014. Differential Responses to Wnt and PCP Disruption Predict Expression and Developmental Function of Conserved and Novel Genes in a Cnidarian. PLoS Genet 10, e1004590. doi:10.1371/journal.pgen.1004590

Ryan, J., Burton, P., Mazza, M., Kwong, G., Mullikin, J., Finnerty, J., 2006. The cnidarian-bilaterian ancestor possessed at least 56 homeoboxes. Evidence from the starlet sea anemone, Nematostella vectensis. Genome Biol. 7, R64–R64. doi:10.1186/gb-2006-7-7-R64

Tsai, Y.S., Gomez, S.M., Wang, Z., 2014. Prevalent RNA recognition motif duplication in the human genome. RNA 20, 702–712. doi:10.1261/rna.044081.113

2.2 PAPER 2: Summary of the Results

The study of the Wnt pathway is one of the main interests of our laboratory. During the course of my PhD I participated in a group project aimed at identifying *via* a comparative transcriptomic approach novel genes involved in embryo patterning directly or indirectly regulated by Wnt signalling.

To gain a more exhaustive understanding of the gene toolkit involved in generating and maintaining *Clytia* axial polarity, the transcriptome of un-manipulated wild type early gastrula stage embryos was compared with that of Wnt3 early gastrula morphants (Figure 43). Previous observations from our group indicated that the first zygotic expression of many genes starts at the beginning of gastrulation.

My participation in this project was mainly in the systematically characterisation of the expression pattern by *in situ* hybridisation of genes significantly over or under expressed in Wnt3 morphant early gastrula embryos. I took advantage of this new transcriptome dataset to look for novel i-cell associated genes. Indeed by comparing the expression patterns of Wnt3 target genes I found that five genes in particular showed expression patterns similar to those of the i-cell markers *Nanos1* and *Piwi*. I went on to investigate in more detail two of these, Mos3 and Znf845 as described in the additional results presented after PAPER 2 in this chapter.

2.2.1 Identification of novel *Clytia* embryos patterning genes

To identify novel regulators implicated in *Clytia* axial polarity and embryogenesis we compared the transcriptome of un-manipulated gastrula embryos with the transcriptome of the Wnt3 early gastrula morphants. To distinguish the influence of Wnt3/Fz/β-catenin signalling and Fz1/PCP we included in this study the transcriptomes of the Fz1 and Stbm early gastrula morphants.

Differential gene expression analysis based on stringent selection of the most significantly over and under expressed genes identified: 1) 40 genes significantly upregulated in Wnt3 early gastrula morphants (negatively regulated by Wnt3) of which 18 were selected for further validation. 2) 114 transcripts downregulated in Wnt3 early gastrula morphants

(positively regulated by Wnt3) from which the top 20 of the list were chosen for further analysis (Figure 43, full list of transcripts identified **PAPER 2, file S1**).

2.2.2 Polarised expression pattern of Wnt3 target genes

In situ hybridisation experiments were performed for the selected transcripts at different developmental stage:

-Early gastrula stage, the same stage that was used to harvest mRNA originally for the differential gene expression analysis.

- 24 hpf planula, when gastrulation is completed, polarity is completely established and presumptive endoderm cells ingressed but endoderm is not yet differentiated.

- 48hpf planula in which ectoderm and endoderm are both well formed and all the differentiated somatic cell types are present.

In situ hybridisation analysis revealed 4 types of spatio-temporal expression profiles, allowing the genes to be grouped in the following 4 categories:

O) Oral genes expressed at oral pole in the ectoderm at all three stages (**Paper 2 Figure 2)**.

A) Aboral genes expressed in the aboral ectoderm at early gastrula stage and maintained during planula stage in different aboral pole cell population (**Paper 2 Figure 3**).

IE) Ingressing/Endoderm genes, detected in different population of ingressing/ingressed cells at oral pole during gastrulation, and restricted to the endodermal region during planula stage (**Paper 2 Figure 2)**

D) Delayed Expressed, these transcripts could be detected only very weakly and uniformly at early gastrula stage, while later expression among the genes of this category was variable, covering both endoderm and ectoderm along the OA axis. (**Paper 2 Figure 3)** These may reflect genes whose expression is generally repressed by Wnt signalling during gastrulation.

The DGE approach was entirely validated by our systematic *in situ* hybridisation analysis. The positive "targets" (direct or indirect) of Wnt3 exclusively had the O and IE expression patterns (oral), and the negative "targets" of Wnt3 exclusively had the A/D patterns (aboral or delayed).

A

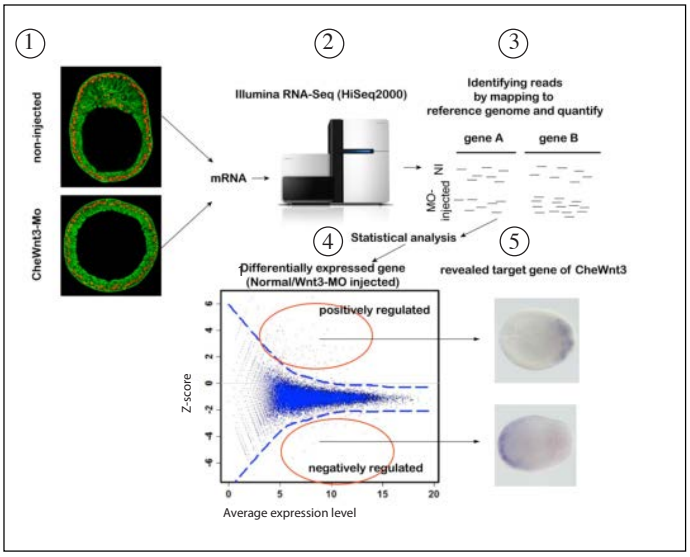

B

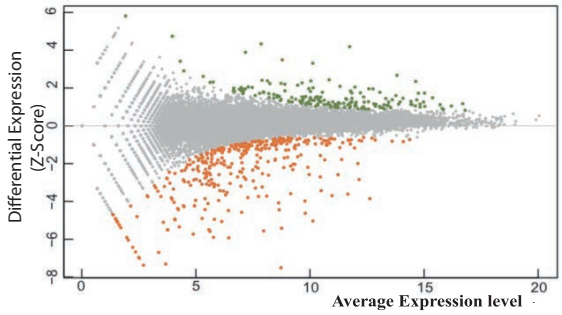

C

Genes differentially expressed (DGE analysis)		
Positively regulated by Wnt3 (downregulated in Wnt3 morphants) 114 genes	**Negatively regulated by Wnt3 (upregulated in Wnt3 morphants)** 40 genes	**Not significantly affected genes**
Profiling ISH 20 genes	**Profiling ISH** 18 genes	
In situ profile IE (Ingressing cell) = 12 genes O (oral) = 8 genes	**In situ profile** A (Aboral) = 7 genes D (Delayed) = 7 genes A\D = 4 genes	
i-cell like profile IE = 5/12: Znf845, HlhIE1, HlhIE2, Mos3, FoxA	**i-cell like profile** 0	**i-cell like profile** Piwi, Nanos1, Nanos2, Vasa

Figure 43: Comparative transcriptomic approach to unravel new genes involved in the establishment of *Clytia* embryo polarity.

A) 1) Experimental design 2) RNA was prepared from large batches of uninjected and Wnt3-MO injected early gastrula (cDNA libraries prepared by *GATC Biotech*) and Illumina sequencing performed. 3) Illumina reads were mapped to a Reference transcriptome compiled from control early gastrula with available EST data mixed stages. 4) Statistical analysis to identify significantly over or under expressed genes in the morpholino sampled compared to controls. 5) Verification of expression profiles by *in situ* hybridization.

B) Graphic representation of the comparison of the expression level between Wnt3 morphants versus wild type early gastrula. Orange dots represent the genes under expressed in Wnt3 morphants, green dots represents over expressed genes in Wnt3 morphants, grey dots represent genes that are not significantly affected.

C) Summary table describing the different categories identified by comparing expression profile of the differentially expressed genes. Amongst the total number of genes differentially expressed, 114 were significantly downregulated in Wnt3 morphants, and 40 significantly upregulated in Wnt3 morphants. The biological validation by *in situ* hybridisation and selected qPCR (not shown) of the more sensitive "top"20 and "top"18 respectively downregulated and upregulated in Wnt3 morphants, allowed us to define four different expression profile groups: O (oral), IE (ingressing endoderm), A(aboral), D(delayed) based on the expression profile. Among the IE genes, 5 genes show an expression profile reminiscent of the germ cell /stem cell genes *Nanos1* and *Piwi*. However *Nanos1*,*Piwi* expression was not significantly affected by Wnt3 disruption.

2.2.3 IE genes show an i-cell like expression pattern

Some of the genes identified as positively regulated by Wnt3 showed an expression pattern reminiscent of the classical i-cell markers Nanos1 and Piwi (Leclère et al. 2012) and so were of particular interest in my study.

All these genes belonged to the IE category and include a Zn-finger domain protein *Znf845*, *Mos3*, two bHLH genes (*HlhIE1* and *HlhIE2*) and the Forkhead transcription factor *Fox-A*. (Figure 34) (**Paper 2 Figure 2 J,K,L,M,Q,).**

These 5 genes have similar expression pattern at early gastrula, the transcripts are localised at oral pole in ingressing/ ingressed cells during gastrulation, while at planula stage, *HlhIE1* (24hpf and 48 hpf stage) is expressed in few cells in the endoderm (**Paper 2 Figure 2 M**).

HlhIE2 is expressed in few cells in the planula 24hpf and all along the endoderm layer in planula 48hpf **(Paper 1 Figure 2 Q)**. *Znf845*, *Mos3* and *Fox-A*, showed in larval stages expression patterns similar to those reported for Nanos1 and Piwi (**Paper 2 Figure 2 J,K,L,Q**).

Since *Fox-A* is considered a conserved endodermal marker (Fritzenwanker et al. 2004; Oliveri et al. 2006) I considered it unlikely that this gene would be associated with i-cells.

2.2.4 Different responses of Wnt3-MO responsive genes to Fz1-MO

We further analysed the response of the transcripts set defined above in Fz1 morphants. The responses were not strictly correlated, implying that Fz1 down-regulation has effects both relating to the Wnt/β-catenin pathway and independent of it. Specifically, we found that the genes with "axial expression" profiles, A and O, were weakly affected in early gastrula Fz1 morphants, while the genes in IE and D expression profile group were more strongly sensitive to Fz-1 MO. In the IE category, genes tend to be strongly down-regulated in Fz1-MO early gastrula and D category genes to be up-regulated in Fz1 morphants, while "axial genes" (O and A) are less affected (**Paper 2 Figure 7).** We were further able to show that this differential response was due to the sensitivity of certain genes to PCP disruption, since Fz1 is a PCP core component. To do that we compared the transcriptome profiles from Fz1 morphants and Stbm morphants as Stbm is exclusively involved in Fz/PCP but not in Wnt/β-catenin signalling, and found that the responses of all 4 categories of genes were very similar under these two conditions.

The fact that IE (ingressing/endoderm) profile genes and D profile genes (repressed until early gastrula) are particularly sensitive to PCP disruption is yet to be fully understood. In *Clytia* PCP disruption by these morpholinos leads to loss of ectodermal planar cell polarity and in to defects in planula elongation as well as altered gastrulation, which could well result in a delay in the expression of genes associated specifically with ingressing cells.

PAPER 2:

Differential Responses to Wnt and PCP Disruption Predict Expression and Developmental Function of Conserved and Novel Genes in a Cnidarian.

Pascal Lapébie, Antonella Ruggiero, Carine Barreau, Sandra Chevalier, Patrick Chang, Philippe Dru, Evelyn Houliston, Tsuyoshi Momose.

Published in PloS Genetics September 2014

OPEN ACCESS Freely available online

PLOS | GENETICS

Differential Responses to Wnt and PCP Disruption Predict Expression and Developmental Function of Conserved and Novel Genes in a Cnidarian

Pascal Lapebie, Antonella Ruggiero, Carine Barreau, Sandra Chevalier, Patrick Chang, Philippe Dru, Evelyn Houliston*, Tsuyoshi Momose

Sorbonne Universite´ s, UPMC Univ Paris 06, and CNRS, Laboratoire de Biologie du De´veloppement de Villefranche-sur-mer, Observatoire Oce´anographique, Villefranche-sur-mer, France

Abstract

We have used Digital Gene Expression analysis to identify, without bilaterian bias, regulators of cnidarian embryonic patterning. Transcriptome comparison between un-manipulated *Clytia* early gastrula embryos and ones in which the key polarity regulator Wnt3 was inhibited using morpholino antisense oligonucleotides (Wnt3-MO) identified a set of significantly over and under-expressed transcripts. These code for candidate Wnt signaling modulators, orthologs of other transcription factors, secreted and transmembrane proteins known as developmental regulators in bilaterian models or previously uncharacterized, and also many cnidarian-restricted proteins. Comparisons between embryos injected with morpholinos targeting Wnt3 and its receptor Fz1 defined four transcript classes showing remarkable correlation with spatiotemporal expression profiles. Class 1 and 3 transcripts tended to show sustained expression at ''oral'' and ''aboral'' poles respectively of the developing planula larva, class 2 transcripts in cells ingressing into the endodermal region during gastrulation, while class 4 gene expression was repressed at the early gastrula stage. The preferential effect of Fz1-MO on expression of class 2 and 4 transcripts can be attributed to Planar Cell Polarity (PCP) disruption, since it was closely matched by morpholino knockdown of the specific PCP protein Strabismus. We conclude that endoderm and post gastrula-specific gene expression is particularly sensitive to PCP disruption while Wnt-/b-catenin signaling dominates gene regulation along the oral-aboral axis. Phenotype analysis using morpholinos targeting a subset of transcripts indicated developmental roles consistent with expression profiles for both conserved and cnidarian-restricted genes. Overall our unbiased screen allowed systematic identification of regionally expressed genes and provided functional support for a shared eumetazoan developmental regulatory gene set with both predicted and previously unexplored members, but also demonstrated that fundamental developmental processes including axial patterning and endoderm formation in cnidarians can involve newly evolved (or highly diverged) genes.

Citation: Lapebie P, Ruggiero A, Barreau C, Chevalier S, Chang P, et al. (2014) Differential Responses to Wnt and PCP Disruption Predict Expression and Developmental Function of Conserved and Novel Genes in a Cnidarian. PLoS Genet 10(9): e1004590. doi:10.1371/journal.pgen.1004590

Editor: Claude Desplan, New York University, United States of America

Received January 2, 2014; Accepted July 9, 2014; Published September 18, 2014

Funding: This study was funded by grants from the ANR (Agence National de la Recherche) project DiploDevo, Coordinator M. Manuel (Paris) #ANR-09-blan-0236-02, ARC grant ARC1098 to TM, and core LBDV funding from the CNRS and UPMC. AR obtained a PhD student fellowship from the MRT (Ministe´re de Recherche et Technologie). The funders had no role in study design, data collection and analysis, decision to publish, or preparation of the manuscript.

Competing Interests: The authors have declared that no competing interests exist.

* Email: houliston@obs-vlfr.fr

Introduction

A major challenge in biology is to understand how the current extraordinary diversity of animal forms has been generated during evolution. Specific goals are to determine which genes were employed to regulate developmental processes in the earliest multicellular animals, and how this set of regulators was expanded during the evolution of different animal branches by diversification of existing gene families or by the acquisition of new genes. To address these questions requires identification and functional analysis of developmental regulatory genes in species from right across the animal kingdom, covering not only the ''bilaterian'' (protostome plus deuterostome) branch including the classic experimental models such as mouse, zebrafish, *Drosophila* and *Caenorhabditis*, but also non-bilaterian phyla such as cnidarians, ctenophores and sponges, which have evolved many distinct forms and body plans.

Following the recent explosion of genome and transcriptome sequencing it has been widely noted that the majority of families of transcription factors and signaling pathway components uncovered as developmental regulators in bilaterian model species are represented in genomes of cnidarians, as well as ctenophores and to a lesser extent sponges [1–9]. This has fuelled the idea that a shared set (or ''common toolkit'') of genes inherited from a common metazoan ancestor is used to regulate development in widely divergent species through differential deployment [1,3,10–17]. The common toolkit idea relies heavily on the assumption that conserved genes have retained largely equivalent developmental functions during the evolution of each animal lineage, for which evidence remains quite patchy. Comparing the expression territories, and in some cases functions, of gene orthologs in families of transcription factors such as Hox, Sox, Fox and T-box genes, and components in signaling pathways such as Wnt, TGFb, FGF, Hedgehog, Notch etc, has provided some support for this

Author Summary

The recent wave of genome sequencing from many species has revealed that most of the gene families known to regulate animal development are shared not only between humans and laboratory favorites such as mice, flies and worms, but also by evolutionarily more distant animals such as jellyfish and sponges. It is often assumed that genes inherited from a common ancestor remain largely responsible for regulating embryogenesis across these animal species, rather than more recently evolved genes. To address this issue we made an unbiased, systematic search for developmental genes in embryos of the jellyfish *Clytia*, selecting genes whose expression altered upon manipulation of the key regulator Wnt3, and comparing their expression in embryos specifically disrupted for Planar Cell Polarity. Identification of evolutionarily conserved and novel genes as developmental regulators was confirmed by demonstrating characteristic expression profiles for a sub-set of genes, and by gene knockdown studies. Conserved genes coded for members of many known signaling pathway and transcription factor families, as well as previously unstudied proteins. Nearly 30% of the identified genes were restricted to cnidarians (the jellyfish-sea anemone-coral group), supporting the idea that the appearance of new genes during evolution contributed significantly to generating animal diversity.

assumption, but also for lineage specific modifications in gene repertoires for example through gene duplications and losses within the transcription factor families [10–21]. Another possibility is that novel regulatory genes have emerged within specific evolutionary lineages to contribute to generating animal diversity [14,18–23]. The significant proportions of cnidarian-specific gene sequences in the fully sequenced genomes of *Hydra* (around 15%) and *Nematostella* (around 13%) is compatible with such a scenario in Cnidaria [14,18,22–26]. Detailed studies involving transcriptome comparisons in *Hydra* have shown that many cnidarian-specific genes are associated with specialized cell types, notably nematocytes (stinging cells) but also nerve and gland cells [22,24–30], while others have been specifically implicated in intercellular signaling and regulating morphological processes [22,27–31]. Furthermore, in a subtractive hybridization search for cnidarian-specific genes involved in embryogenesis, 30 of 88 distinct partial cDNA clones recovered did not match known bilaterian sequences, including one corresponding to a *Hydra* specific gene (HyEMB-1) expressed in the ovary and early embryo [31].

To gain a fresh perspective on the gene repertoires that regulate metazoan development, we employed a systematic unbiased comparative transcriptomics approach to identify potential regulators of embryonic patterning at gastrula stage in the cnidarian experimental model *Clytia hemisphaerica* [32]. Clytia is a typical hydrozoan species that includes a jellyfish form as well as a polyp form in its life cycle, unlike anthozoan cnidarians such as the popular sea anemone model *Nematostella vectensis*. After gastrulation, a torpedo-shaped ''planula'' larva is formed, whose organization shows the characteristic cnidarian body plan: a single ''oral-aboral'' axis and two germ layers. The outer ectoderm of the *Clytia* planula features ciliated epitheliomuscular cells for motility, and an internal endodermal (or ''entodermal'') region including a population of interstitial stem cells (i-cells) specific to hydrozoans, which generate a variety of cell types for each germ layer [33–36]. Gastrulation proceeds by unipolar cell ingression to fill the blastocoel prior to endoderm cell epithelialization [37]. The gastrulation site derives from the egg animal pole and corresponds to the pointed oral pole of the larva, giving rise after metamorphosis to the mouth region of the polyp form [38].

Establishment of the oral pole in *Clytia* critically depends on Wnt/Fz signaling activity through the Wnt/b-catenin pathway. Maternally-provided transcripts for the ligand Wnt3 and the receptors Fz1 (activatory) and Fz3 (inhibitory) are pre-localized along the egg animal-vegetal axis to drive activation of this pathway on the future gastrulation site/oral side during cleavage and blastula stages [39,40]. This activation establishes distinct regional identities characterized by specific sets of transcribed genes at the oral and aboral poles of the developing embryo, including those required for cell ingression at gastrulation. Fz-PCP signaling, dependent on the conserved transmembrane protein Strabismus (Stbm), is activated in parallel along the same axis to coordinate cell polarity in the ectoderm and to guide embryo elongation [41]. Since multi-member Wnt families with early polarized embryonic expression have also been uncovered in other cnidarians [42,43], ctenophores and sponges [44–47] as well as in a range of bilaterian models [48,49], it seems highly probable that Wnt/Fz signaling regulated embryonic patterning in ancestral metazoans, specifying the primary body axes and/or presumptive germ layer regions.

To identify genes potentially involved in *Clytia* embryogenesis without favoring gene families identified as developmental regulators from bilaterians, we compared transcriptomes at the onset of gastrulation between normal embryos and ones strongly ''aboralized'' by Wnt3 morpholino (Wnt3-MO) injection prior to fertilization [40]. In many animals gastrulation coincides with, or closely follows, a significant stepping up of transcription from the zygotic genome, taking over from an initial phase of development predominantly dependent on maternally supplied mRNAs and proteins. By comparing transcriptomes from undisturbed and Wnt3-MO early gastrulae by Digital Gene Expression (DGE) we compiled lists of significantly over- and under-expressed genes. These included orthologs of known conserved developmental regulators but also members of unexplored metazoan conserved gene families, and in addition many sequences restricted to cnidarians. Expression profiling for an unbiased subset of these transcripts systematically revealed spatially or temporally restricted expression profiles of four types. Further transcriptome and *in situ* hybridization comparisons with Fz1-MO and Stbm-MO embryos revealed expression-pattern-related differences in the responses of genes to disruption of Wnt/b-catenin versus PCP. Finally, roles in developmental processes for the identified genes, both conserved and cnidarian–restricted, were supported both by their characteristic expression patterns and by correlated phenotypes obtained following morpholino injection for a subset of 8 genes.

Overall our unbiased screen allowed systematic identification of developmental genes regulated by the Wnt/ß-catenin pathway and by Fz-PCP. It provided functional support for a shared eumetazoan developmental regulatory gene set with both predicted and previously unexplored members, while also showing that axial patterning and endoderm formation in cnidarians can involve taxon restricted genes.

Results

A systematic approach to identify cnidarian developmental genes

To identify genes regulated transcriptionally in relation to Wnt dependent embryo patterning we compared transcriptomes from unmanipulated early gastrula stage embryos and from embryos injected prior to fertilization with a morpholino antisense oligonucleotide targeting Wnt3 [40]. Digital Gene Expression

analysis (DGE) was performed using an Illumina HiSeq sequencing platform. The number of mapped reads onto a reference transcriptome data set was taken as a measure of transcript level, and the statistical significance of differences in these levels between samples assessed using the DEGseq package (Figure 1; see Materials and Methods for technical details). Plotting for each transcript the expression ratio between two samples against the global average expression (Figure 1A,C) allowed visualization of sets of transcripts that showed significant differential expression, defined as ones that cannot be accounted for by sampling variation according to Random Sampling Model. We used the MATR method [50], justified by the Normal distribution of the data (Figure 1B), to adjust the cutoff to take into account experimental noise, based on comparison of replicate samples (blue line in Figure 1A: compare with the red line delimiting the theoretical random distribution). For subsequent analyses we routinely used a corresponding ''z-score'' value as an index of significant differences between samples (see Methods).

Comparisons between Wnt3-MO and uninjected embryo samples (Figure 1C) identified 375 assembled transcript sequences as differentially expressed according to the z-score +/23.3 cutoff, which corresponds to a probability threshold (p-value) of 0.01 (colored dots in Figure 1C). Detailed analyses were performed for a more restricted set of 179 sequences with z-scores of less than -5 or greater than +5 (see insert in Figure 1C; list of transcripts and their characteristics in File S1). We could eliminate transcripts whose expression levels were affected non-specifically by the morpholino injection procedure by comparing the Wnt3-MO embryo differentially regulated transcripts with those identified in embryo populations generated using morpholinos targeting two other genes, Fz1 and Fz3, which respectively activate and repress Wnt/b-catenin signaling leading to aboralized and oralized phenotypes, respectively [39]. Genes non-specifically affected by the morpholino injection procedure are expected to respond in the same way in all three experimental groups, whereas genes regulated specifically downstream of Wnt3 are expected to respond distinctly following Fz1-MO compared to Fz3-MO injection. Comparison between these groups allowed us to identify 4 sequences with high z-scores (.5) in Fz1-MO and in Fz3-MO (opposite phenotypes) as well as Wnt3-MO samples (purple dots in Figure 1D,E; DGE class 5 in File S1). Two of these code for Ubiquitin ligases, implicated in protein degradation, and one for a secreted cyclase, suggesting a possible association with lysis of damaged cells in injected embryos. In addition the Fz3 transcript was itself detected at high levels in Fz3-MO embryos, probably due to the stabilizing effect of the morpholino. An additional set of 10 transcripts were eliminated as coming from likely bacterial contaminants, because they clearly stood apart as strongly under-represented (z-scores ,25) in both Fz3-MO and Wnt3-MO samples (and also for Fz1-MO in 9 cases) compared with uninjected controls (blue dots in Fig 1D, E.). The sequences of these transcripts had no similarity with any known eukaryotic genes but rather included genes from bacteria. Contamination from bacteria may be higher in uninjected embryos due to reduced manipulation of the egg and thus more frequent retention of the jelly coat and associated contaminants.

Conserved and novel transcripts are differentially expressed in Wnt3-MO embryos

After elimination of the 13 non-specifically affected sequences, our final validated transcriptome comprised 166 differentially expressed transcripts. 153 of these 166 had clear predicted full or partial ORFs, comprising 40 over-expressed in Wnt3-MO embryos and 114 under-expressed. Detailed analysis of these sequences (File S1) revealed conserved and novel genes.

Conserved developmental regulators. *Clytia* developmental regulatory genes already known to be expressed in a polarized manner were present as expected. These included the orally expressed Brachyury (Bra), Frizzled-1 (Fz1) and WntX1A in the Wnt3-MO under-expressed list, and the aborally expressed FoxQ2a, Frizzled-3 (Fz3), Hox9/14B and Sox15 in the over-expressed list [15–17,39,40]. Many additional *Clytia* orthologs of bilaterian developmental regulators were also identified (phylogenetic analyses in File S2). Amongst the transcription factors were an ortholog of the hydrozoan-duplicated T-box Brachyury gene Bra2 [11], two forkhead family proteins frequently associated with endoderm formation (FoxA, FoxC), a previously uncharacterized FoxQ2 paralog (FoxQ2c), a T-box transcription factor (Tbx: no clear orthology to vertebrate T box genes), a member of the Pox-neuro branch of the Pax family (PaxA) [10], orthologs of Six4/5 and *Nematostella* DMRT-E [51], the Ets transcription factor Erg and the ANTP family non-hox/parahox homeodomain protein HD02 [16]. We also identified a Myb transcription factor belonging to the HTH class and several zinc finger domain transcription factors whose metazoan orthologs have not been characterized. Signaling pathway mediators notably included not only Wnt ligands and receptors but also many potential modulators of Wnt signaling including members of three families of secreted antagonists: Dkk (Dickkopf family), sFRP-A (a secreted frizzled-related protein) and Dan1(Cerberus/Dan family of Wnt and TGFb antagonists) [52]. We also identified secreted proteins that modify the extracellular environment, potentially capable of modulating ligand-receptor interactions through many pathways including Wnt as well as BMP and Hedgehog. Of particular note in relation to Wnt signaling were three heparan sulfate proteoglycan modifiers: two lipases implicated in glycipan cleavage closely related to Notum, and an endosulfatase related to vertebrate Sulf1/Sulf 2 [53,54]. The *Clytia* Notum sequences, derived from a hydrozoan-specific gene duplication, were named NotumA and NotumO because of their aboral and oral expression territories (see below). The second main signaling pathway that emerged in this analysis was the Notch pathway, with transcripts in the Wnt3-MO embryo-upregulated list coding for the Notch ligand and for two proteins related to Botch, whose *Drosophila* and mouse counterparts inhibit Notch protein processing [55].

Further signaling pathway components and transcription factors with likely conserved developmental roles featured in an extended list of transcripts differentially expressed in Wnt3-MO embryos with significance at p = 0.01 level (z-score +/23. 3 cutoff; list of additional sequences in File S3). These included yet more potential Wnt regulators: another Wnt ligand WntX1A [40], the transcription factor TCF, and Naked cuticle [56,57] were under-expressed, while another sFRP in the same orthology group as sFRP-A (named sFRP-B) and MESD (which interacts with the co-receptor LRP5/6 [58,59]) were overexpressed. Components of other signaling pathways also figured in this extended list, including a TGFb pathway ligand and cytoplasmic inhibitor (SMAD 6/7), a putative FGF receptor and a VEGF-related ligand. *Clytia* orthologs of the developmentally important transcription factors Gooseco¨id (Gsc), Iroquois (Irx), Hox9/14B [16] and Rfx were also identified.

Other conserved metazoan genes. The developmental regulator gene orthologs listed above were known through functional studies in classic experimental model species such as *Drosophila*, mouse and zebrafish. Additional ancient metazoan genes conserved during evolution may also have roles in regulating development that have yet to come to light. As well as genes

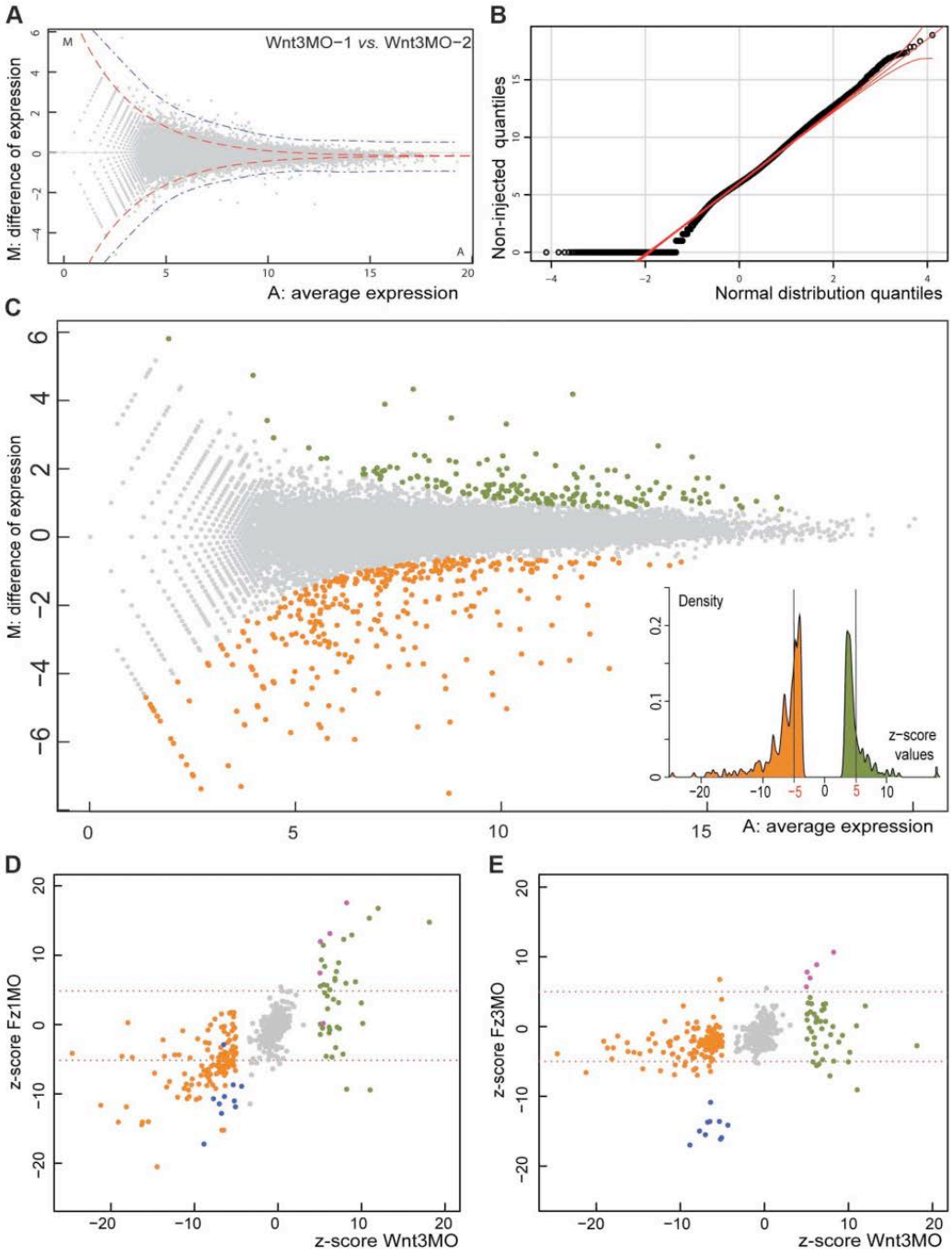

Figure 1. Identifying Clytia early gastrula patterning genes by DGE. A) Visualization of variation between two independent Wnt3-MO early gastrula replicate samples (''MA plot''). For each reference transcript (grey dots), M is the difference of read density between the two samples and A its average expression level in the combined samples (see Methods). Red and blue dotted lines give estimates of the distribution zone outside which values are statistically significant, based on the standard deviation (4xSD) of a theoretical distribution (red) calculated using the random sampling model, or real variation (blue) estimated by the comparison of technical replicates [50]. B) Demonstration of the near-normal distribution of the $\log_2$

counts of the mapped reads from one of the non-injected embryo samples by a QQ plot, a necessary condition to use the Random Sampling Model assumption in DGE analysis. C) MA plot of read data from Wnt3-MO versus non-injected embryo samples. Applying the 1% cut-off p-value for statistical significance corresponding to the threshold z-score of +/2 3.3 identifies 148 transcript sequences as over-expressed (green dots) and 232 as under-expressed (orange dots) in Wnt3-MO embryos. The more stringent +/2 5.0 threshold for z-score values eliminates a cluster of genes with expression characteristics very close to the overall population of non-differentially expressed genes, as demonstrated in the histogram (insert) and reduces the number of transcripts to 44 and 135 for Wnt3-MO embryo over- and under-expressed transcripts respectively. D, E) Z-scores for the Wnt3-MO embryo over- (green dots) and under- (orange dots) expressed transcripts plotted against those for two other morpholino-injected embryo groups harvested at the same developmental stage. Z-scores were calculated for experimental versus non-injected values in each case. D: Wnt3-MO versus Fz1-MO; E: Wnt3-MO versus Fz3 MO. Transcripts significantly under-expressed in all three MO groups (z-scores less than -5: probably from bacterial contaminants) are represented as blue dots and over-expressed (z-scores greater than 5; probably injection damage-related) as purple dots.
doi:10.1371/journal.pgen.1004590.g001

probably associated with the differentiation of larval cell types such as myophilin, calmodulin and innexin, our analysis provided a number of candidate-conserved developmental regulators, falling into three categories: 1) Known genes with little or no previously known involvement in development, for instance, coding for the amino acid transporter Aat or other solute carriers; 2) Members of large gene families associated with developmental regulation but lacking clear bilaterian orthologs, including putative transcription factors containing helix-loop-helix or zinc finger domains as well as 7-pass transmembrane (7tm) proteins (a large and diverse family of receptors for cytokines, hormones, peptides and other ligands with the potential to evolve developmental cell-cell signaling roles, as has occurred in the Frizzled family). 3) As yet uncharacterized genes that have homologs in bilaterians. This third category includes proteins containing conserved domains identified in the PFAM database such as the Domains of Unknown Function DUF4323 and DUF3504.

Cnidarian restricted genes. A considerable proportion of the sequences with complete predicted ORFs (37/126 = 29%) did not have identifiable orthologs among known bilaterian genes or any other non-cnidarian sequences in the NCBI databases (see Methods for details), as defined by a lack of significant similarity by reciprocal BLAST along the length of the sequence. These 'cnidarian restricted' sequences included the transcript most strongly under-expressed (highest z-score) in Wnt3-MO embryos, WegO1. In some cases, despite the absence of any identifiable ortholog, recognizable conserved motifs such as SAM or PH domains could be detected within the sequence of these transcripts using domain prediction software, suggesting involvement in mediating protein–protein or protein-membrane interactions. These domains are common to many diverse bilaterian proteins and cannot be taken as indicating homology. Such sequences could have originated through domain recombination or through extreme divergence of surrounding sequences during cnidarian evolution. Six of the novel cnidarian-restricted sequences identified in our study had clear counterparts in the fully sequenced genomes of *Nematostella* and/or *Hydra* but the others (31/37) are unique to *Clytia* amongst available sequences. Genome sequences for a larger range of cnidarian species will be required to assess the degree of taxonomic restriction of these genes. Thirteen possessed predicted 59 signal peptide sequences indicating that they code for secreted proteins varying in length from 77–526 predicted amino acids (average about 260). These characteristics are compatible with roles as novel signaling ligands, antagonists or extracellular regulators.

In situ hybridization analysis reveals four spatiotemporal expression profile types

We undertook detailed characterization of spatial expression and sequence analysis (Table 1) non-selectively for the top 20 under-expressed transcripts (Figure 2) and top 18 over-expressed transcripts (Figure 3) in Wnt3-MO early gastrulae. Expression territories for all 38 transcripts were determined by *in situ* hybridization at three stages: early gastrula, 24 hpf planula (just completed gastrulation, endoderm still undifferentiated), and 48 hpf old planula (cell differentiation ongoing in both endodermal and ectodermal regions). We found that almost all the *in situ* hybridization profiles could be assigned to one of four types, which we termed Oral (O), Aboral (A), Ingressing/Endodermal (IE) and Delayed expression (D) types, as described in more detail below and summarized in Figure 4. Briefly, O and A type profiles are characterized by polarized expression with respect to the developing oral-aboral axis at all stages, suggesting ongoing patterning roles during embryonic and larval development. The IE type profile corresponds to cells destined to contribute to the complex endodermal region including the i-cell stem cells and their derivatives. The D type profile transcripts were barely detectable in early gastrulae but showed at larval stages expression in diverse patterns in the ectoderm and/or later in the endoderm. Overall, our approach to identify new candidates for roles in cnidarian embryonic development was completely validated by these analyses. Without any selection based on sequence identity, all the transcripts we tested showed expression restricted in space and/or time during gastrulation and planula development.

Names were assigned to the analyzed transcripts on the basis of orthology and/or membership of known gene families (all phylogenetic analyses in File S2). Multiple members of known gene families were distinguished by suffixes designating the 4 main expression profile types: O, A, IE or D. Cnidarian-specific transcripts lacking any recognizable orthologs from non-cnidarian species in NCBI databases, and those with non-cnidarian orthologs that had not previously been characterized, were assigned novel names using the same suffixes, prefixed by ''Weg'' to denote differential expression in Wnt3-MO early gastrulae, or given names based on recognizable repeats when present.

Wnt3-MO embryo under-expressed transcripts show oral and endodermal profiles. Consistent with the aboralized phenotype of the Wnt3-MO-embryos, the twenty top under-expressed transcripts were all strongly localized during normal development to cells at the future oral pole (site of gastrulation) at the early gastrula stage (Figure 2). Their expression profiles could all be designated unambiguously as either O or IE type. The eight O type profile transcripts (Figure 2B-I) were detected strongly in the oral pole ectoderm in both gastrula and planula larva stages. These included the Wnt ligand WntX1A [40], three transcription factors (*Clytia* Bra2, Myb and ZnfO), and two novel cnidarian genes designated WegO1 and WegO2. None of these transcripts were significantly detected in cells ingressing during gastrulation, indicating either expression in exclusively ectodermal cells or down-regulated in ingressing cells upon their separation from the oral ectoderm. Two additional O-type profile genes showed later additional expression in cells of the endodermal region at the planula stage (Aat and Akr; panels H and I). Expression domains for these two genes and for the two Wnt ligands extended across the oral third of the larva [40]. In contrast, expression of the other

Table 1. Characteristics of all transcripts analyzed in detail in this study.

Name	Wnt3-MO response (z-score)	Identity/domains	Cnidarian specificity for novel transcripts	Domains	Expression pattern type	DGE class
TRANSCRIPTS UNDER-EXPRESSED IN Wnt3-MO						
WegO1	24.6	Cnidarian-restricted	*Clytia*		O	1
Znf845	21.2	Zn-finger domain, expressed in *Hydra* i-cells		DNA binding	IE	2
DMRT-E	19.1	DM-DNA binding domain. Doublesex and mab-3 related transcription factor		DNA binding	IE	2
HlhlE1	18.7	HLH domain		DNA binding	IE	1
Mos3	18.2	Mos kinase			IE	2
Bra2	18	Brachyury 2 ; T-box transcription factor		DNA binding	O	1
Sulf	17.5	Extracellular Sulfatase related to Sulf1/Sulf2 (modulates ligand signalling)		Signal peptide	IE	1
FoxA	16.2	FoxA; Forkhead-domain transcription factor		DNA binding	IE	2
FoxC	15.5	FoxC; Forkhead-domain transcription factor		DNA binding	IE	2
ZnfO	14.8	Zn-finger domain		DNA binding	O	2
Sox15	14.5	Sox domain (Jager et al 2010)		DNA binding	IE	2
WntX1A	13.8	Wnt ligand, (Momose et al 2008)		Signal peptide	O	1
Akr	13.6	Small protein with 2 Ankyrin repeats.			O (+ endo)	1
WeglE1	13.3	Cnidarian-restricted , SAM domain	Hydrozoan		IE	2
HlhlE2	12.9	HLH domain		DNA binding	IE	2
Aat	12.4	Amino acid transporter		Trans-membrane	O (+ endo)	1
WeglE2	12	Cnidarian-restricted, secreted protein	Clytia	Signal peptide	IE	2
WegO2	11.8	Cnidarian-restricted	Clytia		O	1
Myb	11.4	Myb-type HTH DNA-binding domain		DNA binding	O	1
Erg	11.2	Ets DNA-binding domain, SAM/pointed domain		DNA binding	IE	2
Bra	*10.6*	*Brachyury 1; T-box transcription factor (Momose & Houliston, 2007)*		*DNA binding*	*O*	*1*
FoxQ2c	*8.4*	*Forkhead-domain transcription factor*		*DNA binding*	*IE*	*2*
NotumO	*8.4*	*Notum ; extracellular Wnt signalling regulator*		*Signal peptide*	*O*	*1*
WegO3	*5*	*related to human CXorf65 (uncharacterized)*			*O (+ endo)*	*1*
Gsc	*4.6*	*Goosecoid, homeodomain protein*		*DNA binding*	*O*	*1*
TRANSCRIPTS OVEREXPRESSED IN Wnt3-MO EMBRYOS						
Botch1	18.1	ChaC domain - related to Botch (Notch antagonist)			D	4
bZip	12	bZip TF, related to CCAAT/enhancer-binding proteins		DNA binding	D/A	4
FoxQ2a	11	Forkhead-domain transcription factor (Chevalier et al 2006)		DNA binding	A	3
Dkk	10.2	Dickkopf family (secreted Wnt antagonist)		Signal peptide	A[#]	3
ZnfA	10	Zn-finger domain (SP1 family)		DNA binding	A	3
NotumA	9.3	Notum ; extracellular Wnt signalling regulator		Signal peptide	A	4
Botch2	8.8	ChaC domain - related to Botch (Notch antagonist)			D/A	4
WegD1	8.2	Cnidarian-Restricted - Pleckstrin Homology domain	Hydrozoan		D	4
WegAI	8.3	DUF3504 domain	Cnidarian		A	3
Asp	7.9	Asparaginase, 5 Ankyrin repeats			D	4
WegD2	7.8	Cnidarian-restricted	Clytia		D	4
Dan1	7.3	Dan/Cerberus family of secreted Wnt/BMP inhibitors		Signal peptide	A	3
ZpdA	7.3	Cell Surface Glycoprotein - zona pellucida domain superfamily		Trans-membrane	D/A	4

Table 1. Cont.

Name	Wnt3-MO response (z-score)	Identity/domains	Cnidarian specificity for novel transcripts	Domains	Expression pattern type	DGE class
Amt	6.9	Ammonium transporter		Trans-membrane	D	4
HD02	7	Antp family homeodomain protein (Chiori et al., 2009)		DNA binding	D	4
WegA2	6.9	Cnidarian-restricted , SAM domain	Clytia		A	3
Notch	6.7	Notch		Trans-membrane	D/A	3
UCP	6.8	Mitochondrial Uncoupling Protein			D	4
Tbx	*6.5*	*T-box transcription factor*		*DNA binding*	*A*	*3*
sFRP-A	*6.2*	*Secreted Fz (sFRP)- lectin domain*		*Signal peptide*	*A*	*3*
Fz3	*5.4*	*Fz family receptor (Momose & Houliston, 2007)*		*Signal peptide*	*A*	*3*

Details of transcripts for which *in situ* hybridization analyses were performed previously or in this study, with corresponding expression pattern type (see Figure 4) and DGE class as defined according to z-scores in Wnt3-MO and Fz1-MO transcriptomes compared to non-injected embryos (see Figure 7). Transcripts selected from outside the "top 20" under and over-expressed list are in italics. See text for details. O= Oral; A= Aboral; IE= Ingressing/Endodermal; D= Delayed. endo= endoderm in 48hpf planula. # = no expression detectable in Early Gastrula.

doi:10.1371/journal.pgen.1004590.t001

five genes was predominantly detected at the oral tip, resembling the previously-described expression of Bra1(initially named Bra) [39]. O type expression patterns were also obtained for three additional transcripts selected from the Wnt3-MO-underexpressed list; Gsc, NotumO and an evolutionarily conserved but previously uncharacterized sequence designated WegO3 (*in situ* hybridization images in File S4). Gsc and WegO3 both showed oral tip expression, supplemented with additional endodermal expression in 48 h planula larvae for WegO3. NotumO expression extended further along the oral-aboral axis, matching that of the two Wnt ligands.

IE type patterns were observed for twelve transcripts, and were characterized by expression mainly in ingressing or ingressed cells during gastrulation, and later in different cell populations within the endodermal region (Figure 2J-U). At the gastrula stage, these transcripts were detected in subpopulations of cells ingressing into the endoderm at the oral pole, as well as in some cases putative pre-ingressing populations in the ectoderm. At planula stages, they were detected predominantly in the endodermal region, in different sub-populations of cells. For the transcription factors Znf845, FoxA and also for the kinase Mos3, the distribution of expressing cells, notably their position in non-polar regions between the endoderm and ectoderm layers in 48 hpf larvae, was reminiscent of previously described germ line/stem cell genes expressed in i-cells such as Nanos1, Vasa and Piwi [60]. Expression in scattered ingressing cells was also observed for HlhIE1 (Figure 2M; fewer cells detected), the Ets family transcription factor Erg (Figure 2N; additional expression in oral ectoderm cells in 48 h planulae), *Clytia* Sulf (Fig 2O; very weak in 48hpf larvae) and Sox15 (Figure 2P; additional expression in various endodermal and ectodermal cells as previously described [17]), and also for an additional FoxQ2 paralog identified in the Wnt3-MO-underexpressed transcript set designated FoxQ2c (File S2). The hypothesis that Znf845 and FoxQ2c were expressed in i-cells or their primary derivatives is consistent with data from a recent study in *Hydra* which compared transcriptomes of sorted endodermal, ectodermal or Nanos-expressing (i-cell lineage) cells from adult polyps [25] (see File S5). HlhIE2, DMRT-E and FoxC were also expressed in early stages of ingression in the early gastrula but adopted more widespread distribution through the endodermal region in the planula. Correspondingly *Hydra* FoxC transcripts are highly enriched in endodermal cells [25] (File S5). Two novel cnidarian transcripts (WegIE1 and WegIE2) were detected predominantly in an extensive population of presumptive endoderm cells, expression only becoming detectable once they have entirely separated from the oral ectoderm (Figure 2T,U). Additional WegIE1 expression in scattered larval ectoderm cell populations was observed, particularly in 24 h planulae (Figure 2T).

Wnt3-MO embryo over-expressed transcripts are detected in aboral territories or repressed in early gastrulae. Spatial expression profiles obtained for the top eighteen Wnt3-MO embryo up-regulated genes (Figure 3) were of the A (Aboral; Figure 3A-G) or D (Delayed; Figure 3L-R) profile types, or in four cases showed characteristics of both profile types (Figure 3H-K). The seven transcripts assigned as having clear A-type profiles, on the basis of sustained expression at the aboral pole, notably included the Wnt regulators Dkk1/2/4, Dan1 and NotumA, the transcription factors FoxQ2a and ZnfA, the novel cnidarian gene WegA2, and WegA, which has no clear non-cnidarian orthologs but contains a conserved 135aa domain (DUF3504). Six of these seven transcripts were detectable from the gastrula stage, while Dkk1/2/4 was only detectable in planulae. The extent of the aboral expression territory varied between genes, with WegA1 expression extending along about half the oral-aboral axis at all stages, while the others were expressed in the aboral third at the early gastrula stage before becoming more tightly restricted to different ectodermal and/or endodermal cell populations at the aboral pole of the planula larva. Consistent with the ectodermal localization of this transcript, a WegA1 ortholog identifiable in published transcriptome data from *Hydra* polyps [25] is also preferentially expressed in ectoderm (File S5). Clear A-type expression profiles were also observed for two additional transcripts selected on the basis of sequence identity from lower down the Wnt3-MO-underexpressed list: Tbx and sFRP-B (File S4).

Four more transcripts from the ''top 18'' showed aborally enhanced expression in at least two of the three stages tested, but also additional expression at other sites. Given their barely-detectable expression at the early gastrula stage they had partial expression features of both the A and D type profiles (see below). The extracellular glycoprotein ZpdA showed enhanced aboral

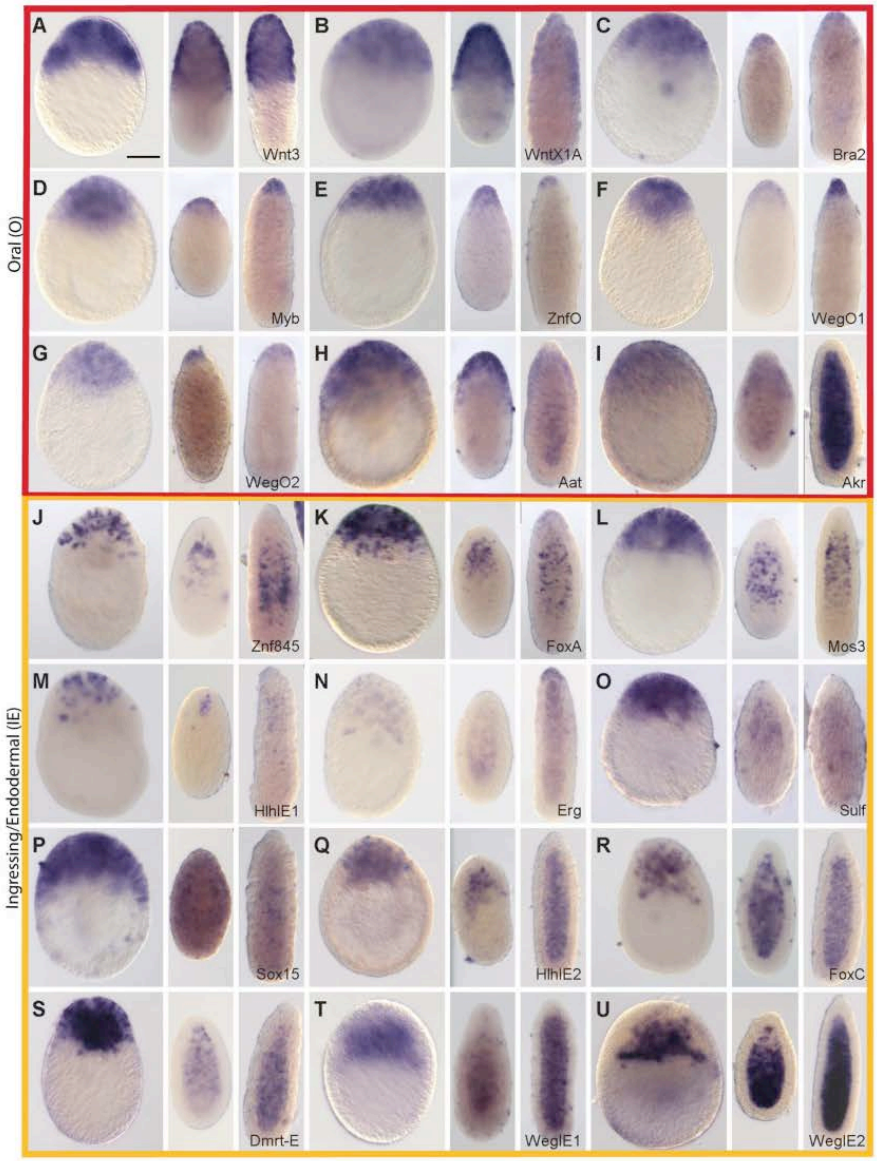

Figure 2. Preferential expression of Wnt3-MO-embryo under-expressed transcripts in oral and ingressing cells. *In situ* hybridization analysis of Wnt3-MO-embryo under-expressed transcripts in early gastrula, 24hpf planula and 48hpf planula stages (from left to right in each panel). The expression of Wnt3 (A; Momose et al., 2008) is compared with that of the 20 down-regulated transcripts with the highest z-scores. All genes showed heavily oral-biased expression at the early gastrula stage, with two principle distribution patterns: Predominantly in the oral ectoderm at all stages (panels A-I; "Oral" expression pattern, outlined in red); Mainly in ingressing/ingressed cells during gastrulation and then in the endodermal region of the planula (panels J-U; 'Ingressing/Endodermal" expression pattern, outlined in orange). Two of the "Oral pattern" transcripts (panels H and I) also showed expression in the endoderm at the planula stage. Representative images of the patterns observed in at least three experiments are shown. All embryos are oriented with the oral pole uppermost. Bottom right: gene name (see Table 1). Scale bar 50 mm.
doi:10.1371/journal.pgen.1004590.g002

expression at the gastrula and 24 h planula stages, but was detected across the whole larva by 48hpf (Figure 3H). Conversely, expression of Botch2 was mainly confined to cells in the aboral half ectoderm at 48hpf, but concentrated in the oral endoderm at 24hpf (Figure 3I), while bZip-expressing cells were concentrated at the aboral pole at planula stages but also detected in more central

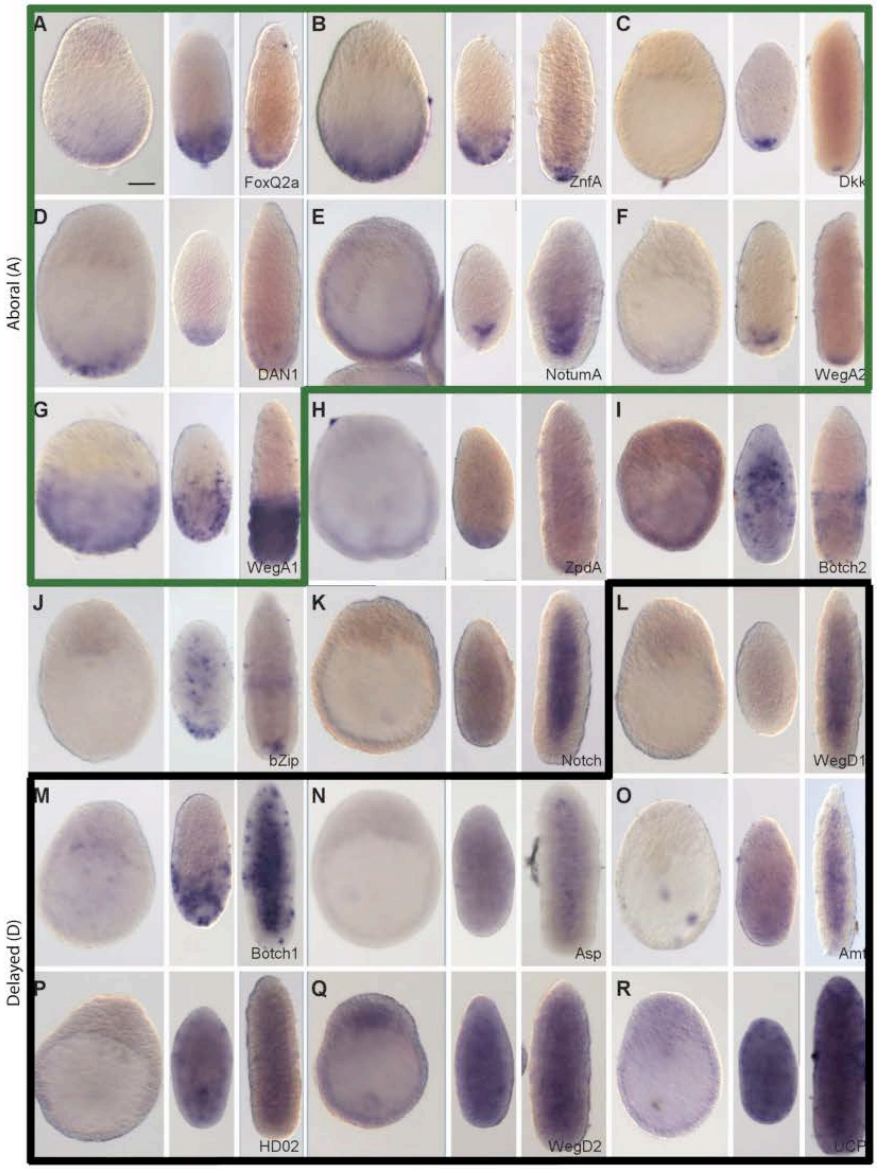

Figure 3. Preferential expression of Wnt3-MO-embryo over-expressed transcripts in aboral domains and planulae. *In situ* hybridization analysis of Wnt3-MO-embryo over-expressed transcripts in early gastrula, 24hpf planula and 48hpf planula stages (from left to right in each panel). The 18 transcripts with the highest z-scores were analyzed. Seven genes showed expression clearly restricted to the aboral territories at planula stages (A-G), already apparent at the early gastrula stage except in in the case of Dkk (C). Two additional transcripts showed an aboral expression pattern but with additional signal in endodermal region of planula larvae: ZpdA (H) and Botch2 (I). 9 transcripts (J-R) showed low ubiquitous or undetectable expression at the gastrula stage followed by a variety of patterns in planula larva including ubiquitous (Q-R), mainly endodermal (K-O) and/or with diverse dynamic distributions of scattered cells in the ectoderm and/or endoderm (J, M, N, O, P). We classified the expression profiles as "Aboral-type" (A-G, panels outlined in green), "Delayed" type (L-R, panels outlined in black) or as showing a mixture of these profiles (4 remaining panels). Representative images from at least three experiments are shown. All embryos are oriented with the oral pole uppermost. Bottom right: gene name (see Table 1). Scale bar 50 mm.
doi:10.1371/journal.pgen.1004590.g003

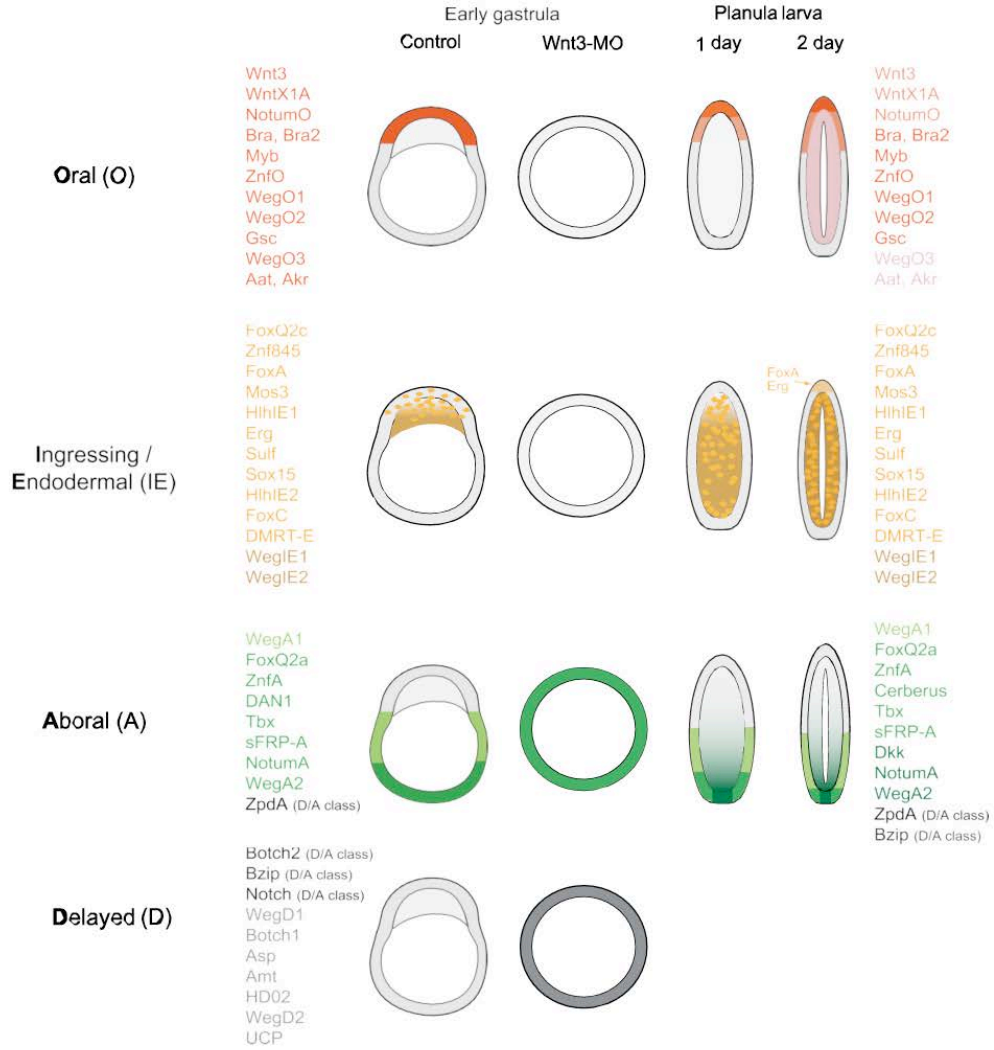

Figure 4. Summary of expression profiles observed for the analyzed transcripts. The differentially expressed transcripts analyzed in this study showed four basic types of expression profile: Oral (oral pole ectoderm at all stages); Ingressing/Endodermal (cells moving into the endodermal region during gastrulation and persisting in this region); Aboral (aboral pole throughout) and Delayed (absent or very low expression at the beginning of gastrulation, then expression in a variety of regions/cell types at the planula stages). Within these four categories there were differences in the limits of detected expression as indicated.
doi:10.1371/journal.pgen.1004590.g004

locations (Figure 3J). Notch expression was not detectable in the gastrula and was predominantly endodermal in planula stages, but with low additional signal detected in the aboral ectoderm (Figure 3K).

The seven transcripts with D type profiles exhibited a heterogeneous array of expression sites (Figure 3L-R). Their main common characteristic was ubiquitous low or undetectable expression at the gastrula stage, later being detected in a variety of distributions. WegD1 transcripts were detected only in the endodermal region at 48hpf (Figure 3L); Botch1 transcripts were detected initially in cells of the aboral ectodermal in 24hpf planulae but at 48h in patches of cells scattered irregularly along the oral-aboral ectoderm as well as through the endodermal region (Figure 3M). The Asparaginase (Asp; Figure 3N) and Ammonium transporter (Amt; Figure 3O) transcripts could be widely detected in cells in both cell layers in 24hpf planulae and then mainly in individual cells of the endodermal layer one day later. Finally the homeodomain protein HD02 (Figure 3P), WegD2 (Figure 3Q)

and the mitochondrial uncoupling protein UCP (Figure 3R) were detected in cells distributed widely across the larva at both 24 and 48hpf.

Unlike the regionalized A, O and IE type patterns, the diverse expression profiles of this D group of transcripts was not anticipated from the aboralized Wnt3-MO phenotype. To check that they did not represent false positives from the DGE screen, we verified expression for representatives of each of the four expression profile types in Wnt3-MO embryos by quantitative PCR (Q-PCR; Figure 5) and *in situ* hybridization (Figure 6). The Q-PCR analysis confirmed the DGE response for all of the10 transcripts tested. By *in situ* hybridization, expression of O and IE profile transcripts was as expected undetectable in Wnt3-MO early gastrula. D-type pattern transcripts showed strongly elevated expression in Wnt3-MO embryos compared to control embryos processed in parallel. The expressing cells lined the blastocoel across the embryo for Botch1, bZip and Amt (Fig 6. J-L); also found for Asp, ZpdA, and Botch2 (File S6). In contrast, A type profile transcripts (Fig 6. G-I) showed expression territories extended spatially though the ectoderm from the aboral side, but without significantly higher expression than in the aboral domain of control embryos. These results indicate that IE, A and O type profile genes are all regulated by regional differences in Wnt signaling activity at the early gastrula stage, whereas D type profile gene transcription is activated temporally between the early gastrula and planula stages following down-regulation of Wnt3 signaling.

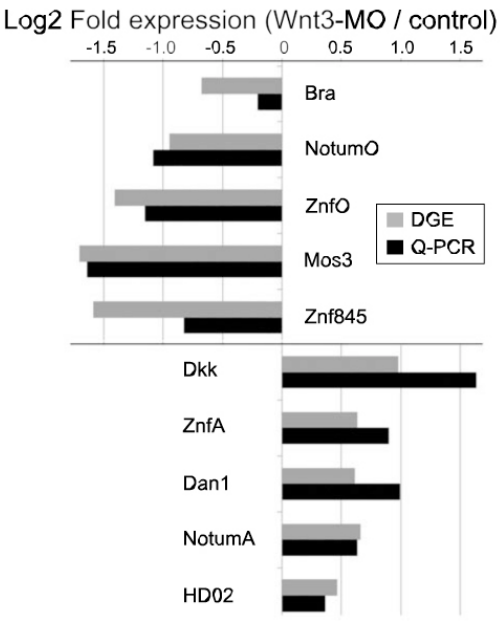

Figure 5. Equivalent differential expression responses determined by DGE and Q-PCR. For ten selected transcripts from different DGE classes and with different expression profiles (see Table 1, Figure 4), transcript levels at the early gastrula stage were determined by Q-PCR in Wnt3-MO and non-injected early gastrula embryos. The ratio of expression levels of selected genes between injected and control embryos, normalized with respect to EF-1a is compared to the DGE data represented in the same way by using the counts of reads mapped rather than the number of cycles of Q-PCR amplification. Transcript identities are shown beside each pair of bars.
doi:10.1371/journal.pgen.1004590.g005

PCP disruption preferentially affects transcripts with non-axial expression profiles

The overall outcome of our *in situ* hybridization analyses was that transcripts identified as Wnt3-MO-underexpressed consistently showed Oral and Ingressing/Endodermal type expression profiles while the overexpressed ones all showed Aboral and Delayed type profiles. The significance level of the response did not, however, correlate with expression patterns (O versus IE or A versus D, respectively; see z-scores in Table 1). Remarkably, we were able in both cases to uncover a strong correlation when we included in the analysis the z-scores obtained for the Fz1-MO sample (Figure 7A). This could be demonstrated by plotting the z-scores calculated for the two experimental conditions (against non-injected) against each other and determining the position of all the transcripts analyzed in Figures 2 and 3, of genes with expression patterns characterized previously (Bra, Fz3) and of five additional examples selected from our primary list (FoxQ2e, Tbx; NotumO, sFRP-A, Gsc, WegO3; File S4; All patterns summarized in Table 1 and Figure 4). Amongst the Wnt3-MO embryo under-expressed transcripts (orange dots in Figure 7A), those with Fz1-MO z-values higher than -5.0, ie not significantly affected or only relatively weakly underexpressed in Fz1-MO embryos, tended to show the O type expression pattern (eleven of the thirteen examined transcripts in the dark orange ''Class 1'' zone). The others (pale orange ''Class 2'' zone) showed IE type expression profiles in eleven of the twelve cases. A similar strong correlation was found for the Wnt3-MO embryo-over-expressed transcripts (green dots in Figure 7). In this case, applying a Fz1-MO z-score value threshold of +5.0 we found that transcripts with higher z-values (grey ''Class 4'' zone) tended to show D or mixed D/A-type patterns (seven and three respectively of the eleven analyzed transcripts), while nine transcripts with z-scores less than 5.0 (green ''Class 3 ''zone) showed A-type patterns and the tenth (Notch) a mixed A/D pattern. In this Class3 zone, responses to Fz1-MO were quite variable, including moderate over-expression, unchanged expression and, in a few cases, under-expression (notably FoxQ2a and WegA1).

From these analyses we defined four ''DGE classes'' on the basis of z-score values in Wnt3-MO and Fz1 MO embryos, as indicated in Figure 7A. Although these classes strongly correlate with the four types of expression profiles (Figure 7; Table 1) there are exceptions, for instance ZnfO is categorized as Class 2 on the basis of z-scores but shows an oral type expression profile, while Sulf is categorized as Class 1 but shows endodermal expression.

Fz1 acts as a receptor for Wnt3 to activate Wnt/b-catenin signaling [39,40], but is also thought to interact with the *Clytia* Strabismus protein to mediate planar cell polarity (PCP), necessary for cell alignment in the ectoderm but also axial elongation during larval development and endoderm formation [41]. We thus hypothesized that the differences in expression responses in Fz1-MO versus Wnt3-MO could be due to the specific involvement of Fz1 in PCP. To test this hypothesis we made additional comparisons using a transcriptome derived from early gastrula embryos in which PCP was specifically disrupted by a morpholino targeting Strabismus (Stbm-MO). Plotting the z-scores (in relation to uninjected embryos) of the Fz1-MO and Stbm-MO transcriptomes against each other revealed a striking similarity (Figure 7B). The linear positive correlation was especially clear between Fz1-MO and Stbm-MO z-scores for the Wnt3-MO over-expressed transcripts (i.e. DGE Classes 3 and 4; green and grey dots respectively in Figure 7B; Pearson correlation coefficient value

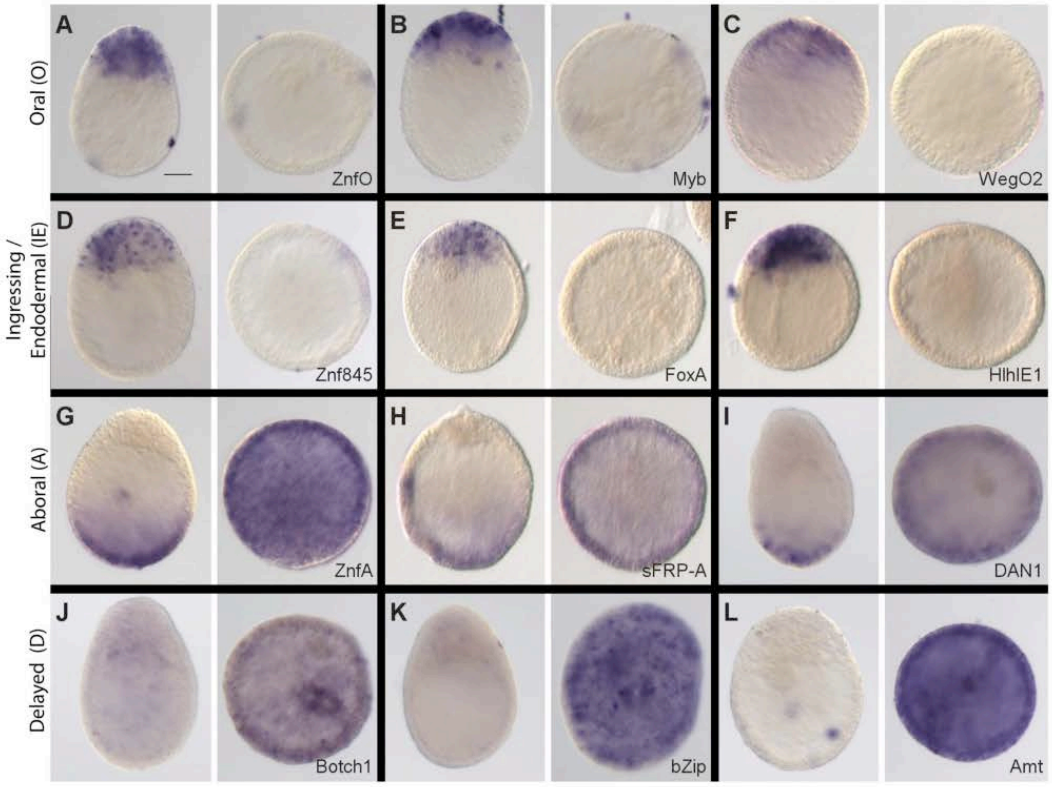

Figure 6. Stereotyped modification of gene expression patterns in Wnt3-MO embryos. *In situ* hybridization analysis of selected transcripts in untreated (left panels) and Wnt3-MO injected (right panels) early gastrulae. Each expression pattern type is represented in the transcripts analyzed, as indicated on the left. A-C: O-type pattern transcripts; D-F: IE-type pattern transcripts, G-I: A-type pattern transcripts; J-L: D-type pattern transcript. For Botch1 (J) and bZip (K), individual cells with high expression on the blastocoelar face of the ectoderm were discernible in the Wnt3-MO embryos. Representative images of the patterns observed in at least three experiments are shown. All control embryos are oriented with the oral pole uppermost. Gene identity is shown in the bottom right of each pair of panels. Scale bar 50 mm.
doi:10.1371/journal.pgen.1004590.g006

0.93). The separation between Class 1 and Class 2 transcripts on the basis of Stbm-MO responses was less strict, with Class 1 transcripts showing moderately increased or decreased levels in these embryos, compared to unaffected or reduced levels in Fz1-MO embryos (compare distribution of orange dots in Figure 7A and 7C). This can be explained by the requirement of Fz1 but not Stbm in Wnt/b-catenin signaling in the presumptive oral territory, We validated the transcriptome comparison analyses by *in situ* hybridization on Fz1-MO and Stbm-MO early gastrula embryos (Figure 8) using a subset of the probes used to examine Wnt3-MO embryos (Figure 5). For each gene the expression patterns in the two morpholino conditions were strikingly similar: The Class 1/O-type pattern transcript Myb, and the Class 3/A-type pattern transcripts ZnfA and sFRP-A showed little change compared with non-injected controls (Figure 8A, E, F). ZnfO, assigned to DGE Class2 despite its O-type expression profile, showed undetectable expression at the early gastrula stage in both Fz1-MO and Stbm-MO embryos (Figure 8B) and thus indeed represents an axially-expressed gene atypically sensitive to PCP perturbation.

The weak change in levels of most axially-expressed genes along with the significant under-expression of FoxQ2a and WegA1 in both Fz1-MO and Stbm-MO early gastrula embryos (Figure 7A, C; File S1) revealed in this study may at first seem difficult to reconcile with the previous description of an ''aboralized'' phenotype including a slight expansion of the FoxQ2a expression domain in Fz1-MO embryos [39], but this can be explained by a difference in the timing of the two studies since the PCP effect is only transient. Thus, analysis of Stbm-MO embryos revealed that while aboral FoxQ2a expression is undetectable by *in situ* hybridization at the early gastrula stage it subsequently becomes restored, while conversely oral expression of Bra1 is transiently expanded but then becomes re-restricted to the oral pole of the planula [41].

The *in situ* analyses performed for Class 2/IE-type and Class4/D-type pattern transcripts also validated the DGE analyses. FoxA and Znf845 were barely detectable by *in situ* hybridization at the early gastrula stage (Figure 8C, D), while Botch1 and bZip were detected strongly across the embryo (Figure 8G, H). As in Wnt3-MO embryos (Figure 5) the signal in these latter cases was mainly

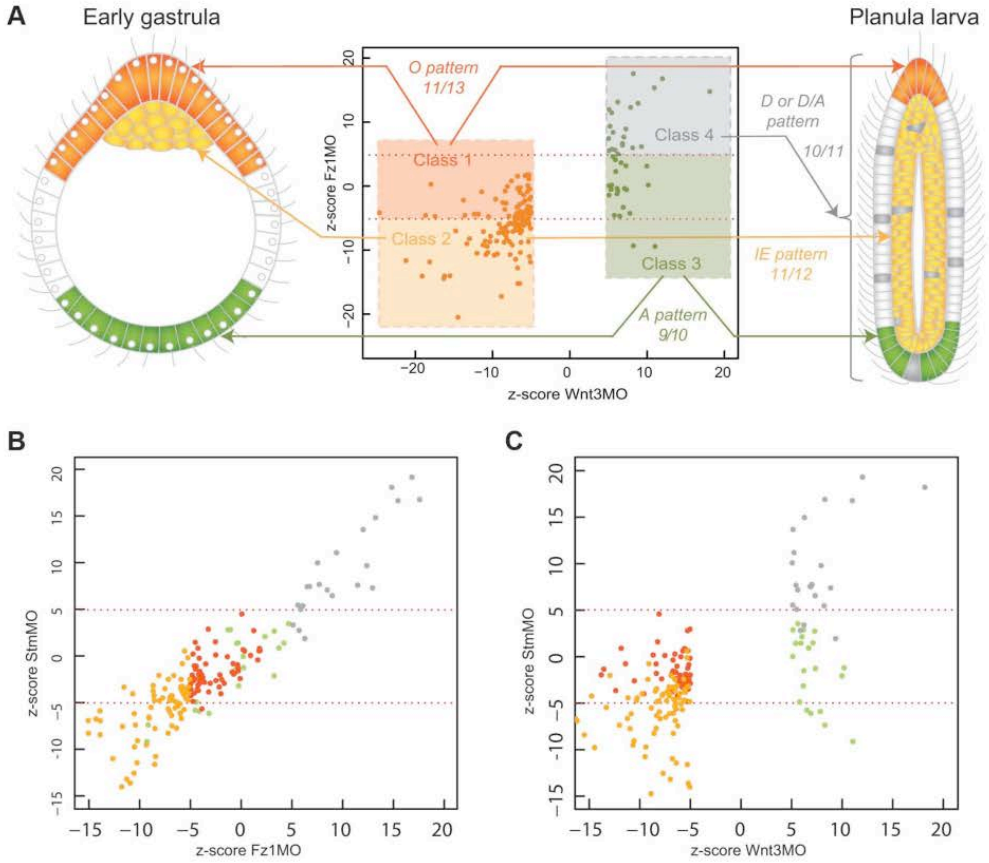

Figure 7. DGE responses correlate with spatial expression profiles. A) Schematic representation of the 4 types of expression profile observed amongst characterized transcripts (see Figure 4) at early gastrula (left) and planula (right) stages, showing their mapping onto the differential responses of the transcripts to Wnt3-MO and Fz1-MO. indicated on the z-score plot in the center. Four DGE classes were defined on the basis of z-scores in Wnt3-MO and Fz1-MO embryos applying cutoffs of -5 for classes 1 and 2, and +5 for classes 3 and 4 as indicated respectively by the dark and light orange, green and gray zones on the graph. The numbers indicate how many of the transcripts for which expression patterns were determined for each class showed the corresponding expression profile. These transcripts are all listed in Table 1 and with expression patterns shown in Figures 2, 3 and 6. B) Equivalent Z-score plot mapping a transcriptome dataset for Stbm-MO early gastrula-stage embryos against the Fz1-MO dataset. Dot colors correspond to the 4 classes defined in A. There is a strong correlation between expression responses in these two conditions, especially for classes 3 and 4 (green and grey dots, ie transcripts over-expressed in Wnt3-MO embryos). C) Z-score plot mapping the Stbm-MO transcriptome dataset embryos against the Wnt3-MO dataset. This illustrates that the 4 DGE classes defined on the basis of Fz1-Mo and Wnt3-MO responses situate largely but not exclusively in the equivalent zones of the Stbm-MO vs Wnt3-Mo graph.
doi:10.1371/journal.pgen.1004590.g007

detected in cells positioned on the basal side of the ectodermal epithelial layer.

We conclude that the relatively strong under-expression (Class 2) or over-expression (Class 4) of certain genes in Fz1-MO embryos is due in whole or part to disruption of PCP. This effect could reflect regulation of gene transcription by specific signaling pathways activated by PCP or be indirect, resulting from disturbed morphogenesis following failure of the ectodermal cells to align, to develop cell polarity and to undergo ciliogenesis [41].

Knockdown of conserved and cnidarian-restricted genes generates developmental defects

To test whether the newly identified genes in *Clytia* were indeed involved with developmental processes as predicted by their expression patterns, we injected antisense morpholino oligonucleotides targeting a selection of identified genes. We included in this analysis transcripts representing each of the four expression profile types including cnidarian-restricted genes (WegO1, WegIE2, WegD1), candidate conserved developmental regulators (Bra1, Bra2, FoxQ2c, FoxQ2a, HD02) and the partly conserved transcript WegA1. For each morpholino tested, developmental defects observed at morphological (Figure 9) and cellular (File S8) levels were coherent with the corresponding expression patterns (Figures 2 and 3), confirming the usefulness of our approach to identify developmental regulators. Wherever possible (6/8 cases, see File S7 for details) morpholinos targeting two different sites in the transcript were used, and in each case similar phenotypes were observed.

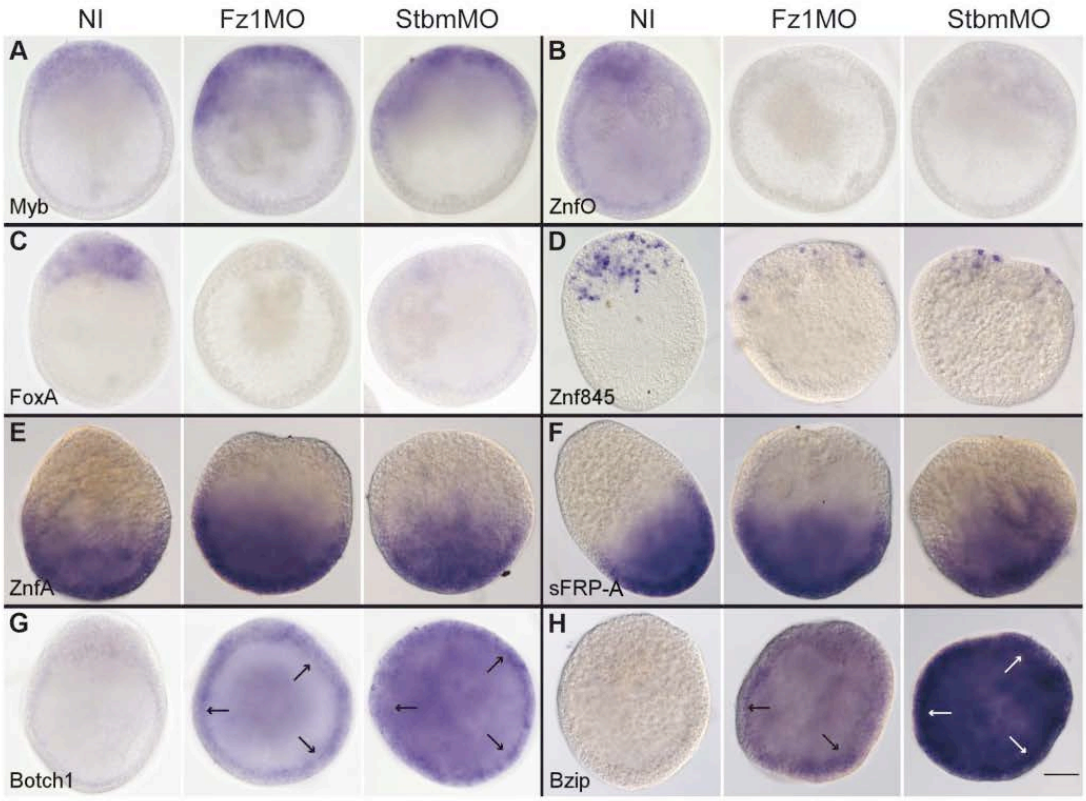

Figure 8. Fz1-MO and Stbm-MO have very similar effects on gene expression profiles. Each set of 3 panels shows typical *in situ* hybridization patterns obtained for uninjected embryos (left), Fz1-MO embryos (center) and Stbm-MO embryos (right) injected, fixed at the early gastrula stage and processed in parallel. A-B: O-type pattern transcripts (Myb and ZnfO); C-D: IE-type pattern transcripts (FoxA and Znf845); E-F: A-type pattern transcripts (ZnfA and sFRP-A); G-H: D-type pattern transcripts (Botch1 and bZip). Cells with high Botch1 and bZip expression on the blastocoelar face of the ectoderm were discernible (narrows) in Fz1MO and StbmMO embryos. Gene identity is shown in the bottom left of each set of panels. For each transcript the two morpholinos have very similar effects on the expression patterns, confirming the z-score comparisons (File S1). Scale bar 50 mm.
doi:10.1371/journal.pgen.1004590.g008

Morpholinos to the three O-type expression pattern transcripts all showed defects in endoderm formation, consistent with endoderm fate specification in the oral territory [61,62]. Morpholinos targeting the two *Clytia* paralogs Bra1 and Bra2 both significantly inhibited endoderm formation. Initial signs of cell ingression at the oral pole occurred with only a slight delay with respect to non-injected controls, but subsequent filling of the blastocoel was strongly retarded, such that by 24hpf Bra1-MO and Bra2-MO embryos (Figure 9C, D) resembled uninjected embryos at the onset of gastrulation (about 11hpf). Bra1-MO and Bra2-MO embryos then elongated somewhat and disorganized cells accumulated in the blastocoel to a variable degree, although often with a significant reduction in the amount of endoderm observed. Confocal microscopy confirmed that the residual ectodermal cells of both Bra1-MO1 and Bra2-MOe/i embryos accumulated in aboral regions and showed signs of epithelialization (File S8 C, D). A similar but much less severe delay in gastrulation was obtained following injection of morpholinos targeting the cnidarian-restricted gene WegO1, whose expression profile is very similar to that of Bra1 and Bra2 (Figure 2). Planulae showed a characteristic tapering of the oral half (Figure 9H), and confocal microscopy revealed that endoderm was reduced in this region (File S8B).

Strikingly, morpholinos targeting the A-type profile transcript WegA1 generated an opposite phenotype from the O-type pattern morpholinos. At the onset of gastrulation, massive cell ingression initiated widely across the embryo (Figure 9F). This is reminiscent of the phenotype previously described for Fz3 MO [39]. During subsequent development, cells from the internal regions were expulsed in most embryos, so that by the planula stage, embryos were commonly smaller and consisted of accumulations of endodermal-type cells surrounded in some cases by a very thin ectoderm layer, in which the cells were stretched over the inner cell mass (Figure 9F; File S8 G, H, I).

Morpholinos targeting the two IE type pattern genes WegIE2 and FoxQ2c both caused only minor disruption of development prior to the end of gastrulation, but subsequent formation of the endodermal cell layer was affected, with in both cases a thin and uneven layer of endodermal cells observed at 48hpf surrounding a distended cavity containing cell debris (Figure 9R, S). WegIE2-

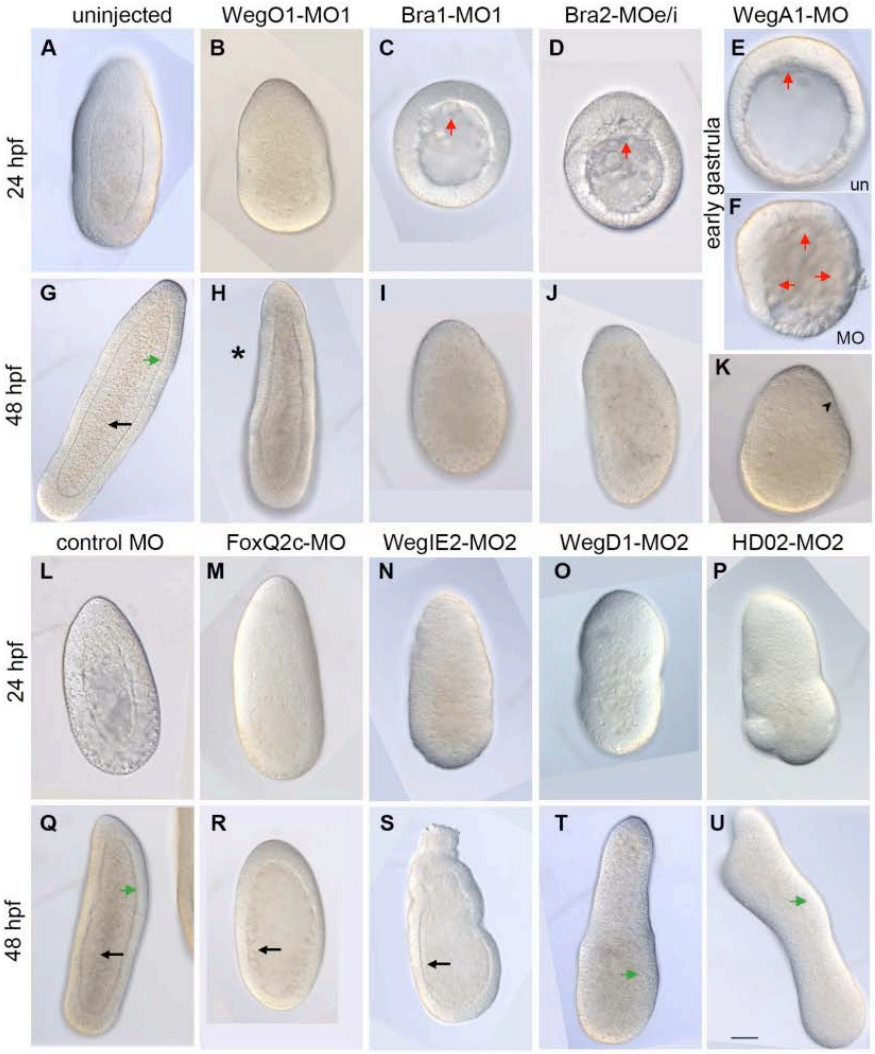

Figure 9. Morpholinos targeting conserved and cnidarian-specific transcripts disrupt development. DIC imaged larvae developed from morpholino-injected eggs after 24hpf and 48hpf development or at the early gastrula stage as indicated. Typical morphology observed at non-toxic morpholino doses are shown in each case, with the oral pole at the top. Similar phenotypes were obtained using a second morpholino in all cases, except FoxQ2c and WegA1, for which no second non-toxic morpholino could be designed. Uninjected embryos (A) and control-MO injected embryos (L) had completed gastrulation at 24hpf with endodermal epithelialisation starting at the aboral pole. By 48hpf uninjected planula larvae (G, Q) had formed with endodermal epithelial layers (black arrows) organized around a central stripe-like cavity and a well-defined lamina layer separating the endoderm and ectoderm (green arrows). WegO1-MO1 embryos showed minor disruption of gastrulation with embryo elongation slightly compromised at 24hpf (B) and the oral half, thin and tapered (asterisk) at 48hpf (H). Morpholinos targeting either Bra1(C, I) or Bra2 (D, J) showed severe delays in gastrulation. By 48 hpf some embryo elongation had occurred but the blastocoel contained only loose, disorganized material. WegA1-MO embryos (F) showed massive cell ingression at the onset of gastrulation, when cell ingression had barely initiated in uninjected embryos cultured in parallel (E). At 48 hpf (K) the endoderm was enlarged and the ectoderm layer was very thin and irregular (black arrowhead). FoxQ2c-MO (M, R) and WegIE2-MO (N, S), showed severely reduced endodermal layer at 48hpf. WegD1-MO and HD02-MO embryos showed severe defects in overall morphology (O, P, T, U), lacking a well defined basal lamina between endoderm and ectoderm. Green arrows indicate the position of this interface. Black arrows indicate the endodermal epithelial layers in G, Q, R and S. Red arrows indicate ingressing cells at the onset of gastrulation in C, D, E and F. Scale bar 50 mm for all panels.
doi:10.1371/journal.pgen.1004590.g009

MO embryos showed additional disorganization of the oral ectoderm. Confocal microscopy confirmed that the endodermal cell layers were severely disorganized (File S8 E,F).

Finally, morpholinos targeting the two D-type profile genes, which are strongly up-regulated at the early gastrula stage upon Wnt3, Fz1 or Stbm disruption, did not markedly disrupt gastrulation but resulted in highly aberrant morphology of the planulae (Figure 9T,U). WegD1-MO embryos showed a distended aboral end with the ectoderm then becoming highly folded, this effect extending along the length of the embryo in the most extreme cases. Injection of morpholinos targeting the ANTP family gene HD02 also resulted in elongated and very irregular shaped planulae. In both cases the interface between the ectoderm and endoderm layers was very irregular with confocal microscopy revealing mixing of cells from the two layers and an absent or highly disrupted basal lamina between them (File S8 P, T). In HD02-MO embryos, anti-tubulin staining revealed an abundance of neurite–like projections traversing irregularly this interface, contrasting with the well defined epithelial basal lamina and regular distribution of orthogonally extending neural projections in undisturbed planulae (File S8; compare K and O).

Preferential association of cnidarian-restricted genes with embryo patterning

We used the strong correlation between DGE classes and expression patterns to assess the relationship between transcript identity and localization, using the 128 transcripts for which complete ORFs were present (Figure 10). The proportions of transcription factors and probable signaling pathway regulators were similar between DGE classes (12–21%; values not significantly different by Fisher's Exact Test). In contrast there was a significantly higher proportion of cnidarian-restricted sequences in DGE classes 1, 2 and 3 than in DGE class 4 which tend to show D-type expression profiles (around 30% vs 6%; Fisher's Exact Test p-value for this comparison = 0.04). This analysis suggests that while cnidarian-restricted developmental regulators contribute significantly to patterning at the early gastrula stage, expression of evolutionary ancient genes predominates during development of the larva following gastrulation.

Discussion

This study successfully identified many potential developmental regulators from the cnidarian experimental model *Clytia hemisphaerica* by analyzing the transcriptome of early gastrula stage embryos aboralized by Wnt3 knockdown, providing a number of new insights into the evolution of developmental patterning mechanisms. Firstly, the key role of Wnt signaling in embryo patterning was confirmed since the identified genes all displayed one of four basic expression profiles, three associated with embryo patterning (through localized expression in the oral, aboral and presumptive endoderm regions) and one with planula formation. Expression profile types could be related to differential expression sensitivity to Wnt3-MO vs Fz1-MO or Stbm-MO, allowing us to separate genes expressed along the oral–aboral axis predominantly under Wnt/b-catenin signaling regulation from genes whose expression at the early gastrula stage is affected by Fz-PCP. Secondly, the identified genes included not only members of known conserved metazoan developmental gene families, but also previously uncharacterized or understudied conserved metazoan genes, providing novel candidates for evolutionary ancient roles in directing developmental processes. Finally, a number of cnidarian-restricted genes emerged as potential developmental regulators. Roles in larval patterning and morphogenesis were confirmed by morpholino analysis for 3 such genes as well as for one that shares a domain of unknown function with bilaterians. Overall our study illustrates the power of systematic transcriptomics-based screens, coupled with functional studies, to identify developmental genes in non-bilaterians and thus to help understand metazoan evolution and diversification.

Wnt signaling and PCP direct gene expression programs in the early gastrula

Our findings confirmed the central importance of Wnt signaling in embryo patterning. The transcripts under–represented in the spherical, aboralized Wnt3-MO embryos were during normal development systematically found expressed either in the oral ectoderm or in cells that contribute to the endodermal region (defining O and IE type profiles respectively), while those from the over–represented set were detected either in the aboral ectoderm (A type profile) or generally repressed throughout the embryo at the early gastrula stage to be expressed in different patterns during planula larva formation (D type profile). The O and A type profile genes displayed sustained localized expression at the poles through gastrulation and larval development and are thus good candidates for roles in patterning along the oral-aboral axis, but may also

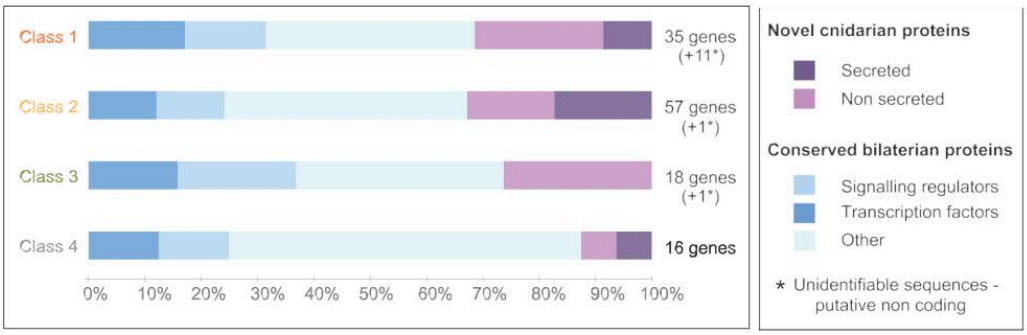

Figure 10. Conserved and cnidarian-specific genes in all DGE classes. Analysis performed on a sub-set of 126 transcript sequences in which predicted ORFs were complete at both 3′ and 5′ ends. Proportions of novel and conserved gene types, including transcription factors and signaling pathway regulators are similar in all groups except DGE class 4, which includes fewer cnidarian-specific genes.
doi:10.1371/journal.pgen.1004590.g010

include precociously expressed gene markers of larval cell types enriched at one pole.

We were intrigued to find that the four types of expression profile for Wnt3-MO-differentially expressed transcripts strongly correlated with four ''DGE classes'', distinguished by the strength of the effect of Fz1-MO on the expression of the same genes. More specifically the axially expressed transcripts tended to show less extreme changes in expression in Fz1-MO early gastrulae than did IE and D-type profile transcripts (Figure 7A). We have shown previously that Wnt/b-catenin signaling activated by Wnt3 and Fz1 is a key regulator of gene expression along the oral-aboral axis [39,40]. The relatively weak difference in expression of the axial genes in Fz1-MO relative to Wnt3-MO early gastrulae documented here could be explained, at least in part, by incomplete inhibition of this pathway by Fz1-MO compared with total extinction by Wnt3-MO, as revealed by b-catenin nuclear localization (compare Figures 3 in [39] and [40]). It is also conceivable that Wnt receptors other than Frizzleds such as RYK or ROR2 [63] could be partly responsible for mediating the Wnt3 responses in oral regions. Our Stbm-MO analyses demonstrate, however, that the main explanation for less marked changes in expression of 'axial' versus 'non-axial' genes in Fz1-MO embryos relates to the involvement of Fz1 in PCP. One aspect of this is that transient up-regulation of some oral genes and down-regulation for some aboral genes due to PCP disruption, as shown in Stbm-MO embryos[41], could in Fz-MO embryos counterbalance and dampen the effects of Wnt/b-catenin signaling. Concerning the non-axial genes the strong effects of PCP disruption could reflect direct signaling through 'non-canonical' intracellular pathways acting downstream of Fz/Dsh [64]. Given the transient nature of the effect, however, we favor the possibility that the effect is indirect, resulting from the developmental programs of the corresponding cell lineages being delayed or accelerated by a changed morphological environment. For cells of the presumptive endodermal region (IE type pattern), lack of detection at the early gastrula stage in Fz1-MO and Stbm-MO embryos could result from disruption of ingression behavior due to loss of polarity of oral ectoderm cells. Conversely the strong over-expression of the D-type profile genes at the early gastrula stage in Fz1-MO and Stbm-MO embryos suggests that epithelial PCP may have a significant effect in delaying the development of certain planula cell types. One attractive possibility is that Fz-PCP disruption affects apical-basal polarity of epithelial cells and thus the generation of new cell types through oriented asymmetric divisions, as has been recently demonstrated in *Xenopus* embryos [65]. Consistent with this hypothesis, cells expressing Botch1, bZip and Amt became prominent in basal regions of the epithelial ectoderm of early gastrulae when PCP was disrupted directly using Stbm-MO or Fz1-MO (Figure 8), or disturbed indirectly in the Wnt3-MO context [41](Figure 6). Furthermore several other D type profile transcripts (HD02, UNC, WegD2 and possibly also Notch and Botch2) also tended to be expressed in basal regions of the ectodermal and/or endodermal epithelia during planula development (Figure 3).

Conserved metazoan developmental regulators in cnidarian embryogenesis

Our study provides further support for the well-known idea that a common set of transcription factors diversified from a common cnidarian-bilaterian ancestor has retained roles in regulating development in individual evolutionary lineages, with some families diversifying functions following lineage-specific gene duplications[4–6,9]. *Clytia* orthologs of many of known developmental regulator genes were identified from our unbiased screen based on sensitivity to Wnt/Fz signaling. All those tested showed characteristic spatiotemporally restricted expression profiles, and for four examples from well-known transcription factor families, roles in developmental regulation were supported by functional studies based on morpholino injection. Analysis of the morphant phenotypes suggested that the two *Clytia Brachury* paralogs Bra1 and Bra2, expressed at the oral pole throughout larval development, both play important roles in controlling the progression of gastrulation. Expression around the blastopore has been proposed to be an ancestral metazoan characteristic of *Brachury*, which during bilaterian evolution became involved in the specification of various mesoderm and endoderm fates from these tissues [66] but with the ancestral role likely to have been in regulating morphogenetic movements [67]. In *Clytia*, although there is no blastopore, the relationship with the gastrulation initiation site is conserved, and our morpholino results suggest that morphogenetic movements upstream of endoderm specification are affected. The *Hydra Bra1* and *Bra2* orthologs have been shown to have subtly distinct roles in endoderm and ectoderm layers of the budding polyp [11], suggesting that while embryogenesis roles for these genes overlap, their functions at other life cycle stages have diverged. A morpholino targeting FoxQ2c, expressed in the developing endodermal region during planula formation, caused severe defects in the organization of the endodermal layer. As with *Brachyury*, gene duplications have expanded the *FoxQ2* gene family in Cnidaria, and in this case the paralogs have adopted clearly distinct expression profiles, FoxQ2a having conserved the likely ancestral aboral (anti-blastoporal) expression [68] while FoxQ2b is only expressed in oocytes [15]. The final member of a known developmental transcriptional regulator gene family we tested functionally was HD02, a non-Hox member of the Antp homeodomain family [16], expressed particularly strongly in cells at the base of the ectoderm and endoderm layers during larval development (Figure 2P). The phenotypes following morpholino injections suggest that HD02 is involved directly or indirectly in regulating development of the neural network that develops at this site [69], perhaps dependent on the correct organization of the basal lamina. Further in depth studies will be required to explore this possibility, as well as to confirm and understand fully all the other morpholino phenotypes documented here.

On the basis of expression patterns it is likely that several other transcription factor genes identified in this study have developmental functions conserved through metazoan evolution. For example FoxA and FoxC are associated with distinct cell populations contributing to the endoderm region during gastrulation, as has also been reported for their *Nematostella* orthologs expressed in distinct regions of the developing pharynx [12,70]. In bilaterian species orthologs of these Fox genes are associated with development of endoderm/axial mesoderm and mesoderm respectively [71–74].

As well as transcription factors from families such as T-box, Fox and Antp, our transcriptome comparison identified likely regulators of a variety of intercellular signaling pathways including Notch, FGF, TGFb and Ras-MAPkinase. These included core components (ligands, receptors and secreted antagonists), but also less well known regulators acting in ligand or receptor processing and/or extracellular interactions, such as the Botch, Sulf and Notum proteins. Most strikingly we identified *Clytia* orthologs of known Wnt pathway regulators acting at all levels: Wnt ligands (WntX1A), receptors (Fz3, Fz2), members of three of the five families of secreted antagonists known from bilaterian models (Dkk1/2/4; Dan1; two sFRPs) [52,75], MESD which specifically

interferes with ligand co-receptor LRP5/6 [58,59], an ortholog of the intracellular negative regulator Naked Cuticle [56], and also the two Notum family lipases and Sulf. Sulf enzymes act on cell surface Heparan Sulphate Proteoglycans and have been reported to modulate Wnt as well as Hedgehog, TGFb and FGF signaling while Notum releases the GPI anchor of glycipans such as Dally [76–79]. The oral expression profile of all the positive Wnt pathway regulators from this and our previous study (five Wnt ligands, Axin and TCF) reinforces the notion that an active Wnt signaling source is maintained at the cnidarian embryo and larval oral pole [40,42,80] as it is at the equivalent 'head organizer'' site in the *Hydra* polyp [81–83]. Co-expression of orally expressed putative pathway inhibitors such as *Clytia* NotumO is consistent with a role in limiting the extent of Wnt activity, equivalent to its action in *Drosophila* imaginal discs [76] or during planarian head regeneration [84]. Most of the putative Wnt antagonists we identified, however, were expressed aborally in the gastrula and in aboral pole subdomains in the planula (demonstrated by *in situ* hybridization for Dkk1/2/4, Dan1, sFRP-A and NotumA, implied by DGE responses for sFRP-B and MESD), suggesting that Wnt signaling is inhibited actively at the aboral pole region in the larva. Future functional studies will be required to examine the functions of each Wnt regulator during *Clytia* development, and to unravel the interactions between them.

New candidate developmental regulators of potentially wide interest

Our study uncovered many potential developmental regulators amongst gene families with orthologs and/or shared domains identifiable from the mass of available genomic and transcriptomic data across bilaterian species, but for which nothing is known about function or expression. These include zinc finger and helix-loop-helix domain transcription factors as well as putative novel signaling pathway components. The prominence of cell surface protein modifiers with known impact on one or several signaling pathways in our screen raises the possibility that some of the other uncharacterized conserved or cell surface proteins may function similarly. In this context it would be interesting, for example, to test the function of the ZpdA and Aat genes, which code for a likely cell surface glycoprotein and a membrane transport protein respectively. Uncovering developmental roles for such proteins in *Clytia* would open the way to explore the involvement of potential novel regulators of key embryonic and cellular processes in bilaterians, and the associated evolutionary and medical implications. WegA1 offers an interesting illustration of this possibility. WegA1-MO injection results in a spectacular developmental defect involving premature cell ingression (a process of epithelial-mesenchymal transition) at gastrulation, and a massive shift in the balance of ectoderm to endoderm formation. This finding implies that this previously unknown protein functions during normal development under the control of Wnt/b-catenin and PCP signaling to inhibit cell ingression in aboral territories. As well as the 135-amino acid, C-terminal DUF3504 domain the WegA1 sequence contains a putative nuclear localization signal. Whether it has true orthologs in bilaterians remains to be established.

Cnidarian restricted genes

Amongst the potential developmental regulators identified in our study, 29% were defined as cnidarian-restricted on the basis that they had no identifiable orthologs in any other metazoans. Previous surveys of available cnidarian genomic and transcriptomic data revealed about 25% in *Clytia* and 15% in the 'polyp only' cnidarian models *Nematostella* and *Hydra* [4,14,18,23]. A few of these match genes previously known only outside Metazoa, and so represent ancient genes lost in bilaterian branches or gained by lateral gene transfer, while the others probably represent cnidarian innovations. Although more in depth studies of each gene are required, the characteristic phenotypes observed in our morpholino experiments support the stereotypical expression pattern data in suggesting roles in regulating developmental processes for these cnidarian-restricted genes: larval oral pole organisation for WegO1, endoderm formation for WegIE2 and epithelial organization for WegD1 respectively.

More than half of the cnidarian-restricted transcripts identified in our study contained secretion signal sequences. These are prime candidates for roles in cell-cell signaling, either as ligands or as modulators of ligand/cell surface/receptor interactions during axis establishment and gastrulation. Candidate receptors for such signaling molecules include the many unclassified 7tm receptors identified particularly amongst IE profile/DGE class 2 transcripts. With notable exceptions such as Frizzled and Patched, members of the 7tm superfamily, including the G–protein coupled receptors (GPCRs), have not been strongly implicated in developmental regulation in bilaterians. This family has expanded independently in cnidarians [14], so its exploitation for developmental signaling might represent a cnidarian specialty, a fascinating possibility to explore in future studies.

Intriguingly, almost all (35/37) of the cnidarian-restricted genes we identified belonged to the three DGE classes associated with regional expression and thus embryo patterning at the gastrula stage (Figure 10). Conversely, the DGE Class 4 transcript set contained a higher proportion of broadly conserved ''ancient'' genes. Recent studies have demonstrated that the extensive variation in modes of early embryogenesis between species correlates with expression of evolutionarily ''newer'' genes, while subsequent 'phylotypic stages' (corresponding to neurula and somatogenic stages in vertebrates and the germ-band segmentation stage in insects) are strongly conserved at the phylum level and tend to express more ancient genes [85,86]. With the caveat that our analysis concerns only a small fraction of the transcriptome and provides only limited coverage of developmental stages, the observation that most (28/35) of the DGE class 1–3 (putative patterning) genes lacked counterparts in *Nematostella* or *Hydra* may reflect the widely divergent modes of early embryo patterning and gastrulation amongst cnidarian species [87]. In contrast several of the DGE class 4 genes, mostly ''ancient'', appeared to be associated with epithelia development and in particular with formation of the basal lamina, a structure considered to be a major innovation in the animal lineage [88,89] and highly conserved in all Eumetazoa. A temporal shift in expression from ''new'' to ''old'' genes between gastrula and larva in cnidarian species is consistent with the idea that the epitheliarized, planula stage-ciliated torpedo larva represents the phylotypic stage [90].

To conclude, from a methodological standpoint, our study demonstrates the power of rigorous unbiased transcriptomic approaches to obtain a fresh view of gene conservation and innovation in the evolution of animal diversity. It also illustrates how transcriptome comparisons can allow prediction of expression characteristics without doing large-scale *in situ* hybridization screens; The differential transcriptional responses in Fz1-MO and Stbm-MO embryos will be very useful for picking candidate genes for future studies targeted to particular developmental processes. From a theoretical standpoint, our findings provide strong support for the notion that many evolutionary-conserved genes are deployed across eumetazoans to regulate development, but also good evidence that developmental regulation in cnidarians may involve a significant number of taxon-restricted genes. Functional

studies of the genes identified here in *Clytia* should provide a fruitful entry for exploring both these possibilities.

Materials and Methods

Embryo manipulation, culture and harvesting

Eggs obtained by light-induced spawning of laboratory-raised medusae were microinjected with morpholino oligonucleotides prior to fertilization as described [39]. Previously unpublished morpholino sequences are provided in File S7. Use of genetically identical female medusae derived from a single individual laboratory polyp colony Z^4B and males from a closely related colony [32] restricted the problems of sequence polymorphism. After culture at 18uC to the four cell stage, any unfertilized or abnormally-dividing embryos were removed. Early gastrula stage embryos, used for RNA extraction or fixed for *in situ* hybridization or confocal microscopy, were obtained after culture at 16uC overnight (17 hours). Planulae were fixed for *in situ* hybridization after 24 or 48 hours of culture at 18uC. Particular care was taken to use identical timing and temperature regimes for all experiments.

DGE analysis

For each experimental condition, total RNA was extracted from batches of 900–1400 early gastrula stage embryos using RNAqueous kit (Life Technologies/Ambion, CA). RNA integrity was confirmed by formaldehyde gel electrophoresis. Two independent biological replicates were performed for the uninjected and Wnt3-MO conditions, and single samples for the other morpholino conditions. Estimated final embryo numbers in each sample, after removal of any showing arrested cleavage or irregular development, were as follows: Uninjected: each 1900; Wnt3-MO: each 2300, Fz1-MO: 900, Fz3-MO: 1600 and Stbm: 1400. Library construction and Illumina short-read (51 bp) sequencing was performed by GATC (Konstanz, Germany).

To quantify gene expression, the number of mapped reads onto a reference transcriptome data set was taken as a measure of transcript level. The reference transcriptome, comprising 24893 distinct (non-overlapping) assembled sequences, was built by combining, using CAP3 software, previous EST data [15,32] and Illumina sequences from one of the untreated early gastrula samples generated in this study. Redundant sequence entries were eliminated by USEARCH (ver. 5.2.32_i86linux32). The longest predicted ORF from each sequence was used as the reference for read mapping. To reduce polymorphism, adaptator sequences and probable 59 UTR sequences upstream of the first ATG in each cDNA contig were removed,

For each experimental condition approximately 80 million of 51pb Illumina reads were mapped on the reference transcriptome using the Bowtie command, with tolerance of two mismatches. Reads that matched to more than one reference sequence were not taken into account. Around 35% of the reads obtained for each condition could be mapped using this method. Statistical analysis was performed using the DEGseq R package [50] to determine for each transcript whether the observed ratio of transcript levels (M) between two samples is significant given the global average expression (A). The Random Sampling Model employed assumes a normal distribution for $\log_2(C)$, where C is the number of counts, as confirmed for our data by a Q-Q plot (Figure 1B). $M = \log_2(C\ sample1) - \log_2(C\ sample2)$ estimates the difference of expression between the conditions; $A = (\log_2(C\ sample1) + \log_2(C\ sample2))/2$ measures the average expression in the two conditions. A p-value was generated for each gene to determine whether the expression difference between samples was significant. A z-score was generated for each transcript, as a measure of the deviation from the random model (z-score = (Mobserved – Mexpected according to random sampling model)/Var(M expected according to random model). The MATR method used an estimation of the variation between duplicate embryo samples (calculated using the CTR method) to generate a second MA plot and to adjusts the z-score accordingly.

Gene sequence analysis

A R-script was devised to analyze automatically the six possible reading frames of each unique assembled transcript sequence and to predict the best ORF (''find. ORF'' script downloadable at http://octopus.obs-vlfr.fr/R_scripts). Sequence comparisons were performed with both BLASTx with the whole sequence and BLASTp with predicted translated ORF against the '''non-redundant''' (nr) NCBI database. Domain analyses (Files S1 and S3) were performed using Interproscan, SignalP for the detection of secreted peptide signals and TMHMM for the prediction of transmembrane domains. Gene identities (column 3 of File S1) were based on BLAST and domain analyses. Gene accession numbers are provided in File S1 and File S3.

Orthology analysis

To determine orthology of the transcript sequences studied in detail (Table 1) we searched for homologs by reciprocal BLASTp. When reciprocal blast and domain analysis (see above) gave unambiguous identities (non-multigene families), gene names were attributed directly (Sulf, Aat, Asparaginase, Amt, UCP). For certain multigenic developmental regulator families, we added our candidate sequence and the retrieved cnidarian sequences to alignments from previously published studies kindly provided by authors (see File S2 and acknowledgements). Where no existing appropriate alignments were available, sequences from a range of eumetazoan genomes (*Drosophila melanogaster, Lottia giganta, Strongylocentrotus purpuratus, Xenopus laevis or Homo sapiens, H. magnipapillata and N. vectensis*) were aligned using MUSCLE, the best fitting model of evolution was determined using ProtTest2.4, and phylogenetic analysis performed using PhyML3.0. The trees are available in File S2.

In cases where clear *Hydra magnipapillata* orthologs were identified, further analysis was performed using the *Hydra vulgaris* transcript dataset (HAEP) available at http://compagen.zoologie.uni-kiel.de/blast.html) [91]. The number of matching reads recorded in each separated cell population (endoderm, ectoderm and *nanos*-positive cells) was normalized with respect to total read number (File S5).

For cnidarian-specific sequences, WegO1, WegO2, WegIE2, WegA2, WegD2, Zpd, had no recognisable homologs in *Hydra* or in *Nematostella* genomes. For WegIE1, WegD1 we identified single orthologs in Hydra: (listed in File S5).

Gene cloning and probe synthesis

In situ hybridization probes were synthesized from cDNA clones corresponding to our EST collection when available. For the remaining sequences, cDNAs were cloned by PCR using the TOPO-TA cloning kit (Invitrogen). All sequences were verified before probe synthesis. DIG-labeled antisense RNA probes for *in situ* hybridization were synthesized using Promega T3/T7/Sp6 RNA polymerases, purified using ProbeQuant G-50 Micro Columns (GE Healthcare) and taken up in 100 ml of 50% formamide.

In situ hybridization

Gastrulae, 24hpf and 48hpf planula larvae were fixed in 3.7% formaldehyde/0.2% glutaraldehyde in PBS for 2 hours on ice, washed five times in PBST (PBS containing 0.1% Tween 20) for 10 minutes, dehydrated in PBST/50% methanol and stored in methanol at 220uC. *In situ* hybridization was performed using the InsituPro robot (Intavis). After rehydratation in PBST/50% methanol and three 5 minute washes in PBST, samples were transferred to the plate. The robot program was as follows: two 20 min washes in PBST; 20 min in PBST/50% hybridization buffer (5X SSC, 50% deionized formamide, 1% dextran sulfate, 1% SDS, 50 mg/ml tRNA, 50 mg/ml heparin); 20 min in hybridization buffer; 2 hours pre-hybridization in hybridization buffer at 62uC; 40 to 63 hours hybridization at 62uC with the denatured DIG-labelled RNA probe; four 30 min washes in 5X SSC, 0.1% Tween 20 and 50% formamide at 62uC; four 30 min washes in 2X SSC, 0.1% Tween 20 and 50% formamide at 62uC; two 20 min washes in 2X SSC, 0.1% Tween 20 at 62uC; two 20 min equilibration steps in MABT (100 mM maleic acid pH 7.5, 150 mM NaCl, 0.1% Triton X-100); 1 hour blocking in MABT/1% blocking reagent (Roche); 3 hours incubation with an alkaline phosphatase labeled anti-DIG antibody diluted 1/2000 in the blocking solution; seven 20 min washes in MABT; three 20 min washes in TMNT (100 mM Tris-HCl pH 9.4, 50 mM $MgCl_2$, 100 mM NaCl and 0.1% Tween 20). The color reaction was performed manually in TMNT containing 0.08 mg/ml NBT and 0.1 mg/ml BCIP (Promega). Color development time varied from 1 hour to 1 day. Samples were then washed twice in water, three times in PBS, post-fixed in PBS/3.7% formaldehyde and washed three times with PBST before mounting in 40% glycerol.

Gene function analysis and microscopy

For the selected candidate genes we addressed phenotype specificity by designing and testing several morpholinos targeting different parts of the sequence, discarding any that proved toxic to cell division during pre-gastrula development. We could only identify 1 non-toxic morpholino targeting FoxQ2c and WegA1, and none for FoxQ2a. For Bra2 one morpholino targeted the predicted AUG translation initiation codon and the other an exon-intron junction (all details in File S7). For each morpholino we first injected a range of concentrations into eggs prior to fertilization, and then assessed planula morphology for the lowest non-toxic dose at 24 h and 48 h. The cellular basis of the observed phenotypes was then further assessed by confocal microscopy. Images of *in situ* hybridization profiles and DIC images of live embryos were acquired on an Olympus BX51 microscope. For confocal imaging of cell boundaries using fluorescent phalloidins and nuclei using Hoechst 33358 or TOPRO-3 dyes, embryos were fixed, processed and imaged on a Leica SP5 microscope as described previously [39]. Microtubules were stained by immunofluorescence using anti-a tubulin rat monoclonal antibody YL1/2 (Sigma) followed by rhodamine-conjugated anti-rat Ig antibodies (Jackson Immunoresearch).

Quantitative RT-PCR

Total RNA from 60 Wnt3-MO injected and 60 non-injected early gastrulae was extracted using RNAqueous-Micro kit according to the manufacturer's instructions (Ambion, Warrington, UK). Genomic DNA was removed by a DNAse I treatment (Ambion) and this step was controlled for each RNA extract. First-strand cDNA was synthesized using 500 ng of total RNA, Random Hexamer Primers and Transcriptor Reverse Transcriptase (Roche Applied Science, Indianapolis, USA). Quantitative PCRs were run in quadruplicate and EF-1alpha used as the reference control gene. Each PCR contained 5 ml cDNA 1/400, 10 ml SYBR Green I Master Mix (Roche Applied Science), and 200 nM of each gene-specific primer, in a 20 ml final volume. PCR reactions were run in 96-well plates, in a LightCycler 480 (Roche Applied Science). Sequences of forward and reverse primers designed for each gene: EF-1alpha-F 59 TGCTGTTGTCCCAATCTCTG 39; EF-1alpha-R 59 AAGACGGAGTGGTTTGGATG 39; Bra-F 59 GCAACACCCACAACAACAAC 39; Bra-R 59 TACGGGAAACATACGCCTTC 39; NotumO-F 59 GGGACATCTAAAACCCATGC 39; NotumO-R 59 CATGGATCTCGCATTGTGAC 39; ZnfO-F 59 TGCTGCTAACAACGACCAAC 39; ZnfO-R 59 TGGTGGAAGTGGAGATTGTG 39; Mos3-F 59 ATCTTACGTCCCGAACAACG 39; mos3-R 59 ATCCACCAATGGCAGCTTAC 39; Znf845-F 59 AGACCGACAGCATTTCATCC 39; Znf845-R 59 TGGCATTCCTTGCATACCTC 39; Dkk1/2/4-F 59 GGGCTTGTTCGTACTTTTCC 39; Dkk1/2/4-R 59 ATTCCATCCCACGACAACAC 39; ZnfA-F 59 CAACAACTTTCACCGAGCTG 39; ZnfA-R 59 TGTCTCTTGTGTTGCCAAGC 39; Dan1-F 59 CATGCCCGTTCATGAGAAAG 39; Dan1-R 59TTTTGGCTGTTCCCACTGTC 39; NotumA-F 59 TGCTGAAGGGTCGTACATTG 39; NotumA-R 59 CGTGTGTCCATTTTCAGTGC 39; HD02-F 59 TT AACAGCCCACCGAAACTC 39; HD02-R 59 CGTCGTGTTTTTCAGTGACG 39.

For each gene studied an expression level N was calculated as 2^{2Ct}, where Ct (Cycle threshold) represents the number of cycles required for the fluorescent signal to cross the threshold.

Supporting Information

File S1 Primary list of transcripts differentially expressed in Wnt3-MO compared to non-injected embryos identified by DGE (z-score cutoff of +/2 5.0), with putative identities, domain analysis, z-scores calculated for three MO–injected embryo conditions, accession numbers and DGE classes assigned in relation to Wnt3-MO and Fz1-MO responses (see text).
(XLS)

File S2 Phylogenetic analyses (using PhyML) to determine the orthology of the *Clytia* sequences studied in detail in this study : Antp family (HD02, Six4/5 and Gsc) ; T-box family (Tbx, Bra1, Bra2); Pax Family (PaxA), Notum family (NotumA, NotumO); Botch Family (Botch1 and Botch2); Dkk; DMRT-E; Forkhead family (FoxA, FoxC, FoxQ2a, FoxQ2b, FoxQ2c,); Frizzled/sFRP family (sFRP-A, sFRP-B, Fz1, Fz2, Fz3, Fz4); Dan family (Dan1); Hlh family (HlhIE1; HlhIE2); Mos family (Mos1, Mos2, Mos3); Erg; Myb; Znf subfamilies for ZnfO, ZnfA and Znf845. For bZip, Asp, Amt, Sulf, phylogenetic analysis was not performed since only one *Clytia* homolog was found. *Hydra* orthologs are provided in File S5. Note that only the *Clytia* genes featured in this study were included, not other related *Clytia* sequences. See Materials and Methods for details of the datasets used.
(DOC)

File S3 Secondary list of differentially expressed sequences in Wnt3-MO compared to non-injected embryos identified by DGE with z-scores outside the +/2 5.0 cutoff but greater than +3.3/less than 23.3.
(XLS)

File S4 Expression patterns of additional selected transcripts. *In situ* hybridization profiles for FoxQ2c (A); NotumO (B); WegO3 (C); Gooseco¨ıd (D); sFRP-A (E) and Tbx (F). FoxQ2c shows an IE-type pattern, NotumO, WegO3 and Gooseco¨ıd show O-type patterns, sFRP-A and Tbx show A-type patterns. The correlation

with DGE responses holds in all cases (see Table 1). Scale bars and panel organization as in Figures 2 and 3.
(TIF)

File S5 *Hydra* orthologs of the *Clytia* gene analyses from genomic and transcriptomic data, along with information where available on differential expression between *Hydra* tissues [25]. Orthology was confirmed by phylogenetic (PhyML) analysis of sets of closely related sequences from cnidarians.
(XLS)

File S6 *In situ* hybridization analysis of selected D-type pattern transcripts in untreated (left panels) and Wnt3-MO injected (right panels) early gastrulae. A: ZpdA transcripts; B: Botch2 transcripts, C: Asp transcripts. Cells with high expression on the blastocoelar face of the ectoderm were discernible (narrows). All control embryos are oriented with the oral pole uppermost. Gene identity is shown in the bottom right of each pair of panels. Scale bar 50 mm.
(EPS)

File S7 Details of all previously unpublished morpholinos used in this study, including injection doses and sequences.
(XLS)

File S8 Confocal images of control and morpholino embryos fixed after about 48 hpf and phalloidin stained for the visualisation of cell contours (A-H, L, M, P-R) or anti-tubulin immunofluorescence (red) and nuclear staining with Hoechst or TOPRO-3 dyes (blue) (I-K, N, O, S). Endogenously expressed GFP-1 [92] provided a marker of the planula ectoderm (green in P, T, U). Oral poles are at the top in all images. Uninjected planula larvae (A) showed well-defined, epithelialized ectoderm and endodermal layers. WegO1 (B), Bra1 (C) and Bra2 (D) showed deficits of endoderm with regions of empty blastocoel still found (asterisks) as well as residual ectodermal cells accumulating towards the aboral pole (white arrowheads). This defect was much less severe in WegO1-MO embryos. FoxQ2c-MO (E) and WegIE2-MO (F) embryos showed severely disrupted endodermal layers (black arrows). WegA1-MO injection generated aggregates of endodermal-like cells of variable sizes covered in some (G, I) but not all (H) cases by a thin layer of ectodermal cells. HD02-MO (L-P) and WegD1-MO (Q-T) embryos had severely disrupted morphology characterized by a disruption of the basal lamina between the endoderm and GFP-expressing ectoderm layers (white arrows in P and T; compare with the uninjected planula in U). The WegD1-MO embryos were filled with disorganized cell sheets and lacked the central stripe of cell destruction characteristic of normal endodermal cavity formation. Anti-tubulin staining revealed disorganized bundles of neurite-like processes in the ectoderm-endoderm interface in HD02-MO embryos contrasting with the more orderly organization in uninjected embryos (pink arrows in confocal images in O and K respectively, acquired at this level) and the lack of this layer in WegD1-MO embryos (S). Scale bar 50 mm.
(TIF)

Acknowledgments

We thank C. Fourrage and A. Charlet for their participation in some experiments, and L. Lecle're, R. Copley and M. Manuel for constructive criticism of the manuscript. PL also thanks L. & X Wang for advice on changing graphic settings in the DEGseq Package, L. Lecle're and F. Gyoja for providing alignments and sequences. We thank the Observatoire de la Co^te d'Azur for use of their calculation capacity.

Author Contributions

Conceived and designed the experiments: TM EH PL. Performed the experiments: PL AR SC CB PC EH TM PD. Analyzed the data: PL EH AR CB PD. Wrote the paper: PL TM CB EH.

References

1. Duboule D, Wilkins AS (1998) The evolution of 'bricolage'. Trends Genet 14: 54–59.
2. Pires-daSilva A, Sommer RJ (2003) The evolution of signalling pathways in animal development. Nat Rev Genet 4: 39–49. doi:10.1038/nrg977.
3. Carroll SB (2008) Evo-devo and an expanding evolutionary synthesis: a genetic theory of morphological evolution. Cell 134: 25–36. doi:10.1016/j.cell.2008.06.030.
4. Technau U, Rudd S, Maxwell P, Gordon PMK, Saina M, et al. (2005) Maintenance of ancestral complexity and non-metazoan genes in two basal cnidarians. Trends Genet 21: 633–639. doi:10.1016/j.tig.2005.09.007.
5. Miller DJ, Ball EE, Technau U (2005) Cnidarians and ancestral genetic complexity in the animal kingdom. Trends in Genetics 21: 536–539. doi:10.1016/j.tig.2005.08.001.
6. Degnan BM, Vervoort M, Larroux C, Richards GS (2009) Early evolution of metazoan transcription factors. Current Opinion in Genetics & Development 19: 591–599. doi:10.1016/j.gde.2009.09.008.
7. Putnam NH, Srivastava M, Hellsten U, Dirks B, Chapman J, et al. (2007) Sea Anemone Genome Reveals Ancestral Eumetazoan Gene Repertoire and Genomic Organization. Science 317: 86–94. doi:10.1126/science.1139158.
8. Chapman JA, Kirkness EF, Simakov O, Hampson SE, Mitros T, et al. (2010) The dynamic genome of Hydra. Nature 464: 592–596. doi:10.1038/nature08830.
9. Larroux C, Luke GN, Koopman P, Rokhsar DS, Shimeld SM, et al. (2008) Genesis and Expansion of Metazoan Transcription Factor Gene Classes. Molecular Biology and Evolution 25: 980–996. doi:10.1093/molbev/msn047.
10. Hoshiyama D, Suga H, Iwabe N, Koyanagi M (1998) Sponge Pax cDNA related to Pax-2/5/8 and ancient gene duplications in the Pax family. J Mol Evol 47: 640–648. doi:10.1007/PL00006421.
11. Bielen H, Oberleitner S, Marcellini S, Gee L, Lemaire P, et al. (2007) Divergent functions of two ancient Hydra Brachyury paralogues suggest specific roles for their C-terminal domains in tissue fate induction. Development 134:4187–4197. doi:10.1242/dev.010173.
12. Magie CR, Pang K, Martindale MQ (2005) Genomic inventory and expression of Sox and Fox genes in the cnidarian Nematostella vectensis. Dev Genes Evol 215: 618–630. doi:10.1007/s00427-005-0022-y.
13. Ryan JF, Burton PM, Mazza ME, Kwong GK, Mullikin JC, et al. (2006) The cnidarian-bilaterian ancestor possessed at least 56 homeoboxes: evidence from the starlet sea anemone, Nematostella vectensis. Genome Biol 7: R64. doi:10.1186/gb-2006-7-7-R64.
14. Fore^t S, Knack B, Houliston E, Momose T, Manuel M, et al. (2010) New tricks with old genes: the genetic bases of novel cnidarian traits. Trends Genet 26: 154–158. doi:10.1016/j.tig.2010.01.003.
15. Chevalier S, Martin A, Lecle're L, Amiel A, Houliston E (2006) Polarised expression of FoxB and FoxQ2 genes during development of the hydrozoan Clytia hemisphaerica. Dev Genes Evol 216: 709–720. doi:10.1007/s00427-006-0103-6.
16. Chiori R, Jager M, Denker E, Wincker P, Da Silva C, et al. (2009) Are Hox Genes Ancestrally Involved in Axial Patterning? Evidence from the Hydrozoan Clytia hemisphaerica (Cnidaria). PLoS ONE 4: e4231. doi:10.1371/journal.pone.0004231.s003.
17. Jager M, Que'innec E, Le Guyader H, Manuel M (2011) Multiple Sox genes are expressed in stem cells or in differentiating neuro-sensory cells in the hydrozoan Clytia hemisphaerica. Evodevo 2: 12. doi:10.1186/2041-9139-2-12.
18. Khalturin K, Hemmrich G, Fraune S, Augustin R, Bosch TCG (2009) More than just orphans: are taxonomically-restricted genes important in evolution? Trends in Genetics 25: 404–413. doi:10.1016/j.tig.2009.07.006.
19. Domazet-Los^o T, Tautz D (2003) An evolutionary analysis of orphan genes in Drosophila. Genome Res 13: 2213–2219. doi:10.1101/gr.1311003.
20. Tautz D, Domazet-Los^o T (2011) The evolutionary origin of orphan genes. Nat Rev Genet 12: 692–702. doi:10.1038/nrg3053.
21. Neme R, Tautz D (2013) Phylogenetic patterns of emergence of new genes support a model of frequent de novo evolution. BMC Genomics 14: 117. doi:10.1186/1471-2164-14-117.
22. Steele RE (2012) The Hydra genome: insights, puzzles and opportunities for Developmental Biologists. Int J Dev Biol 56: 535–542. doi:10.1387/ijdb.113462rs.
23. Steele RE, David CN, Technau U (2011) A genomic view of 500 million years of cnidarian evolution. Trends Genet 27: 7–13. doi:10.1016/j.tig.2010.10.002.
24. Hwang JS, Ohyanagi H, Hayakawa S, Osato N, Nishimiya-Fujisawa C, et al. (2007) The evolutionary emergence of cell type-specific genes inferred from the

gene expression analysis of Hydra. Proceedings of the National Academy of Sciences 104: 14735–14740. doi:10.1073/pnas.0703331104.
25. Hemmrich G, Khalturin K, Boehm A-M, Puchert M, Anton-Erxleben F, et al. (2012) Molecular signatures of the three stem cell lineages in hydra and the emergence of stem cell function at the base of multicellularity. Molecular Biology and Evolution 29: 3267–3280. doi:10.1093/molbev/mss134.
26. Milde S, Hemmrich G, Anton-Erxleben F, Khalturin K, Wittlieb J, et al. (2009) Characterization of taxonomically restricted genes in a phylum-restricted cell type. Genome Biol 10: R8. doi:10.1186/gb-2009-10-1-r8.
27. Grens A, Shimizu H, Hoffmeister SA, Bode HR, Fujisawa T (1999) The novel signal peptides, pedibin and Hym-346, lower positional value thereby enhancing foot formation in hydra. Development 126: 517–524.
28. Lohmann JU, Endl I, Bosch TC (1999) Silencing of developmental genes in Hydra. Dev Biol 214: 211–214. doi:10.1006/dbio.1999.9407.
29. Lohmann JU, Bosch TC (2000) The novel peptide HEADY specifies apical fate in a simple radially symmetric metazoan. Genes Dev 14: 2771–2777.
30. Khalturin K, Anton-Erxleben F, Sassmann S, Wittlieb J, Hemmrich G, et al. (2008) A novel gene family controls species-specific morphological traits in Hydra. PLoS Biol 6: e278. doi:10.1371/journal.pbio.0060278.
31. Genikhovich G, Kürn U, Hemmrich G, Bosch TCG (2006) Discovery of genes expressed in Hydra embryogenesis. Dev Biol 289: 466–481. doi:10.1016/j.ydbio.2005.10.028.
32. Houliston E, Momose T, Manuel M (2010) Clytia hemisphaerica: a jellyfish cousin joins the laboratory. Trends Genet 26: 159–167. doi:10.1016/j.tig.2010.01.008.
33. David CN (2012) Interstitial stem cells in Hydra: multipotency and decision-making. Int J Dev Biol 56: 489–497. doi:10.1387/ijdb.113476cd.
34. Bosch TCG, Anton-Erxleben F, Hemmrich G, Khalturin K (2010) The Hydra polyp: nothing but an active stem cell community. Dev Growth Differ 52: 15–25. doi:10.1111/j.1440-169X.2009.01143.x.
35. Martin VJ, Archer WE (1986) Migration of interstitial cells and their derivatives in a hydrozoan planula. Dev Biol 116: 486–496. doi:10.1016/0012-1606(86)90149-1.
36. Martin VJ (1990) Development of Nerve Cells in Hydrozoan Planulae: III. Some Interstitial Cells Traverse the Ganglionic Pathway in the Endoderm. Biol Bull 178: 10–20.
37. Byrum CA (2001) An Analysis of Hydrozoan Gastrulation by Unipolar Ingression. Dev Biol 240: 627–640. doi:10.1006/dbio.2001.0484.
38. Freeman G (1981) The cleavage initiation site establishes the posterior pole of the hydrozoan embryo. Wilhelm Rouxs Arch Dev Biol 190: 123–125. doi:10.1007/BF00848406.
39. Momose T, Houliston E (2007) Two oppositely localised frizzled RNAs as axis determinants in a cnidarian embryo. PLoS Biol 5: e70. doi:10.1371/journal.pbio.0050070.
40. Momose T, Derelle R, Houliston E (2008) A maternally localised Wnt ligand required for axial patterning in the cnidarian Clytia hemisphaerica. Development 135: 2105–2113. doi:10.1242/dev.021543.
41. Momose T, Kraus Y, Houliston E (2012) A conserved function for Strabismus in establishing planar cell polarity in the ciliated ectoderm during cnidarian larval development. Development 139: 4374–4382. doi:10.1242/dev.084251
42. Kusserow A, Pang K, Sturm C, Hrouda M, Lentfer J, et al. (2005) Unexpected complexity of the Wnt gene family in a sea anemone. Nature 433: 156–160. doi:10.1038/nature03158.
43. Plickert G, Jacoby V, Frank U, Mü ller WA, Mokady O (2006) Wnt signaling in hydroid development: Formation of the primary body axis in embryogenesis and its subsequent patterning. Dev Biol 298: 368–378. doi:10.1016/j.ydbio.2006.06.043.
44. Adamska M, Larroux C, Adamski M, Green K, Lovas E, et al. (2010) Structure and expression of conserved Wnt pathway components in the demosponge Amphimedon queenslandica. Evol Dev 12: 494–518. doi:10.1111/j.1525-142X.2010.00435.x.
45. Adamska M, Degnan SM, Green KM, Adamski M, Craigie A, et al. (2007) Wnt and TGF-beta expression in the sponge Amphimedon queenslandica and the origin of metazoan embryonic patterning. PLoS ONE 2: e1031. doi:10.1371/journal.pone.0001031.
46. Windsor PJ, Leys SP (2010) Wnt signaling and induction in the sponge aquiferous system: evidence for an ancient origin of the organizer. Evol Dev 12: 484–493. doi:10.1111/j.1525-142X.2010.00434.x.
47. Pang K, Ryan JF, NISC Comparative Sequencing Program, Mullikin JC, Baxevanis AD, et al. (2010) Genomic insights into Wnt signaling in an early diverging metazoan, the ctenophore Mnemiopsis leidyi. Evodevo 1: 10. doi:10.1186/2041-9139-1-10.
48. Petersen CP, Reddien PW (2011) Polarized notum Activation at Wounds Inhibits Wnt Function to Promote Planarian Head Regeneration. Science 332: 852–855. doi:10.1126/science.1202143.
49. Schneider SQ, Bowerman B (2013) Animal Development: An Ancient b-Catenin Switch? Current Biology 23: R313–R315. doi:10.1016/j.cub.2013.03.011.
50. Wang L, Feng Z, Wang X, Wang X, Zhang X (2010) DEGseq: an R package for identifying differentially expressed genes from RNA-seq data. Bioinformatics 26: 136–138. doi:10.1093/bioinformatics/btp612.
51. Parlier D, Moers V, Van Campenhout C, Preillon J, Lecle¨re L, et al. (2013) The Xenopus doublesex-related gene Dmrt5 is required for olfactory placode neurogenesis. Dev Biol 373: 39–52. doi:10.1016/j.ydbio.2012.10.003.
52. Kawano Y, Kypta R (2003) Secreted antagonists of the Wnt signalling pathway. J Cell Sci 116: 2627–2634. doi:10.1242/jcs.00623.
53. Filmus J, Capurro M, Rast J (2008) Glypicans. Genome Biol 9: 224. doi:10.1186/gb-2008-9-5-224.
54. Dhoot GK, Gustafsson MK, Ai X, Sun W, Standiford DM, et al. (2001) Regulation of Wnt signaling and embryo patterning by an extracellular sulfatase. Science 293: 1663–1666. doi:10.1126/science.293.5535.1663.
55. Chi Z, Zhang J, Tokunaga A, Harraz MM, Byrne ST, et al. (2012) Botch promotes neurogenesis by antagonizing Notch. Developmental Cell 22: 707–720. doi:10.1016/j.devcel.2012.02.011.
56. Wharton Jr KA, Zimmermann G, Rousset R, Scott MP (2001) Vertebrate Proteins Related to Drosophila Naked Cuticle Bind Dishevelled and Antagonize Wnt Signaling. Dev Biol 234: 93–106. doi:10.1006/dbio.2001.0238.
57. Van Raay TJ, Fortino NJ, Miller BW, Ma H, Lau G, et al. (2011) Naked1 antagonizes Wnt signaling by preventing nuclear accumulation of b-catenin. PLoS ONE 6: e18650. doi:10.1371/journal.pone.0018650.
58. Hsieh J-C, Lee L, Zhang L, Wefer S, Brown K, et al. (2003) Mesd encodes an LRP5/6 chaperone essential for specification of mouse embryonic polarity. Cell 112: 355–367.
59. Lin C, Lu W, Zhai L, Bethea T, Berry K, et al. (2011) Mesd is a general inhibitor of different Wnt ligands in Wnt/LRP signaling and inhibits PC-3 tumor growth in vivo. FEBS Letters 585: 3120–3125. doi:10.1016/j.febslet.2011.08.046.
60. Lecle¨re L, Jager M, Barreau C, Chang P, Le Guyader H, et al. (2012) Maternally localized germ plasm mRNAs and germ cell/stem cell formation in the cnidarian Clytia. Dev Biol 364: 236–248. doi:10.1016/j.ydbio.2012.01.018.
61. Freeman G (1981) The role of polarity in the development of the hydrozoan planula larva. Dev Genes Evol 190: 168–184. doi:10.1007/BF00867804.
62. Momose T, Schmid V (2006) Animal pole determinants define oral-aboral axis polarity and endodermal cell-fate in hydrozoan jellyfish Podocoryne carnea. Dev Biol 292: 371–380. doi:10.1016/j.ydbio.2006.01.012.
63. Angers S, Moon RT (2009) Proximal events in Wnt signal transduction. Nat Rev Mol Cell Biol 10: 468–477. doi:10.1038/nrm2717.
64. Lape¨bie P, Borchiellini C, Houliston E (2011) Dissecting the PCP pathway: one or more pathways?: Does a separate Wnt-Fz-Rho pathway drive morphogenesis? Bioessays 33: 759–768. doi:10.1002/bies.201100023.
65. Huang Y-L, Niehrs C (2014) Short Article. Developmental Cell 29: 250–257. doi:10.1016/j.devcel.2014.03.015.
66. Technau U (2001) Brachyury, the blastopore and the evolution of the mesoderm. Bioessays 23: 788–794. doi:10.1002/bies.1114.
67. Yamada A, Martindale MQ, Fukui A, Tochinai S (2010) Highly conserved functions of the Brachyury gene on morphogenetic movements: insight from the early-diverging phylum Ctenophora. Dev Biol 339: 212–222. doi:10.1016/j.ydbio.2009.12.019.
68. Sinigaglia C, Busengdal H, Lecle¨re L, Technau U, Rentzsch F (2013) The Bilaterian Head Patterning Gene six3/6 Controls Aboral Domain Development in a Cnidarian. PLoS Biol 11: e1001488. doi:10.1371/journal.pbio.1001488.s010.
69. Thomas MB, Freeman G, Martin VJ (1987) The Embryonic Origin of Neurosensory Cells and the Role of Nerve Cells in Metamorphosis in Phialidium gregarium(Cnidaria, Hydrozoa). International Journal of Invertebrate Reproduction and Development 11: 265–285. doi:10.1080/01688170.1987.10510286.
70. Fritzenwanker JH, Saina M, Technau U (2004) Analysis of forkhead and snail expression reveals epithelial–mesenchymal transitions during embryonic and larval development of Nematostella vectensis. Dev Biol 275: 389–402. doi:10.1016/j.ydbio.2004.08.014.
71. Dal-Pra S, Thisse C, Thisse B (2011) Developmental Biology. Dev Biol 350: 484–495. doi:10.1016/j.ydbio.2010.12.018.
72. Oliveri P, Walton KD, Davidson EH, McClay DR (2006) Repression of mesodermal fate by foxa, a key endoderm regulator of the sea urchin embryo. Development 133: 4173–4181. doi:10.1242/dev.02577.
73. Wotton KR, Mazet F, Shimeld SM (2008) Expression of FoxC, FoxF, FoxL1, and FoxQ1 genes in the dogfishScyliorhinus canicula defines ancient and derived roles for fox genes in vertebrate development. Dev Dyn 237: 1590–1603. doi:10.1002/dvdy.21553.
74. Koinuma S, Umesono Y, Watanabe K, Agata K (2000) Planaria FoxA (HNF3) homologue is specifically expressed in the pharynx-forming cells. Gene 259: 171–176. doi:10.1016/S0378-1119(00)00426-1.
75. Niehrs C (2006) Function and biological roles of the Dickkopf family of Wnt modulators. Oncogene 25: 7469–7481. doi:10.1038/sj.onc.1210054.
76. Gira´ldez AJ, Copley RR, Cohen SM (2002) HSPG Modification by the Secreted Enzyme Notum Shapes the Wingless Morphogen Gradient. Dev Cell 2: 667–676. doi:10.1016/S1534-5807(02)00180-6.
77. Traister A, Shi W, Filmus J (2008) Mammalian Notum induces the release of glypicans and other GPI-anchored proteins from the cell surface. Biochem J 410: 503–511. doi:10.1042/BJ20070511.
78. Flowers GP, Topczewska JM, Topczewski J (2012) A zebrafish Notum homolog specifically blocks the Wnt/b-catenin signaling pathway. Development 139: 2416–2425. doi:10.1242/dev.063206.
79. Kleinschmit A, Takemura M, Dejima K, Choi PY, Nakato H (2013) Drosophila heparan sulfate 6-O-endosulfatase Sulf1 facilitates wingless (Wg) protein degradation. Journal of Biological Chemistry 288: 5081–5089. doi:10.1074/jbc.M112.447029.
80. Marlow H, Matus DQ, Martindale MQ (2013) Ectopic activation of the canonical wnt signaling pathway affects ectodermal patterning along the primary

axis during larval development in the anthozoan Nematostella vectensis. Dev Biol 380: 324–334. doi:10.1016/j.ydbio.2013.05.022.
81. Hobmayer B, Rentzsch F, Kuhn K, Happel CM, Laue von CC, et al. (2000) WNT signalling molecules act in axis formation in the diploblastic metazoan Hydra. Nature 407: 186–189. doi:10.1038/35025063.
82. Broun M (2005) Formation of the head organizer in hydra involves the canonical Wnt pathway. Development 132: 2907–2916. doi:10.1242/dev.01848.
83. Bode HR (2012) The head organizer in Hydra. Int J Dev Biol 56: 473–478. doi:10.1387/ijdb.113448hb.
84. Petersen CP, Reddien PW (2011) Polarized notum activation at wounds inhibits Wnt function to promote planarian head regeneration. Science 332: 852–855. doi:10.1126/science.1202143.
85. Domazet-Los˘o T, Tautz D (2010) A phylogenetically based transcriptome age index mirrors ontogenetic divergence patterns. Nature 468: 815–818. Available: http://dx.doi.org/10.1038/nature09632.
86. Kalinka AT, Varga KM, Gerrard DT, Preibisch S, Corcoran DL, et al. (2010) Gene expression divergence recapitulates the developmental hourglass model. Nature 468: 811–814. Available: http://dx.doi.org/10.1038/nature09634.
87. Rodimov AA (2005) Development of Morphological Polarity in Embryogenesis of Cnidaria. Russ J Dev Biol 36: 298–303. doi:10.1007/s11174-005-0047-1.
88. Tyler S (2003) Epithelium—The Primary Building Block for Metazoan Complexity. Integr Comp Biol 43: 55–63. doi:10.1093/icb/43.1.55.
89. Leys SP, Riesgo A (2012) Epithelia, an evolutionary novelty of metazoans. J Exp Zool B Mol Dev Evol 318: 438–447. doi:10.1002/jez.b.21442.
90. Raff R (1996) The Shape of Life: Genes, Development, and the Evolution of Animal Form. University Of Chicago Press. 544 p.
91. Hemmrich G, Bosch TCG (2008) Compagen, a comparative genomics platform for early branching metazoan animals, reveals early origins of genes regulating stem-cell differentiation. Bioessays 30: 1010–1018. doi:10.1002/bies.20813.
92. Fourrage C, Swann K, Gonzalez Garcia JR, Campbell AK, Houliston E (2014) An endogenous green fluorescent protein-photoprotein pair in Clytia hemisphaerica eggs shows co-targeting to mitochondria and efficient bioluminescence energy transfer. Open Biol 4: 130206. doi:10.1098/rsob.130206.

2.3 Additional Results: Characterisation of putative novel i-cell genes under-expressed in Wnt3 morphant early gastrulae.

- *Znf845 and Mos3 are not expressed in Nanos1 and Piwi expressing i-cells*

The *Znf845* and *Mos3* genes both showed expression territories very similar to *Piwi* and *Nanos1* expression at different stages of planula development (Figure 44A). To examine whether *Znf845* and *Mos3* are expressed in multipotent i-cells I assessed the expression of these two transcripts in the medusa in the gonads, in the base of the manubrium (Leclère et al. 2012) and in tentacle bulbs (the proximal part close to the umbrella) (Denker et al. 2008) where i-cells are concentrated.

Unlike *Piwi* and *Nanos1* neither *Znf845* nor *Mos3* mRNAs could be detected in the gonads or in spawned eggs (Figure 44B). The four genes were expressed in the tentacle bulbs and in the manubrium, although their patterns were slightly different (Figure 44B).

Znf845 expression was also detected in tentacle bulbs and in the base of the manubrium, as is the case of *Mos3*. However *Znf845* expression in the tentacles bulbs was detected in two patches of cells located between endoderm and ectoderm in a similar position of *Nanos1* and *Piwi* (Figure 44B). In contrast, in the manubrium *Znf845* mRNA was detected in fewer cells than *Nanos1* and *Piwi* mRNA, localised in the ectoderm at the base of the manubrium, *Mos3* was strongly detected in the tentacle bulb ectoderm in wider domain in comparison in *Nanos1* and Piwi, and in ectodermal cells in the manubrium (Figure 44B). These expression profiles suggest that in medusa this gene is expressed in a more extensive cell population than the i-cells.

The absence of *Znf845* and *Mos3* expression in the gonads means that neither gene is expressed in all i-cells. Thus I investigated the possibility that *Znf845* and *Mos3* are expressed in i-cells, committed to a somatic fate, by co-localisation studies using either *Mos3* or *Znf845* probes in combination with *Piwi* and with the somatic early precursors (*e.g. Mcol3-4a*, *Antistasin*).

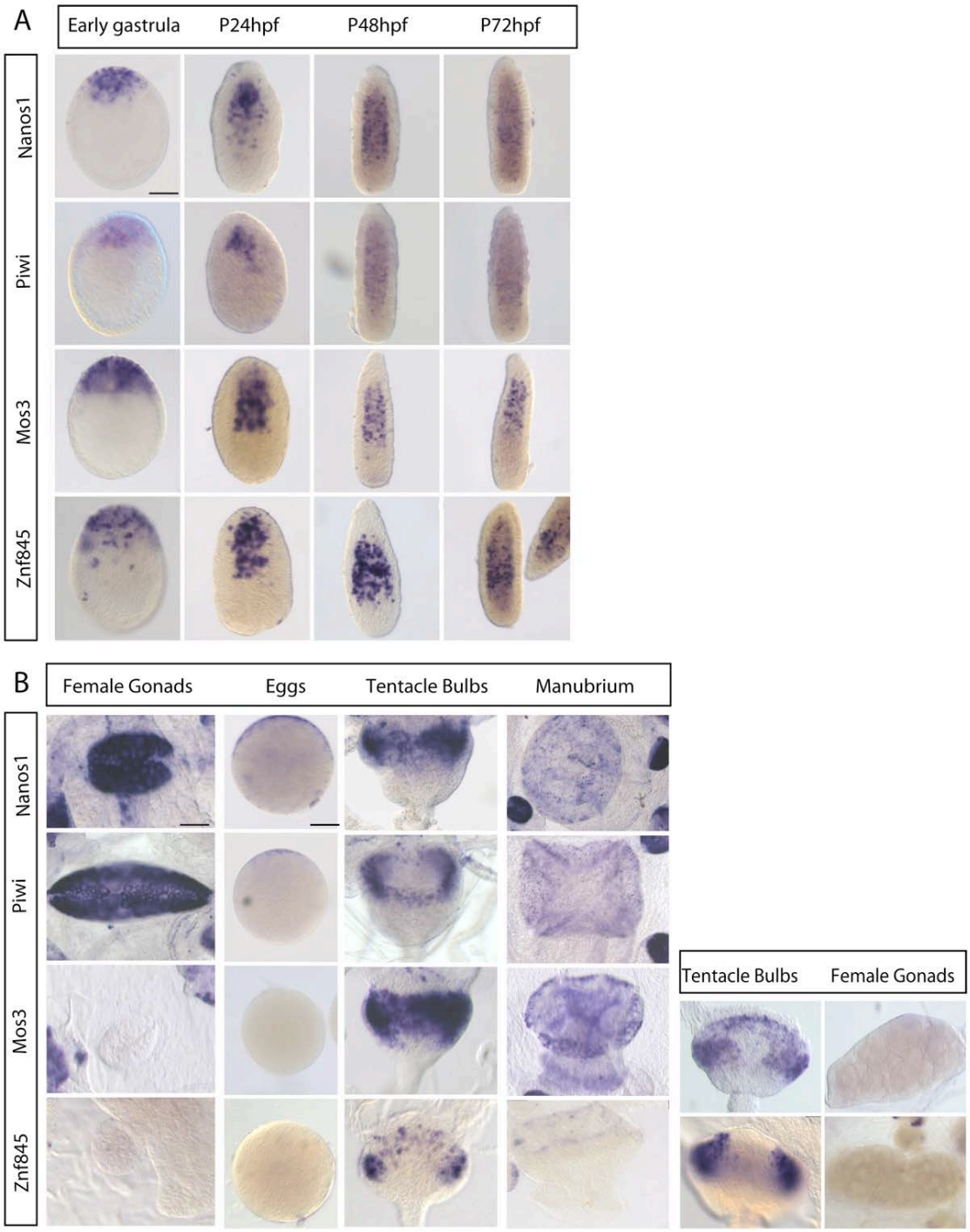

Figure 44: *Nanos1*, *Piwi*, *Mos3* and *Znf845* expression during larval development in young and in adult jellyfishes. A) Expression pattern of the four genes during embryonic development. For each gene expression pattern is shown (from left to the right): early gastrula, 24,48,72hpf. At the early gastrula stage, *Nanos*1,*Piwi*, *Znf845* and *Mos3* transcripts are detected at the oral pole in a group of ingressing cells at site of gastrulation and in the larval stages in the central endodermal region . B) Expression in the young medusa and in the unfertilised eggs. Gonads, eggs, tentacle bulbs, manubrium. *Mos3* and *Znf845* transcripts were not detected in the gonads or in the eggs. In the young and in the adult medusa (C) their expression is restricted to the tentacle bulbs and to the manubrium ectoderm. Tentacle bulbs are oriented with the proximal side on the top, base of the manubrium at the top. Scale bar 50μm.

- *Mos3 is not expressed in the same cells as Piwi*

The kinase Mos has been widely investigated for its role in oocyte development in numerous taxa. Mos is a serine–threonine protein kinase, which activates the MAPK (mitogen-activated protein kinase) pathway and regulates meiotic divisions and oocyte specific processes such as polar body formation and the "cytostatic" (CSF) cell cycle arrest of the egg awaiting fertilisation (Dupré et al. 2011).

MAPK/ERK signalling is activated in both eggs and in somatic cells where it plays a pivotal role in regulating cellular proliferation, cellular differentiation and in some circumstances apoptosis (Yoon and Seger 2006). In somatic cells the activation of this pathway depends on extracellular stimuli such as grow factors and mitogens. Growth factors such as FGF and EGF bind to transmembrane Tyrosine Kinase receptor, which in turn activates the small GTPase protein Ras. Ras recruits the MAPKKK (= Raf) to the membrane, modulating its activation. Phosphorylated (active) MAPKKK phosphorylates and activates MAPKK (=MEK), which in turn activates the MAPK (= ERK). Phosphorylated ERK in turn phosphorylates substrates in the cytosol or can translocate in the nucleus where it modulates gene expression. In the nucleus it can phosphorylate a series of transcription factors like c-Fos and Ets1/2, to control cell proliferation. Mos can be considered as the Raf counterpart in eggs, but its activation is very different; the MAPK pathway in oocytes is activated independently of growth factors and Tyrosine Kinase receptors. *Mos* mRNA is pre-synthesised during oogenesis and production of the protein is activated only when meiotic maturation is triggered. At the end of oocyte maturation Mos process accumulated in the eggs activates the MAPK signalling cascade arresting cell cycle progression until fertilisation. This so called cytostatic factor (CSF) arrest (Schmidt et al. 2006; Masui 2001) is released by the fertilisation. This egg cell cycle arrest function for Mos is very highly conserved across the animal kingdom.

Phylogenetic analysis shows that in bilaterian genomes the Mos gene is present in one copy. In cnidarians, however multiple Mos genes have been identified (Amiel et al. 2009), suggesting lineage specific duplication events. *Nematostella* has four Mos genes and *Clytia* has three copies, *Mos1, Mos2* and *Mos3*, while only one copy has been found in *Hydra*. Clytia Mos1 and Mos2 protein functions are oocyte specific and have been previously studied (Amiel et al. 2009) whereas Mos3 has been identified in our transcriptome analysis (Lapebie et al 2014) as an early-gastrula expressed gene and positively regulated by Wnt3.

Functional studies of *Clytia* Mos1 and Mos2 have shown that these kinases share most of the biological activities of their bilaterians orthologs, including a conserved role for Mos1 in CSF arrest. *Clytia Mos1* and *Mos2* mRNAs are detected in oocytes and also in spermatids. Surprisingly *Mos3* shows a completely different expression pattern. *Mos3* is not expressed in the gonads and it is expressed during larval development stage, starting for early gastrula stage. (Figure 44A-B). Moreover is transcription is regulated, directly or indirectly, by Wnt signalling (Lapebie et al 2014).

To address how *Mos3* expression relates to i-cells, I assessed *Mos3* and *Piwi* co-localisation at early gastrula stage using the double fluorescent *in situ* approach. This revealed two distinct cell populations, one expressing only *Piwi* and one expressing only *Mos3* (Figure 45). Surprisingly *Mos3* and *Piwi* transcripts were are detected in the same cell population even though their localization at oral pole is very similar (Figure 45 A-B). These observations demonstrate that *Mos3* is not expressed in *Nanos1* and *Piwi* expressing i-cell population and also suggest that it does not distinguish a subpopulation of i-cell derived-early precursor, although it remains possible that it is expressed during development of a particular somatic fate, immediately following Nanos and Piwi down regulation. To test this hypothesis co-localisation should be assessed using *Mos3* and somatic fate early precursor such as *Mcol3-4a*. To investigate the role of Mos3 I started functional studies using a Morpholino targeting Mos3. I could not observe, at any dose, any obvious phenotype, although at higher doses the organisation of the planula endoderm appeared to be disrupted. Further analysis will be required to determine if the phenotype is specific to Mos3-MO or is due to the high dose used.

To further investigate this intriguing gene, with its unexpected expression pattern in the embryo, several basic aspects need to be clarified. First of all it would be useful to determine if Mos3 kinase has "CSF" activity, assayed as the ability to cause arrest of blastomere division via the activation of the MAPK cascade by the classical assay of mRNA injection into *Xenopus* embryos, as performed previously for *Mos1* and *Mos2* (Amiel et al. 2009). It would also be interesting to verify if in Mos3 expressing cells MAPK/ERK is active by double labelling (IF-FISH) using Mos3 probe and an antibody recognising the phosphorylated (active) form of ERK, in order to see when during development the pathway becomes active.

- *Znf845 is expressed in i-cells subpopulation*

Znf845 is a conserved zinc finger domain protein. *Znf845* genes have been little studied and their role has not previously been investigated. The *Hydra Znf845* ortholog is highly expressed in *Nanos* positive cells (i-cells) and it s transcript is thus strongly represented in the i-cell population (Hemmrich et al. 2012) (Table1 Annexe).

My co-localisation studies in *Clytia* using *Znf845* probe in combination with *Piwi* probe showed that a subpopulation of *Piwi* expressing cells also expressed *Znf845,* but no cells could be identified expressing *Znf845* alone (Figure 48C-D). By quantification of a total of 5 planulae I found that around 50% of the *Piwi* positive cells also expresses *Znf845*, although the total number of cells was variable between different planula (Table 1). These observations suggest that the *Znf845* gene may be expressed in a subpopulation of i-cells committed to a somatic cell fate corresponding to half of the total *Piwi* positive population.

To narrow down the possible identity of the cells expressing Znf845, I compared its expression pattern in larval development and in the medusa to that of known i-cell derivative markers characterised in Results-I.

Among these genes, *Mcol3-4a* (nematoblast marker*)* and *Antistasin (*gland cell marker*)* showed an expression profile that resembled the *Znf845* profile in the larval and in medusa stages (see Result-I Figure 33). I thus performed co-localization experiments using the *Znf845* probe in combination with *Mcol3-4*a and *Antistasin* probes at different developmental stages.

Sample number	Znf845 alone	Piwi alone	Znf845 and Piwi % of the total	TOT
1	0	145	154 (52%)	299
2	0	129	142 (52%)	271
3	0	71	70 (50%)	140
4	0	51	44 (46%)	95
5	0	98	99 (50%)	197

Table 1: *Znf845* is expressed in about 50% of the total Piwi expressing i-cell population. Quantification performed for 5 planulae. Columns indicate the sample number, the number cells positive only for Znf845, only for Piwi and for both probes.

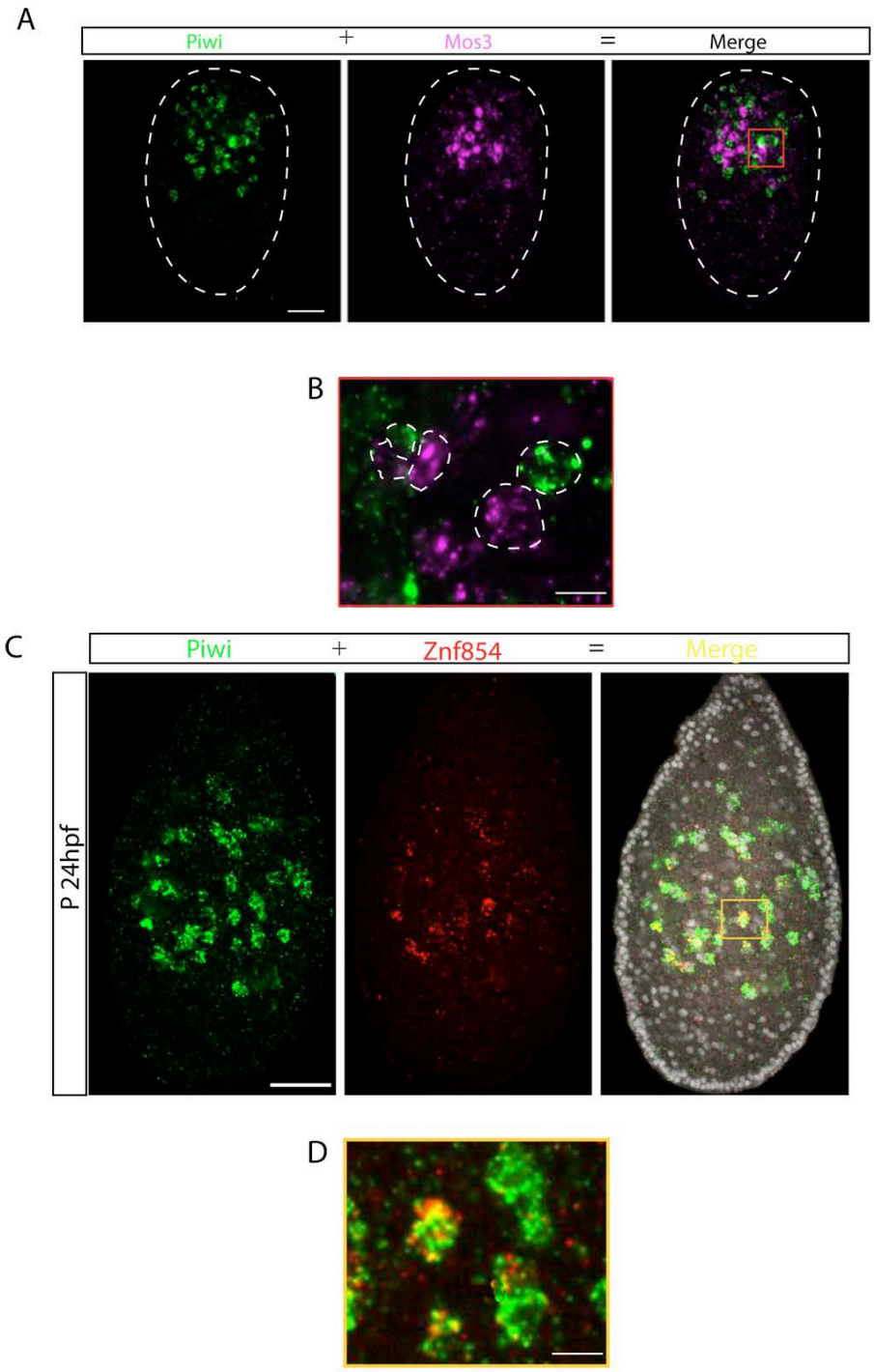

Figure 45: Co-localisation of *Piwi* with *Mos3* and *Znf845*. A) Representative confocal images of double *in situ* experiments using *Piwi* and *Mos3* probes at early gastrula stage. From left to right: *Piwi* (in red) *Mos3* (in green), last panel merged. Cell expressing both *Piwi* and *Mos3* are concentrated in ingressing cells positioned at oral pole. Scale bar 50µm. B) Detailed view of the area boxed in last panel in A. High magnification image showing that *Piwi* and *Mos3* genes are not expressed in the same cell population. Dashed line represent the contour of the early gastrula. Scale bar 10µm. **C) Representative confocal image demonstrating the co-localisation of *Piwi* (green) *Znf845* (red) in planula 24hpf.** Merged images show that *Piwi* and *Znf845* co-localise in same cells. Yellow colour in the merged image indicates co-expression. Scale bar 50µm D) Detailed view of the area boxed in last panel in C. High magnification image showing that *Piwi* and *Znf845* co-localise in some cells. Scale bar 10µm.

- *Znf845 does not co-localise with Antistasin in medusae*

Co-localisation studies were performed at the medusa stage, when *Antistasin* expression is much stronger then in the planula. As showed in Result I, *Antistasin* expression is restricted to gland cells, positioned in the manubrium endoderm, distributed along the four ridges of the mouth. *Znf845* expression in medusae was detected in the ectoderm in a few cells showing i- cell like morphology (Figure 46A). No cells expressing both probes could be identified (Figure 46C). Furthermore these cells were located in two different germ layers: *Antistasin*-expressing cells were located in the endoderm, while *Znf845*-expressing cells were located in the ectoderm at the base of the manubrium. However since i-cells are highly migratory cells it is possible that the few ectodermal cells, could correspond to gland cell early precursors that then migrate into the endodermal layer before differentiation. The absence of detectable co-localization between *Znf845* and *Antistasin* expression does not allow to be ruled out this possibility.

- *No Znf845 expression in nematoblasts*

Co-localisation studies using the *Mcol3-4a* probe in combination with *Znf845* at 24hpf revealed only cells expressing either *Znf845* or *Mcol3-4a (*Figure 41D). The cells expressing *Znf845* and *Mcol3-4a* are clearly distinct although they are localised in a similar region of the planula endoderm. Again, it remains possible that *Znf845* is involved in the specification of early nematoblasts, despite the lack of co-localisation, given its early expression at early gastrula. To test this idea I performed co-localisation studies using Znf845 in combination with Sox15 (Result 1) at the early gastrula stage and at 48hpf. The early gastrula experiment unfortunately failed to give any reliable results (probably due to the timing of the fixation of the embryos) while at 48hpf no co-expression was observed (Figure 47). From these preliminary observations I can conclude only that if *Znf845* is involved in nematogenesis, it is expressed only transiently in early precursors. To address this hypothesis it would be necessary to repeat the double *in situ* hybridisation experiment at the early gastrula stage. Another possibility is that *Znf845* is expressed early during development of the neuronal lineage. To distinguished between these hypothesises it would be useful to perform functional studies by morpholino injection, followed by assaying using gene marker expression to determine whether nematoblasts, nematocytes and/or other somatic cells types are affected by *Znf845* down-regulation.

These studies of i-cell fate pathways would obviously be greatly aided by the development of transgenic lines expressing a fluorescent reporter in i-cells as has been developed in *Hydra* (Wittlieb et al. 2006b) or under the control of linage specific promoters as achieved for SoxB(2) in *Nematostella* (Richards & Rentzsch 2014). Such transgenic reporter lines would enable more easily to relate the expression of different genes to the development of each particular derivative cell type.

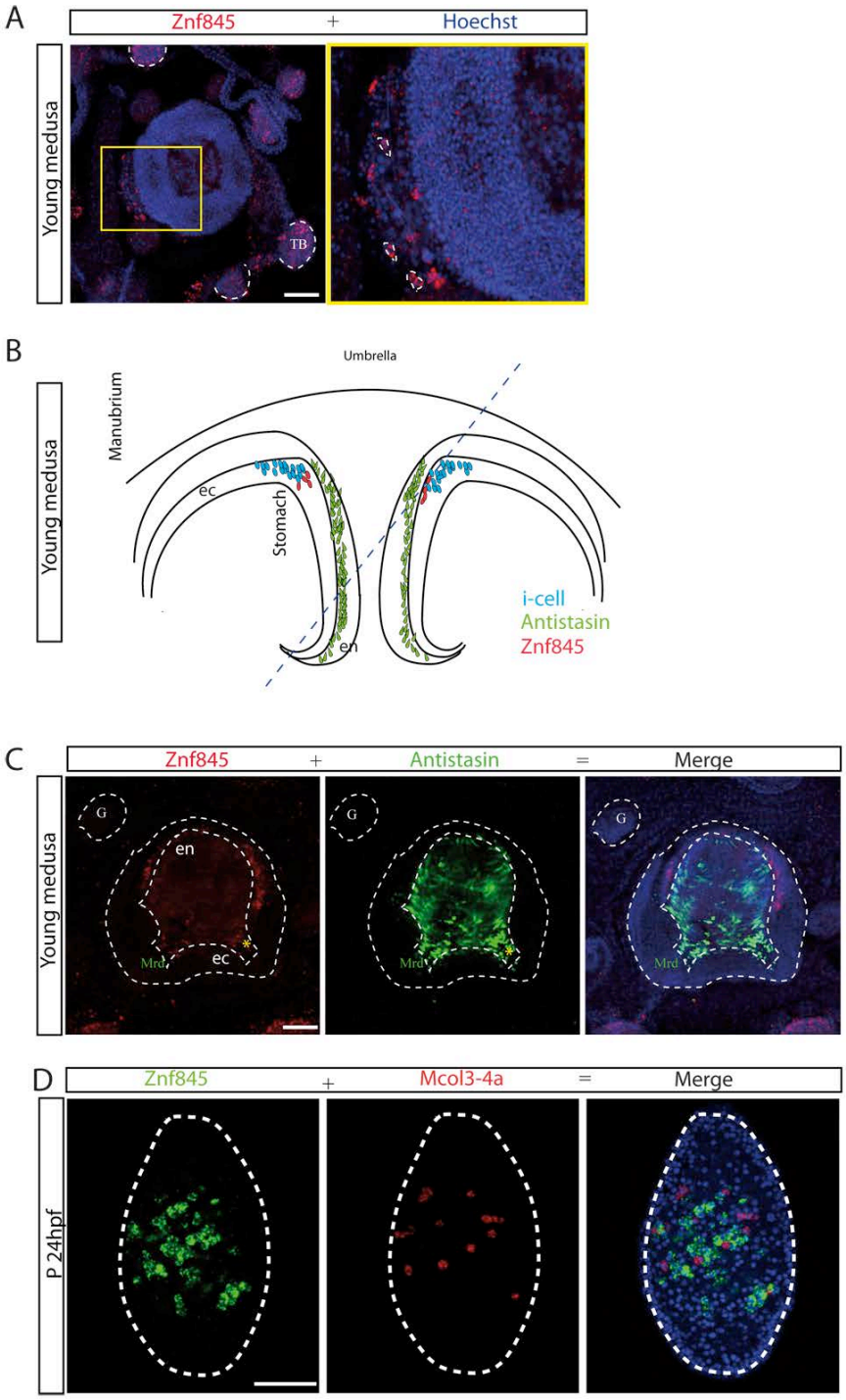

Figure 46: *Znf845* is not expressed in gland cells or in nematoblasts. A) Representative confocal image of *Znf845* positive cells, highlighting the i-cell like morphology of the *Znf845* expressing cells in the manubrium ectoderm. Highlighted cell with an i-cell like morphology (outlined by dashed lines in the left panel). B) Schematic drawing showing the distribution of *Znf845* and *Antistasin* positive cells in the medusa manubrium. *Znf845* (in red) and *Antistasin* (in green). Piwi positive cells are also shown (cyan). C) Representative confocal images of *Znf845* and *Antistasin* expression patterns in young medusa. The orientation of the images follows the section traced in the scheme in B. *Znf845* (red), *Antistasin* (green), merged image. Dashed lines mark endoderm (en), ectoderm (ec). Yellow asterisks indicated unspecific *Znf845*red signal bleeding through from *Antistasin* strong staining. D) Representative confocal image of double *in situ* hybridisation using *Mcol3/4a* and *Znf845* at planula 24hpf stage. From right to the left: *Znf845* (green), *Mcol3-4a* (red), last panel merge. Scale bar 50µm.

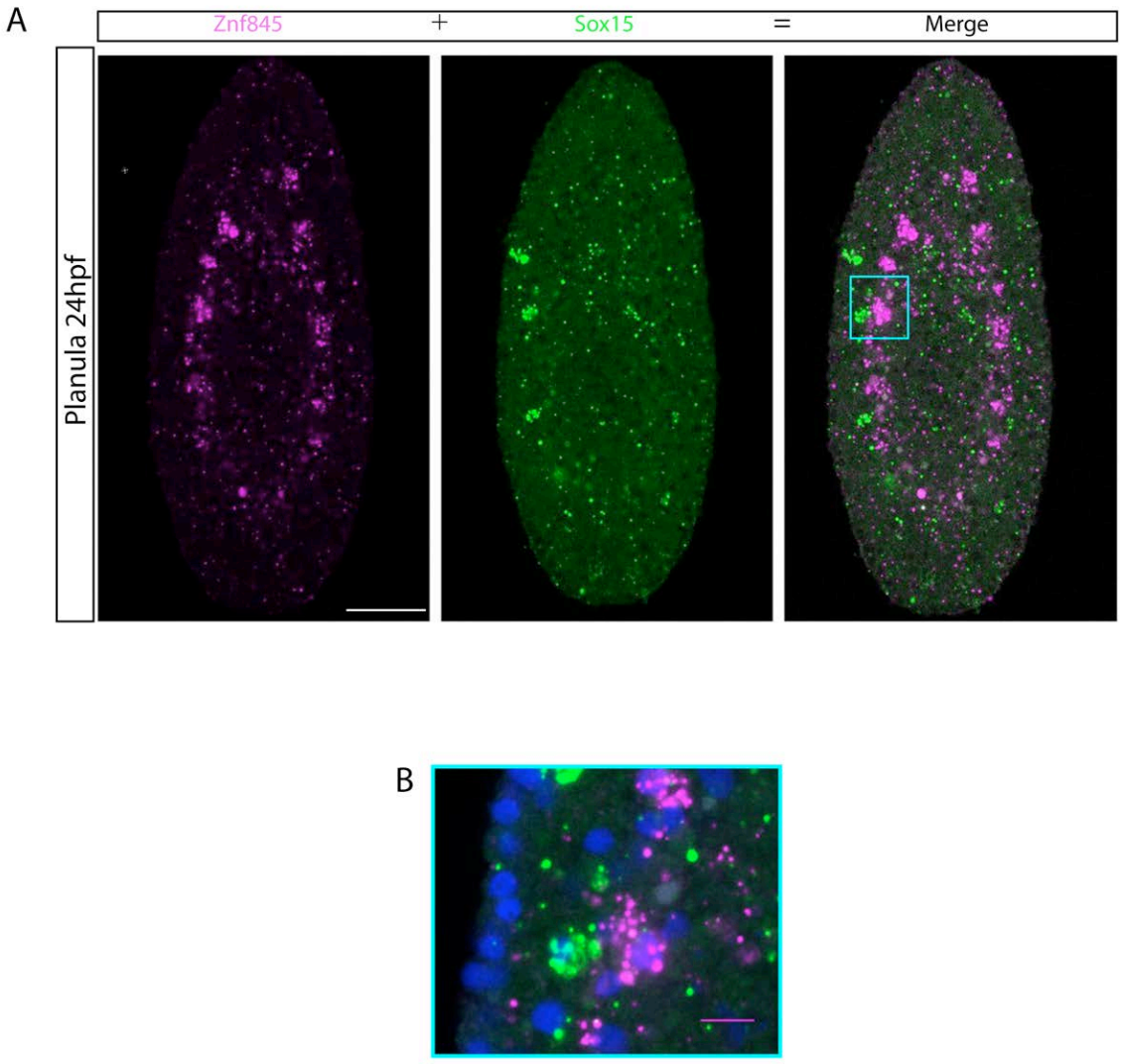

Figure 47: *Znf845* is not expressed in *Sox15* positive cells. A) Representative confocal images of double *in situ* experiments using *Znf845* and *Sox15* probes at p48hpf stage. From left to right: *Znf845* (in magenta) *Sox15* (in green), last panel merged. Scale bar 50μm. B) Detailed view of the area boxed in last panel in A. High magnification image showing that *Znf845* and *Sox15* genes are not expressed in the same cell population. Scale bar 10μm.

Discussion & Perspectives

The study presented in this thesis should be placed in a wider context of stem cell biology. An important aim of stem cell research is to understand the intrinsic and extrinsic mechanisms regulating proliferation and differentiation of multipotent undifferentiated stem cells. Knowledge in this field has come from a broad range of model organisms as well as from *in vitro* stem cells systems like mammalian ES cells.

Among these models are hydrozoan i-cells, which have long been appreciated to provide a great opportunity to study the mechanisms responsible for fate choices and differentiation signals from a multipotent stem cell population (Bode 1996; Plickert &. Müller 2009; Plickert et al. 2012). Previous studies in the *Clytia* medusa have further demonstrated that this "full life-cycle" species could be an attractive model for the study of ordered nematogenesis from i-cells in the tentacle bulb (Denker et al. 2008; Jager, et al. 2011). My work has focussed on developing the *Clytia* larva as a model system to experimentally address the embryonic origin of i-cells, as it is more accessible than the medusa for analysing gene function (via microinjection of Morpholinos /synthetic RNAs etc. into the egg). I hope that the work reported here has illustrated the potential of this system to provide new insights into metazoan stem cell research.

The particular focus of my project was to address the impact of Wnt/β-catenin signalling on i-cell dynamics during *Clytia* larval development; I use the term "dynamics" here to include i-cell formation during embryogenesis, as well as fate specification and differentiation of i-cell derivatives.

To unravel the effects of Wnt/β-catenin signalling on i-cells dynamics I first had to determine the distribution of i-cells and their derivatives. To do this I characterised molecular markers for each i-cell derived cell type lineage. I then exploited these molecular markers to outline a spatial and a temporal map of i-cell derivatives during larval development.

The data collected through this study provided a first framework for investigating several different aspects relating to the origin of i-cells and of their derivatives. In the first section of this general discussion chapter, I will focus on the origin and the regulation (in particular by Wnt/β-catenin signalling) of the cells that make up the hydrozoan nervous system: nematocytes and nerve cells. The second section is dedicated to the embryological

origins of the *Nanos1* and *Piwi* expressing i-cells and the relationship between i-cell formation and germ line segregation mechanisms.

Neurogenesis and Nematogenesis

The expression patterns of gene markers coupled with other methods to detect differentiated nematocytes and RFamide-expressing ganglion/intermediate neurons was used to characterise the appearance and distribution of i-cell derivative intermediates space during larval development, and in the adult, as summarised in Figure 48. This i-cell cartography, based on the expression of selected genes at successive stages, revealed that nematoblasts expressing the capsule protein *Mcol3-4a* appear earlier (at 24hpf, *i.e.* just at the end of the gastrulation) than expression of the neurogenesis gene *Prdl-a* (first detected at 36hpf). In *Hydra Prdl-a* is expressed in a particular sub-population of developing apical neurons (Gauchat et al. 1998; Miljkovic-Licina et al. 2004). The relative timing of *Mcol3-4a* and *Prdl-a* expression suggests that specification of the nematocyte lineage may occur before that of the nerve cell lineage in the *Clytia* larva. In *Hydra* it has been proposed that neurons and nematocytes derive from a common precursor expressing the parahox gene *Gsx/Cnox-2*, which regulates the expression of other transcription factors present early in both lineages such as *Prdl-b* and *Coup-TF*. *Prdl-b* and *Coup-TF* are expressed both in nematoblast nests (Gauchat et al. 1998), and also in single cells with neural morphology that also express *Prdl-a* (Miljkovic-Licina et al. 2004). Experimental downregulation of the *Cnox-2* gene by RNAi treatment causes reduction in the expression of the nerve cell markers *Prdl-a*, *RFamideB* and *RFamideC* precursors as well as the nematogenesis genes *Zic* and *Prdl-b* (Miljkovic-Licina et al. 2007). Conversely the expression of *Coup-TF,* which is thought to repress nematocyte proliferation, was upregulated (Gauchat et al., 2004).

In *Clytia Cnox-2*/*Gsx* is expressed only in the medusa, in the distal part of the tentacle bulbs, described as the nematocyte differentiation zone (Chiori et al. 2009) but where neural differentiation may also be occurring (see *Prdl-a* expression in Figure 26, Results-I).

If *Gsx* function is conserved *in* Clytia, this lack of expression in the larva could suggest that nematogenesis and neurogenesis at this stage do not involve a common precursor, although it remains possible that another regulatory transcription factor substitutes for *Gsx* at the larval stage.

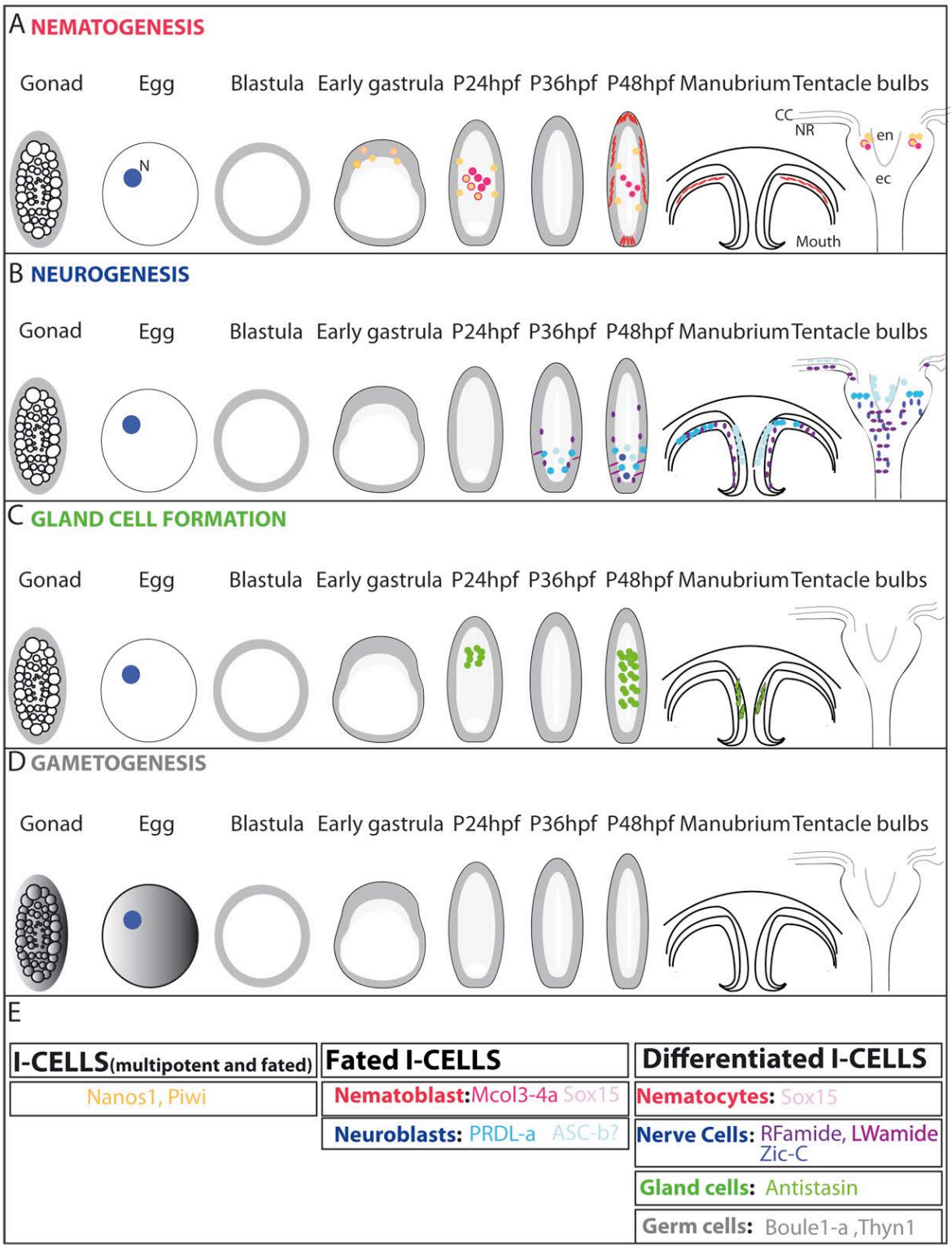

Figure 48: I-cell cartography.
Schematic representation of the distribution of i-cell derivatives during larval development and in the adult medusa. Each putative i-cell derived lineage is illustrated on separate lines: A) Nematogenesis B) Neurogenesis C) Gland cell formation D) Gametogenesis. Nanos- and Piwi-expressing i-cells (in orange) are represented only in the nematogenesis line (A), indicate the co-expression of *Piwi* with *Mcol3-4a*. *Nanos1* and *Piwi* i-cell population is detected throughout larval development and in the medusa (see Figure 12). The colours correspond to the genes listed in E. Bi-coloured dots indicate co-localisation. At 36hpf only the expression of the putative neural genes was verified. E). Table summarising the cell types and the assigned markers.

One possible candidate regulatory transcription factor that could be expressed in bi-potent progenitors or be involved exclusively in the nematogenesis pathway in *Clytia* larvae is Sox15. SOX genes have been shown in *Clytia* to be expressed in developing neurosensory cells and in nematoblasts (Jager et al. 2011). In vertebrates, SOX transcription factors have been widely investigated for their role in pluripotency (see Introduction section 2.3.2). Some have dual functions, for instance mouse Sox2 can regulate both neural stem cell maintenance and nerve cell differentiation in the eye and the brain (Wegner 2011).

Bilaterian SOX genes can be classified in five major groups (named B, C, D, E and F), with SoxB genes being commonly expressed only transiently during neurogenesis. Phylogenetic analysis was not able to assign *Clytia Sox15* to any of the previously identified *SOX* gene groups, so the exact identity of *Sox15* is still obscure, however it fulfils several criteria to be considered as gene expressed in early neural /nematocyte precursors. As shown in Results-I, section 1.2.2, *Sox15* mRNA can be detected at the early gastrula stage in *Piwi* positive cells, as well as in differentiating nematoblasts in the endoderm, where it is co-expressed with *Mcol3-4a* (Figure 24). Its expression territory in the larva ectodermal includes differentiating nematocytes but could also include nerve cells. *Sox15* is the only *Clytia* SOX gene to have detectable expression in both germ layers, while the other putative nematogenic SOX markers, *Sox14*, *Sox5* and *Sox2* were detected exclusively in populations of endodermal cells (Jager et al. 2011). Furthermore *Sox15* expression is Wnt3 dependent at early gastrula stage (Lapébie et al. 2014), which could explain the delay in *Mcol3-4a* expression in Wnt3-MO embryos (Figure 40 ResultsII). The expression pattern and the Wnt3-MO response are compatible with a role for Sox15 in a bi-potent progenitor population, or as a nematogenesis specific gene.

SOX gene function has not been studied so far in hydrozoans, but in anthozoans the neural functions of certain SOX genes have been suggested or demonstrated. In the coral *Acropora* analysis by *in situ* hybridisation showed the expression of the gene *SoxC* (which belongs to the SoxC family) in a sub population of ectodermal neurosensory cells (Shinzato et al. 2008). A recent study in *Nematostella* demonstrated that SoxB(2) regulates neurogenesis (Richards & Rentzsch 2014). By using a stable transgenic line in which the SoxB(2) promoter drives the expression of the fluorescent reporter mOrange it was shown that *SoxB(2)* is expressed in sensory neurons, ganglionic cells and nematocytes (by co-localisation studies using *Nematostella* minicollagen specific antibody). Furthermore

morpholino injection experiments show that *SoxB(2)* functions upstream in the development of all these three neural cell populations.

To complete our study of *Clytia Sox15* in i-cells and to test whether it regulates neurogenesis and/or nematogenesis it would be interesting to perform functional studies using morpholino injection following by *in situ* hybridisation of neural and nematocyte markers. In addition, double staining with the anti-RFamide antibody could help determine whether *Sox15* is also expressed in neural cell types in the planula ectoderm.

Other transcription factor families involved in neurogenesis /nematogenesis should also be investigated. It would be particularly informative to perform co-expression studies, combining for example the neuronal marker *Prdl-a* (this study) and orthologs of genes expressed early during nematogenesis in *Hydra* like *Prdl-b* and *COUP-TF*. I identified a *Clytia Prdl-b* ortholog sequence (Figure 25, Results-I), but no clear ortholog of *Hydra COUP-TF* in the extensive transcriptome data available for *Clytia* (data not shown).

COUP-TF in *Hydra* and in *Hydractinia* is thought to promote neural differentiation and to down-regulate nematogenesis (see above; Miljkovic-Licina et al. 2007; Duffy & Frank 2011). In *Hydractinia COUP-TF* is positively regulated by the Wnt/β-catenin pathway. Thus *Hydractinia* polyps treated with LiCl (which inhibits GSK3β) show increased *COUP-TF* expression. Although Wnt pathway disruption during *Clytia* embryogenesis did not prevent *Prdl-a* expression, it caused a transient delay in the appearance of early nematogenesis markers (Mcol3-4a). Whether this represents a direct of indirect consequence of the Wnt3-MO phenotype, the transcriptomic data derived from the Wnt3 early gastrula morphants (Lapébie et al. 2014) could provide some good candidate transcription factors with possible roles in early fate specification events. Among the genes under-expressed in Wnt3 morphants, the gene *HlhIE1* shows an expression profile that could fulfil the criteria required to be considered as gene expressed in the neural precursor cells (Figure 2M, PAPER 2). *HlhIE1* can be placed by phylogenetic analysis (Figure 27, Results-I) into the Achaete Scute family, whose members are often involved in neural fate commitment (see Introduction 2.3.2 and ResultsI). During *Clytia* development *HlhIE1* mRNA is detected at the early gastrula stage in a population of 'i-cell like' ingressing cells at the oral pole and at larval stages in a few cell located in the endodermal core region, that could correspond to an i-cell sub-population on the way to a particular neuronal fate. Future research could involve detailed characterisation of genes such as *HlhIE*1 by

expression pattern analysis including double in *situ* to verify an i-cell origin, followed by functional studies.

Impact of Wnt/β-catenin signalling on i-cell dynamics

- *I-cell population maintenance is not dependent on Wnt signalling*

Wnt signalling can promote cell proliferation and stem cell renewal (see Introduction 1.6.4). In *Clytia* larvae I found no evidence for a role for Wnt signalling in i-cell renewal. The development and maintenance of *Nanos1* and *Piwi* i-cell expressing populations were not affected in Wnt3 morphants (see Figure 39). This finding is supported by transcriptome analysis, which reveals that the *Nanos1* and *Piwi* expression levels are not significantly affected by Wnt3 disruption (Figure 43C).

The *Nanos1* and *Piwi*- expressing i-cell population includes not only multipotent cells, but also some "fated" cells, probably committed towards different somatic fates, as identified by co-expression of cell type specific marker genes such as *Mcol3-4a*. The size of this population did not change between uninjected embryos and morphants, (at early gastrula, p24 and p48hpf). The conclusion that neither i-cell population maintenance nor somatic fate specification are Wnt sensitive in *Clytia* is supported also by the observation that expression of the nematoblast marker *Mcol3-4* and the neurogenesis marker *Prdl-a* expression were not prevented in Wnt3 morphants. Expression of *Mcol3-4* was delayed but this effect was probably not specific but due to delay in gastrulation, since these cells ingressing along with the presumptive endoderm cells. To test whether Wnt3 signalling is involved in early precursor specification, it would be useful to perform double *in situ* hybridisation with *Piwi* and *Mcol3-4a* in Wnt3 morphants to verify the presence of an early nematoblast population (ResultsI).

To conclude, the results reported here suggest that Wnt signalling is not involved either in i-cell maintenance or early precursor specification, even though more early makers need to be tested in Wnt3 morphants. These findings are in contrast with the results obtained in *Hydractinia (*discussed also in the section 2.1.1, ResultII) in which the hyperactivation of the Wnt signalling boost the number of S-phase cells in stolons. It is possible that is effect is due to the global polyp treatment, and that not only i-cell are responsive to Wnt signalling.

As discussed in the Introduction (section 1.4), stem cell maintenance is regulated at several levels, including transcriptional control by the means of transcription factor. In vertebrates a set of transcriptional factors have been well characterised as regulators of embryonic stem cells, including Nanog, Oct4, Klf4 and Sox2, which act to repress somatic differentiation programs. These genes do not have clear ortholog in invertebrates. Event though recent study in *Hydractinia* revealed the presence of a POU domain-containing gene, the *Polynem* gene (*Pln*), which phylogenetic analysis could not assign to a specific POU gene class. *Pln e*ctopic expression in polyp epithelial cells induces the formation of neoplasm, mostly composed by morphologically recognisable *Nanos* and *Piwi* expressing i-cells (Millane et al. 2011). Downregulation by RNAi treatment in polyp increases the number of mature nematocytes. These findings suggest that POU class gene could have a role in stem cell maintenance and in differentiation also in early branch metazoan. Studies in *Hydra* show that FoxO plays a crucial role in the regulation of stemness (Boehm et al. 2012). The FoxO gene is expressed in all three the stem cell lineage (*i.e.* ectodermal cells, endodermal cell and i-cells), all along the *Hydra* body column Boehm et al. 2012). Overexpression of FoxO in i-cell lineage increases the proliferation ratio and forces stem cell to differentiate into nematocytes as shown by the atypical *Piwi* expression in fully differentiated nematocytes. *Clytia* FoxO (Chevalier et al. 2006) is ubiquitously expressed at early stages of embryogenesis and at both poles in the planula. Thus in *Clytia* too FoxO may control stem cell behaviour, not only in i-cells but more widely in epithelial stem cells. In other biological systems FoxO proteins often play a role in regulating cell proliferation and growth in response to a variety of extracellular signals, notably via the TOR pathway but also Wnt signalling (Eijkelenboom & Burgering 2013). A functional characterisation of FoxO in *Clytia* larvae and in adult medusa in relation to homeostasis of different cell populations would be very interesting.

- *Differentiation of some neural subtypes requires Wnt signalling*

Wnt signalling has been variously implicated in each step of neural development: neural stem cell population maintenance, neural lineage specification, neural precursor proliferation and differentiation (Reviewed in Inestrosa & Arenas 2010; Mulligan & Cheyette 2012).

Our findings suggest that in *Clytia* Wnt/β-catenin signalling does not prevent specification of nematoblasts or neuroblasts, but impairs the differentiation of nematocytes and of some neural sub-types. Particularly sensitive was the differentiation of ganglion cells expressing a RFamide precursor distributed laterally in the planula between the endoderm and ectoderm epithelial layers, while aboral sensory neurons expressing GLWamide, which are involved in mediating the settlement response, were prevented by β-catenin/TCF pharmacological inhibition but not by Wnt-3 MO (Figure 6 PAPER 1).

One possible explanation for this discrepancy is that the drug treatment had non-specific effects, causing loss of all late cell type markers. Following TCF inhibitor (PKF-118) treatment, embryos morphology was not well maintained. To test whether it has a general toxic effect on development, it would be useful to monitor the expression of other late-expressed genes in drug treated embryos.

On the other hand, it is possible that the inhibition of GLWamide sensory neuron development in PKF-118 treated embryos but not in Wnt3 morphants reflects the requirement for a low level of Wnt/b-catenin signalling for the differentiation of aboral type neurons and a higher dose for oral ones. Under this hypothesis the aboral GLWamide subpopulation would need a lower level of active nuclear b-catenin/TCF to acquire its fate, still available in Wnt3-MO embryos but not following PKF-118 treatment. In this context the *Clytia* planula O-A Wnt gradient can be compared to the A-P Wnt gradient along the vertebrate neural plate. In vertebrates, an anterior-posterior Wnt gradient is crucial for the specification of positional information along the neural plate. For instance in the fish *Medaka* this gradient has been shown to be achieved via modulation of Wnt signalling by the inhibitor *SRFP1* which defines the anterior neural plate domain. *SFRP1* over-expression thus induces expansion of the forebrain territory (anterior neural plate) accompanied by axis duplication and posterior truncation (Lopez-Rios et al. 2008).

Similarly in cnidarians it the oral-aboral Wnt activity gradient specifies positional values (Marlow et al. 2013) that could influence neural differentiation *via* the production of local cues. In *Hydra,* neuroblasts after entering the neuronal fate lineage migrate to their site of differentiation, at the oral and oral extremities of the polyp, and their final identity is then specified in relation to their position along the O-A axis by neuropeptides (Takahashi et al. 2000; Bosch 2007). One example is the neuropeptide Hym355. Hym355 precursor is expressed in neuronal cell population present both in the foot and in the tentacle. In adult

polyps treated with this neuropeptide, the number of nerve cells increases initiating a positive regulation of neural cell differentiation. Other secreted peptides are specifically expressed either in the foot or the head region, and so can influence the regional identity of neuron differentiation.

Our findings in *Clytia* planulae, along with the stimulation of nematocyte and RFamide nerve cell differentiation by Wnt signalling hyperactivation in *Hydra* and *Hydractinia* polyps (discussed also in the section 2.1.1, Result-II), indicate that Wnt signalling may have a role in neural differentiation directly and/or *via* its role in defining positional values. We can speculate that Wnt signalling could also have an active role in nematogenesis and in neurogenesis in the *Clytia* medusa, since Wnt3 is expressed, among other sites, at the opening of the mouth and in the nematogenic ectoderm in the tentacle bulbs, (T. Condamine and M. Jager, personal communication). Involvement of Wnt/β-catenin signalling in the neural lineage has been proposed also from studies in the ctenophore *P.Pileus*. Expression studies show that Wnt signalling genes are expressed in various neural structures throughout the adult ctenophore body (Jager et al. 2013). The majority of the Wnt gene expression has been reported in the Polar field, which is an aboral neuro-sensory complex in which a neural structures have been identified together with sub population of RFamide immunoreactive neural subpopulation (Jager et al. 2011).

Equating i-cell formation to germ line segregation mechanisms

The germ line is the cell lineage that will give rise to gametes carrying the genetic information to the next generation. The segregation of germ line from somatic cell lineages, with the subsequent formation of primordial germ cells (PGC), can occur through two different mechanisms termed preformation and epigenesis. In preformation (*Drosophila*, zebrafish, *Xenopus*), germ cells can be identified very early in embryogenesis. Their identity is determined by inheriting localised germ plasm (see Introduction section 1.5). For example the specification of germ line in the crustacean *Parhyale* occurs by early germ plasm segregation, starting at first cleavage. The blastomere bearing germ plasm, named g, it is able to generate the germ line (Extavour 2005). Single blastomere isolation experiments demonstrated that all isolated blastomeres are able to develop independently of each other, but only the germ plasm-inheriting blastomere (tracked using a Vasa

antibody) is able to develop germ cell features, suggesting that germ plasm is instructive for germ line segregation.

The second mechanism of germ line specification involves extrinsic signals from surrounding tissues to a group of embryonic or other undifferentiated cells that will acquire germ cell identity. A recent study in the cricket (Donoughe et al. 2014) showed that BMP signalling, as is the case for mouse (Saitou & Yamaji 2012), is the signalling pathway responsible for PGC induction. Alteration of BMP signalling by RNAi tretments targetting BMP pathway components (*e.g.* the BMP ligands BMP2/4, BMP5/7/8 and the effector Smad1/5/8) impairs PGC formation independently of the effect on mesoderm induction.

Given the scattered distribution of epigenesis and preformation as modes of germ cell development across the metazoan phylogeny (Figure 49), there is still much debate concerning which of the two mechanisms is ancestral. The observation that late germ line segregation (after embryogenesis) occurs in several animals and does not appear to rely on maternally localised factors, supports the idea that epigenesis is the ancestral mechanism and that probably preformation derived from epigenesis multiple times during evolution (Extavour, 2007; Extavour and Akam, 2003). This view is supported also in a recent study in which molecular evolution rates were correlated with PGC specification (Evans et al. 2014). Evolution rates of protein coding sequences were compared between two sister taxa that segregate their germ lines by epigenesis vs preformation (urodele vs. anuran amphibians), using mammals as out-group. It was shown that the taxa that use the preformation mechanism show a faster rate of sequence evolution, suggesting that the acquisition of germ plasm is an evolutionary advantage.

On the other hand, the recent identification of germ plasm in an increasing number of taxa and of its presence in basal branch metazoans such as *Clytia*, indicates that the preformation mechanism in the common metazoan ancestor should be not ruled out (Leclère et al. 2012), perhaps originally existing in parallel with epigenetic mechanisms.

A previous study showed the presence of localised "germ plasm" in *Clytia* oocytes and eggs (Leclère et al. 2012) by morphological criteria in electron microscopy oocyte sections and by detection of localised mRNAs for *Vasa*, *PL10*, *Nanos2*, *Nanos1* and *Piwi* in spawned eggs (Figure 18). These 'germ plasm' mRNAs are aggregated in granules at the animal pole

from the egg, inherited through cleavage stages until the blastula stage. They continue to be detected, probably as a result of new transcription from the zygotic genome, in cells that form at a corresponding position at the early gastrula stage, which then migrate into the endodermal region of the planula during late gastrulation (Figure 12). Despite this spatial "continuity" in the expression of germ plasm genes during *Clytia* development (Leclère et al 2012) we could not conclude prior to this study that in *Clytia* germ cell lineage fate is determined by germ plasm inheritance. On one hand, it was not known whether at the larval stage the i-cell population was uniform in terms of potential, or whether a sub-population was already committed to an exclusive germ line fate and thus represents a true germ line. On the other hand, there was no functional evidence that the maternal germ plasm had a determinant function. Although not conclusive, my study provides new evidence relating to both of these points.

- *Is hydrozoan Germ plasm inherited by the i-cell lineage or a dedicated germ line?*

Given that the "germ line" markers including *Nanos1* and *Piwi* in *Clytia* show wider expression in i-cells and their derivatives, to monitor the appearance of germ cell precursors during development I searched for genes involved specifically in gametogenesis. Among the conserved family genes implicated in gametogenesis I focussed on the Boule and Tudor families.

In the available *Clytia* transcriptome dataset I found 10 boule-like genes, including one, *Boule1-a*, that fulfilled the criteria to be considered a germ cell markers. Phylogenetic analysis revealed that *Boule1-a* is an ortholog of the vertebrate Boule/Daz family gene group (Figure 34 ResultI), and possesses two conserved amino acids at positions considered as the Boule signature (Shah et al. 2010; Kuales et al. 2011). *In situ* hybridisation analysis showed that *Boule1-a* expression is restricted to medusa gonads (both female and male) and is not detected in other stem cell areas, like tentacle bulbs. Importantly no *Boule1-a* expression was detected in larval stages, suggesting that germ cell specification occurs only in the sexual medusa. A second gene with an identical expression profile was also identified (*Thyn*). Neither of the tudor domain containing genes selected, *TDCP1* and *TDCP2*, showed an expression pattern compatible with a germ cell marker (Figure 36). These observations indicate that despite the presence of localised germ plasm in the eggs,

the germ line is segregated later in development. If germ plasm has a determinant role in *Clytia* embryo development it should thus specify general i-cell fate, not germ cell fate.

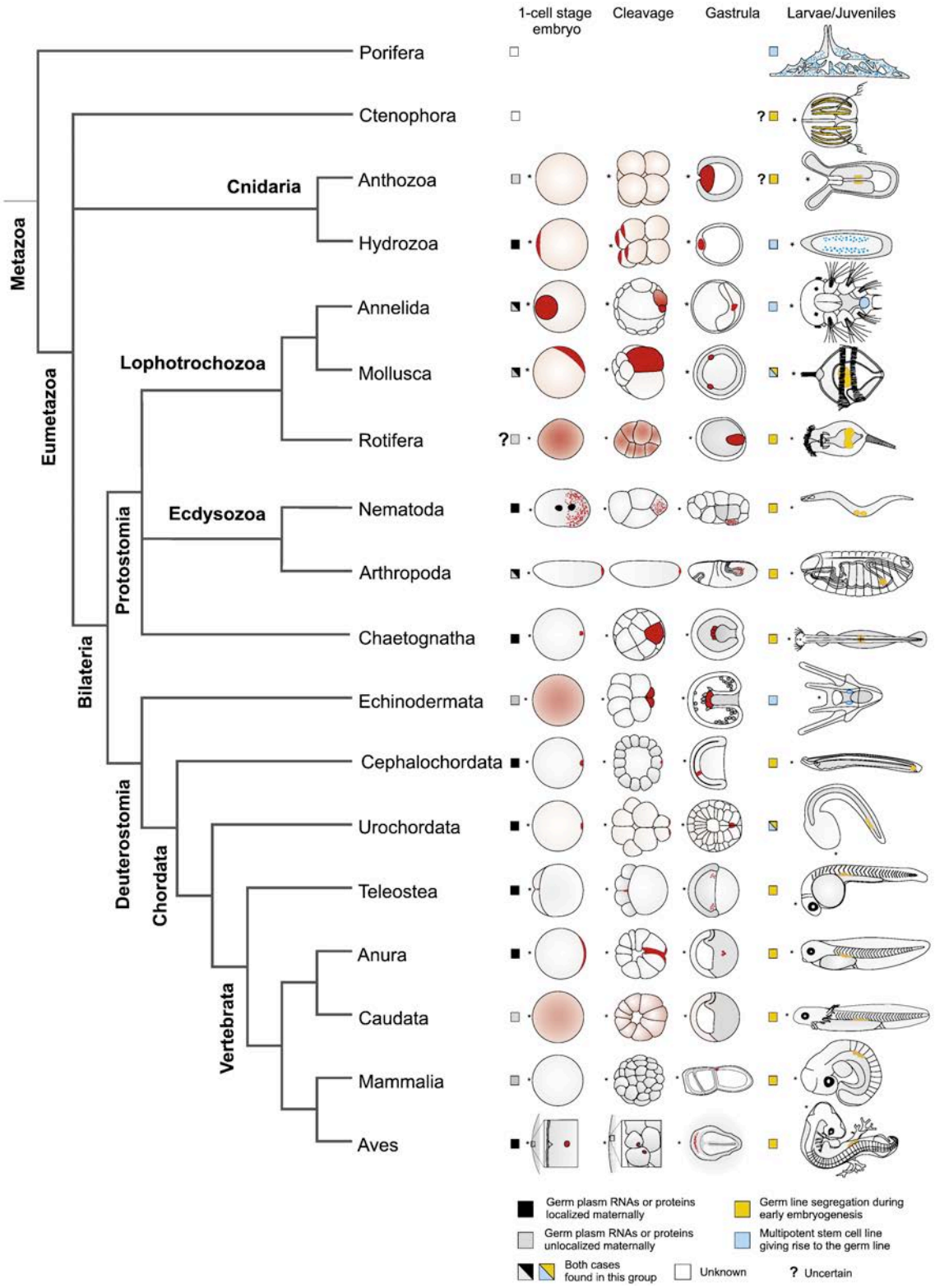

Figure 49: Germ plasm distribution in metazoans.
Phylogenetic tree illustrating the different mechanisms of germ line segregation across metazoans. Black squares represent germ plasm or protein localised maternally. From Leclère et al 2012.

- *Does germ plasm determine i-cell fate?*

Hydrozoan i-cells can be considered as an atypical germ line since they give rise to both germ cells and somatic cells. The i-cell formation mechanism in *Clytia* can thus be equated with the mechanism of germ line formation. To determine whether germ plasm has an instructive role in i-cell formation (and as a consequence in germ line development), embryo fragments in which germ plasm was absent (vegetal halves) were produced by embryo bisection or blastomeres isolation (Leclère et al 2012; see also Results II section 2.1.1, Figure 42). Vegetal fragments lacking germ plasm were able to develop Piwi - expressing cells by the planula stage. The planulae derived from the vegetal halves (germ plasm absent) and animal halves (germ plasm present) were similar with respect to the time and number of Piwi-expressing cells. This result indicates that in vegetal fragments at least germ plasm is not instructive in the formation of i-cells, and that an inductive signal is able to promote i-cell *de novo* formation during embryo re-patterning. In this study we addressed whether Wnt/β-catenin signalling was involved in this process. Critically, we found that vegetal fragments from Wnt3-MO injected embryos had a reduced capacity to recover *Piwi*/*Nanos1* expressing cells at the planula stage compared to vegetal fragments from uninjected embryos (Figure 1 and Table 1 in PAPER1). These results indicate that in the absence of germ plasm, Wnt3 function is necessary (directly or indirectly) for *de novo* i-cell formation. Conversely Wnt3 is not required for i-cell formation during normal development (see Figure 39, ResultsII), suggesting that Wnt3 is involved in i-cell ontogeny exclusively during axis re-establishment. A correlation between *de novo* i-cell formation and axis regulation was observed also in some embryo fragments derived from uninjected embryos; when the embryos halves were not able to regulate their axis, as indicated by the loss of elongated embryo shape and directed swimming, *Piwi* expressing cells tended to be absent. Wnt-dependent *de novo* i-cell formation during embryo re-patterning thus quite possibly relates to the critical role of Wnt signalling in establishing axial properties during embryogenesis. Oral-aboral axis development is initiated in *Clytia* from the egg, building on the asymmetrical distribution of the Wnt3 and Fz mRNAs (Momose & Houliston 2007; Momose et al. 2008). During re-patterning of vegetal fragments a sufficient quantity of Wnt3 and Fz1 from the animal region is presumably required to allow re-establish an oral-aboral axis through feedback mechanisms involving unknown secreted molecules. In vegetal fragments, the lack of germ plasm combined with the Wnt/β-catenin

downregulation prevents i-cell *de novo* formation, suggesting that axis formation is required. In animal fragments germ plasm can determine i-cell fate even in the absence of oral-aboral polarity.

Taken together these results indicate that since embryos lacking germ plasm and Wnt3 signalling are not able to form i-cells, germ plasm normally has an instructive function, not directly linked to early germ lineage segregation but to i-cell lineage segregation.

How Wnt3 drives the *de novo* i-cell formation is not yet understood. One hypothesis could be that following blastomere isolation or blastula bisection, reactivation of Wnt signalling via Wnt3 causes re-aggregation of pre-existing *Nanos1* and *Piwi* mRNAs, allowing reformation of the germ plasm and thus i-cell formation. In this context is important to note that the concentrations of Nanos and Piwi mRNAs between the vegetal and the animal halves at the blastula stage are surprisingly similar (Leclère et al. 2012), despite the presence of germ plasm in the animal fragments. However we should not rule out another possibility, involving traces of Wnt3 protein that could persist in the animal hemisphere of Wnt3 morphant embryos. In this scenario, in both Wnt3-MO whole embryos and animal halves, residual maternal localised Wnt3 protein could be sufficient to promote i-cell formation independently of its role in OA axis formation.

Signalling pathways other than Wnt may also be involved in de novo i-cell formation in *Clytia* reformed oral territories. During mouse embryogenesis BMP signalling and Wnt/β-catenin signalling collaborate to induce PGC formation (Ohinata et al. 2009). In the mouse epiblast, PGCs are specified by BMP signalling coming from the extra embryonic ectoderm. BMP signalling induces the expression of the gene *Blimp1*. Blimp1 protein is a repressor of transcription of somatic genes and it is a key factor in PGCs specification. Wnt3 function is also essential to induce the expression of Blimp1, ensuring that these cells can respond correctly to BMP4 to be specified as germ cells (Ohinata et al. 2009). Interestingly, transcripts of the potential BMP and Wnt inhibitor Cerberus are under-expressed in *Clytia* Wnt3 early gastrula morphants (Figure 3 PAPER 2), suggesting that also in *Clytia* BMP and Wnt signalling might collaborate.

The *Clytia* transcriptome contains several probable BMP ligands and Smad effectors (Lapébie unpublished data). Preliminary expression pattern analysis has shown that the *Clytia* eggs and/or embryos express mRNAs for a BMP5/8 ortholog and a possible BMP2/4 ortholog as well as Smad1/5 and Smad 2/3 orthologs.

The expression pattern of BMP signalling molecules had already been associated with germ cells development in other cnidarians. For example in *Hydra* Hysmad1 levels are upregulated during oogenesis in *Hydra* sexual strains (Hobmayer et al. 2001) while in *Nematostella* the expression domain of BMP 2/4 ortholog coincides with clusters of cells localised in the mesenteries that correspond to presumptive *Nematostella* PGCs (Extavour et al. 2005; Finnerty et al. 2004). To test the involvement of BMP signalling in i-cell formation during embryogenesis in *Clytia*, one approach would be to hyper-activate the pathway by injection into egg of 4-hydroxychalcone, a recently identified chemical activator of the BMP pathway (Vrijens et al. 2013). In crickets, hyperactivation of the BMP pathway using 4-hydroxychalcone increased the number of PGCs clusters and the level of phosphorylated Smad4 indicative of the pathway activation. It will be interesting to investigate the role of these molecules both in the formation of i-cells during normal development and during embryo re-patterning.

To conclude, this study has provided experimental support for the hypothesis that two different mechanisms for the formation of i-cells coexist in *Clytia*. During undisturbed development, germ plasm appears to have an instructive role, while in re-patterning conditions signalling molecules participate in an inductive process.
From an evolutionary point of view, these findings can contribute to the debate concerning which mechanism, epigenesis or preformation, was present in the common metazoan ancestor (Leclère et al. 2012; Extavour & Akam 2003). Specifically, they support the possibility that both mechanisms were available in the common ancestor of metazoans, and that in certain animal lineages either epigenesis or preformation was reinforced as the primary mechanism (Kumano 2015).

Annexe 1: Comparison of expression levels of selected *Hydra* genes in separated cell populations

Clytia gene name	accession number	Ortholog in Hydra magnipapillata	Ortholog in Nematostella vectensis	Ortholog in H. vulgaris transcriptomic dataset HAEP-T-CDS	ECTO	ENDO	NANOS	Podocoryne Orthologs
Asc-b	CEG06181.1	AAR0587.1	001622360.1	HAEP_T-CDS_v02_14032	0	7	4	AAQ75376.1
Prdl-a		CAA75668.1		HAEP_T-CDS_v02_8796	3	0	22	
Zic-C		XP_002154855.1	BAE94127.1		0	0	1	
Boule-1		None						
Boule-3		XP_002157877.1		HAEP_T-CDS_v02_9288	0	0	0	
Boule-2		AFM91092.1		HAEP_T-CDS_v02_9098	0	0	0	
TDP-1		XP_012563744.1		HAEP_T-CDS_v02_6974	12	13	107	
TDP-2		XP_012556899.1		HAEP_T-CDS_v02_5242	33	24	69	
Thyn1		XP002162584.1		HAEP_T-CDS_v02_4726	134	180	1685	
Antistasin		CAA47864.1		HAEP_T-CDS_v02_5764	5	109	16	
				HAEP_T-CDS_v02_5763	4	76	17	
Piwi	EU199802	XM_002155877		HAEP_T-CDS_v02_104 l	134	45	192	
RFamide		XP_002164214.3		HAEP_T-CDS_v02_1089	5	0	0	
				HAEP_T-CDS_v02_12198	2	0	0	
GLW		XP_002164748		HAEP_T-CDS_v02_43727	15	8	7	
				HAEP_T-CDS_v02_8405	2	9	3	
Minicollagen 3/4a	ABW02882.1	DAA34982.1 (minicollagen8)		HAEP_T-CDS_v02_48708	10	0	26	
		DAA34987.1 (minicollagen 13)		HAEP_T-CDS_v02_859	4	2	1	
Sox15		XP_002156236		HAEP_T-CDS_v02_12860	0,2	0	1,5	
Mos3	GBGP01000159	XP_002154855.1		HAEP_T-CDS_v02_16459	0,4	0	0,5	
				HAEP_T-CDS_v02_14617	0,8	0	0,5	
Znf845	GBGP01000085	XP_0021583		HAEP_T-CDS_v02_16460	1,5	0	16,5	

This table lists *Hydra magnipapillata* and *Hydra vulgaris* orthologs of selected *Clytia* genes analysed in this study, and the number of matching reads from the transcript dataset (HAEP) available at http://compagen.zoologie.uni-kiel.de/blast.html (Hemmrich et al. 2012) for separated cell populations (endoderm, ectoderm and nanos-positive cells), normalized with respect to total read number.

BIBLIOGRAPHY

A.Hall, T., 1999. BioEdit: a user friendly biological sequence alignement editor and analysis program for Windows 95/98/NT. *Nucleic Acids Symposium*, N°41.

Alberts B, Johnson A, Lewis J, et al. M., 2002. *Molecular Biology of the Cell. 4th edition.*,

Alié, A. et al., 2011. Somatic stem cells express Piwi and Vasa genes in an adult ctenophore: ancient association of "germline genes" with stemness. *Developmental biology*, 350(1), pp.183–97.

Van Amerongen, R. & Nusse, R., 2009. Towards an integrated view of Wnt signaling in development. *Development (Cambridge, England)*, 136(19), pp.3205–3214.

Amiel, A. et al., 2010. Clytia hemisphaerica: A Cnidarian Model for Studying Oogenesis. In *Oogenesis*. John Wiley & Sons, Ltd, pp. 81–101.

Amiel, A. et al., 2009. Conserved Functions for Mos in Eumetazoan Oocyte Maturation Revealed by Studies in a Cnidarian. *Current Biology*, 19(1), pp.305–311.

Amiel, A. & Houliston, E., 2009. Three distinct RNA localization mechanisms contribute to oocyte polarity establishment in the cnidarian Clytia hemisphærica. *Developmental Biology*, 327(1), pp.191–203

Andreu, P. et al., 2008. A genetic study of the role of the Wnt/beta-catenin signalling in Paneth cell differentiation. *Developmental biology*, 324(2), pp.288–96.

Androutsellis-Theotokis, A. et al., 2006. Notch signalling regulates stem cell numbers in vitro and in vivo. *Nature*, 442(7104), pp.823–826.

Aruga, J. et al., 2006. A wide-range phylogenetic analysis of Zic proteins: Implications for correlations between protein structure conservation and body plan complexity. *Genomics*, 87(6), pp.783–792.

Baguna J, 1981. Planarian neoblast. *Nature*, 290.

Ball, E.E. et al., 2002. Coral development: From classical embryology to molecular control. *International Journal of Developmental Biology*, 46(4 SPEC.), pp.671–678.

Bertrand, N., Castro, D.S. & Guillemot, F., 2002. Proneural genes and the specification of neural cell types. *Nature reviews. Neuroscience*, 3(7), pp.517–30.

Betschinger, J. & Knoblich, J.A., 2004. Dare to be different: asymmetric cell division in Drosophila, C. elegans and vertebrates. *Current biology : CB*, 14(16), pp.R674–85.

Bode, H.R., 1996. The interstitial cell lineage of hydra: a stem cell system that arose early in evolution. *Journal of cell science*, 109.

Bodo, F. and Bouillon, J. (1968) Etude histologique du developpement embryonnaire de quelques Hydrome ´duses de Roscoff. Cahiers Biol. Mar. IX, 69–104 56

Boehm, A.-M. et al., 2012. FoxO is a critical regulator of stem cell maintenance in immortal Hydra. *Proceedings of the National Academy of Sciences of the United States of America*, 109(48), pp.19697–702.

Boehm, A.-M. & Bosch, T.C.G., 2012. Migration of multipotent interstitial stem cells in Hydra. *Zoology (Jena, Germany)*, 115(5), pp.275–82.

Boero, F., Bouillon, J. & Piraino, S., 1992. On the origins and evolution of hydromedusan life cycles (Cnidaria , Hydrozoa). *Sex Origian and Evolution (R. Dallai, ed.), Vol. 6, Selected Symposia and Monographs U.Z.I., Mucchi, Modena, Italy*, (October 2015), pp.59–68.

Bosch, T.C.G., 2009. Hydra and the evolution of stem cells. *BioEssays : news and reviews in molecular, cellular and developmental biology*, 31(4), pp.478–86.

Bosch, T.C.G., 2007. Symmetry Breaking in Stem Cell of the Basal Metazoan Hydra. , pp.62–78.

Bosch, T.C.G. et al., 2010. The Hydra polyp: nothing but an active stem cell community. *Development, growth & differentiation*, 52(1), pp.15–25.

Bosch, T.C.G. & David, C.N., 1987. Stem cells of Hydra magnipapillata can differentiate into somatic cells and germ line cells. *Developmental Biology*, 121(1), pp.182–191.].

Boyer, L.A. et al., 2005. Core transcriptional regulatory circuitry in human embryonic stem cells. *Cell*, 122(6), pp.947–56.

Bradshaw, B., Thompson, K. & Frank, U., 2015. Distinct mechanisms underlie oral vs aboral regeneration in the cnidarian *Hydractinia echinata*. *eLife*, 4, pp.1–19.

Brechbiel, J.L. & Gavis, E.R., 2008. Spatial regulation of nanos is required for its function in dendrite morphogenesis. *Current biology : CB*, 18(10), pp.745–50.

Brennecke, J. et al., 2007. Discrete Small RNA-Generating Loci as Master Regulators of Transposon Activity in Drosophila. *Cell*, 128(6), pp.1089–1103.

Broun, M. et al., 2005. Formation of the head organizer in hydra involves the canonical Wnt pathway. *Development (Cambridge, England)*, 132(12), pp.2907–2916.

Brusca and Brusca, 2003. *Invertebrates* second. S. Associates, ed.,

Bouillon, J., 1966. Les cellules glandulaires des hydroïdes et hydroméduses. Leur structure et la nature de leurs sécrétions. *Cah. Biol. mar 7.2*, 157-205.

Byrum, C.A., 2001. An analysis of hydrozoan gastrulation by unipolar ingression. *Developmental biology*, 240(2), pp.627–40.

Campbell, R.D., 1976. Elimination by Hydra interstitial and nerve cells by means of colchicine. *Journal of cell science*, 21, pp.1–13.

Campos, L.S. et al., 2004. Beta1 integrins activate a MAPK signalling pathway in neural stem cells that contributes to their maintenance. *Development (Cambridge, England)*, 131(14), pp.3433–3444.

Chambers, I. et al., 2003. Functional Expression Cloning of Nanog, a Pluripotency Sustaining Factor in Embryonic Stem Cells. *Cell*, 113(5), pp.643–655.

Chapman, J. a et al., 2010. The dynamic genome of Hydra. *Nature*, 464(7288), pp.592–596.

Chera, S. et al., 2006. Silencing of the hydra serine protease inhibitor Kazal1 gene mimics the human SPINK1 pancreatic phenotype. *Journal of cell science*, 119(Pt 5), pp.846–857.

Chevalier, S. et al., 2006. Polarised expression of FoxB and FoxQ2 genes during development of the hydrozoan Clytia hemisphaerica. *Development Genes and Evolution*, 216(11), pp.709–720.

Chiori, R. et al., 2009. Are hox genes ancestrally involved in axial patterning? Evidence from the hydrozoan Clytia hemisphaerica (cnidaria). *PLoS ONE*, 4(1).

Cho, E. & Irvine, K.D., 2004. Action of fat, four-jointed, dachsous and dachs in distal-to-proximal wing signaling. *Development (Cambridge, England)*, 131(18), pp.4489–4500.

Chuma, S. et al., 2006. Tdrd1/Mtr-1, a tudor-related gene, is essential for male germ-cell differentiation and nuage/germinal granule formation in mice. *Proceedings of the National Academy of Sciences of the United States of America*, 103(43), pp.15894–15899.

Clevers, H., 2006. Wnt/beta-catenin signaling in development and disease. *Cell*, 127(3), pp.469–80.

Conzelmann, M. & Jékely, G., 2012. Antibodies against conserved amidated neuropeptide epitopes enrich the comparative neurobiology toolbox. *EvoDevo*, 3(1), p.23.

Cox, D.N. et al., 1998. A novel class of evolutionarily conserved genes defined by. *Genes & Development*, pp.3715–3727.

Croce, J.C. & McClay, D.R., 2008. Evolution of the Wnt pathways. *Methods in molecular biology (Clifton, N.J.)*, 469, pp.3–18.

Darling, J. a. et al., 2005. Rising starlet: The starlet sea anemone, Nematostella vectensis. *BioEssays*, 27(2), pp.211–221.

Darras, S. et al., 2011. -Catenin specifies the endomesoderm and defines the posterior organizer of the hemichordate Saccoglossus kowalevskii. *Development*, 138(5), pp.959–970.

David, C.N., 1973. A Quantitative Method for Maceration of Hydra Tissue. *Wilhelm Roux' Archiv*, 171,259--2.

David, C.N. et al., 2008. Evolution of complex structures: minicollagens shape the cnidarian nematocyst. *Trends in genetics : TIG*, 24(9), pp.431–8.

David, C.N., 2012. Interstitial stem cells in Hydra: multipotency and decision-making. *The International journal of developmental biology*, 56(6-8), pp.489–97.

David, C.N. & Gierer, a, 1974. Cell cycle kinetics and development of Hydra attenuata. III. Nerve and nematocyte differentiation. *Journal of cell science*, 16(2), pp.359–375.

David, C.N. & Plotnick, I., 1980. Distribution of interstitial stem cells in Hydra. *Developmental Biology*, 76(1), pp.175–184.

De, A., 2011. Wnt / Ca 21 signaling pathway : a brief overview The Non-canonical Wnt Signaling Cascade. *Acta Biochimica et Biophysica Hungarica*, 43(10), pp.745–756.

Deng, W., Lin, H. & Carolina, N., 2002. miwi , a Murine Homolog of piwi , Encodes a Cytoplasmic Protein Essential for Spermatogenesis. , 2, pp.819–830.

Denker, E. et al., 2008. Ordered progression of nematogenesis from stem cells through differentiation stages in the tentacle bulb of Clytia hemisphaerica (Hydrozoa, Cnidaria). *Developmental Biology*, 315(1), pp.99–113.

Devenport, D., 2014. The cell biology of planar cell polarity. , 207(2), pp.171–180.

Dorsky, R.I., Moon, R.T. & Raible, D.W., 2000. Environmental signals and cell fate specification in premigratory neural crest. *BioEssays*, 22(8), pp.708–716.

Duffy, D.J. & Frank, U., 2011. Modulation of COUP-TF expression in a cnidarian by ectopic Wnt signalling and allorecognition. *PloS one*, 6(4), p.e19443.

Dupré, A., Haccard, O. & Jessus, C., 2011. Mos in the oocyte: how to use MAPK independently of growth factors and transcription to control meiotic divisions. *Journal of signal transduction*, 2011, p.350412.

Eberhart, C.G., Maines, J.Z. & Wasserman, S.A., 1996. Meiotic cell cycle requirement for a fly homologue of human Deleted in Azoospermia. *Nature*, 381(6585), pp.783–785.

Edgar, R.C., 2004. MUSCLE: Multiple sequence alignment with high accuracy and high throughput. *Nucleic Acids Research*, 32(5), pp.1792–1797.

Eijkelenboom, A. & Burgering, B.M.T., 2013. FOXOs: signalling integrators for homeostasis maintenance. *Nat Rev Mol Cell Biol*, 14(2), pp.83–97.

Eirín-López, J.M. & Ausió, J., 2011. Boule and the Evolutionary Origin of Metazoan Gametogenesis: A Grandpa's Tale. *International Journal of Evolutionary Biology*, 2011, pp.1–7.

Evans, T. et al., 2014. Acquisition of germ plasm accelerates vertebrate evolution. *Science (New York, N.Y.)*, 344(6180), pp.200–3. Extavour, C.G., 2005. The fate of isolated blastomeres with respect to germ cell formation in the amphipod crustacean Parhyale hawaiensis. *Developmental Biology*, 277(2), pp.387–402.

Extavour, C.G. et al., 2005. Vasa and Nanos Expression Patterns in a Sea Anemone and the Evolution of Bilaterian Germ Cell Specification Mechanisms. *Evolution and Development*, 7, pp.201–215.

Extavour, C.G. & Akam, M., 2003. Mechanisms of germ cell specification across the metazoans: epigenesis and preformation. *Development (Cambridge, England)*, 130(24), pp.5869–84.

Finnerty, J.R. et al., 2004. Origins of bilateral symmetry: Hox and dpp expression in a sea anemone. *Science (New York, N.Y.)*, 304(5675), pp.1335–1337.

Flynn, R.A. & Chang, H.Y., 2014. Long noncoding RNAs in cell-fate programming and reprogramming. *Cell stem cell*, 14(6), pp.752–61.

France Bodo et Jean Bouillon, 1968. France Bodo et Jean Bouillon. , (L), pp.69–104.

Frank, U., Plickert, G. & Müller, W. a, 2009. *Stem Cells in Marine Organisms*,

Frank, U., Plickert, G. & Müller, W.A., 2009. Stem Cells in Marine Organisms B. Rinkevich & V. Matranga, eds. , pp.33–59.

Freeman, G., 1981a. The Cleavage Initiation Site Establishes the Posterior Pole of the Hydrozoan Embryo 1981b. *Journal Of Cell Biology*, pp.123–125.

Freeman, G., 1981b. The Role of Polarity in the Development of the Hydrozoan Planula Larva. *Wilhelm Roux's Archives of Developmental Biology*, 190(3), pp.168–184.

Fritzenwanker, J.H., Saina, M. & Technau, U., 2004. Analysis of forkhead and snail expression reveals epithelial-mesenchymal transitions during embryonic and larval development of Nematostella vectensis. *Developmental biology*, 275(2), pp.389–402.

Funayama, N., 2010. The stem cell system in demosponges: Insights into the origin of somatic stem cells. *Development Growth and Differentiation*, 52(1), pp.1–14.

Funayama, N., 2013. The stem cell system in demosponges: Suggested involvement of two types of cells: Archeocytes (active stem cells) and choanocytes (food-entrapping flagellated cells). *Development Genes and Evolution*, 223, pp.23–38.

Gaino, E. et al., 1984. Origin of male gametes from choanocytes in Spongia officinalis (Porifera, Demospongiae). *International journal of invertebrate reproduction and development*, 7(2), pp.83–93.

Gajewski, M. et al., 1996. LWamides from Cnidaria constitute a novel family of neuropeptides with morphogenetic activity. *Roux's Archives of Developmental Biology*, 205(5-6), pp.232–242.

Galliot, B., 2012. Hydra, a fruitful model system for 270 years. *International Journal of Developmental Biology*, 56(July), pp.411–423.

Galliot, B. et al., 2009. Origins of neurogenesis, a cnidarian view. *Developmental biology*, 332(1), pp.2–24.

Galliot, B. & Quiquand, M., 2011. A two-step process in the emergence of neurogenesis. *European Journal of Neuroscience*, 34(6), pp.847–862.

Galliot, B. & Schmid, V., 2002. Cnidarians as a model system for understanding evolution and regeneration. *International Journal of Developmental Biology*.

Gauchat, D. et al., 1998. Prdl-a, a Gene Marker for Hydra Apical Differentiation Related To Triploblastic Paired-Like Head-Specific Genes. *Development (Cambridge, England)*, 125, pp.1637–1645.

Gauchat, D. et al., 2004. The orphan COUP-TF nuclear receptors are markers for neurogenesis from cnidarians to vertebrates. *Developmental biology*, 275(1), pp.104–1

Genikhovich, G. et al., 2006. Discovery of genes expressed in Hydra embryogenesis. *Developmental biology*, 289(2), pp.466–81.

Giani, V.C. et al., 2011. Somatic and germline expression of piwi during development and regeneration in the marine polychaete annelid Capitella teleta. *EvoDevo*, 2(1).

Gold, D. a., Gates, R.D. & Jacobs, D.K., 2014. The Early Expansion and Evolutionary Dynamics of POU Class Genes. *Molecular Biology and Evolution*, 31(12), pp.3136–3147.

Gold, D. a. & Jacobs, D.K., 2012. Stem cell dynamics in Cnidaria: are there unifying principles? *Development Genes and Evolution*, 223(1-2), pp.53–66.

Grimmelikhuijzen, C.J.P. & Hauser, F., 2012. Mini-review: the evolution of neuropeptide signaling. *Regulatory peptides*, 177 Suppl, pp.S6–9.

Grimmelikhuijzen, C.J.P., Leviev, I. & Carstensen, K., 1996. Peptides in the Nervous Systems of Cnidarians: Structure, Function, and Biosynthesis. *International Review of Cytology*, 167, pp.37–89.

Gubb, D. & Garcia-Bellido, a., 1982. A genetic analysis of the determination of cuticular polarity during development in Drosophila melanogaster. *Journal of Embryology and Experimental Morphology*, 68, pp.37–57.

Guder, C. et al., 2006. The Wnt code: cnidarians signal the way. *Oncogene*, 25(57), pp.7450–7460.

Guo, S. & Kemphues, K.J., 1995. par-1, a gene required for establishing polarity in C. elegans embryos, encodes a putative Ser/Thr kinase that is asymmetrically distributed. *Cell*, 81(4), pp.611–620.

Guttman, M. et al., 2011. lincRNAs act in the circuitry controlling pluripotency and differentiation. *Nature*, 477(7364), pp.295–300.

Gyoja, F., Kawashima, T. & Satoh, N., 2012. A genomewide survey of bHLH transcription factors in the coral Acropora digitifera identifies three novel orthologous families, pearl, amber, and peridot. *Development Genes and Evolution*, 222(2), pp.63–76.

Habas, R. & Dawid, I.B., 2005. Dishevelled and Wnt signaling: is the nucleus the final frontier? *Journal of biology*, 4(1), p.2.

Hansen, D., 2004. Control of the proliferation versus meiotic development decision in the C. elegans germline through regulation of GLD-1 protein accumulation. *Development*, 131(1), pp.93–104.

Hari, L. et al., 2002. Lineage-specific requirements of β-catenin in neural crest development. *Journal of Cell Biology*, 159, pp.867–880.

Haueschild, V.C., 1956. Experimentelle Untersuchungen über die Entstehung asexueller Klone bei der Hydromeduse Eleutheria dichotoma. *Z. Naturforsdig.*, 11 b, pp.394–402.

Hayakawa, E., Fujisawa, C. & Fujisawa, T., 2004. Involvement of Hydra achaete-scute gene CnASH in the differentiation pathway of sensory neurons in the tentacles. *Development Genes and Evolution*, pp.486–492.

Hemmrich, G. et al., 2012. Molecular signatures of the three stem cell lineages in hydra and the emergence of stem cell function at the base of multicellularity. *Molecular biology and evolution*, 29(11), pp.3267–80.

Hobmayer, B. et al., 2000. WNT signalling molecules act in axis formation in the diploblastic metazoan Hydra. *Nature*, 407(6801), pp.186–189.

Hobmayer, B., Rentzsch, F. & Holstein, T.W., 2001. Identification and expression of HySmad1, a member of the R-Smad family of TGFβ signal transducers, in the diploblastic metazoan Hydra. *Development Genes and Evolution*, 211(12), pp.597–602.

Holstein, T.W. et al., 1994. Fibrous mini-collagens in hydra nematocysts. *Science (New York, N.Y.)*, 265(5170), pp.402–4.

Holstein, T.W. et al., 1992. The primitive metazoan Hydra expresses antistasin, a serine protease inhibitor of vertebrate blood coagulation: cDNA cloning, cellular localisation and developmental regulation. *FEBS Letters*, 309(3), pp.288–292.

Horvitz, H.R. & Herskowitz, I., 1992. Mechanisms of asymmetric cell division: Two Bs or not two Bs, that is the question. *Cell*, 68(2), pp.237–255.

Houliston, E., Momose, T. & Manuel, M., 2010. Clytia hemisphaerica: a jellyfish cousin joins the laboratory. *Trends in Genetics*, 26(4), pp.159–167.

Houtmeyers, R. et al., 2013. The ZIC gene family encodes multi-functional proteins essential for patterning and morphogenesis. *Cellular and Molecular Life Sciences*, 70(20), pp.3791–3811.

Houwing, S. et al., 2007. A Role for Piwi and piRNAs in Germ Cell Maintenance and Transposon Silencing in Zebrafish. *Cell*, 129(1), pp.69–82.

Hudson, C. et al., 2013. β-Catenin-Driven Binary Fate Specification Segregates Germ Layers in Ascidian Embryos. *Current Biology*, 23(6), pp.491–495.

Hwang, J.S. et al., 2007. The evolutionary emergence of cell type-specific genes inferred from the gene expression analysis of Hydra. *Proceedings of the National Academy of Sciences of the United States of America*, 104(37), pp.14735–40.

Imai, K. et al., 2000. (Beta)-Catenin Mediates the Specification of Endoderm Cells in Ascidian Embryos. *Development*, 127(14), pp.3009–3020.

Inestrosa, N.C. & Arenas, E., 2010. Emerging roles of Wnts in the adult nervous system. *Nature Reviews Neuroscience*, 11(2), pp.77–86.

Jager, M. et al., 2013. Evidence for Involvement of Wnt Signalling in Body Polarities, Cell Proliferation, and the Neuro-Sensory System in an Adult Ctenophore. *PLoS ONE*, 8(12), p.e84363.

Jager, M. et al., 2006. Expansion of the SOX gene family predated the emergence of the Bilateria. *Molecular phylogenetics and evolution*, 39(2), pp.468–77.

Jager, M., Quéinnec, E., et al., 2011. Multiple Sox genes are expressed in stem cells or in differentiating neuro-sensory cells in the hydrozoan Clytia hemisphaerica. *EvoDevo*, 2, p.12.

Jager, M., Chiori, R., et al., 2011. New insights on ctenophore neural anatomy: Immunofluorescence study in Pleurobrachia pileus (Müller, 1776). *Journal of Experimental Zoology Part B: Molecular and Developmental Evolution*, 316 B(3), pp.171–187.

Juliano, C.E., Swartz, S.Z. & Wessel, G.M., 2010. A conserved germline multipotency program. *Development*, 137(24), pp.4113–4126.

Kageyama, R. et al., 2005. Roles of bHLH genes in neural stem cell differentiation. *Experimental Cell Research*, 306(2), pp.343–348.

Kanska, J. & Frank, U., 2013. New roles for Nanos in neural cell fate determination revealed by studies in a cnidarian. *Journal of cell science*, 126(Pt 14), pp.3192–203.

Karashima, T., Sugimoto, a & Yamamoto, M., 2000. Caenorhabditis elegans homologue of the human azoospermia factor DAZ is required for oogenesis but not for spermatogenesis. *Development (Cambridge, England)*, 127(5), pp.1069–1079.

Khalturin, K. et al., 2007. Transgenic stem cells in Hydra reveal an early evolutionary origin for key elements controlling self-renewal and differentiation. *Developmental biology*, 309(1), pp.32–44.

Kimble, J.E. & White, J.G., 1981. On the control of germ cell development in Caenorhabditis elegans. *Developmental Biology*, 81(2), pp.208–219.

Kloc, M., Bilinski, S. & Etkin, L.D., 2004. The Balbiani body and germ cell determinants: 150 years later. *Curr Top Dev Biol*, 59, pp.1–36.

Knoblich, J.A., 2001. Asymmetric cell division during animal development . *Nat Rev Mol Cell Biol*, 2(1), pp.11–20. Kobayashi, S. et al., 1996. Essential role of the posterior morphogen nanos for germline development in Drosophila. *Nature*, 380(6576), pp.708–711.

Koizumi, O. et al., 2014. The nerve ring in cnidarians: its presence and structure in hydrozoan medusae. *Zoology (Jena, Germany)*.

Koprunner, M. et al., 2001. A zebrafish nanos -related gene is essential for the development of primordial germ cells. *Genes & development*, 15, pp.2877–2885.

Kraemer, B. et al., 1999. NANOS-3 and FBF proteins physically interact to control the sperm–oocyte switch in Caenorhabditis elegans. *Current Biology*, 9(18), pp.1009–1018.

Kuales, G. et al., 2011. Boule-like genes regulate male and female gametogenesis in the flatworm Macrostomum lignano. *Developmental Biology*, 357(1), pp.117–132.

Kumano, G., 2015. Evolution of germline segregation processes in animal development. *Development, Growth & Differentiation*, 57(4), pp.324–332.

Kurz, E.M. et al., 1991. Mini-collagens in hydra nematocytes. *Journal of Cell Biology*, 115(4), pp.1159–1169.

Kusserow, A. et al., 2005. Unexpected complexity of the Wnt gene family in a sea anemone. *Nature*, 433(7022), pp.156–160.

Kuznetsov, S., Lyanguzowa, M. & Bosch, T.C., 2001. Role of epithelial cells and programmed cell death in Hydra spermatogenesis. *Zoology (Jena, Germany)*, 104(1), pp.25–31.

Lai, F., Singh, a. & King, M.L., 2012. Xenopus Nanos1 is required to prevent endoderm gene expression and apoptosis in primordial germ cells. *Development*, 139(8), pp.1476–1486.

Lapébie, P. et al., 2014. Differential Responses to Wnt and PCP Disruption Predict Expression and Developmental Function of Conserved and Novel Genes in a Cnidarian. *PLoS Genetics*, 10(9), p.e1004590.

Lapébie, P., Borchiellini, C. & Houliston, E., 2011. Dissecting the PCP pathway: One or more pathways?: Does a separate Wnt-Fz-Rho pathway drive morphogenesis? *BioEssays*, 33(10), pp.759–768.

Layden, M.J. et al., 2010. Expression and phylogenetic analysis of the zic gene family in the evolution and development of metazoans. *EvoDevo*, 1(1), p.12.

Leclère, L. et al., 2012. Maternally localized germ plasm mRNAs and germ cell/stem cell formation in the cnidarian Clytia. *Developmental biology*, 364(2), pp.236–48.

Leclère, L. & Rentzsch, F., 2014. RGM Regulates BMP-Mediated Secondary Axis Formation in the Sea Anemone Nematostella vectensis. *Cell Reports*, 9(5), pp.1921–1930.

Lee, P.N. et al., 2006. A WNT of things to come: evolution of Wnt signaling and polarity in cnidarians. *Seminars in cell & developmental biology*, 17(2), pp.157–67.

Leininger, S. et al., 2014. Developmental gene expression provides clues to relationships between sponge and eumetazoan body plans. *Nature communications*, 5(May), p.3905.

Leitz, T., Morand, K. & Mann, M., 1994. Metamorphosin A: a novel peptide controlling development of the lower metazoan Hydractinia echinata (Coelenterata, Hydrozoa). *Developmental biology*, 163(2), pp.440–6.

Lentz, T.L., 1965. THE FINE STRUCTURE OF DIFFERENTIATING INTERSTITIAL CELLS IN HYDRA. *Zeitschrift fiir Zellforschung*, 560(67), pp.547–560.

Lichtneckert, R. et al., 2002. Evolutionary conservation of the chromatin modulator Polycomb in the jellyfish Podocoryne carnea. *Differentiation; research in biological diversity*, 70(8), pp.422–8.

Lin, H. & Spradling, a C., 1997. A novel group of pumilio mutations affects the asymmetric division of germline stem cells in the Drosophila ovary. *Development (Cambridge, England)*, 124(12), pp.2463–2476.

Lindgens, D., 2004. Hyzic, the Hydra homolog of the zic/odd-paired gene, is involved in the early specification of the sensory nematocytes. *Development*, 131(1), pp.191–201

Logan, C.Y. et al., 1999. Nuclear beta-catenin is required to specify vegetal cell fates in the sea urchin embryo. *Development (Cambridge, England)*, 126, pp.345–357.

Lopez-Rios, J. et al., 2008. The Netrin-related domain of Sfrp1 interacts with Wnt ligands and antagonizes their activity in the anterior neural plate. *Neural Development*, 3(1), p.19.

Ma, Y. et al., 2013. Bioinformatic analysis of the four transcription factors used to induce pluripotent stem cells. *Cytotechnology*, pp.967–978.

Magie, C.R., Pang, K. & Martindale, M.Q., 2005. Genomic inventory and expression of Sox and Fox genes in the cnidarian Nematostella vectensis. *Development Genes and Evolution*, 215(12), pp.618–630.

Marlow, H., Matus, D.Q. & Martindale, M.Q., 2013. Ectopic activation of the canonical wnt signaling pathway affects ectodermal patterning along the primary axis during larval development in the anthozoan Nematostella vectensis. *Developmental biology*, 380(2), pp.324–34.

Martin, G.R., 1981. Isolation of a pluripotent cell line from early mouse embryos cultured in medium conditioned by teratocarcinoma stem cells. *Proceedings of the National Academy of Sciences of the United States of America*, 78(12), pp.7634–7638.

Martin, V.J., 1992. Characterization of a RFamide-positive subset of ganglionic cells in the hydrozoan planular nerve net. *Cell & Tissue Research*, 269(3), pp.431–438.

Martin, V.J., 1988. Development of Nerve Cells in Hydrozoan Planulae: I. Differentiation of Ganglionic Cells. *The Biological Bulletin*, 174(3), pp.319–329.

Masui, Y., 2001. From oocyte maturation to the in vitro cell cycle: the history of discoveries of Maturation-Promoting Factor (MPF) and Cytostatic Factor (CSF). *Differentiation; research in biological diversity*, 69(1), pp.1–17.

Miljkovic-Licina, M. et al., 2007. Head regeneration in wild-type hydra requires de novo neurogenesis. *Development (Cambridge, England)*, 134(6), pp.1191–201.

Miljkovic-Licina, M., Gauchat, D. & Galliot, B., 2004. Neuronal evolution: analysis of regulatory genes in a first-evolved nervous system, the hydra nervous system. *Bio Systems*, 76(1-3), pp.75–87.

Millane, R.C. et al., 2011. Induced stem cell neoplasia in a cnidarian by ectopic expression of a POU domain transcription factor. *Development (Cambridge, England)*, 138(12), pp.2429–2439.

Mitgutsch, C., Hauser, F. & Grimmelikhuijzen, C.J., 1999. Expression and developmental regulation of the Hydra-RFamide and Hydra-LWamide preprohormone genes in Hydra: evidence for transient phases of head formation. *Developmental biology*, 207(1), pp.189–203.

Miyaji, H. et al., 2002. Molecular cloning and characterization of the mouse thymocyte protein gene. *Gene*, 297(1-2), pp.189–96.

Mochizuki, K. et al., 2000. Expression and evolutionary conservation of nanos-related genes in Hydra. *Development genes and evolution*, 210(12), pp.591–602.

Momose, T., Derelle, R. & Houliston, E., 2008. A maternally localised Wnt ligand required for axial patterning in the cnidarian Clytia hemisphaerica. *Development*, 135(12), pp.2105–2113.

Momose, T. & Houliston, E., 2007. Two oppositely localised frizzled RNAs as axis determinants in a cnidarian embryo. *PLoS Biology*, 5(4), pp.889–899.

Momose, T., Kraus, Y. & Houliston, E., 2012. A conserved function for Strabismus in establishing planar cell polarity in the ciliated ectoderm during cnidarian larval development. *Development*, 4382, pp.4374–4382.

Morrison, S.J. & Spradling, A.C., 2008. Stem cells and niches: mechanisms that promote stem cell maintenance throughout life. *Cell*, 132(4), pp.598–611.

Müller, P. et al., 2003. Evolutionary aspects of developmentally regulated helix-loop-helix transcription factors in striated muscle of jellyfish. *Developmental Biology*, 255(2), pp.216–229.

Muller, W. et al., 2007. Wnt signaling in hydroid development: ectopic heads and giant buds induced by GSK-3beta inhibitors. *The International Journal of Developmental Biology*, 51(3), pp.211–220.

Mulligan, K. a. & Cheyette, B.N.R., 2012. Wnt Signaling in Vertebrate Neural Development and Function. *Journal of Neuroimmune Pharmacology*, 7(4), pp.774–787.

Murata, Y. & Wharton, R., 1995. Binding of Pumilio to maternal hunchback mRNA is required for posterior patterning in Drosophila embryos. *Cell*, 80, pp.747–756.

Nakagawa, T. et al., 2010. Functional Hierarchy and Reversibility Within the Murine Spermatogenic Stem Cell Compartment. *Science* , 328 (5974), pp.62–67.

Nichols, J. et al., 1998. Formation of Pluripotent Stem Cells in the Mammalian Embryo Depends on the POU Transcription Factor Oct4. *Cell*, 95(3), pp.379–391. A

Nishimiya-Fujisawa, C. & Kobayashi, S., 2012. Germline stem cells and sex determination in Hydra. *International Journal of Developmental Biology*, 56(6-8), pp.499–508.

Nishimura, E.K. et al., 2002. Dominant role of the niche in melanocyte stem-cell fate determination. *Nature*, 416(6883), pp.854–860.

Niwa, H., 2007. How is pluripotency determined and maintained? *Development (Cambridge, England)*, 134(4), pp.635–646.

Niwa, H., Miyazaki, J. & Smith, a G., 2000. Quantitative expression of Oct-3/4 defines differentiation, dedifferentiation or self-renewal of ES cells. *Nature genetics*, 24(4), pp.372–376.

Nusse, R., Fuerer, C. & Ching, W., 2008. Wnt Signaling and Stem Cell Control. , LXXIII, pp.59–66.

Ohinata, Y. et al., 2009. A Signaling Principle for the Specification of the Germ Cell Lineage in Mice. *Cell*, 137(3), pp.571–584.

Okamura, K. et al., 2004. Distinct roles for Argonaute proteins in small RNA-directed RNA cleavage pathways. *Genes and Development*, 18, pp.1655–1666.

Oliveri, P. et al., 2006. Repression of mesodermal fate by foxa, a key endoderm regulator of the sea urchin embryo. *Development*, 133(21), pp.4173–4181.

P, Tardent, H.T., 1984. An Ultrahigh-Speed Analysis of Exocytosis: Nematocyst Discarge. *Science*, 223.

Pan, G. & Pei, D., 2005. The stem cell pluripotency factor NANOG activates transcription with two unusually potent subdomains at its C terminus. *Journal of Biological Chemistry*, 280(2), pp.1401–1407.

Petersen, C.P. & Reddien, P.W., 2009. Wnt Signaling and the Polarity of the Primary Body Axis. *Cell*, 139(6), pp.1056–1068.

Pevny, L. & Placzek, M., 2005. SOX genes and neural progenitor identity. *Current Opinion in Neurobiology*, 15(1), pp.7–13.

Philipp, I. et al., 2009. Wnt/beta-catenin and noncanonical Wnt signaling interact in tissue evagination in the simple eumetazoan Hydra. *Proceedings of the National Academy of Sciences of the United States of America*, 106(11), pp.4290–4295.

Pinto, D. et al., 2003. Canonical Wnt signals are essential for homeostasis of the intestinal epithelium service Canonical Wnt signals are essential for homeostasis of the intestinal epithelium. , pp.1709–1713.

Piraino, S. et al., 2011. Complex neural architecture in the diploblastic larva of Clava multicornis (Hydrozoa, Cnidaria). *The Journal of Comparative Neurology*, 519(10), pp.1931–1951.

Piraino, S. et al., 2004. Reverse development in Cnidaria. *Canadian Journal of Zoology*, 82(11), pp.1748–1754.

Plickert, G. et al., 2003. The role of alpha-amidated neuropeptides in hydroid development--LWamides and metamorphosis in Hydractinia echinata. *The International journal of developmental biology*, 47(6), pp.439–450.

Plickert, G., Frank, U. & Müller, W. a, 2012. Hydractinia, a pioneering model for stem cell biology and reprogramming somatic cells to pluripotency. *The International journal of developmental biology*, 56(6-8), pp.519–34.

Plickert, G., Kroiher, M. & Munck, a, 1988. Cell proliferation and early differentiation during embryonic development and metamorphosis of Hydractinia echinata. *Development (Cambridge, England)*, 103(4), pp.795–803.

Ponting, C.P., 1997. Tudor domains in proteins that interact with RNA. *Trends in Biochemical Sciences*, 22(2), pp.51–52.

Putnam, N., Srivastava, M. & Hellsten, U., 2007. Sea anemone genome reveals ancestral eumetazoan gene repertoire and genomic organization. *science*.

Rebscher, N. et al., 2008. The germ plasm component Vasa allows tracing of the interstitial stem cells in the cnidarian Hydractinia echinata. *Developmental dynamics : an official publication of the American Association of Anatomists*, 237(6), pp.1736–45.

Reddien, P.W. et al., 2005. SMEDWI-2 is a PIWI-like protein that regulates planarian stem cells. *Science (New York, N.Y.)*, 310, pp.1327–1330.

Richards, G.S. & Rentzsch, F., 2014. Transgenic analysis of a SoxB gene reveals neural progenitor cells in the cnidarian Nematostella vectensis. *Development*, 141, pp.4681–4689.

Rigo-Watermeier, T. et al., 2012. Functional conservation of Nematostella Wnts in canonical and noncanonical Wnt-signaling. *Biology Open*, 1(1), pp.43–51.

Roberts, a & Mackie, G.O., 1980. The giant axon escape system of a hydrozoan medusa, *Aglantha digitale*. *The Journal of Experimental Biology*, 84, pp.303–18.

Rothbächer, U. et al., 2000. Dishevelled phosphorylation, subcellular localization and multimerization regulate its role in early embryogenesis. *The EMBO journal*, 19(5), pp.1010–22.

Röttinger, E., Dahlin, P. & Martindale, M.Q., 2012. A Framework for the Establishment of a Cnidarian Gene Regulatory Network for "Endomesoderm" Specification: The Inputs of ß-Catenin/TCF Signaling. *PLoS Genetics*, 8(12), p.e1003164.

Ryan, J. et al., 2006. The cnidarian-bilaterian ancestor possessed at least 56 homeoboxes. Evidence from the starlet sea anemone, Nematostella vectensis. *Genome Biology*, 7, pp.R64–R64.

Ryan, J.F. & Baxevanis, A.D., 2007. Hox, Wnt, and the evolution of the primary body axis: insights from the early-divergent phyla. *Biology Direct*, 2(1), p.37.

Sandberg, M., Kallstrom, M. & Muhr, J., 2005. Sox21 promotes the progression of vertebrate neurogenesis. *Nat Neurosci*, 8(8), pp.995–1001.

Sato, N. et al., 2004. Maintenance of pluripotency in human and mouse embryonic stem cells through activation of Wnt signaling by a pharmacological GSK-3-specific inhibitor. *Nature medicine*, 10(1), pp.55–63.

Satou, Y. et al., 2008. Regulatory genes in the ancestral chordate genomes. *Development Genes and Evolution*, 218(11-12), pp.715–721.

Satterlie, R. a, 2002. Neuronal control of swimming in jellyfish: a comparative story. *Canadian Journal of Zoology*, 80(10), pp.1654–1669.

Scadden, D.T., 2006. The stem-cell niche as an entity of action. *Nature*, 441(7097), pp.1075–1079.

Schmid, V., Wydler, M. & Alder, H., 1982. Transdifferentiation and regeneration in vitro. *Developmental Biology*, 92(2), pp.476–488.

Schmidt, A. et al., 2006. Cytostatic factor: an activity that puts the cell cycle on hold. *Journal of cell science*, 119(Pt 7), pp.1213–1218.

Schmidt, T. & David, C.N., 1986. Gland cells in Hydra: cell cycle kinetics and development. *Journal of cell science*, 85, pp.197–215.

Seipel, K., Yanze, N. & Schmid, V., 2004a. Developmental and evolutionary aspects of the basic helix–loop–helix transcription factors Atonal-like 1 and Achaete-scute homolog 2 in the jellyfish. *Developmental Biology*, 269(2), pp.331–45.

Seipel, K., Yanze, N. & Schmid, V., 2004b. The germ line and somatic stem cell gene Cniwi in the jellyfish Podocoryne carnea. *The International Journal of Developmental Biology*, 48(1), pp.1–7.

Shah, C. et al., 2010. Widespread presence of human BOULE homologs among animals and conservation of their ancient reproductive function. *PLoS genetics*, 6(7), p.e1001022.

Shinzato, C. et al., 2008. Sox genes in the coral Acropora millepora: divergent expression patterns reflect differences in developmental mechanisms within the Anthozoa. *BMC Evolutionary Biology*, 8(1), p.311.

Siebert, S. et al., 2014. Stem cells in a colonial animal with localized growth zones. *EvoDevo*.

Siebert, S., Anton-Erxleben, F. & Bosch, T.C.G., 2008. Cell type complexity in the basal metazoan Hydra is maintained by both stem cell based mechanisms and transdifferentiation. *Developmental biology*, 313(1), pp.13–24.

Simon, J.A. & Kingston, R.E., 2013. Occupying chromatin: Polycomb mechanisms for getting to genomic targets, stopping transcriptional traffic, and staying put. *Molecular cell*, 49(5), pp.808–24.

Simpson, T.L., 1984. Cell Biology Sponges. *Springer*.

Sinigaglia, C. et al., 2013. The Bilaterian Head Patterning Gene six3/6 Controls Aboral Domain Development in a Cnidarian. *PLoS Biology*, 11(2).

Siomi, M.C., Mannen, T. & Siomi, H., 2010. How does the royal family of tudor rule the PIWI-interacting RNA pathway? *Genes and Development*, 24(7), pp.636–646.

Slautterback, D.B. & Fawcett, D.W., 1959. The development of the cnidoblasts of Hydra; an electron microscope study of cell differentiation. *The Journal of biophysical and biochemical cytology*, 5(3), pp.441–452.

Sokol, S.Y., 2011. Maintaining embryonic stem cell pluripotency with Wnt signaling. *Development*, 138(20), pp.4341–4350.

Song, A.-X. et al., 2005. Identification, expression, and purification of a unique stable domain from human HSPC144 protein. *Protein expression and purification*, 42(1), pp.146–52.

Soza-Ried, J. et al., 2010. The transcriptome of the colonial marine hydroid Hydractinia echinata. *FEBS Journal*, 277(1), pp.197–209.

Srivastava, M. et al., 2010. The Amphimedon queenslandica genome and the evolution of animal complexity. *Nature*, 466(7307), pp.720–726.

Steinmetz, P.R.H. et al., 2012. Independent evolution of striated muscles in cnidarians and bilaterians. *Nature*, 487(7406), pp.231–234.

Summers, R.G. & Naynes, J.F., 1969. The Ontogeny o f Interstitial Cells in Pennaria tiarella. *Journal of Morphology*, 129, pp.81–87.

Szczepanek, S., Cikala, M. & David, C.N., 2002. Poly- γ -glutamate synthesis during formation of nematocyst capsules in Hydra. , pp.745–751.

Takahashi, T. et al., 2000. A novel neuropeptide, Hym-355, positively regulates neuron differentiation in Hydra. *Development (Cambridge, England)*, 127(5), pp.997–1005.

Takahashi, T. & Hatta, M., 2011. The Importance of GLWamide Neuropeptides in Cnidarian Development and Physiology. *Journal of Amino Acids*, 2011, pp.1–8.

Tang, K. et al., 2010. COUP-TFs regulate eye development by controlling factors essential for optic vesicle morphogenesis. *Development (Cambridge, England)*, 137(5), pp.725–734.

Technau, U. & Steele, R.E., 2011. Evolutionary crossroads in developmental biology: Cnidaria. *Development*, 138(8), pp.1447–1458.

Teo, R. et al., 2006. An evolutionary conserved role of Wnt signaling in stem cell fate decision. *Developmental biology*, 289(1), pp.91–9.

Thomas, M.B & Martin G.F 1987. The Embryionic Origin of Neurosensory Cells and the Role of Nerve cells in Metamorphosis in Phialidium gregarium. *international journal of invertebrate reproduction and development*, 11.

Thomson, T. & Lasko, P., 2005. Tudor and its domains: germ cell formation from a Tudor perspective. *Cell Research*, 15(4), pp.281–291.

Thomson, T. & Lin, H., 2009. The biogenesis and function of PIWI proteins and piRNAs: progress and prospect. *Annual review of cell and developmental biology*, 25, pp.355–376.

Torras, R. & González-Crespo, S., 2005. Posterior expression of nanos orthologs during embryonic and larval development of the anthozoan Nematostella vectensis. *International Journal of Developmental Biology*, 49, pp.895–899.

Toyota, H. et al., 2012. Thy28 partially prevents apoptosis induction following engagement of membrane immunoglobulin in WEHI-231 B lymphoma cells. *Cellular & Molecular Biology Letters*, 17(1), pp.36–48.

Tsai, Y.S., Gomez, S.M. & Wang, Z., 2014. Prevalent RNA recognition motif duplication in the human genome. *RNA*, 20(5), pp.702–712.

Tuszynskisb, G.P., Gasicll, T.B. & Gasicll, J., 1987. Isolation and Characterization of Antistasin. , 262(20), pp.9718–9723.

Vrijens, K. et al., 2013. Identification of Small Molecule Activators of BMP Signaling. *PLoS ONE*, 8(3), p.e59045.

Wang, Y. et al., 2007. Nanos Function Is Essential for Development and Regeneration of Planarian Germ Cells. *Proceedings of the National Academy of Sciences of the United States of America*, 104(32), pp.5901–5906.

Watanabe, H. et al., 2009. Immortality and the base of multicellular life: Lessons from cnidarian stem cells. *Seminars in cell & developmental biology*, 20(9), pp.1114–25.

Weber, J., 1990. Poly(-glutamic Acid)s Are the Major Constituents Hydra of Nematocysts Hydroxoa , Cnidaria)*. *J. Biol. Chem.*, 265(17), pp.9664–9669.

Wegner, M., 2011. SOX after SOX: SOXession regulates neurogenesis. *Genes and Development*, 25(23), pp.2423–2428.

Weismann A, 1883. The origin of the sexual cells in hydromedusae. *Gustav Fischer*.

Wharton, R.P. & Struhl, G., 1991. RNA regulatory elements mediate control of Drosophila body pattern by the posterior morphogen nanos. *Cell*, 67(5), pp.955–967.

Wikramanayake, a. H. et al., 2003. An ancient role for nuclear β-catenin in the evolution of axialpolarity and germ layer segregation. *Nature*, 426(November), pp.446–450. A

Wilson, A. & Trumpp, A., 2006. Bone-marrow haematopoietic-stem-cell niches. *Nature reviews. Immunology*, 6(2), pp.93–106.

Wittlieb, J. et al., 2006a. Transgenic Hydra allow in vivo tracking of individual stem cells during morphogenesis. *Proceedings of the National Academy of Sciences of the United States of America*, 103(16), pp.6208–6211.

Wittlieb, J. et al., 2006b. Transgenic Hydra allow in vivo tracking of individual stem cells during morphogenesis. *Proceedings of the National Academy of Sciences of the United States of America*, 103(16), pp.6208–6211.

Wutz, A., 2013. Transcriptional and Translational Regulation of Stem Cells. *Transcriptional and Translational Regulation of Stem Cells*, 786, pp.307–328.

Xu, E.Y., Moore, F.L. & Pera, R. a. R., 2001. A gene family required for human germ cell development evolved from an ancient meiotic gene conserved in metazoans. *Proceedings of the National Academy of Sciences*, 98(13), pp.7414–7419.

Yoon, S., & Seger, R. (2006). The extracellular signal-regulated kinase: multiple substrates regulate diverse cellular functions. *Growth factors*, *24*(1), 21-44.

Zhang, J. & Li, L., 2005. BMP signaling and stem cell regulation. *Developmental biology*, 284(1), pp.1–11.